

The Molecular Basis of Sexual Dimorphism

Experimental and Theoretical Characterization of Phenotypic,
Transcriptomic and Genetic Patterns of Sex-Specific Adaptation

by

Gemma Puixeu

August, 2023

A thesis submitted to the
Graduate School of the
Institute of Science and Technology Austria
in partial fulfillment of the requirements
for the degree of Doctor of Philosophy

Committee in charge:
Christoph Lampert, Chair
Beatriz Vicoso
Nick Barton
Fyodor Kondrashov
John Pannell



The thesis of Gemma Puixeu, titled “The Molecular Basis of Sexual Dimorphism: Experimental and Theoretical Characterization of Phenotypic, Transcriptomic and Genetic Patterns of Sex-Specific Adaptation” is approved by:

Supervisor: Beatriz Vicoso, Institute of Science and Technology Austria, Klosterneuburg, Austria

Signature:

Supervisor: Nick Barton, Institute of Science and Technology Austria, Klosterneuburg, Austria

Signature:

Internal committee member: Fyodor Kondrashov, Okinawa Institute of Science and Technology, Okinawa, Japan

Signature:

External committee member: John Pannell, University of Lausanne, Lausanne, Switzerland

Signature:

Defense chair: Christoph Lampert, Institute of Science and Technology Austria, Klosterneuburg, Austria

Signature:

Signed page is on file

© by Gemma Puixeu, August, 2023
All Rights Reserved for the Creative Commons Attribution 4.0 International
License (CC BY 4.0)

ISTA Thesis, ISSN: 2663-337X
ISBN: 978-3-99078-035-0

CC BY 4.0 The copyright of this thesis rests with the author. Unless otherwise indicated, its contents are licensed under a Creative Commons Attribution 4.0 International License. Under this license, you may copy and redistribute the material in any medium or format. You may also create and distribute modified versions of the work. This is on the condition that you credit the author.

I hereby declare that this thesis is my own work and that it does not contain other people's work without this being so stated; this thesis does not contain my previous work without this being stated, and the bibliography contains all the literature that I used in writing the dissertation.

I declare that this is a true copy of my thesis, including any final revisions, as approved by my thesis committee, and that this thesis has not been submitted for a higher degree to any other university or institution.

I certify that any republication of materials presented in this thesis has been approved by the relevant publishers and co-authors.

Signature: _____

Gemma Puixeu

August, 2023

Signed page is on file

Abstract

Females and males across species are subject to divergent selective pressures arising from different reproductive interests and ecological niches. This often translates into a intricate array of sex-specific natural and sexual selection on traits that have a shared genetic basis between both sexes, causing a genetic sexual conflict. The resolution of this conflict mostly relies on the evolution of sex-specific expression of the shared genes, leading to phenotypic sexual dimorphism. Such sex-specific gene expression is thought to evolve via modifications of the genetic networks ultimately linked to sex-determining transcription factors. Although much empirical and theoretical evidence supports this standard picture of the molecular basis of sexual conflict resolution, there still are a few open questions regarding the complex array of selective forces driving phenotypic differentiation between the sexes, as well as the molecular mechanisms underlying sex-specific adaptation. I address some of these open questions in my PhD thesis.

First, how do patterns of phenotypic sexual dimorphism vary within populations, as a response to the temporal and spatial changes in sex-specific selective forces? To tackle this question, I analyze the patterns of sex-specific phenotypic variation along three life stages and across populations spanning the whole geographical range of *Rumex hastatulus*, a wind-pollinated angiosperm, in the first Chapter of the thesis.

Second, how do gene expression patterns lead to phenotypic dimorphism, and what are the molecular mechanisms underlying the observed transcriptomic variation? I address this question by examining the sex- and tissue-specific expression variation in newly-generated datasets of sex-specific expression in heads and gonads of *Drosophila melanogaster*. I additionally used two complementary approaches for the study of the genetic basis of sex differences in gene expression in the second and third Chapters of the thesis.

Third, how does intersex correlation, thought to be one of the main aspects constraining the ability for the two sexes to decouple, interact with the evolution of sexual dimorphism? I develop models of sex-specific stabilizing selection, mutation and drift to formalize common intuition regarding the patterns of covariation between intersex correlation and sexual dimorphism in the fourth Chapter of the thesis.

Alltogether, the work described in this PhD thesis provides useful insights into the links between genetic, transcriptomic and phenotypic layers of sex-specific variation, and contributes to our general understanding of the dynamics of sexual dimorphism evolution.

Acknowledgements

Many layers of support have made this work possible, all of which I want to acknowledge, from farthest to closest.

First, I want to thank the funding institutions: the European Union's Horizon 2020 research and innovation program for partially financing the first two years of my PhD (2016-2018) under the Marie Skłodowska-Curie Grant (agreement no. 665385) and the Austrian Academy of Sciences for granting me a DOC fellowship at ISTA (DOC 25817), which has co-funded the last 3 years of the PhD.

Second, I want to thank ISTA as an institution. For the trust now 7 years ago as I was accepted in the PhD program; for embracing my erratic walking; for witnessing my personal and professional growth throughout the years – which has turned out to be reciprocal; for the administrative and technical support (particularly the HR and IT units) that made life easier in the crucial moments; for the opportunities for involvement as a Student Representative, and for the co-growth in the international community throughout the years; and for the daily bike rides along the Donau.

Third, I want to thank my community at work. Beatriz and Nick for the trust, the supervision and the attempts to work jointly, which I feel have slightly improved through the years; all my direct and indirect collaborators, for the opportunity to learn from and with each other; the Barton and Vicoso groups for their support, for making me feel part of something larger, and reminding me of the importance of 'all this' in the moments when I most needed it; my friendships at ISTA, which by now are some of my longest-term and most stable relationships in Vienna, and which I hope to carry with me anywhere else I might be.

Fourth, I want to thank Vienna. For hosting this experience, which was orders of magnitude longer than originally expected; for the German slang, its controversial history, the greenness, the international community, the drums and the beautiful people I have met along the way; and for making me appreciate more what I left back home.

Last, I want to thank my safety net. My parents, for bringing me here, and Raissa, for reminding me why.

About the author

Gemma Puixeu completed a BSc in Genetics at the Autonomous University of Barcelona in 2016 after defending a Bachelor thesis on the "Evolution and Medical Implications of Sexual Dimorphism". She joined ISTA in early 2016 for an internship in the Siekhaus group, where she studied *Drosophila* development. Sexual dimorphism and flies came together for her PhD, which she started in September 2016 under the supervision of Beatriz Vicoso and Nick Barton, and where she has studied the evolution of sexual dimorphism using a combination of theoretical and experimental work – and flies as the main model organism.

During these years she has published some of her results in high impact journals (like *G3* and *New Phytologist*), and has presented them in conferences, most recently at the ESEB conference in Prag last summer.

She is also a feminist, committed to establishing a conversation on the biological basis of sex and gender beyond the canonical picture of gender binarism and inequality that we inherited from the last couple of centuries. Committed to stressing how important it is to study sex and gender by transcending, but also understanding, their biological basis.

List of Collaborators and Publications

Chapter 1

Publication

Puixeu G, Pickup M, Field DL, Barrett SCH. Variation in sexual dimorphism in a wind-pollinated plant: the influence of geographical context and life-cycle dynamics. *New Phytol.* 2019 Nov;224(3):1108-1120. doi: 10.1111/nph.16050. Epub 2019 Aug 12. PMID: 31291691; PMCID: PMC6851585.

Contributions to the manuscript: MP, DF and SCHB conceived the study and designed the research experiment; MP and DLF undertook the experiment and data collection; GP, MP and DLF performed the data analyses; all authors contributed to writing of the manuscript.

Chapter 2

Publication

Puixeu G, Macon A, Vicoso B. Sex-specific estimation of cis and trans regulation of gene expression in heads and gonads of *Drosophila melanogaster*. *G3 (Bethesda)*. 2023 Jun 1;jkad121. doi: 10.1093/g3journal/jkad121. Epub ahead of print. PMID: 37259621.

Contributions to the manuscript: GP and BV conceived the study and designed the research experiment; GP and AM obtained the experimental dataset; GP performed the data analysis and GP and BV wrote the manuscript.

Chapter 3

Publication in preparation

Puixeu G, Syrowatka C, Macon A, L Scolari, N Barton, B Vicoso. Characterizing the regulatory architecture of sex differences in expression via sex-bias eQTL analysis in heads and gonads of *Drosophila melanogaster*

Contributions to the current version of the manuscript: GP, NB and BV conceived the study; GP, AM and BV designed the research experiment; GP, AM, LS obtained the experimental dataset; GP and CS performed the data analyses; GP wrote the manuscript.

Chapter 4

Publication in preparation

Puixeu G, Hayward LK. When and why should we expect a negative correlation between intersex correlation and sexual dimorphism?

Contributions to the current version of the manuscript: GP and LKH conceived the study, performed the analyses and wrote the manuscript.

Publications not included in the thesis

Fraïsse C, Puixeu Sala G, Vicoso B. Pleiotropy Modulates the Efficacy of Selection in *Drosophila melanogaster*. *Mol Biol Evol.* 2019 Mar 1;36(3):500-515. doi: 10.1093/molbev/msy246. PMID: 30590559; PMCID: PMC6389323.

Puixeu G. The causes and consequences of sex differences. *STEB Series.* 2020 Jun

Table of Contents

Abstract	iv
Acknowledgements	v
About the author	vi
List of Collaborators and Publications	vii
Table of Contents	ix
List of Figures and Tables	xiii
General introduction	1
Chapter 1. Variation in sexual dimorphism in a wind-pollinated plant: the influence of geographical context and life-cycle dynamics?	20
Introduction	21
Materials and Methods	24
Study species and population sampling	24
Experimental design and traits measured	24
Statistical analysis	25
Percent sexual dimorphism	26
Variation in sexual dimorphism among populations along de- mographic, geographical and bioclimatic gradients	26
Intersex and inter-trait correlations	27
Results	29
Sexual dimorphism in vegetative traits	29
Sexual dimorphism in reproductive traits	29
Variation in sexual dimorphism among chromosome races and popu- lations	30
Intersex and inter-trait correlations	33
Discussion	35
Temporal variation and reproductive roles of the sexes	37
Geographical variation in sexual dimorphism	38
Phenotypic correlations and the evolution of sexual dimorphism	40
Acknowledgements	41
Author Contributions	41

References	41
Chapter 2. Sex-specific estimation of <i>cis</i> and <i>trans</i> regulation of gene expression in heads and gonads of <i>Drosophila melanogaster</i>	49
Introduction	50
Materials and Methods	52
Sample preparation and sequencing	52
Data processing and (allele-specific) expression estimation	53
Estimation of <i>cis</i> -regulatory (CR), parent-of-origin (PO) and maternal genotype (MG) effects	54
Sex- and tissue-dependent CR effects	55
Extent of CR effects across sex bias levels	55
Overlap of CR effects between samples	56
<i>Cis</i> - and <i>trans</i> -regulatory divergence assignment	56
Inheritance patterns classification	57
Results	57
More <i>cis</i> -variation in the testes than in ovaries and heads	58
Extensive sex-specific CR effects in the gonads	60
Sex-specific CR effects across sex bias categories	62
Additive genes have more CR effects	63
Discussion	64
Absence of PO and MG effects, and inconsistent <i>trans</i> -regulatory effects between crosses and tissues	64
Testis-specific regulatory architecture of gene expression	65
Selective pressures acting on sex-biased expression	66
Data Availability	68
Acknowledgements	68
Author Contributions	68
References	68
Chapter 3. Characterizing the regulatory architecture of sex differences in expression via sex bias eQTL analysis in heads and gonads of <i>Drosophila melanogaster</i>	76
Introduction	77
Materials and Methods	82
Sample preparation and sequencing	82
Data processing and gene expression estimation	83

eQTL analyses	84
Results	84
More sex bias in gonads than in heads	85
The regulatory variation underlying sex-specific and sex bias in heads and gonad gene expression in <i>D. melanogaster</i>	85
The modus operandi of sex bias eQTLs	88
Enrichment of <i>cis</i> -acting associations among those shared between sexes	89
Genes with shared genetic architecture between sexes have higher intersex correlation in expression	91
Discussion and work in progress	92
Acknowledgements	100
Author Contributions	100
References	101

Chapter 4. When and why should we expect a negative correlation between intersex correlation and sexual dimorphism? 113

1 Introduction	114
2 Methods	117
2.1 The model	117
2.2 Parameter ranges and choice of units	119
2.3 Simulations	120
2.4 Empirical calculation of sex-specific variances, intersex covariance and intersex correlation	122
3 Results	123
3.1 The relationship between r_{fm} and sexual dimorphism at equilibrium 125	
3.1.1 At equilibrium, expected sexual dimorphism and intersex corre- lation are independent of each other	125
3.1.1.1 Parametrization of sex-specific allele effects	125
3.1.1.2 The intersex correlation at equilibrium	126
3.1.2 At equilibrium, drift can generate a negative correlation between r_{fm} and sexual dimorphism	128
3.2 A negative relationship between r_{fm} and sexual dimorphism out of equilibrium – exploring common hypotheses	130
3.2.1 Exploring H1 (low r_{fm} precedes): lower intersex correlation leads to more sexual dimorphism – after a given period of time	131

3.2.1.1	Adaptation in the infinitesimal limit: r_{fm} determines the relative rate of sexually-concordant vs sexually-dimorphic evolution	132
3.2.1.2	Adaptation with a multigenic genetic architecture: transient changes in the 2 nd and 3 rd order moments of the phenotype distribution alter the dynamics of phenotypic adaptation	136
3.2.1.3	Higher intersex correlation delays equilibration for sex differences	137
3.2.1.4	H1 holds – given an additional assumption	139
3.2.2	Exploring H2 (low r_{fm} follows): sex-specific directional selection acts to <i>transiently</i> reduce intersex correlation	140
4	Discussion	141
	Acknowledgements	151
	Author Contributions	151
	References	151
Joint discussion across thesis chapters		160
	Sexual dimorphism, as well as its regulatory variation, varies in time, space and across genetic backgrounds	160
	Two complementary approaches to the study of the regulatory basis of sex- and tissue-specific gene expression	162
	How data can inform the theory: on the distribution of mutations underlying sexual dimorphism	165
	How theory can inform the data: on the relationship between intersex correlation and sexual dimorphism	166
	References	167
Supplementary Material		171
	Chapter 1. Supplementary Material	171
	Chapter 2. Supplementary Material	186
	Chapter 3. Supplementary Material	199
	Chapter 4. Supplementary Material	204

List of Figures and Tables

Chapter 1. Variation in sexual dimorphism in a wind-pollinated plant: the influence of geographical context and life-cycle dynamics?	20
Figure 1. Sexual dimorphism in vegetative traits at four and eight weeks in <i>Rumex hastatulus</i>	28
Figure 2. Sexual dimorphism in reproductive traits at four and eight weeks in <i>Rumex hastatulus</i>	30
Figure 3. Percentage of sexual dimorphism (%SD) per trait and at different life-cycle stages in <i>Rumex hastatulus</i>	31
Figure 4. The relation between percent sexual dimorphism (%SD) and mean plant density (plants m ⁻²) for 29 populations of <i>Rumex hastatulus</i>	32
Figure 5. Patterns of sexual dimorphism along climatic gradients for populations of <i>Rumex hastatulus</i>	34
Figure 6. Intersex and inter-trait raw and partial correlations for <i>Rumex hastatulus</i>	36
Chapter 2. Sex-specific estimation of <i>cis</i> and <i>trans</i> regulation of gene expression in heads and gonads of <i>Drosophila melanogaster</i>	49
Figure 1. Sex-, tissue- and cross-specific proportion of <i>cis</i> -regulatory (CR) effects	60
Figure 2. Patterns of <i>cis</i> and <i>trans</i> regulatory variation	61
Figure 3. Deviance in allelic gene expression explained by <i>cis</i> -regulatory effects (CR) in each sex bias category for each tissue and cross in females and males	62
Figure 4. Proportion of additive and non-additive genes with CR divergence	64
Chapter 3. Characterizing the regulatory architecture of sex differences in expression via sex bias eQTL analysis in heads and gonads of <i>Drosophila melanogaster</i>	76
Figure 1. On the expression dataset	86
Figure 2. Sharing of eQTL-gene associations between analyses	90
Figure 3. The regulatory basis of the various categories of associations	91
Figure 4. Intersex correlation (r_{fm}) and sex bias	93
Table 1. Summary of eQTL results for each analysis	87
Chapter 4. When and why should we expect a negative correlation	

between intersex correlation and sexual dimorphism?	113
Figure 1. Relationship between expected intersex correlation (r_{fm}) and sexual dimorphism at equilibrium	129
Figure 2. Phenotypic evolution with an approximately infinitesimal genetic architecture	135
Figure 3. Transient decrease in r_{fm} during sexually-dimorphic (divergent and convergent) evolution	142
Table 1. Summary of notation	150

General introduction

On the biological basis of sex and gender

Gemma Puixeu

“Men are from Mars, women are from Venus”. This statement, popularized by the relationship counselor John Gray (2012) to illustrate that most of the relationship problems between men and women derive from fundamental psychological differences between them, comes in all shapes and flavours in our everyday life. Indeed, it is remarkable what a big role sex and gender play in our societies – but why? A very large body of research in the last couple of hundred years has provided multiple lines of biological evidence for the gendered societies we live in. I, as a young gender-aware geneticist, curious as much as skeptical, set out to examine for myself what biology has to contribute to the picture. What does it fundamentally mean to be a female, or a male? What are the selective forces that shape sex and gender, and the molecular mechanisms allowing populations to adapt to them? How predictable are these evolutionary patterns, and how stable are they across species?

Although many fields of biology provide valuable contribution to the characterization of sex and gender, my ‘whys’ and ‘hows’-related questions suggested evolutionary biology as the most appropriate discipline to inform my journey; a journey that began at the very fundamental difference between sexes, which is thought to rely on anisogamy, i.e. gamete size differences, predicted to have evolved to resolve a size-amount trade-off in gamete production (Parker et al., 1972; Bulmer & Parker, 2002). Thus, anyone can sex individuals of any species given they have access to their gametes: females produce larger, fewer gametes, while males’ gametes are smaller and more numerous; and then there are various types of cosexuals, which produce both types of gametes. The evolution of higher levels of phenotypic dimorphism is thought to derive from the fact that each individual female gamete is more expensive, so females will maximize their fitness by taking care of their ‘costly’ offspring, while males will do so by mating more often (Darwin, 1871; Bateman, 1948). So, this post-ejaculatory struggle for higher reproductive success based on gamete size

is partially translated into pre-ejaculatory mating strategies as well as parental investment after fertilization, along the so-called sexual cascade (Lehtonen & Parker, 2014; Parker, 2014).

This outlines the standard paradigm of the main evolutionary drivers of sex differences, underlying our common understanding of sex and gender in the present days – and mapping back to Charles Darwin (1871), the first to state that stronger sexual selection in males, ultimately driven by anisogamy, implies that males would be the active agents in the evolution of many traits, while females would passively adopt them by ‘transference’. This would provide biological support for the biological superiority of males, as well as for why females and males, and so women and men, were naturally driven to fulfill differential roles in the Victorian society he was embedded in. Since then, many authors across different fields in biology have studied the biological dimension of sex and gender differences – providing, however, a somewhat inconsistent picture.

On the one hand, many studies have gathered evidence for a fundamental difference between sexes. Evolutionary biology focussed on discussing evolutionary drivers for female-biased parental care and male-biased sexual dimorphism, most notably derived from Bateman (1948)’s gradients, ideas that were mirrored by evidence gathered in other fields of biology. For example, testosterone has been discussed since the discovery of sexual hormones in the 1980s (Brown-Séquard, 1889; Berthold, 1944) until our days (Herbert, 2015), as a key driver of male masculinization and sexual dimorphism, leading to marked sexual dimorphism in the most complex phenotypic traits such as brain structure (e.g. Gur et al., 1982, 1999), which in turn should underlie fundamental differences in preferences, attitudes and behaviors, making up the most intricate aspects of gender expression (Connellan et al., 2000). On the other hand, however, these multiple sources of evidence for fundamental differences between sexes and genders were overlooked in fields like biomedicine, where a ‘uni-sex’ catalogue of drugs, developed by using almost exclusively male samples until very recently (Liu & Mager, 2016), was distributed to individuals across sexes. This somewhat inconsistent take on the biological basis of sex and gender, systematically supporting gender binarism and inequality, seems not independent of political agendas and general social values (Fausto-Sterling, 2000; Fine, 2017; Saini, 2018; Criado Perez, 2020).

Indeed, a whole body of research has more recently contested this general paradigm of the biological basis of sex and gender, illustrating that, when surveying a wider

range of species with (crucially) different questions and expectations in mind, the general picture becomes more complex and nuanced (Fine, 2017; Saini, 2018). They provide evidence for sex differences in phenotypic traits (e.g. Klein & Flanagan, 2016; Karp et al., 2017), including brain structure (Joel et al., 2015) and preferences (Hyde, 2005; Hines, 2020), likely underlain by metabolic (Mogil, 2020), hormonal (Marrocco & McEwen, 2016; Yao et al., 2019) and generally molecular (Rawlik et al., 2016; Bernabeu et al., 2021; Arnold, 2022) sex differences. Differences which, crucially, are quantitative rather than qualitative, derived from highly-overlapping distributions between sexes (Ah-King & Ahnesjö, 2013), and which are moreover context-dependent (Kleisner et al., 2021), generated by a seemingly more symmetrical picture of sexual selection, where both sexes experience within-sex competition, exert mate choice (Berglund et al., 2006; Brown et al., 2009; Tang-Martínez, 2010; Edward & Chapman, 2011; Schlupp, 2018; Parish, 2022) and share parental care in a wide range of species (A. S. Griffin et al., 2013; Saltzman et al., 2017).

This illustrates two points: first, how important it is to examine patterns of sexual dimorphism, here understood as a quantitative measure of sex differences (and not implying bimodal distributions or necessarily qualitative differences between sexes), across species and phenotypic levels, in order to get a more complete picture of sex differences, as well as the selective forces and molecular mechanisms that underlie them. Second, more generally, that the scientific community, as does society as a whole, builds on inherited knowledge and ideas established through historical processes, sometimes manifested in verbal arguments and general beliefs that are taken for granted rather than explicitly challenged.

With this preamble in mind, of which I have become more aware throughout these last few years, my PhD has focussed on characterizing various aspects of sexual dimorphism evolution, both empirically and theoretically. Concretely, I explored a wide range of questions using very diverse methodology and data across species and phenotypic levels in order to get a first-hand, deeper understanding of the biological dimension of sex, as well as the evolutionary forces and molecular mechanisms shaping it.

The first project involved analyzing the spatial and temporal patterns of sexual dimorphism of *Rumex hastatulus*, a dioecious wind-pollinated plant. I found the invitation to study sex differences in plants very appealing, since most of our notion of sex and gender is based on their expression in animals. However, the more

recent evolution of dioecy and sex chromosomes in angiosperms than most animals (Charlesworth, 2002; Ming et al., 2011), as well as a greater diversity of mating systems in closely-related species (from dioecy, to various types of cosexuality, and andro- and gyno-dioecy, Barrett, 2010), and only indirect interaction between female and male components via various types of biotic and abiotic factors (Lloyd & Webb, 1977; Moore & Pannell, 2011), offers a great opportunity to study sex-specific selective forces underlying sex differences in plants, and find generalizable processes across plant and animal kingdoms.

Concretely, we analyzed patterns of genetically-based sex-specific phenotypic variation, as well as sexual dimorphism, along 3 life-cycle stages and across 30 populations spanning the whole geographic range and representing two sex-chromosome races of *R. hastatulus*. We found that patterns of sexual dimorphism did not differ between the chromosome races; however, they vary along lifespan and geographical space consistent with sex-specific natural and sexual selection shaping overall sex differences in reproductive roles. For example, we found that males are taller at peak flowering, and have overall fewer but larger inflorescences than females, likely to optimize pollen dispersal (Niklas, 1985). This is likely driven by pollen-pollen competition, one of the main drivers of plant sexual selection, particularly strong in wind-pollinated plants, since flowers are commonly uniovulate (Friedman & Barrett, 2009). On the other hand, females spread their flowers across a higher number of smaller inflorescences, likely to facilitate pollen capture, and grow to be taller than males at maturity (leading to a temporal reversal in sexual dimorphism for height), likely to facilitate seed dispersal (Thomson et al., 2011; Bullock et al., 2017). We also find that females invest more in vegetative tissue, consistent with their higher carbon requirements for seed production, as opposed to the relatively higher nitrogen requirement for pollen production in males (Delph, 1999; Harris & Pannell, 2008). Further evidence for natural selection shaping local patterns of sexual dimorphism was provided by the fact that a large proportion (up to 43%) of inter-population variation in sexual dimorphism for some traits can be attributed to differential response to climatic clines between the two sexes.

We also examined the patterns of intertrait and intersex correlations, and how they might affect phenotypic evolution. Contrary to the expectation and general observation in other studies (Lande, 1980; Ashman, 2003; Poissant et al., 2010) of a negative correlation between both, we found that intersex correlation did not significantly covary with sexual dimorphism across traits. However, we found substantial differences in inter-trait correlations between sexes. Concretely, we found

that males had more significant among-trait correlations and trade-offs than females, consistent with previous results (Steven et al., 2007; Delph et al., 2010), as well as general evidence for correlated evolution between traits potentially contributing to the observed patterns of sex-specific variation.

This study was, to our knowledge, the first account of clinal variation in sexual dimorphism in plants, and provided an in-depth picture of phenotypic sexual dimorphism, illustrating how it evolves as a consequence of multivariate sex-specific selection, corresponding to intricate compromises between natural and sexual selection acting on both sexes, which moreover change through time and space. This motivated what would be the main focus of the rest of the PhD, a question that has long fascinated evolutionary biologists: how does a single genome manage to decouple the genotype-to-phenotype map between the sexes, responding to such a complex array of time-, space- and generally context-dependent sex-specific selective pressures?

The molecular mechanisms that resolve sexual conflict into sexual dimorphism typically involve sex-linkage and sex-biased expression (R. M. Griffin et al., 2013; Mank, 2017). The first implies genetic linkage of sexually-antagonistic alleles with sex-determining regions (Dean & Mank, 2014; Wright et al., 2017), and so is limited to loci with differential representation in both sexes, most typically the sex chromosomes, but also mitochondrial or chloroplast DNA, which represent a small proportion of the genome. The second, however, refers to differential expression of the shared genes, which include most of the genome, and so it is thought to be the main mechanism underlying phenotypic sexual dimorphism (Stewart et al., 2010; Mank, 2017).

For the next two projects, which constituted the main body of this PhD, I worked on the characterization of the molecular basis of sexual dimorphism, with particular focus on understanding the genetic variation underlying sex differences in expression.

For this, we chose *Drosophila melanogaster*, a well-studied model organism that witnessed the ever-first genetic mapping of a phenotype by Thomas Hunt Morgan in 1910 (Green, 2010), which happened to be the sex-linked white mutation on the X chromosome. Now, over a century later, we have extensively examined molecular and phenotypic variation, including gene expression, in various species of *Drosophila* (R. M. Griffin et al., 2013; Huang et al., 2014; Meiklejohn et al., 2014; Hales et al., 2015), and even linked the two (e.g. Mackay & Huang, 2018) – something only

imaginable in Morgan’s times.

For the next project, second in the overall count, we characterized various aspects of the regulatory variation underlying sex- and tissue-specific gene expression using a newly-obtained dataset including replicate sex-specific gene expression of heads and gonads of within- and reciprocal between-line crosses between inbred lines of the *Drosophila* Genetic Reference Panel (DGRP, Mackay et al., 2012; Huang et al., 2014). This dataset provides a nice add-on to current studies analyzing similar patterns, which often rely on whole-body data in single crosses (Wittkopp et al., 2004; McManus et al., 2010; Coolon et al., 2013), even though patterns of gene expression (regulation) are very tissue-specific (e.g. Urbut et al., 2019; Oliva et al., 2020) and often variable across genetic backgrounds.

First, we found no evidence of maternal genotype or parent-of-origin effects on gene expression in our data, as was previously reported for *Drosophila* (Wittkopp et al., 2006; Coolon et al., 2012; Chen et al., 2015; Takada et al., 2017). Second, our results suggest that while ovaries and heads of both sexes have similar *cis*-regulatory architectures, testes display more and substantially different *cis*-regulatory effects. This suggests that the sex differences in regulatory architecture that had been previously observed in whole-body data may largely derive from testes-specific effects. Third, we examine the patterns of *cis*-regulatory variation across genes with different levels of sex bias in gonads and heads. We find more *cis* variation in unbiased and moderately-biased genes in heads, consistent with the hypothesis that genes with low sex bias should be subject to strongest sexual conflict (Cheng & Kirkpatrick, 2016), potentially presenting more variation maintained by balancing selection (e.g. Kidwell et al., 1977; Morrow & Connallon, 2013). While no clear pattern in *cis*-regulatory variation across sex bias categories was found in testes, we observe reduced *cis* variation for male-biased genes in ovaries, suggesting that the *cis* variants acting on these genes in males do not lead to changes in ovary expression. Last, we examine the dominance patterns of gene expression, and find an enrichment of *cis*-regulatory effects in additive genes compared with non-additive genes consistently across samples, as expected (Lemos et al., 2008; McManus et al., 2010; Zhang et al., 2011; Gruber et al., 2012; Meiklejohn et al., 2014), a pattern that is most marked in testes. However, sex- and tissue-specific general patterns of inheritance as well as *trans*-regulatory variation are highly variable across biological crosses, although these were performed in very controlled experimental conditions. This finding suggests that these aspects are highly dependent on genetic effects and

highlights the importance of using various genetic backgrounds to infer generalizable patterns.

The results from this project provide substantial evidence of differential sex-specific regulatory architecture of gene expression between tissues, but do not allow us to get a mechanistic understanding of this variation, nor how it operates to generate variation for sex differences, which is expected to substantially differ between tissues with different levels of sexual dimorphism (Stewart et al., 2010).

To explore these questions, we needed higher resolution. Concretely, we used a complementary approach that allowed us to identify individual mutations underlying the differential regulatory architecture for gene expression between sexes we had generally observed, with a particular focus on the identification of the genetic variation underlying sex differences in expression. This consisted in detecting eQTLs associated with sex bias in gene expression, calculated as $\log_2(\text{exp}_f/\text{exp}_m)$, as a direct measure of sex differences in expression. To achieve more power, we ideally want an estimate of sex bias per genetic background, requiring sex-specific gene expression per genotype, which is not available for wild, outbred populations.

To this end, we generated another dataset, this time consisting of replicated sex-specific gene expression for heads and gonads of 95 crosses between 190 *Drosophila melanogaster* inbred lines from the DGRP, where F1 individuals are outbred, but genetically identical within each line, allowing us to obtain a measure of sex bias in gene expression per genotype. We used this dataset to characterize the molecular basis underlying sex differences in expression, with a particular focus on understanding how this compares between tissues with high and low levels of sexual dimorphism.

The molecular patterns we find strongly reflect the differences in phenotypic dimorphism between the two tissues, with gonads having more sex bias in expression as well as more sex-specific regulatory architecture than heads. We find that a third (two thirds) of mutations associated with sex bias in heads (gonads) act by affecting expression in a sex-specific manner, with a greater proportion being male-specific; also, we detect sex-biased and sexually-antagonistic associations, which generate variation for sex bias by affecting sex-specific expression in different magnitudes and directions, respectively. However, these are very rare, as previous studies have reported (Meiklejohn et al., 2014; Oliva et al., 2020). Also consistent with previous results, we detect an enrichment of *cis*-regulatory effects and a higher intersex correlation among associations that are shared between sexes.

At this point we have a good picture of the three relevant layers of sexual dimorphism: first, how phenotypic dimorphism varies across time and space, but also across traits and tissues; second, how differential gene expression is likely to underlie most patterns of complex sexual dimorphism; third, how individual mutations operate to generate sex differences in gene expression. However, they say one only understands a process if one can predict it. And this is what we do in this last project: define models of sex-specific stabilizing selection, mutation and drift in order to explore various aspects of the dynamics of sexual dimorphism evolution, and how they vary across selection regimes and genetic architectures.

Concretely, we focus on the relationship between intersex correlation and sexual dimorphism. Intersex correlation, defined as the phenotypic correlation of individual genotypes when expressed in either sex, is thought to quantitatively constrain the evolution of sexual dimorphism: with a high intersex correlation, the genotype-to-phenotype relationship is more similar and thus difficult to decouple between sexes, potentially leading to a negative covariance between the two. This pattern has been generally (Preziosi & Roff, 1998; Delph et al., 2004, 2010; Bonduriansky & Rowe, 2005; McDaniel, 2005; Poissant et al., 2010 – but not universally: Cowley & Atchley, 1988; Ashman, 2003; Chenoweth & Blows, 2003; Leinonen et al., 2011, Chapter 1 of this thesis) observed across traits and species, and is usually interpreted to derive from the fact that either a low intersex correlation allows for more sexual dimorphism evolution, or that intersex correlation is reduced under sex-specific selection leading to dimorphic evolution (Bonduriansky & Rowe, 2005; R. M. Griffin et al., 2013; Stewart & Rice, 2018; McGlothlin et al., 2019). These seemingly logical hypotheses seem to trace back to Lande (1980, 1987) and Fisher (1958), who did not illustrate them with mathematical models, and rather seem to rely on their intuition on how such correlations should evolve; an intuition that has been reproduced multiple times in the field of sex-specific selection even though no study to date has provided mechanistic understanding for it.

This is what we do here: we jointly examine intersex correlation and sexual dimorphism both at steady state under stabilizing selection and as the population adapts under directional selection, in order to test the conditions in which this general pattern is expected to arise, with a special focus on testing these two commonly-stated hypothesis. On the one hand, we reproduce the classical result that expected r_{fm} and sexual dimorphism at equilibrium are independent (Lande, 1980), and demonstrate that a negative association between both at steady state can be generated by genetic drift. Also, we show that the two common hypotheses

imply the expected negative association only weakly, and only when three additional assumptions are met. Specifically, that 1) some traits are sex-specifically adapting under directional selection, 2) that this sex-specific adaptation is more commonly divergent than convergent and 3) that some subset of traits has a non-infinitesimal genetic architecture. This study is, to our knowledge, the first mechanistic exploration of various scenarios with potential to generate a negative correlation between intersex correlation and sexual dimorphism, and the assumptions that they require. We show that this negative association only arises under a very specific set of conditions, and that the common intuition is not generalizable across selection regimes and genetic architectures. Generally, this illustrates how historical heritage can influence how we think of problems, and the importance of taking a step back to challenge it.

Besides the specific technical points each project has illustrated, through this PhD I have learned a few lessons about (the study of) the biological dimension of sex.

First, that sexes differ. Sexual dimorphism is prevalent across species, populations, traits and tissues, something that is very important to acknowledge in fields like biomedicine but also conservation.

Second, that such differences are quantitative rather than qualitative, and vary along time and space as a consequence of sex-specific selective forces, reflecting intricate compromises between sexual and natural selection. In other words, that there is much beyond the canonical picture where males actively compete to be the favourite of a passively choosing female.

Third, that a comprehensive understanding of sex differences relies on integrating information on the historical process of selective forces driving sex-specific adaptation, as well as the molecular mechanisms that operate to facilitate or constrain sex-specific adaptation.

Fourth, that all this has to be done with a critical eye, aware of the biases of the scientific method, and ready to question current assumptions and expand knowledge beyond common intuition. A gender-aware perspective is crucial to interpret biology-informed data (e.g. [Zuk, 1993](#); [Hrdy, 1999](#); [Fausto-Sterling, 2000](#); [Fine, 2017](#); [Saini, 2018](#); [Shansky & Murphy, 2021](#)) and facilitate a more egalitarian implementation of societal gender expression, that transcends but also recognizes its biological drivers.

References

- Ah-King, M., & Ahnesjö, I. (2013, December). The “Sex Role” Concept: An Overview and Evaluation. *Evolutionary Biology*, 40(4), 461–470. Retrieved 2023-06-07, from <https://doi.org/10.1007/s11692-013-9226-7> doi: 10.1007/s11692-013-9226-7
- Arnold, A. P. (2022, September). X chromosome agents of sexual differentiation. *Nature Reviews Endocrinology*, 18(9), 574–583. Retrieved 2023-06-07, from <https://www.nature.com/articles/s41574-022-00697-0> (Number: 9 Publisher: Nature Publishing Group) doi: 10.1038/s41574-022-00697-0
- Ashman, T.-L. (2003, September). Constraints on the evolution of males and sexual dimorphism: field estimates of genetic architecture of reproductive traits in three populations of gynodioecious *Fragaria virginiana*. *Evolution; International Journal of Organic Evolution*, 57(9), 2012–2025. doi: 10.1111/j.0014-3820.2003.tb00381.x
- Barrett, S. C. H. (2010, January). Understanding plant reproductive diversity. *Philosophical Transactions of the Royal Society B: Biological Sciences*, 365(1537), 99–109. Retrieved 2023-05-24, from <https://www.ncbi.nlm.nih.gov/pmc/articles/PMC2842705/> doi: 10.1098/rstb.2009.0199
- Bateman, A. J. (1948, December). Intra-sexual selection in *Drosophila*. *Heredity*, 2(3), 349–368. Retrieved 2023-06-07, from <https://www.nature.com/articles/hdy194821> (Number: 3 Publisher: Nature Publishing Group) doi: 10.1038/hdy.1948.21
- Berglund, A., Rosenqvist, G., & Robinson-Wolrath, S. (2006). Food or Sex: Males and Females in a Sex Role Reversed Pipefish Have Different Interests. *Behavioral Ecology and Sociobiology*, 60(2), 281–287. Retrieved 2023-06-14, from <https://www.jstor.org/stable/25063813> (Publisher: Springer)
- Bernabeu, E., Canela-Xandri, O., Rawlik, K., Talenti, A., Prendergast, J., & Tenesa, A. (2021, September). Sex differences in genetic architecture in the UK Biobank. *Nature Genetics*, 53(9), 1283–1289. doi: 10.1038/s41588-021-00912-0
- Berthold, A. A. (1944). The Transplantation of Testes (D. P. Quiring, Trans.). *Bulletin of the History of Medicine*, 16(4), 399–401. Retrieved 2023-05-24, from <https://www.jstor.org/stable/44442835> (Publisher: The Johns Hopkins University Press)
- Bonduriansky, R., & Rowe, L. (2005, September). Intralocus sexual conflict and the genetic architecture of sexually dimorphic traits in *Prochyliza xanthostoma*

- (Diptera: Piophilidae). *Evolution; International Journal of Organic Evolution*, 59(9), 1965–1975.
- Brown, G. R., Laland, K. N., & Mulder, M. B. (2009, June). Bateman’s principles and human sex roles. *Trends in Ecology & Evolution*, 24(6-14), 297–304. Retrieved 2023-06-14, from <https://www.ncbi.nlm.nih.gov/pmc/articles/PMC3096780/> doi: 10.1016/j.tree.2009.02.005
- Brown-Séguard, E. (1889). The effects produced on man by subcutaneous injections of a liquid obtained from the testicles of animals. *Lancet*, 20, 105–107.
- Bullock, J. M., González, L. M., Tamme, R., Götzenberger, L., White, S. M., Pärtel, M., & Hooftman, D. A. P. (2017). A synthesis of empirical plant dispersal kernels. *Journal of Ecology*, 105(1), 6–19. Retrieved 2023-05-15, from <https://www.jstor.org/stable/26177054> (Publisher: [Wiley, British Ecological Society])
- Bulmer, M. G., & Parker, G. A. (2002, November). The evolution of anisogamy: a game-theoretic approach. *Proceedings. Biological Sciences*, 269(1507), 2381–2388. doi: 10.1098/rspb.2002.2161
- Charlesworth, D. (2002, February). Plant sex determination and sex chromosomes. *Heredity*, 88(2), 94–101. doi: 10.1038/sj.hdy.6800016
- Chen, J., Nolte, V., & Schlötterer, C. (2015, February). Temperature Stress Mediates Decanalization and Dominance of Gene Expression in *Drosophila melanogaster*. *PLOS Genetics*, 11(2), e1004883. Retrieved 2023-05-14, from <https://journals.plos.org/plosgenetics/article?id=10.1371/journal.pgen.1004883> (Publisher: Public Library of Science) doi: 10.1371/journal.pgen.1004883
- Cheng, C., & Kirkpatrick, M. (2016, September). Sex-Specific Selection and Sex-Biased Gene Expression in Humans and Flies. *PLOS Genetics*, 12(9), e1006170. Retrieved 2023-05-14, from <https://journals.plos.org/plosgenetics/article?id=10.1371/journal.pgen.1006170> (Publisher: Public Library of Science) doi: 10.1371/journal.pgen.1006170
- Chenoweth, S. F., & Blows, M. W. (2003). Signal Trait Sexual Dimorphism and Mutual Sexual Selection in *Drosophila Serrata*. *Evolution*, 57(10), 2326–2334. Retrieved 2023-04-27, from <https://onlinelibrary.wiley.com/doi/abs/10.1111/j.0014-3820.2003.tb00244.x> (_eprint: <https://onlinelibrary.wiley.com/doi/pdf/10.1111/j.0014-3820.2003.tb00244.x>) doi: 10.1111/j.0014-3820.2003.tb00244.x
- Connellan, J., Baron-Cohen, S., Wheelwright, S., Batki, A., & Ahluwalia, J. (2000).

- Sex differences in human neonatal social perception. *Infant Behavior & Development*, 23, 113–118. (Place: Netherlands Publisher: Elsevier Science) doi: 10.1016/S0163-6383(00)00032-1
- Coolon, J. D., Stevenson, K. R., McManus, C. J., Graveley, B. R., & Wittkopp, P. J. (2012, July). Genomic imprinting absent in *Drosophila melanogaster* adult females. *Cell Reports*, 2(1), 69–75. doi: 10.1016/j.celrep.2012.06.013
- Coolon, J. D., Webb, W., & Wittkopp, P. J. (2013, December). Sex-Specific Effects of Cis-Regulatory Variants in *Drosophila melanogaster*. *Genetics*, 195(4), 1419–1422. Retrieved 2023-05-14, from <https://www.ncbi.nlm.nih.gov/pmc/articles/PMC3832283/> doi: 10.1534/genetics.113.156331
- Cowley, D. E., & Atchley, W. R. (1988, June). Quantitative Genetics of *Drosophila Melanogaster*. II. Heritabilities and Genetic Correlations between Sexes for Head and Thorax Traits. *Genetics*, 119(2), 421–433. doi: 10.1093/genetics/119.2.421
- Criado Perez, C. (2020). *Invisible Women: the Sunday Times number one bestseller exposing the gender bias women face every day* (1st edition ed.). London: Vintage.
- Darwin, C. (1871). *The Descent of Man, and Selection in Relation to Sex*. D. Appleton. (Google-Books-ID: LYEQAAAAYAAJ)
- Dean, R., & Mank, J. E. (2014). The role of sex chromosomes in sexual dimorphism: discordance between molecular and phenotypic data. *Journal of Evolutionary Biology*, 27(7), 1443–1453. Retrieved 2023-05-23, from <https://onlinelibrary.wiley.com/doi/abs/10.1111/jeb.12345> (eprint: <https://onlinelibrary.wiley.com/doi/pdf/10.1111/jeb.12345>) doi: 10.1111/jeb.12345
- Delph, L. F. (1999). Sexual Dimorphism in Life History. In M. A. Geber, T. E. Dawson, & L. F. Delph (Eds.), *Gender and Sexual Dimorphism in Flowering Plants* (pp. 149–173). Berlin, Heidelberg: Springer. Retrieved 2023-05-15, from https://doi.org/10.1007/978-3-662-03908-3_6 doi: 10.1007/978-3-662-03908-3_6
- Delph, L. F., Arntz, A. M., Scotti-Saintagne, C., & Scotti, I. (2010, October). The genomic architecture of sexual dimorphism in the dioecious plant *Silene latifolia*. *Evolution; International Journal of Organic Evolution*, 64(10), 2873–2886. doi: 10.1111/j.1558-5646.2010.01048.x
- Delph, L. F., Frey, F. M., Steven, J. C., & Gehring, J. L. (2004). Investigating the independent evolution of the size of floral organs via G-matrix estimation and

- artificial selection. *Evolution & Development*, 6(6), 438–448. doi: 10.1111/j.1525-142X.2004.04052.x
- Edward, D. A., & Chapman, T. (2011, December). The evolution and significance of male mate choice. *Trends in ecology & evolution*, 26(12), 647–654. Retrieved 2023-06-07, from <https://doi.org/10.1016/j.tree.2011.07.012> doi: 10.1016/j.tree.2011.07.012
- Fausto-Sterling, A. (2000). *Sexing the Body: Gender Politics and the Construction of Sexuality* (Revised ed. edition ed.). New York, NY: Basic Books.
- Fine, C. (2017). *Testosterone Rex: Myths of Sex, Science, and Society* (First Edition ed.). New York, N.Y: W. W. Norton & Company.
- Fisher, R. (1958). *The Genetical Theory of Natural Selection* (Second edition ed.). New York: dover.
- Friedman, J., & Barrett, S. C. H. (2009, June). Wind of change: new insights on the ecology and evolution of pollination and mating in wind-pollinated plants. *Annals of Botany*, 103(9), 1515–1527. doi: 10.1093/aob/mcp035
- Gray, J. (2012). *Men Are from Mars, Women Are from Venus: The Classic Guide to Understanding the Opposite Sex*. Harper Paperbacks.
- Green, M. M. (2010, January). 2010: A Century of Drosophila Genetics Through the Prism of the white Gene. *Genetics*, 184(1), 3–7. Retrieved 2023-05-24, from <https://www.ncbi.nlm.nih.gov/pmc/articles/PMC2815926/> doi: 10.1534/genetics.109.110015
- Griffin, A. S., Alonzo, S. H., & Cornwallis, C. K. (2013, March). Why Do Cuckolded Males Provide Paternal Care? *PLoS Biology*, 11(3), e1001520. Retrieved 2023-06-07, from <https://www.ncbi.nlm.nih.gov/pmc/articles/PMC3608547/> doi: 10.1371/journal.pbio.1001520
- Griffin, R. M., Dean, R., Grace, J. L., Rydén, P., & Friberg, U. (2013, September). The shared genome is a pervasive constraint on the evolution of sex-biased gene expression. *Molecular Biology and Evolution*, 30(9), 2168–2176. doi: 10.1093/molbev/mst121
- Gruber, J. D., Vogel, K., Kalay, G., & Wittkopp, P. J. (2012, February). Contrasting properties of gene-specific regulatory, coding, and copy number mutations in *Saccharomyces cerevisiae*: frequency, effects, and dominance. *PLoS genetics*, 8(2), e1002497. doi: 10.1371/journal.pgen.1002497
- Gur, R. C., Gur, R. E., Obrist, W. D., Hungerbuhler, J. P., Younkin, D., Rosen, A. D., ... Reivich, M. (1982, August). Sex and handedness differences in cerebral blood flow during rest and cognitive activity. *Science (New York,*

- N. Y.*), 217(4560), 659–661. doi: 10.1126/science.7089587
- Gur, R. C., Turetsky, B. I., Matsui, M., Yan, M., Bilker, W., Hughett, P., & Gur, R. E. (1999, May). Sex differences in brain gray and white matter in healthy young adults: correlations with cognitive performance. *The Journal of Neuroscience: The Official Journal of the Society for Neuroscience*, 19(10), 4065–4072. doi: 10.1523/JNEUROSCI.19-10-04065.1999
- Hales, K. G., Korey, C. A., Larracunte, A. M., & Roberts, D. M. (2015, November). Genetics on the Fly: A Primer on the *Drosophila* Model System. *Genetics*, 201(3), 815–842. doi: 10.1534/genetics.115.183392
- Harris, M. S., & Pannell, J. R. (2008, November). Roots, shoots and reproduction: sexual dimorphism in size and costs of reproductive allocation in an annual herb. *Proceedings. Biological Sciences*, 275(1651), 2595–2602. doi: 10.1098/rspb.2008.0585
- Herbert, J. (2015). *Testosterone: Sex, Power, and the Will to Win* by Joe Herbert. Oxford University Press.
- Hines, M. (2020, January). Neuroscience and Sex/Gender: Looking Back and Forward. *The Journal of Neuroscience*, 40(1), 37–43. Retrieved 2023-06-07, from <https://www.ncbi.nlm.nih.gov/pmc/articles/PMC6939487/> doi: 10.1523/JNEUROSCI.0750-19.2019
- Hrdy, S. B. (1999). *The Woman That Never Evolved: With a New Preface and Bibliographical Updates, Revised Edition*. Cambridge, MA: Harvard University Press.
- Huang, W., Massouras, A., Inoue, Y., Peiffer, J., Ràmia, M., Tarone, A. M., ... Mackay, T. F. C. (2014, July). Natural variation in genome architecture among 205 *Drosophila melanogaster* Genetic Reference Panel lines. *Genome Research*, 24(7), 1193–1208. doi: 10.1101/gr.171546.113
- Hyde, J. S. (2005, September). The gender similarities hypothesis. *The American Psychologist*, 60(6), 581–592. doi: 10.1037/0003-066X.60.6.581
- Joel, D., Berman, Z., Tavor, I., Wexler, N., Gaber, O., Stein, Y., ... Assaf, Y. (2015, December). Sex beyond the genitalia: The human brain mosaic. *Proceedings of the National Academy of Sciences of the United States of America*, 112(50), 15468–15473. doi: 10.1073/pnas.1509654112
- Karp, N. A., Mason, J., Beaudet, A. L., Benjamini, Y., Bower, L., Braun, R. E., ... White, J. K. (2017, June). Prevalence of sexual dimorphism in mammalian phenotypic traits. *Nature Communications*, 8(1), 15475. Retrieved 2023-06-07, from <https://www.nature.com/articles/ncomms15475> (Number: 1

- Publisher: Nature Publishing Group) doi: 10.1038/ncomms15475
- Kidwell, J. F., Clegg, M. T., Stewart, F. M., & Prout, T. (1977, January). Regions of stable equilibria for models of differential selection in the two sexes under random mating. *Genetics*, *85*(1), 171–183. doi: 10.1093/genetics/85.1.171
- Klein, S. L., & Flanagan, K. L. (2016, October). Sex differences in immune responses. *Nature Reviews Immunology*, *16*(10), 626–638. Retrieved 2023-06-14, from <https://www.nature.com/articles/nri.2016.90> (Number: 10 Publisher: Nature Publishing Group) doi: 10.1038/nri.2016.90
- Kleisner, K., Tureček, P., Roberts, S. C., Havlíček, J., Valentova, J. V., Akoko, R. M., ... Saribay, S. A. (2021, March). How and why patterns of sexual dimorphism in human faces vary across the world. *Scientific Reports*, *11*(1), 5978. Retrieved 2023-06-14, from <https://www.nature.com/articles/s41598-021-85402-3> (Number: 1 Publisher: Nature Publishing Group) doi: 10.1038/s41598-021-85402-3
- Lande, R. (1980, March). SEXUAL DIMORPHISM, SEXUAL SELECTION, AND ADAPTATION IN POLYGENIC CHARACTERS. *Evolution; International Journal of Organic Evolution*, *34*(2), 292–305. doi: 10.1111/j.1558-5646.1980.tb04817.x
- Lande, R. (1987). Genetic correlations between the sexes in the evolution of sexual dimorphism and mating preferences. In J. W. Bardbury & M. B. Andersson (Eds.), *Sexual Selection: Testing the Alternatives : Report of the Dahlem Workshop on Sexual Selection: Testing the Alternatives, Berlin 1986, August 31-September 5*. Wiley. (Google-Books-ID: Z9lqAAAAMAAJ)
- Lehtonen, J., & Parker, G. A. (2014, December). Gamete competition, gamete limitation, and the evolution of the two sexes. *Molecular Human Reproduction*, *20*(12), 1161–1168. doi: 10.1093/molehr/gau068
- Leinonen, T., Cano, J. M., & Merilä, J. (2011, February). Genetic basis of sexual dimorphism in the threespine stickleback *Gasterosteus aculeatus*. *Heredity*, *106*(2), 218–227. doi: 10.1038/hdy.2010.104
- Lemos, B., Araripe, L. O., Fontanillas, P., & Hartl, D. L. (2008, September). Dominance and the evolutionary accumulation of cis- and trans-effects on gene expression. *Proceedings of the National Academy of Sciences of the United States of America*, *105*(38), 14471–14476. doi: 10.1073/pnas.0805160105
- Liu, K. A., & Mager, N. A. D. (2016). Women’s involvement in clinical trials: historical perspective and future implications. *Pharmacy Practice*, *14*(1), 708. Retrieved 2023-05-24, from <https://www.ncbi.nlm.nih.gov/pmc/articles/>

[PMC4800017/](#) doi: 10.18549/PharmPract.2016.01.708

- Lloyd, D. G., & Webb, C. J. (1977). Secondary Sex Characters in Plants. *Botanical Review*, 43(2), 177–216. Retrieved 2023-05-15, from <https://www.jstor.org/stable/4353917> (Publisher: New York Botanical Garden Press)
- Mackay, T. F. C., & Huang, W. (2018, January). Charting the Genotype-Phenotype Map: Lessons from the *Drosophila melanogaster* Genetic Reference Panel. *Wiley interdisciplinary reviews. Developmental biology*, 7(1), 10.1002/wdev.289. Retrieved 2023-05-26, from <https://www.ncbi.nlm.nih.gov/pmc/articles/PMC5746472/> doi: 10.1002/wdev.289
- Mackay, T. F. C., Richards, S., Stone, E. A., Barbadilla, A., Ayroles, J. F., Zhu, D., . . . Gibbs, R. A. (2012, February). The *Drosophila melanogaster* Genetic Reference Panel. *Nature*, 482(7384), 173–178. doi: 10.1038/nature10811
- Mank, J. E. (2017, January). The transcriptional architecture of phenotypic dimorphism. *Nature Ecology & Evolution*, 1(1), 6. doi: 10.1038/s41559-016-0006
- Marrocco, J., & McEwen, B. S. (2016, December). Sex in the brain: hormones and sex differences. *Dialogues in Clinical Neuroscience*, 18(4), 373–383. doi: 10.31887/DCNS.2016.18.4/jmarrocco
- McDaniel, S. F. (2005, November). Genetic correlations do not constrain the evolution of sexual dimorphism in the moss *Ceratodon purpureus*. *Evolution; International Journal of Organic Evolution*, 59(11), 2353–2361.
- McGlothlin, J. W., Cox, R. M., & Brodie, E. D. (2019, July). Sex-Specific Selection and the Evolution of Between-Sex Genetic Covariance. *The Journal of Heredity*, 110(4), 422–432. doi: 10.1093/jhered/esz031
- McManus, C. J., Coolon, J. D., Duff, M. O., Eipper-Mains, J., Graveley, B. R., & Wittkopp, P. J. (2010, June). Regulatory divergence in *Drosophila* revealed by mRNA-seq. *Genome Research*, 20(6), 816–825. doi: 10.1101/gr.102491.109
- Meiklejohn, C. D., Coolon, J. D., Hartl, D. L., & Wittkopp, P. J. (2014, January). The roles of cis- and trans-regulation in the evolution of regulatory incompatibilities and sexually dimorphic gene expression. *Genome Research*, 24(1), 84–95. doi: 10.1101/gr.156414.113
- Ming, R., Bendahmane, A., & Renner, S. S. (2011). Sex chromosomes in land plants. *Annual Review of Plant Biology*, 62, 485–514. doi: 10.1146/annurev-arplant-042110-103914
- Mogil, J. S. (2020, July). Qualitative sex differences in pain processing: emerging evidence of a biased literature. *Nature Reviews Neuroscience*, 21(7),

- 353–365. Retrieved 2023-06-07, from <https://www.nature.com/articles/s41583-020-0310-6> (Number: 7 Publisher: Nature Publishing Group) doi: 10.1038/s41583-020-0310-6
- Moore, J. C., & Pannell, J. R. (2011, March). Sexual selection in plants. *Current biology: CB*, *21*(5), R176–182. doi: 10.1016/j.cub.2010.12.035
- Morgan, T. H. (1910, July). SEX LIMITED INHERITANCE IN DROSOPHILA. *Science (New York, N.Y.)*, *32*(812), 120–122. doi: 10.1126/science.32.812.120
- Morrow, E. H., & Connallon, T. (2013, December). Implications of sex-specific selection for the genetic basis of disease. *Evolutionary Applications*, *6*(8), 1208–1217. doi: 10.1111/eva.12097
- Niklas, K. J. (1985). The Aerodynamics of Wind Pollination. *Botanical Review*, *51*(3), 328–386. Retrieved 2023-05-15, from <https://www.jstor.org/stable/4354060> (Publisher: New York Botanical Garden Press)
- Oliva, M., Muñoz-Aguirre, M., Kim-Hellmuth, S., Wucher, V., Gewirtz, A. D. H., Cotter, D. J., ... Stranger, B. E. (2020, September). The impact of sex on gene expression across human tissues. *Science (New York, N.Y.)*, *369*(6509), eaba3066. doi: 10.1126/science.aba3066
- Parish, A. R. (2022, October). Two Sides of the Same Coin: Females Compete and Cooperate. *Archives of Sexual Behavior*, *51*(7), 3283–3286. doi: 10.1007/s10508-021-02230-2
- Parker, G. A. (2014, August). The sexual cascade and the rise of pre-ejaculatory (Darwinian) sexual selection, sex roles, and sexual conflict. *Cold Spring Harbor Perspectives in Biology*, *6*(10), a017509. doi: 10.1101/cshperspect.a017509
- Parker, G. A., Baker, R. R., & Smith, V. G. F. (1972, September). The origin and evolution of gamete dimorphism and the male-female phenomenon. *Journal of Theoretical Biology*, *36*(3), 529–553. Retrieved 2023-06-07, from <https://www.sciencedirect.com/science/article/pii/0022519372900070> doi: 10.1016/0022-5193(72)90007-0
- Poissant, J., Wilson, A. J., & Coltman, D. W. (2010, January). Sex-specific genetic variance and the evolution of sexual dimorphism: a systematic review of cross-sex genetic correlations. *Evolution; International Journal of Organic Evolution*, *64*(1), 97–107. doi: 10.1111/j.1558-5646.2009.00793.x
- Preziosi, R. F., & Roff, D. A. (1998, July). Evidence of genetic isolation between sexually monomorphic and sexually dimorphic traits in the water strider *Aquarius remigis*. *Heredity*, *81*(1), 92–99. Retrieved 2023-04-27, from <https://www.nature.com/articles/6883800> (Number: 1 Publisher: Na-

- ture Publishing Group) doi: 10.1046/j.1365-2540.1998.00380.x
- Rawlik, K., Canela-Xandri, O., & Tenesa, A. (2016, July). Evidence for sex-specific genetic architectures across a spectrum of human complex traits. *Genome Biology*, 17(1), 166. Retrieved 2023-06-07, from <https://doi.org/10.1186/s13059-016-1025-x> doi: 10.1186/s13059-016-1025-x
- Saini, A. (2018). *Inferior: How Science Got Women Wrong-and the New Research That's Rewriting the Story* (Reprint edition ed.). Boston: Beacon Press.
- Saltzman, W., Harris, B. N., De Jong, T. R., Perea-Rodriguez, J. P., Horrell, N. D., Zhao, M., & Andrew, J. R. (2017, September). Paternal Care in Biparental Rodents: Intra- and Inter-individual Variation. *Integrative and Comparative Biology*, 57(3), 589–602. Retrieved 2023-06-14, from <https://doi.org/10.1093/icb/icx047> doi: 10.1093/icb/icx047
- Schlupp, I. (2018, June). Male mate choice, female competition, and female ornaments as components of sexual selection. *Current Zoology*, 64(3), 321–322. Retrieved 2023-06-14, from <https://doi.org/10.1093/cz/zoy037> doi: 10.1093/cz/zoy037
- Shansky, R. M., & Murphy, A. Z. (2021, April). Considering sex as a biological variable will require a global shift in science culture. *Nature Neuroscience*, 24(4), 457–464. Retrieved 2023-06-07, from <https://www.nature.com/articles/s41593-021-00806-8> (Number: 4 Publisher: Nature Publishing Group) doi: 10.1038/s41593-021-00806-8
- Steven, J. C., Delph, L. F., & Brodie, E. D. (2007, January). Sexual dimorphism in the quantitative-genetic architecture of floral, leaf, and allocation traits in *Silene latifolia*. *Evolution; International Journal of Organic Evolution*, 61(1), 42–57. doi: 10.1111/j.1558-5646.2007.00004.x
- Stewart, A. D., Pischedda, A., & Rice, W. R. (2010). Resolving intralocus sexual conflict: genetic mechanisms and time frame. *The Journal of Heredity*, 101 Suppl 1(Suppl 1), S94–99. doi: 10.1093/jhered/esq011
- Stewart, A. D., & Rice, W. R. (2018, September). Arrest of sex-specific adaptation during the evolution of sexual dimorphism in *Drosophila*. *Nature Ecology & Evolution*, 2(9), 1507–1513. doi: 10.1038/s41559-018-0613-4
- Takada, Y., Miyagi, R., Takahashi, A., Endo, T., & Osada, N. (2017, July). A Generalized Linear Model for Decomposing Cis-regulatory, Parent-of-Origin, and Maternal Effects on Allele-Specific Gene Expression. *G3 (Bethesda, Md.)*, 7(7), 2227–2234. doi: 10.1534/g3.117.042895
- Tang-Martínez, Z. (2010, January). Bateman's Principles: Original Experiment and

- Modern Data For and Against. In M. D. Breed & J. Moore (Eds.), *Encyclopedia of Animal Behavior* (pp. 166–176). Oxford: Academic Press. Retrieved 2023-06-07, from <https://www.sciencedirect.com/science/article/pii/B9780080453378001820> doi: 10.1016/B978-0-08-045337-8.00182-0
- Thomson, F. J., Moles, A. T., Auld, T. D., & Kingsford, R. T. (2011). Seed dispersal distance is more strongly correlated with plant height than with seed mass. *Journal of Ecology*, *99*(6), 1299–1307. Retrieved 2023-05-15, from <https://onlinelibrary.wiley.com/doi/abs/10.1111/j.1365-2745.2011.01867.x> (_eprint: <https://onlinelibrary.wiley.com/doi/pdf/10.1111/j.1365-2745.2011.01867.x>) doi: 10.1111/j.1365-2745.2011.01867.x
- Urbut, S. M., Wang, G., Carbonetto, P., & Stephens, M. (2019, January). Flexible statistical methods for estimating and testing effects in genomic studies with multiple conditions. *Nature Genetics*, *51*(1), 187–195. doi: 10.1038/s41588-018-0268-8
- Wittkopp, P. J., Haerum, B. K., & Clark, A. G. (2004, July). Evolutionary changes in cis and trans gene regulation. *Nature*, *430*(6995), 85–88. doi: 10.1038/nature02698
- Wittkopp, P. J., Haerum, B. K., & Clark, A. G. (2006, July). Parent-of-origin effects on mRNA expression in *Drosophila melanogaster* not caused by genomic imprinting. *Genetics*, *173*(3), 1817–1821. doi: 10.1534/genetics.105.054684
- Wright, A. E., Darolti, I., Bloch, N. I., Oostra, V., Sandkam, B., Buechel, S. D., ... Mank, J. E. (2017, January). Convergent recombination suppression suggests role of sexual selection in guppy sex chromosome formation. *Nature Communications*, *8*, 14251. doi: 10.1038/ncomms14251
- Yao, Q., Zhou, G., Xu, M., Dai, J., Qian, Z., Cai, Z., ... Hu, R. (2019, November). Blood metal levels and serum testosterone concentrations in male and female children and adolescents: NHANES 2011–2012. *PLoS ONE*, *14*(11), e0224892. Retrieved 2023-06-14, from <https://www.ncbi.nlm.nih.gov/pmc/articles/PMC6837506/> doi: 10.1371/journal.pone.0224892
- Zhang, X., Cal, A. J., & Borevitz, J. O. (2011, May). Genetic architecture of regulatory variation in *Arabidopsis thaliana*. *Genome Research*, *21*(5), 725–733. doi: 10.1101/gr.115337.110
- Zuk, M. (1993). Feminism and the Study of Animal Behavior. *BioScience*, *43*(11), 774–778. Retrieved 2023-06-07, from <https://www.jstor.org/stable/1312322> (Publisher: [American Institute of Biological Sciences, Oxford University Press]) doi: 10.2307/1312322

CHAPTER 1

Variation in sexual dimorphism in a wind-pollinated plant: the influence of geographical context and life-cycle dynamics¹

Gemma Puixeu², Melinda Pickup², David L. Field
and Spencer C.H. Barrett

Abstract

Understanding the mechanisms causing phenotypic differences between females and males has long fascinated evolutionary biologists. An extensive literature exists on animal sexual dimorphism but less is known about sex differences in plants, particularly the extent of geographical variation in sexual dimorphism and its life-cycle dynamics.

Here, we investigate patterns of genetically-based sexual dimorphism in vegetative and reproductive traits of a wind-pollinated dioecious plant, *Rumex hastatulus*, across three life-cycle stages using open-pollinated families from 30 populations spanning the geographic range and chromosomal variation (XY and XY₁Y₂) of the species.

The direction and degree of sexual dimorphism was highly variable among populations and life-cycle stages. Sex-specific differences in reproductive function explained a significant amount of temporal change in sexual dimorphism. For several traits, geographical variation in sexual dimorphism was associated with bioclimatic parameters, likely due to the differential responses of the sexes to climate. We found no systematic differences in sexual dimorphism between chromosome races.

Sex-specific trait differences in dioecious plants largely result from a balance between sexual and natural selection on resource allocation. Our results indicate that abiotic factors associated with geographical context also play a role in modifying sexual dimorphism during the plant life cycle.

¹This work has been published at <https://doi.org/10.1111/nph.16050>

²These authors contributed equally to this work.

Introduction

Trait differences between females and males (sexual dimorphism) reflect sex-specific optima related to their different reproductive roles (Darwin, 1871; Andersson, 1994). In dioecious plants, the strength and direction of sex-specific selection can vary within species, providing opportunities to examine the genetic and evolutionary drivers of sexual dimorphism (Lloyd & Webb, 1977; Delph, 1999; Geber et al., 1999; Barrett & Hough, 2013). Mechanisms of pollen and seed dispersal may mediate the strength of sex-specific selection because female and male components interact indirectly through biotic or abiotic vectors (Lloyd & Webb, 1977; Moore & Pannell, 2011). Male-male competition can be particularly intense in wind-pollinated species, compared to animal-pollinated systems, because flowers are commonly uniovulate (Friedman & Barrett, 2011). Consequently, conspicuous sexual dimorphism is predicted to evolve for traits related to pollination success in anemophilous species including plant height, flower number and inflorescence deployment (Eppley & Pannell, 2007; Friedman & Barrett, 2009; Tonnabel et al., 2019). Specifically, males are expected to invest in fewer, but larger and taller inflorescences, whereas females are predicted to have flowers spread throughout the air stream and distributed across more inflorescences. Yet sexual selection may also interact with the different resource requirements of the sexes to influence the level and direction of sexual dimorphism. For example, whereas males may have higher nitrogen demands for pollen production, females require a greater investment in photosynthetic tissues to produce carbon for seeds and fruits (Delph, 1999; Harris & Pannell, 2008), which may result in females having higher vegetative investment (Teitel et al., 2016). Consequently, sex-specific trait differences in anemophilous plants may reflect both wind-mediated selection for proficient pollen and seed dispersal, and optimal resource allocation between vegetative and reproductive structures.

Variation in sexual dimorphism within species may occur at both temporal and geographical scales (Lloyd & Webb, 1977; Barrett & Hough, 2013). Temporal changes in patterns of sexual dimorphism during plant life cycles can result from the timing of the different reproductive roles of the sexes (Delph, 1999; Hesse & Pannell, 2011; Sánchez Vilas & Pannell, 2011). For species with wind-mediated pollen and seed dispersal, males optimize pollen dispersal during peak flowering, whereas females maximize pollen receipt during flowering and seed dispersal at reproductive maturity. Thus, selection is likely to favour taller males at peak flowering and taller females at reproductive maturity, leading to temporal changes in sexual dimorphism for plant height (Pickup & Barrett, 2012). These dynamics highlight the value of

measuring sexual dimorphism at different life-cycle stages to capture the complexity of sex-specific roles (Harris & Pannell, 2008; Hesse & Pannell, 2011; Sánchez Vilas & Pannell, 2011; Teitel et al., 2016).

Differences in sex-specific trait optima among populations can reflect the balance between sexual and natural selection mediated by local ecological conditions (Lande, 1980). Sex-specific differences in reproductive costs and allocation trade-offs (Lloyd & Webb, 1977; Delph, 1999; Obeso, 2002) may result in differential responses of each sex to environmental gradients (e.g. rainfall, temperature, Delph, Andicoechea, et al., 2011), thereby contributing to heterogeneity in patterns of dimorphism, which in some cases may result in geographical clines. Although sex-specific plasticity in trait expression across environmental conditions has been reported in several dioecious plant species (Delph & Bell, 2008; Teitel et al., 2016), among-population variation in sexual dimorphism has not been investigated in detail (but see Delph et al., 2002). Moreover, to date, no studies have used common gardens to examine population-level variation in sexual dimorphism in relation to the environment of source populations.

For wind-pollinated species, demographic factors including population size and plant density will likely influence sexual selection by mediating the degree of male-male competition (Steven & Waller, 2007; Stehlik et al., 2008; Friedman & Barrett, 2009; Tonnabel et al., 2019). Biased sex ratios can also influence the strength of sexual selection by varying the degree of pollen competition (Compagnoni et al., 2017), with less competition expected in populations with female-biased sex ratios. Disentangling the relative importance of these processes requires investigation of patterns of sexual dimorphism in different environmental and demographic contexts and for multiple populations spanning a species' geographic range, an approach we use here.

The evolution of sexual dimorphism results from the interplay between sex-specific selection and the underlying genetic architecture of traits (Delph et al., 2002, 2010; Ashman, 2003; Weller et al., 2006). Strong intersex genetic correlations may constrain the evolution of sexual dimorphism (Lande, 1980; Meagher, 1992) and inter-trait correlations can lead to the evolution of sexual dimorphism for traits that are not directly under selection (Delph et al., 2002). Finally, sex-specific differences in correlation among clusters of traits may impose constraints or result in trait coevolution in a sex-specific manner (Meagher, 1992; Delph et al., 2002, 2005). These complexities highlight the importance of sex-specific inter-trait and intersex correlations for predicting responses to selection and the evolution of sexual

dimorphism.

The more recent evolution of dioecy and sex chromosomes in angiosperms (Charlesworth, 2002; Ming et al., 2011) than in most animals provides the potential to examine sexual dimorphism in relation to sex chromosome variation (Govindarajulu et al., 2013; Charlesworth, 2018). In dioecious *Rumex* (Polygonaceae), sex chromosome systems vary both within and between species (Navajas-Pérez et al., 2005; Cuñado et al., 2007). *Rumex hastatulus* possesses two distinct karyotype races with different sex chromosomes (Texas race XY; North Carolina XY₁Y₂; Smith, 1963; Bartkowiak, 1971). Karyotype differences may affect divergence between male and female phenotypes in two ways. First, sex-linked genes may contribute disproportionately to the patterns of phenotypic and genetic differentiation between the races (Beaudry et al., 2020). Second, sex chromosomes may influence patterns of sex-specific adaptation and intersex correlations through differences in dosage compensation and/or unequal transmission between the sexes (Rice, 1984; Dean & Mank, 2014). This species therefore provides a unique opportunity to determine whether sex chromosome variation contributes to patterns of sexual dimorphism.

Here, we examine spatial and temporal variation in genetically-based sexual dimorphism in *R. hastatulus*. We measured quantitative traits under uniform glasshouse conditions across three life-cycle stages corresponding to pre-reproduction, peak flowering and reproductive maturity in 30 populations sampled from across the geographical range of the species, including the two chromosome races. Specifically, we asked the following questions: (i) does sexual dimorphism in reproductive and vegetative traits vary among life-cycle stages in relation to the different reproductive roles of females and males? (ii) Does sexual dimorphism vary among populations across its geographic range and between chromosome races? (iii) Can demographic, geographical and bioclimatic variables explain among-population variation in sexual dimorphism? Having established the overall patterns of sexual dimorphism in *R. hastatulus* we then investigated trait correlations within and between the sexes to ask if intra- and intersex correlations vary across the life-cycle for reproductive and vegetative traits. Our findings demonstrate that patterns of sexual dimorphism vary across the life cycle associated with differences between the sexes in reproductive roles, but also geographically likely because of sex-specific responses to bioclimatic parameters.

Materials and Methods

Study species and population sampling

Rumex hastatulus (Polygonaceae) is a largely annual colonizer of open sites distributed across the southern regions of the USA from Texas to North Carolina and Florida. Both pollen and seed of *R. hastatulus* are wind dispersed. The species is cytologically complex with two main chromosome races (Smith, 1963); the North Carolina karyotype (females = XX, $2n = 8$; males = XY_1Y_2 , $2n = 9$) and the Texas karyotype (females XX, males XY, $2n = 10$). Populations of the Texas race are distributed across four states: Texas (TX), Oklahoma (OK), Arkansas (AK) and Louisiana (LA), whereas populations of the North Carolina race occur in North Carolina (NC), South Carolina (SC), Georgia (GA), Alabama (AL) and Florida (FL).

To examine geographical variation in sexual dimorphism we sampled 30 populations of *R. hastatulus*, including 15 from each chromosome race (Figure S1). The populations represent a sub-sample of 46 populations previously used to examine sex-ratio variation (see Pickup & Barrett, 2013). The 30 populations included here were chosen based on available seed from at least 20 maternal plants and to span the observed variation in population size (TX race range = $66 - \approx 2,000,000$, NC race range = $10 - \approx 556,000$) and plant density (TX race range = $0.21 - 122.4$ plants m^{-2} , NC race range = $0.04 - 34.3$ plants m^{-2}) within each chromosome race. For each population, open-pollinated seed families were collected from randomly chosen females along transects (for further details see Pickup & Barrett, 2013).

Experimental design and traits measured

In June 2010, we germinated 6 seeds from 15 randomly chosen maternal plants (90 seeds per population) from each of the 30 populations (2700 seeds in total). Seeds were soaked in water for 24 hours at 4°C and transferred to moist filter paper in petri dishes in a growth cabinet maintained at 20°C for 12 hours and 10°C for 12 hours with continuous light. After ~ 14 days we randomly chose and transplanted 60 seedlings (four from each of the 15 families) per population individually to 5 cm pots containing Pro-Mix BX (peat moss, vermiculate and perlite) and NPK fertilizer (20:20:20) and these were grown in a glasshouse at $20 - 24^\circ\text{C}$. Due to maternal variation in germination, 48 – 64 seedlings were planted per population (mean = 59.7; average of 3.4 seedlings per family, all with male and female representation,

with sex determined at flowering). The 1792 seedlings were positioned in a complete randomised block design in the glasshouse.

To examine variation in sexual dimorphism among populations and during the life cycle, we measured traits at three growth stages: pre-reproduction (2 weeks), peak flowering (4 weeks), and reproductive maturity (8 weeks) from planting date. (i) Plant height (vertical height from the pot surface to the tallest point on the plant), (ii) number of leaves and (iii) leaf size were measured at each life-cycle stage. At four and eight weeks, we measured several reproductive traits: (iv) flowering (presence of flowers in anthesis), (v) number of stems, (vi) number of flowering stems, (vii) number of inflorescences, and (viii) length of three representative inflorescences (as a surrogate for the number of flowers per inflorescence, [Pickup & Barrett, 2013](#)). We additionally calculated: (ix) flowering as a binary variable (yes/no), (x) proportion of flowering stems for those individuals flowering and (xi) an estimate of total flower number, by multiplying the number of inflorescences (vii) by average inflorescence length (viii). Sex (male, female), was determined at week 4 or 8 by flower morphology. Non-flowering individuals could not be sexed and were therefore not considered in the analyses. At reproductive maturity (8 weeks) we harvested plants and separated the above ground biomass into (xii) vegetative biomass (including rosette leaves, stem leaves and stems), and (xiii) reproductive biomass (including inflorescences, and seeds and fruit for females). Total biomass (xiv) is represented as the sum of vegetative and reproductive biomass. We obtained dried weights for each biomass component by drying samples at 55°C for three days before weighing them on a four decimal place gram balance.

Statistical analysis

To examine if sexual dimorphism in morphological and reproductive traits varied with chromosome race, population and life-cycle stage we used generalized linear mixed models (GLMMs, function “glmer” of the R package “lme4”). For overall models of sexual dimorphism, sex, chromosome race (or population) and life-cycle stage were included as fixed effects, and maternal parent (nested within population) as a random effect. In models analyzing temporal variation, life-cycle stage was additionally included as a fixed effect, and individual as a random effect to correct for non-independence of observations across time points. However, given a significant interaction between life-cycle stage and sex (particularly strong between the first time point and the other two – see Table S1), the effect of chromosome race and population were examined using models for each life-cycle stage separately. In

sex x chromosome race models, population was included as a random effect. The probability distribution and link function used for each specific model were chosen by considering the (i) nature of the response variable, (ii) relation between the mean and variance of the response variable, and (iii) quantile-to-quantile plots of the response variable versus data generated under different candidate distributions. Model choice was based on: (1) Akaike information criterion (AIC) values, (2) normal independent and identically distributed (iid) residuals, and (3) low correlation between residuals and fitted values and high correlation between predicted and observed values. These are standard criteria to decide on modeling strategy when using GLMMs (Bolker et al., 2009). We checked for overdispersion in Poisson and binomial models, and these were resolved by including “individual” as a random effect. We determined the overall effects and significance of the fixed factors using type 2 ANOVA. When there was a significant interaction between sex and chromosome race, we used chromosome race-specific models to examine overall sexual dimorphism and among population variation. For each model, we used the “predictmeans” (R package) to obtain predicted means (conditional on all other sources of variation included in the models) and 95% confidence intervals, which were used for display and posterior analyses. These, and all subsequent statistical analyses, were performed using R version 3.4.4 (R Core Team, 2022).

Percent sexual dimorphism

To evaluate patterns of sexual dimorphism we calculated percent sexual dimorphism (%SD) as $(\text{mean}_f - \text{mean}_m) / \text{mean}_m \times 100$, where mean_f and mean_m are the predicted means for females and males respectively (see Delph et al., 2002) for each trait and time point, both within and among populations and chromosome races. Positive values indicate female-biased, while negative values male-biased, sexual dimorphism. We calculated the confidence intervals as $\sqrt{(\text{min}_f^2 + \text{min}_m^2)}$, where min_f and min_m are the lower (or upper) bound of the 95% confidence interval for females and males given by the “predictmeans” function from the GLM models.

Variation in sexual dimorphism among populations along demographic, geographical and bioclimatic gradients

We used multiple linear regression to examine if demographic (population size, population density and sex ratio), geographical (altitude, latitude and longitude) and bioclimatic parameters could explain among-population variation in percent sexual

dimorphism. We measured demographic parameters in the field in May-June 2009. For populations with < 200 individuals, total population size, density (plants m^{-2}) and sex ratio as no. females/(no. females + no. males) were obtained by direct counts. For large populations (> 200 individuals), demographic parameters were estimated from stratified quadrats along four randomly positioned transects (see [Pickup & Barrett, 2013](#) for full details on sampling and the data obtained). For each population, we obtained data for 19 bioclimatic variables (see Figure S4A) from WorldClim version 1.4. ([Hijmans et al., 2005](#)), which provides high-resolution ($\sim 1\text{km}$) interpolated climate surfaces based on monthly averages from 1960-90.

To examine if these parameters explained significant variation in percent sexual dimorphism we used separate models for: (i) demographic, (ii) geographical, and (iii) bioclimatic variables. For the set of models examining bioclimatic variables, we first reduced the number of predictors to ensure their independence (determined using Spearman rank correlations, r_s , Figure S4A), and also that the predictors recapitulated the observed geographical clines by examining the two first principal components of the selected bioclimatic variables in comparison to all variables (Figure S4B). In all models and for all traits and life-cycle stages, explanatory variables were added sequentially to models of increasing complexity and ANOVA was used for model selection to identify the variable(s) that best explained differences in sexual dimorphism. For each model, we tested for homogeneity of residuals using the Shapiro-Wilk normality test. To facilitate interpretation of the contribution of bioclimatic variables to variation in sexual dimorphism, we regressed sex-specific means on these variables for traits where multiple regressions were significant (Table S3). We also visualized the relations between each parameter and sexual dimorphism to assess the direction of the correlations and whether heterogeneity in sexual dimorphism scaled with each predictor using funnel plots.

Intersex and inter-trait correlations

We estimated intersex and inter-trait correlations at weeks 4 and 8 separately as Spearman rank correlation coefficients (r_s) across predicted means including all populations. Given that our experiment was designed to maximize the number of populations sampled, there were too few individuals within families in each population to enable maternal variation to be taken into account in the calculation of population-level correlations. To account for the potential effect of confounding variables on trait correlations, partial intersex and inter-trait correlations were additionally calculated using “`pcor.test`” function from the “`ppcor`” R package with the

Spearman method, by controlling for the predicted population means of the rest of the trait values (and averaged across sexes for the intersex partial correlations). We determined whether pairwise inter-trait correlations differed significantly between the sexes via bootstrapping: we calculated sex-specific 95% confidence intervals for correlations between all pairs of traits by selecting 25 out of all populations 1000 times. If the sex-specific confidence intervals did not overlap we concluded that there was a significant difference in inter-trait correlations. Pairwise correlations between absolute values of percent sexual dimorphism and intersex correlation were computed as Spearman rank correlation coefficients. For all analyses, P-values indicate probability that $r_s=0$.

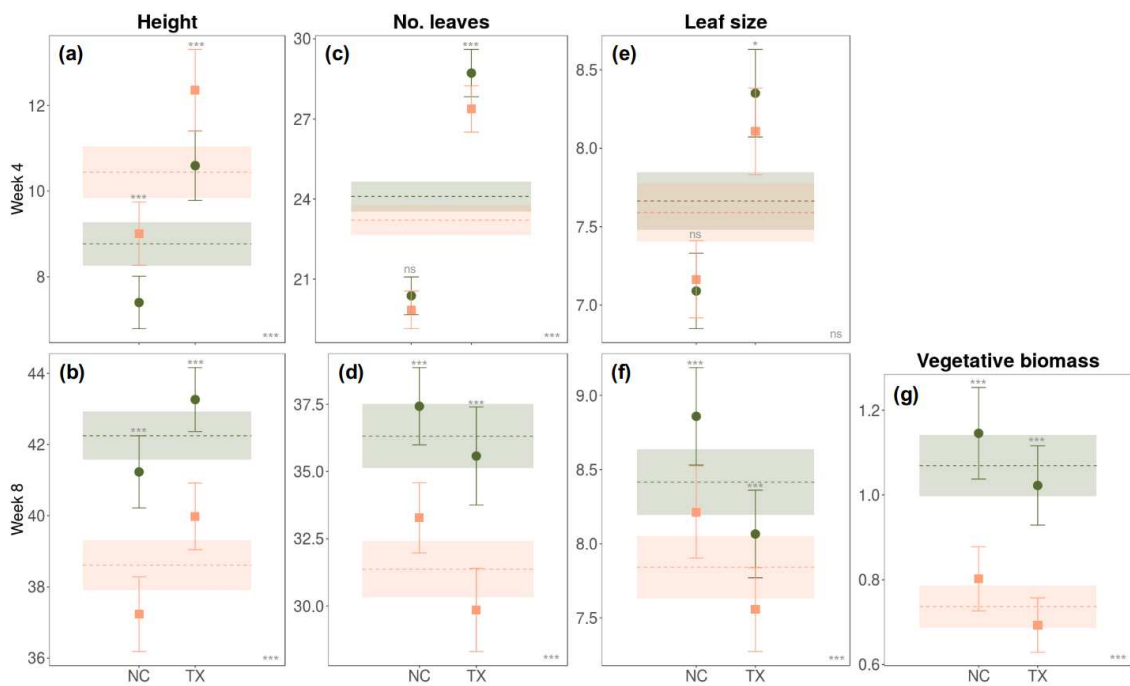


Figure 1: Sexual dimorphism of vegetative traits at four and eight weeks in *Rumex hastatulus*. Predicted means and 95% confidence intervals at two time points (4 weeks and 8 weeks) for males (orange squares) and females (green circles) of the Texas (TX) and North Carolina (NC) chromosome races (individual points) and overall values for each sex (dashed lines and color shading). Traits measured at four and eight weeks were (A, B) height (cm), (C, D) number of leaves and (E, F) leaf size (cm), while (G) vegetative biomass (grams) was measured at harvest. The significance of sex differences for each chromosome race and across both races is indicated by stars above the individual bars and in the lower right corner of each plot, respectively. *, $0.01 < P < 0.05$; ***, $P < 0.001$; ns = not statistically significant.

Results

Sexual dimorphism in vegetative traits

Sexual dimorphism in plant height changed significantly across the life cycle of *R. hastatulus*. There was no sexual dimorphism at week 2 prior to flowering (Figure S2A), but at week four (peak flowering) males were significantly taller than females (%SD = -16.1; Figure 1A, Figure 3 and Figure S2B), and at week 8 (reproductive maturity and seed dispersal) sexual dimorphism for height reversed, with females taller than males (%SD = 9.4; Figure 1B, Figure 3 and Figure S2C). The reversal in height was indicated by the significant interaction between sex and life-cycle stage when the model included both 4 and 8 weeks (Table S1). These patterns of sexual dimorphism were consistent across populations and chromosome races, as indicated by the non-significant sex x population and sex x chromosome race interactions (Table S1). At week 8, females produced more (%SD leaf number = 15.8) and larger leaves (%SD leaf size = 7.3; Figure 1D,F and Figure 3) and this was reflected in female-biased sexual dimorphism in vegetative biomass at harvest (%SD = 45.2; Figure 1G and Figure 3). However, this pattern varied significantly among populations and between chromosome races (Table S1).

Sexual dimorphism in reproductive traits

At week 4, even though males had more stems than females (Figure 2A), the proportion of plants flowering was female-biased, and this was the most sexually-dimorphic trait overall (%SD = 163.2; Figure 2C and Figure 3), suggesting that males may delay flowering and invest in stem growth. Indeed, we found a significant positive correlation ($r_s = 0.81$, $P < 0.0001$) between height and total flower number in males at this life-cycle stage. Among those individuals flowering at week 4, males produced more and larger inflorescences than females (Figure 2D,F). At reproductive maturity (week 8), both sexes had equal numbers of stems (Figure 2B), all of which were flowering. At week 8 females produced more inflorescences (Figure 2E), whereas in males inflorescences were larger (Figure 2G). This difference resulted in a temporal reversal in sexual dimorphism from male-biased at week 4 to female-biased at week 8 for inflorescence number (%SD week 4 = -18.6, %SD week 8 = 73.7) and total flower number (inflorescence number x size, %SD week 4 = -30.2, %SD week 8 = 24.6; Figure 3).

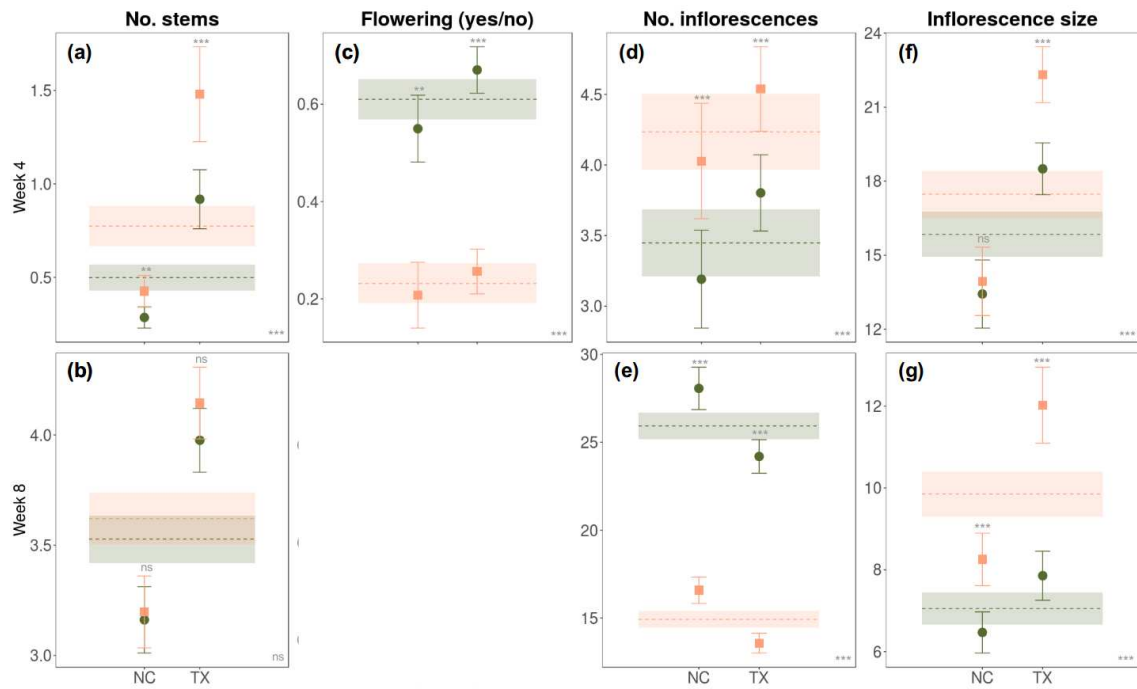


Figure 2: Sexual dimorphism of reproductive traits at four and eight weeks in *Rumex hastatulus*. Predicted means and 95% confidence intervals at two time points (4 weeks and 8 weeks) for males (orange squares) and females (green circles) of the Texas (TX) and North Carolina (NC) chromosome races (individual points) and overall for each sex (dashed lines and color shading). Traits measured: (A, B) number of stems, (C) presence of flowering (yes/no) at week 4; at week 8 all individuals are flowering, and (D, E) number of inflorescences and (F, G) inflorescence size (mm) for those individuals flowering. The significance of sex differences for each chromosome race and across both races is indicated by stars above the individual bars and in the lower right corner of each plot, respectively. **, $0.001 < P < 0.01$; ***, $P < 0.001$; ns = not statistically significant.

Variation in sexual dimorphism among chromosome races and populations

There were no clear differences in the degree of sexual dimorphism between the Texas and North Carolina chromosome races of *R. hastatulus* (Figure 1 and 2). For some traits (height, leaf size, number, amount of stems and inflorescence size and number), however, we found significantly higher sexual dimorphism in the Texas race compared to the North Carolina race at week 4 (peak flowering) but not at week 8 (Figure 1 and 2, and Table S1). This may reflect a developmental difference between the chromosome races, which could contribute to the earlier onset of sexual dimorphism in populations of the Texas karyotype. However, there was large among-population variation in sexual dimorphism for many traits and across different life-

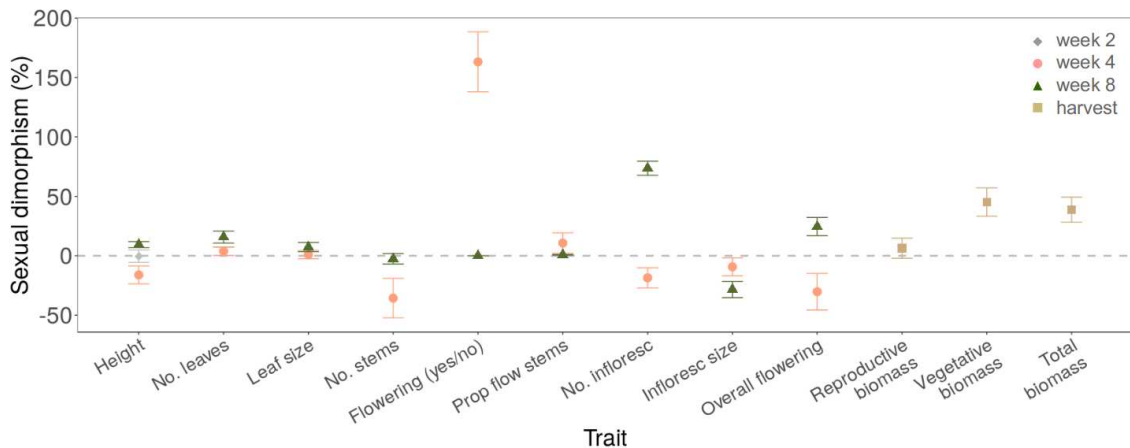


Figure 3: Percentage of sexual dimorphism (%SD) per trait and at different life-cycle stages in *Rumex hastatulus*. Percent sexual dimorphism was calculated as $(\text{mean}_f - \text{mean}_m) / \text{mean}_m \times 100$ where mean_f and mean_m are the predicted means for females and males respectively. Error bars represent 95% confidence intervals. Values above and below zero (dashed line) represent female-biased and male-biased sexual dimorphism, respectively.

cycle stages (Figure S3; see sex x population interactions in Table S1, and Figure S2 for more details of inter-population variability for height across time points, as an example). Traits with a significant sex x population interaction were height at week 2, inflorescence number and size at week 4, number of leaves, proportion of flowering stems and inflorescence number and size at week 8, and reproductive biomass at harvest (see Table S1).

Next, we assessed whether the observed genetically-based sexual dimorphism under glasshouse conditions could be explained by demographic, geographical and environmental variables of the population of origin. Population size, density and sex ratio did not explain significant variation in the degree of sexual dimorphism. Only sexual dimorphism in inflorescence size at week 8 decreased with plant density (%SD inflorescence size, week 8 = $-23.124 - 0.167 \text{ Density}$; $R^2 = 0.28$, $P = 0.0017$). However, greater variability in sexual dimorphism for vegetative and reproductive traits at both weeks 4 and 8 was evident in less dense populations (Figure 4). Among populations, both male- and female-biased sexual dimorphism were evident at low density for height, total flower number, number of leaves and biomass, but at higher density sexual dimorphism was more consistent in the direction of bias, which varied among traits (Figure 4).

Geographical parameters (longitude, latitude and altitude) of the population of origin explained between 14-35% of the inter-population variation in sexual dimor-

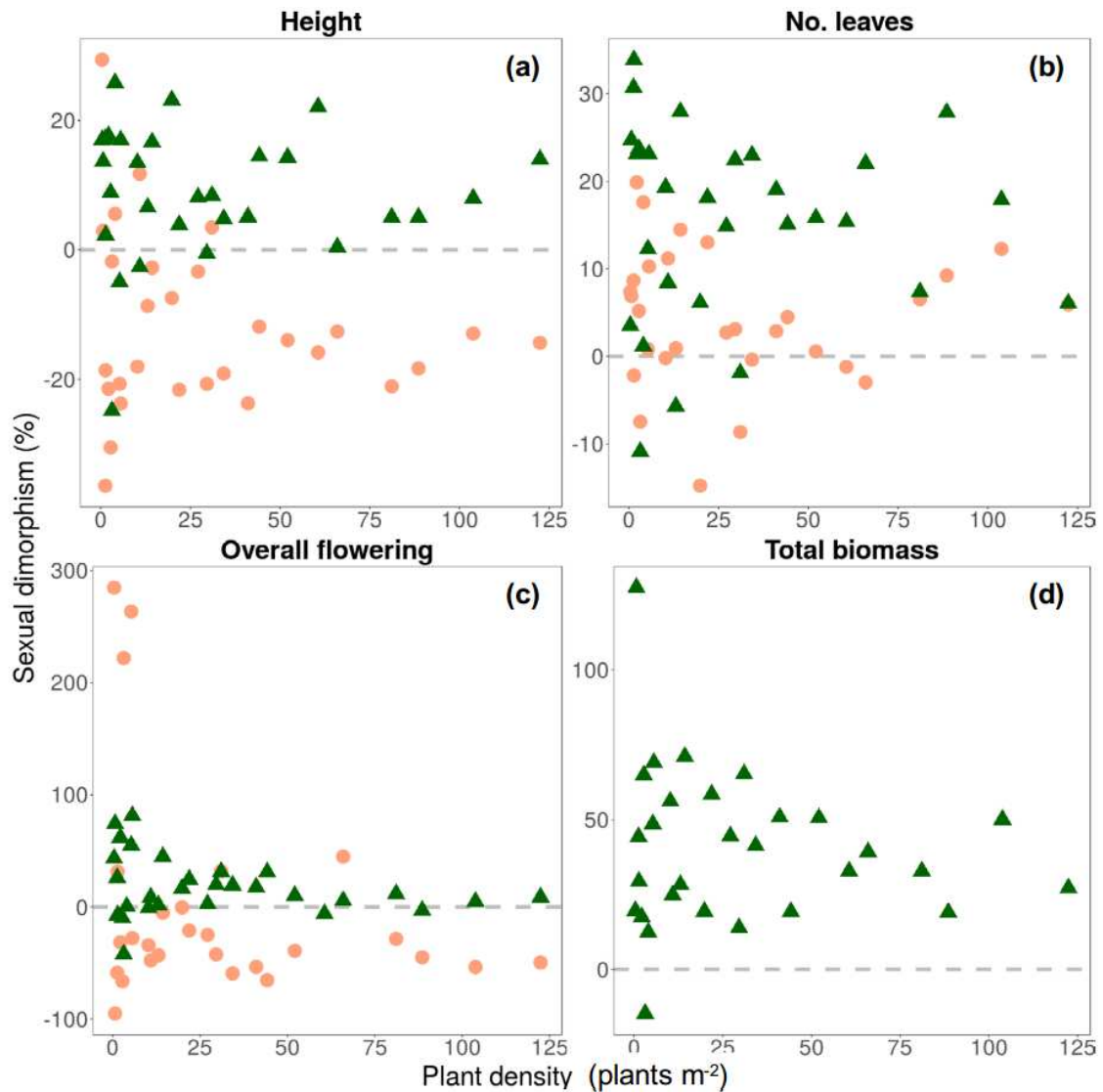


Figure 4: The relation between percent sexual dimorphism (%SD) and mean plant density (plants m^{-2}) for 29 populations of *Rumex hastatulus* for: (A) plant height (cm), (B) number of leaves and (C) total flower number (number of inflorescences \times inflorescence size) at weeks 4 (orange circles) and 8 (green triangles). Total biomass (D) was measured at harvest. Values above and below zero (dashed line) represent female-biased and male-biased sexual dimorphism, respectively.

phism for several vegetative and flowering traits in the glasshouse (see Table S2). Given that these patterns likely reflect underlying bioclimatic variation along geographical clines, we examined sexual dimorphism in relation to three bioclimatic parameters of the source populations: total annual precipitation, annual mean temperature and annual temperature range (based on reduced dimensionality of 19 WorldClim bioclimatic parameters, see Figure S4 and Methods for details), which

were indeed correlated with longitude, latitude and altitude (Figure S4C). At week 4, male-biased sexual dimorphism in height increased with mean temperature ($R^2 = 0.24$, $P = 0.004$; Figure 5A), whereas for inflorescence size, the degree of sexual dimorphism changed from female-biased to male-biased with increasing mean temperature ($R^2 = 0.25$, $P = 0.0048$; Figure 5B). At week 8, we found that mean temperature explained 31% ($P = 0.001$) and 19% ($P = 0.011$) of the variation in female-biased sexual dimorphism in number of leaves and stems, respectively (Figure 5C,D). At this life-cycle stage, male-biased dimorphism in inflorescence size was greater in populations with higher mean annual temperature and a smaller annual temperature range ($R^2 = 0.43$, $P = 0.002$, Figure 5E).

A more complex relationship between sexual dimorphism and bioclimatic variables was evident for number of stems and total flower number at 4 weeks. For total flower number, sexual dimorphism was more male-biased in populations with higher and more variable temperatures and greater annual precipitation, with these three variables explaining 34% of the variation in sexual dimorphism (total flower number = $3270.29 - 8.32$ mean temperature - 4.09 temperature range - 0.36 precipitation; $P = 0.006$). Sexual dimorphism in the number of stems was more male-biased in populations with higher precipitation and annual variation in temperature, but lower average temperature (number of stems = $726.53 - 1.12$ mean temperature - 1.28 temperature range - 0.12 precipitation; $R^2 = 0.37$, $P = 0.003$). Sex-specific regression of trait means on bioclimatic variables revealed that several such patterns probably resulted from differences between sexes in their sensitivity to environmental heterogeneity. For example, the increase in male-biased sexual dimorphism in flowering at week 4 at higher temperatures was likely due to males increasing flower production relative to females with increasing temperature (Table S3).

Intersex and inter-trait correlations

We analyzed intersex and inter-trait correlations using the predicted means of populations at each life-cycle stage separately, because the correlation among traits within each stage was higher than the within-trait correlations across life-cycle stages (data not shown). We found significant pairwise correlations between many traits, which in some cases differed between sexes (Figure 6A,B). For example, height was positively correlated with leaf size in females and with inflorescence size in males, whereas inflorescence size was strongly negatively correlated with leaf production and inflorescence number in males but not females. These results are consistent with greater male investment in inflorescences, at the expense of vegetative traits,

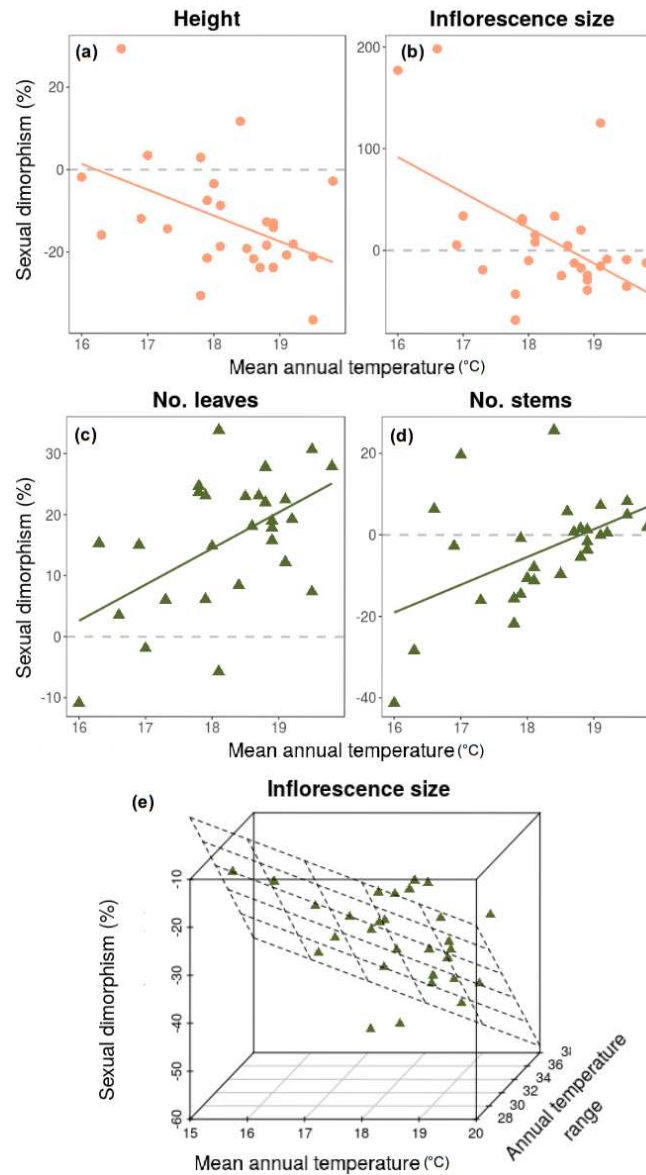


Figure 5: Patterns of sexual dimorphism along climatic gradients for populations of *Rumex hastatulus*. Percent sexual dimorphism (%SD) among populations for different vegetative and reproductive traits at weeks 4 (orange circles) and 8 (green triangles) plotted against mean annual temperature (bio1) and annual temperature range (bio7; see Figure S4 for more details on climatic variables). (A) Height (week 4) = $99.40 - 0.61 \text{ bio1}$ ($R^2 = 0.24$, $P = 0.004$); (B) inflorescence size (week 4) = $647.71 - 3.48 \text{ bio1}$ ($R^2 = 0.25$, $P = 0.005$); (C) number of leaves (week 8) = $-86.17 + 0.56 \text{ bio1}$ ($R^2 = 0.31$, $P = 0.001$); (D) number of stems (week 8) = $-103.10 + 0.55 \text{ bio1}$ ($R^2 = 0.19$, $P = 0.011$); (E) inflorescence size (week 8) = $179.61 - 0.45 \text{ bio1} - 0.39 \text{ bio7}$ ($R^2 = 0.43$, $P = 0.0003$).

whereas females invest in both vegetative and reproductive structures.

We also detected significant temporal differences in inter-trait correlations (Fig-

ure 6A,B). Whereas sex differences and negative values of inter-trait correlations were only apparent at week 8, at week 4 all inter-trait correlations were positive and highly concordant between the sexes. This concordance at week 4 likely reflects developmental variation, and that specific inter-trait correlations may result from indirect interactions with other traits. Indeed, when examined via partial correlations (accounting for other traits as covariates), we found that trade-offs between pairs of traits were more consistent across sexes and time points (Figure 6C,D). For example, partial correlations showed that both sexes displayed a trade-off between inflorescence size and number (which was stronger in males than females). Yet for the uncorrected correlations, this was masked by indirect interactions with other traits at week 4 for both sexes, and for females at week 8.

We then explored the relations between intersex correlation and the extent of sexual dimorphism. Interestingly, number of inflorescences, which had the lowest intersex correlation both at weeks 4 and 8, also displayed temporal reversal in sexual dimorphism (Figure 3). However, we found no significant covariation between intersex correlation and the extent of sexual dimorphism ($r_s = -0.095$, $P = 0.6745$). Moreover, the most sexually dimorphic traits (flowering at week 4 and inflorescence number at week 8) had very similar correlations with other traits in both sexes.

Discussion

We compared patterns of sexual dimorphism for reproductive and vegetative traits measured under uniform glasshouse conditions at three life-cycle stages in 30 populations of dioecious wind-pollinated *Rumex hastatulus*. Genetically-based sexual dimorphism was evident for most traits and often changed during the life cycle, with a reversal of dimorphism between peak flowering and reproductive maturity for some traits (e.g., height, flowering). We detected no systematic sex differences between the chromosome races, but there was striking among-population variation in sexual dimorphism, which was partially explained by bioclimatic variables along geographical clines. We now discuss how these patterns of sexual dimorphism relate to the reproductive roles of the sexes and their life-cycle dynamics, and consider explanations for the among-population variation in sexual dimorphism and how inter-trait and intersex correlations may influence the evolution of sexual dimorphism.

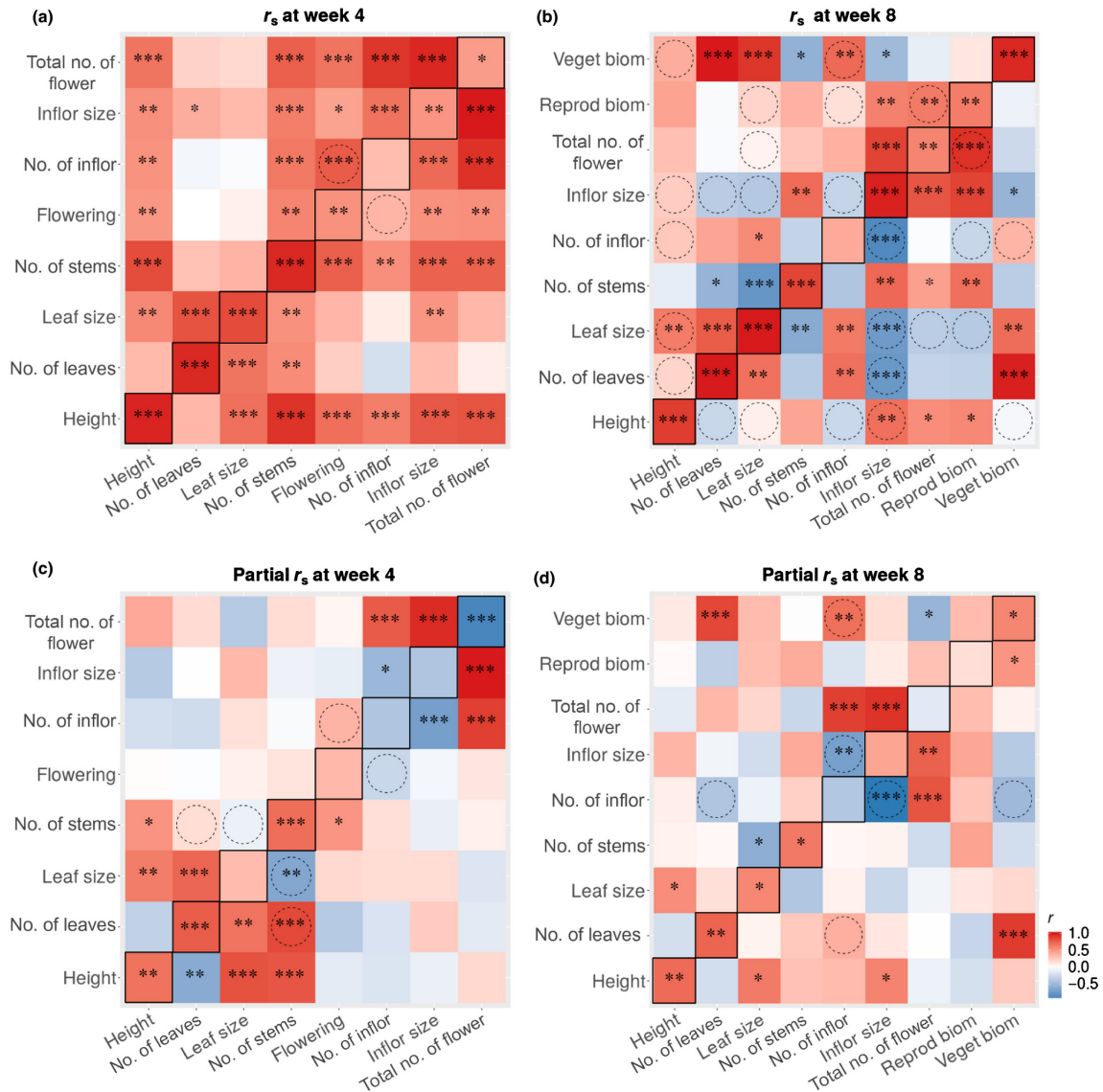


Figure 6: Intersex and inter-trait raw and partial correlations for *Rumex hastatulus* using predicted population means at (A, C) 4 and (B, D) 8 weeks. For each plot, above diagonal are the inter-trait correlations among females, below diagonal are the inter-trait correlations among males and on-diagonal are the intersex correlations for each trait. Reproductive and vegetative biomass were measured at harvest. Flowering (yes/no) is not included at week 8 since all individuals flowered. For the raw correlations (A-B) values correspond to Spearman rank correlation on predicted population means. Partial correlations (C-D) control for potential confounding interactions with other traits. Colour indicates the direction of the correlation (red for positive and blue for negative), while the strength of the correlation is indicated by the colour bar. * $0.01 < P < 0.05$, ** $0.001 < P < 0.01$, *** $P < 0.001$. Dashed circles denote significant differences between pairwise inter-trait correlations between sexes, determined via bootstrapping (see Materials and Methods for more details).

Temporal variation and reproductive roles of the sexes

Sexual dimorphism of reproductive and vegetative traits is widespread among dioecious plant species (Delph, 1999; Barrett & Hough, 2013), reflecting the different reproductive roles of females and males (Lloyd & Webb, 1977), sex-specific trade-offs in resource use (Moore & Pannell, 2011) and interactions with underlying intersex genetic correlations (Delph et al., 2002, 2010; Delph, Steven, et al., 2011). The patterns of sexual dimorphism we observed in *R. hastatulus* are consistent with temporal differences in the reproductive roles of the sexes. For example, males were taller at peak flowering, which likely facilitates wind-mediated pollen dispersal in males and pollen receipt in females (Okubo & Levin, 1989; Friedman & Barrett, 2009), whereas females were taller at reproductive maturity, which likely increases the dispersal distance of wind-dispersed seeds (Tackenberg et al., 2003; Soons et al., 2004; Thomson et al., 2011; Bullock et al., 2017; Figure 1A,B). The benefit of increased seed dispersal distance in plants includes reduced sib-competition and greater potential access to favourable microsites (Howe & Smallwood, 1982; Levin et al., 2003). Our finding of reversal in sexual dimorphism for height in *R. hastatulus*, extends previous results (Pickup & Barrett, 2012; Teitel et al., 2016), which involved many fewer populations of this species, and demonstrates that this pattern of height reversal is a fundamental feature of the growth strategy of this species.

Although we did not directly evaluate the reproductive success of males in relation to height, several lines of evidence suggest that male height reflects wind-mediated sex-specific selection (e.g. Tonnabel et al., 2019). First, we observed a significant positive relation between flowering onset and height in this sex, suggesting that males delay flowering to achieve increased stem elongation. This may be particularly important in *R. hastatulus* as this species occurs in monospecific stands in open habitats in which height – relative to conspecifics – likely promotes more effective pollen dispersal (Niklas, 1985). Second, male-biased dimorphism in height at peak flowering was consistent across most populations (Figure S2B, non-significant sex x population interaction in Table S1). Significantly, the only populations where this was not evident were those at low plant density (Figure 4A), where male-male competition may be less intense due to the positive relation between plant density and stigmatic pollen loads in wind-pollinated herbs (Steven & Waller, 2007; Friedman & Barrett, 2009; Hesse & Pannell, 2011), including *R. hastatulus* (M. Pickup, D.L. Field and S.C.H. Barrett, unpublished) and other *Rumex* species (Stehlik & Barrett, 2006; Stehlik et al., 2008). Accordingly, other vegetative and reproductive traits showed higher consistency in sexual dimorphism in denser populations (Fig-

ure 4). Third, in males, height was correlated with inflorescence size (indicative of flower number; Figure 6), suggesting that taller males have a higher reproductive investment and male siring success.

Wind-mediated sexual selection also likely acts on females of *R. hastatulus*. Although shorter stature facilitates pollen receipt during peak flowering, taller females probably have increased seed dispersal at reproductive maturity, consistent with the temporal reversal of sexual dimorphism in height we observed (Figure 1A,B). We also found evidence for sexual selection shaping patterns of sexual dimorphism in inflorescence traits. Overall, males produced fewer but taller and larger inflorescences (Figure 2E,G), facilitating pollen dispersal, whereas females had more smaller inflorescences, which may optimize pollen receipt by distributing flowers over a larger portion of the air stream. We found greater vegetative biomass in females at reproductive maturity, a pattern reported in other herbaceous wind-pollinated species (Korpelainen, 1992; Harris & Pannell, 2008; Hesse & Pannell, 2011), and a previous study of *R. hastatulus* (Teitel et al., 2016). Sex-specific differences in vegetative investment in wind-pollinated herbaceous plants have been explained by contrasting resource requirements, in that females need more carbon for seed and fruit production (Harris & Pannell, 2008; Teitel et al., 2016). We found greater female investment in leaves consistently across populations, especially at reproductive maturity (Figure 1D,F,G). Female-bias in vegetative biomass at reproductive maturity, but no difference between the sexes in number of stems (Figure 2A), likely reflects greater investment in longer stems to support developing fruit and aid in their dispersal. Overall, we found higher sexual dimorphism in reproductive than vegetative traits, as reported for several other dioecious species (Delph et al., 2002; Barrett & Hough, 2013; Figure 3).

Geographical variation in sexual dimorphism

Understanding the drivers of geographical variation in sexual dimorphism can provide insights into the importance of sexual selection, sex-specific plasticity and genetic divergence of sex-specific trait differences (Delph et al., 2002; Delph & Bell, 2008). Our common garden study revealed extensive genetically-based among-population variation in sexual dimorphism across the life cycle. We investigated several genetic and ecological correlates of this variation in an effort to provide insights into potential contributing factors. First, we predicted that genetic divergence at sex-linked genes across the two karyotypic races (Beaudry et al., 2020) might contribute to sexual dimorphism because sex chromosomes may be enriched

for variation influencing sex-specific adaptations (Rice, 1984; Dean & Mank, 2014). However, we found no systematic sex differences between the chromosome races (Figure 1 and 2). Significant among-race differences in sexual dimorphism at week 4 for some traits likely reflect a developmental difference associated with the earlier onset of dimorphism in populations of the Texas race.

Second, sex ratio might influence patterns of sex differences by mediating the degree of pollen-pollen competition, with greater pollen competition expected in populations with more males. Although populations of *R. hastatulus* varied in degree of female-bias (sex ratio: 0.54 – 0.68; Pickup & Barrett, 2013), sex ratio did not explain variation in sexual dimorphism. Third, differences in sexual dimorphism can also arise through a greater response of one sex than the other to environmental heterogeneity (Delph & Bell, 2008; Delph, Andicoechea, et al., 2011). For example, sex-specific responses to environmental variables have been reported in natural populations of *Salix* (Dudley, 2006), although it is difficult to disentangle plasticity from genetically-based dimorphism by observing natural variation. We regressed genetically-based sexual dimorphism and sex-specific trait means on the bioclimatic parameters of source populations of *R. hastatulus* to determine: (i) if sexual dimorphism varied across bioclimatic clines and, (ii) whether these patterns are due to a greater response of one sex than the other. We found that a large proportion (up to 43%) of variation in sexual dimorphism in some traits was explained by bioclimatic variables, likely due to sex-differential responses. Mean annual temperature is expected to provide more favourable growing conditions during the year. In our study, populations from sites with higher mean annual temperatures had greater male-biased sexual dimorphism for plant height at peak flowering (Figure 5A), perhaps due to a higher relative investment in stem growth in males than females at higher temperatures (Table S3). We also found a positive correlation between temperature and female-biased sexual dimorphism for leaf production at reproductive maturity (Figure 5C). In females, a slower rate of decline in mean leaf production with increasing annual temperature (see Table S3) suggests that they maintain a greater investment in leaves than males over this gradient, which was reflected in increased female-biased dimorphism.

To our knowledge, our finding of correlations between geographical and bioclimatic variables and sexual dimorphism in *R. hastatulus*, provides the first evidence for clinal variation in sexual dimorphism in plants. Our results strongly suggest that both variation in sexual selection, mediated by intra-sex competition, and sex-specific differences in resource allocation trade-offs, modulated by bioclimatic vari-

ables, shape patterns of sexual dimorphism. Experimental manipulation of growing conditions could be used to further investigate these hypotheses and, combined with studies of selection gradients (see Delph & Herlihy, 2012), could provide more information on how these different factors interact in the evolution of sex differences.

Phenotypic correlations and the evolution of sexual dimorphism

Our study examined intersex and inter-trait correlations at the phenotypic level to understand how they interact with the evolution of sex differences. First, we found many pairwise trait correlations (Figure 6A,B), yet, for many pairs of traits, the correlations changed in strength and direction when assessed using partial correlations conditioned on other traits (Figure 6C,D). This suggests an extensive shared genetic basis across traits and that there is the potential for correlated evolution to drive sexual dimorphism (Lande, 1980; Delph et al., 2002; Delph, Gehring, et al., 2004; Delph, Frey, et al., 2004). We observed extensive sex-specific differences in both the direction and magnitude of inter-trait correlations for some traits, which may reflect sex differences in selective pressures and trait architecture (Ashman, 2003; Delph et al., 2010). For example, inflorescence size was negatively correlated with inflorescence number and leaf size in males but not females indicating that males invest in inflorescence size at the expense of the other traits, whereas females strike a compromise between reproductive and vegetative investment (Delph et al., 2005; Figure 6). In general, males had more significant among-trait correlations and trade-offs than females, which is consistent with previous findings in *Silene latifolia* (Steven et al., 2007; Delph et al., 2010), *Ceratodon purpureous* (McDaniel, 2005) and *R. hastatulus* (Teitel et al., 2016). Importantly, in our study negative correlations among traits only became evident at week 8, indicating that week 4 probably captured mostly developmental variation. This finding highlights the importance of examining intersex and inter-trait correlations across the life cycle to capture functionally relevant patterns.

High intersex correlations in trait expression can limit the evolution of sex differences (Meagher, 1992; Ashman, 2003) and as a result constrain the evolution of sexual dimorphism (Poissant et al., 2010; Griffin et al., 2013). However, we found no association between the intersex correlation and extent of sexual dimorphism. The most dimorphic traits (flowering at week 4 and inflorescence number at week 8) had very similar correlations with other traits in both sexes (Figure 6B). These

results therefore suggest that although intersex correlations contribute to patterns of sexual dimorphism they are capable of evolving and are not inflexible constraints to the evolution of sex differences (Delph, Steven, et al., 2011).

Understanding the link between sex-specific phenotypic variation and the different reproductive roles of the sexes has long intrigued evolutionary biologists. For plants, pollen and seed dispersal vectors can mediate the strength of sex-specific selection, leading to trait changes in relation to the timing of the reproductive roles of males (pollen dispersal) and females (pollen receipt and seed dispersal). Similarly, interaction between environmental gradients and sex-specific resource requirement may result in clinal variation in patterns of dimorphism. By examining geographical and temporal variation in sexual dimorphism our study has provided novel insights into how sexual and natural selection contribute to sex-phenotype variation in a wide-ranging plant species.

Acknowledgements

We thank Allison Kwok for assistance with the glasshouse experiment and Caroli de Waal for help with field collections. Thanks to Carina Baskett for assistance with Figure S1. Research and post-doctoral fellowships to MP and DF funded by a Discovery Grant from the Natural Sciences and Engineering Research Council of Canada to SCHB. GP received funding from the European Union's Horizon 2020 research and innovation programme under the Marie Skłodowska-Curie Grant Agreement No. 665385.

Author Contributions

MP, DF and SCHB conceived the study and designed the research experiment, MP and DLF undertook the experiment and data collection, GP, MP and DLF performed the data analyses and all authors contributed to writing of the manuscript.

References

- Andersson, M. (1994). *Sexual Selection* (Second Edition ed.). Princeton, N.J: Princeton University Press.
- Ashman, T.-L. (2003, September). Constraints on the evolution of males and sexual dimorphism: field estimates of genetic architecture of reproductive

- traits in three populations of gynodioecious *Fragaria virginiana*. *Evolution; International Journal of Organic Evolution*, 57(9), 2012–2025. doi: 10.1111/j.0014-3820.2003.tb00381.x
- Barrett, S. C. H., & Hough, J. (2013, January). Sexual dimorphism in flowering plants. *Journal of Experimental Botany*, 64(1), 67–82. doi: 10.1093/jxb/ers308
- Bartkowiak, E. (1971, January). Mechanism of sex determination in *Rumex hastatulus* Baldw. *TAG. Theoretical and applied genetics. Theoretische und angewandte Genetik*, 41(7), 320–326. doi: 10.1007/BF00577104
- Beaudry, F. E. G., Barrett, S. C. H., & Wright, S. I. (2020, February). Ancestral and neo-sex chromosomes contribute to population divergence in a dioecious plant. *Evolution; International Journal of Organic Evolution*, 74(2), 256–269. doi: 10.1111/evo.13892
- Bolker, B. M., Brooks, M. E., Clark, C. J., Geange, S. W., Poulsen, J. R., Stevens, M. H. H., & White, J.-S. S. (2009, March). Generalized linear mixed models: a practical guide for ecology and evolution. *Trends in Ecology & Evolution*, 24(3), 127–135. doi: 10.1016/j.tree.2008.10.008
- Bullock, J. M., González, L. M., Tamme, R., Götzenberger, L., White, S. M., Pärtel, M., & Hooftman, D. A. P. (2017). A synthesis of empirical plant dispersal kernels. *Journal of Ecology*, 105(1), 6–19. Retrieved 2023-05-15, from <https://www.jstor.org/stable/26177054> (Publisher: [Wiley, British Ecological Society])
- Charlesworth, D. (2002, February). Plant sex determination and sex chromosomes. *Heredity*, 88(2), 94–101. doi: 10.1038/sj.hdy.6800016
- Charlesworth, D. (2018, February). Does sexual dimorphism in plants promote sex chromosome evolution? *Environmental and Experimental Botany*, 146, 5–12. Retrieved 2023-08-01, from <https://www.sciencedirect.com/science/article/pii/S0098847217302769> doi: 10.1016/j.envexpbot.2017.11.005
- Compagnoni, A., Steigman, K., & Miller, T. E. X. (2017, October). Can't live with them, can't live without them? Balancing mating and competition in two-sex populations. *Proceedings. Biological Sciences*, 284(1865), 20171999. doi: 10.1098/rspb.2017.1999
- Cuñado, N., Navajas-Pérez, R., de la Herrán, R., Ruiz Rejón, C., Ruiz Rejón, M., Santos, J. L., & Garrido-Ramos, M. A. (2007). The evolution of sex chromosomes in the genus *Rumex* (Polygonaceae): Identification of a new species with heteromorphic sex chromosomes. *Chromosome Research: An Interna-*

- tional Journal on the Molecular, Supramolecular and Evolutionary Aspects of Chromosome Biology*, 15(7), 825–833. doi: 10.1007/s10577-007-1166-6
- Darwin, C. (1871). *The Descent of Man, and Selection in Relation to Sex*. D. Appleton. (Google-Books-ID: LYEQAAAAYAAJ)
- Dean, R., & Mank, J. E. (2014, July). The role of sex chromosomes in sexual dimorphism: discordance between molecular and phenotypic data. *Journal of Evolutionary Biology*, 27(7), 1443–1453. doi: 10.1111/jeb.12345
- Delph, L. F. (1999). Sexual Dimorphism in Life History. In M. A. Geber, T. E. Dawson, & L. F. Delph (Eds.), *Gender and Sexual Dimorphism in Flowering Plants* (pp. 149–173). Berlin, Heidelberg: Springer. Retrieved 2023-05-15, from https://doi.org/10.1007/978-3-662-03908-3_6 doi: 10.1007/978-3-662-03908-3_6
- Delph, L. F., Andicoechea, J., Steven, J. C., Herlihy, C. R., Scarpino, S. V., & Bell, D. L. (2011, October). Environment-dependent intralocus sexual conflict in a dioecious plant. *The New Phytologist*, 192(2), 542–552. doi: 10.1111/j.1469-8137.2011.03811.x
- Delph, L. F., Arntz, A. M., Scotti-Saintagne, C., & Scotti, I. (2010, October). The genomic architecture of sexual dimorphism in the dioecious plant *Silene latifolia*. *Evolution; International Journal of Organic Evolution*, 64(10), 2873–2886. doi: 10.1111/j.1558-5646.2010.01048.x
- Delph, L. F., & Bell, D. L. (2008). A test of the differential-plasticity hypothesis for variation in the degree of sexual dimorphism in *Silene latifolia*. *Evolutionary Ecology Research*. Retrieved 2023-05-15, from <https://www.semanticscholar.org/paper/A-test-of-the-differential-plasticity-hypothesis-in-Delph-Bell/f7fb1a8386c628ca47ecd37dd98991b0efb92708>
- Delph, L. F., Frey, F. M., Steven, J. C., & Gehring, J. L. (2004). Investigating the independent evolution of the size of floral organs via G-matrix estimation and artificial selection. *Evolution & Development*, 6(6), 438–448. doi: 10.1111/j.1525-142X.2004.04052.x
- Delph, L. F., Gehring, J. L., Arntz, A. M., Levri, M., & Frey, F. M. (2005, October). Genetic correlations with floral display lead to sexual dimorphism in the cost of reproduction. *The American Naturalist*, 166 Suppl 4, S31–41. doi: 10.1086/444597
- Delph, L. F., Gehring, J. L., Frey, F. M., Arntz, A. M., & Levri, M. (2004, September). Genetic constraints on floral evolution in a sexually dimorphic plant

- revealed by artificial selection. *Evolution; International Journal of Organic Evolution*, 58(9), 1936–1946. doi: 10.1111/j.0014-3820.2004.tb00481.x
- Delph, L. F., & Herlihy, C. R. (2012, April). Sexual, fecundity, and viability selection on flower size and number in a sexually dimorphic plant. *Evolution; International Journal of Organic Evolution*, 66(4), 1154–1166. doi: 10.1111/j.1558-5646.2011.01510.x
- Delph, L. F., Knapczyk, F. N., & Taylor, D. R. (2002). Among-population variation and correlations in sexually dimorphic traits of *Silene latifolia*. *Journal of Evolutionary Biology*, 15(6), 1011–1020. Retrieved 2023-05-15, from <https://onlinelibrary.wiley.com/doi/abs/10.1046/j.1420-9101.2002.00467.x> (.eprint: <https://onlinelibrary.wiley.com/doi/pdf/10.1046/j.1420-9101.2002.00467.x>) doi: 10.1046/j.1420-9101.2002.00467.x
- Delph, L. F., Steven, J. C., Anderson, I. A., Herlihy, C. R., & Brodie, E. D. (2011, October). Elimination of a genetic correlation between the sexes via artificial correlational selection. *Evolution; International Journal of Organic Evolution*, 65(10), 2872–2880. doi: 10.1111/j.1558-5646.2011.01350.x
- Dudley, L. S. (2006, December). Ecological correlates of secondary sexual dimorphism in *Salix glauca* (Salicaceae). *American Journal of Botany*, 93(12), 1775–1783. doi: 10.3732/ajb.93.12.1775
- Eppley, S. M., & Pannell, J. R. (2007, October). Density-dependent self-fertilization and male versus hermaphrodite siring success in an androdioecious plant. *Evolution; International Journal of Organic Evolution*, 61(10), 2349–2359. doi: 10.1111/j.1558-5646.2007.00195.x
- Friedman, J., & Barrett, S. C. H. (2009, June). Wind of change: new insights on the ecology and evolution of pollination and mating in wind-pollinated plants. *Annals of Botany*, 103(9), 1515–1527. doi: 10.1093/aob/mcp035
- Friedman, J., & Barrett, S. C. H. (2011, February). The evolution of ovule number and flower size in wind-pollinated plants. *The American Naturalist*, 177(2), 246–257. doi: 10.1086/657954
- Geber, M. A., Dawson, T. E., & Delph, L. F. (Eds.). (1999). *Gender and Sexual Dimorphism in Flowering Plants*. Berlin, Heidelberg: Springer. Retrieved 2023-05-15, from <http://link.springer.com/10.1007/978-3-662-03908-3> doi: 10.1007/978-3-662-03908-3
- Govindarajulu, R., Liston, A., & Ashman, T.-L. (2013, May). Sex-determining chromosomes and sexual dimorphism: insights from genetic mapping of sex expression in a natural hybrid *Fragaria* × *ananassa* subsp. *cuneifolia*. *Heredity*,

- 110(5), 430–438. doi: 10.1038/hdy.2012.96
- Griffin, R. M., Dean, R., Grace, J. L., Rydén, P., & Friberg, U. (2013, September). The shared genome is a pervasive constraint on the evolution of sex-biased gene expression. *Molecular Biology and Evolution*, 30(9), 2168–2176. doi: 10.1093/molbev/mst121
- Harris, M. S., & Pannell, J. R. (2008, November). Roots, shoots and reproduction: sexual dimorphism in size and costs of reproductive allocation in an annual herb. *Proceedings. Biological Sciences*, 275(1651), 2595–2602. doi: 10.1098/rspb.2008.0585
- Hesse, E., & Pannell, J. R. (2011, May). Sexual dimorphism in a dioecious population of the wind-pollinated herb *Mercurialis annua*: the interactive effects of resource availability and competition. *Annals of Botany*, 107(6), 1039–1045. doi: 10.1093/aob/mcr046
- Hijmans, R. J., Cameron, S. E., Parra, J. L., Jones, P. G., & Jarvis, A. (2005). Very high resolution interpolated climate surfaces for global land areas. *International Journal of Climatology*, 25(15), 1965–1978. Retrieved 2023-05-15, from <https://onlinelibrary.wiley.com/doi/abs/10.1002/joc.1276> (_eprint: <https://onlinelibrary.wiley.com/doi/pdf/10.1002/joc.1276>) doi: 10.1002/joc.1276
- Howe, H. F., & Smallwood, J. (1982). Ecology of Seed Dispersal. *Annual Review of Ecology and Systematics*, 13(1), 201–228. Retrieved 2023-05-15, from <https://doi.org/10.1146/annurev.es.13.110182.001221> (_eprint: <https://doi.org/10.1146/annurev.es.13.110182.001221>) doi: 10.1146/annurev.es.13.110182.001221
- Korpelainen, H. (1992, January). Patterns of resource allocation in male and female plants of *Rumex acetosa* and *R. acetosella*. *Oecologia*, 89(1), 133–139. doi: 10.1007/BF00319025
- Lande, R. (1980, March). SEXUAL DIMORPHISM, SEXUAL SELECTION, AND ADAPTATION IN POLYGENIC CHARACTERS. *Evolution; International Journal of Organic Evolution*, 34(2), 292–305. doi: 10.1111/j.1558-5646.1980.tb04817.x
- Levin, S. A., Muller-Landau, H. C., Nathan, R., & Chave, J. (2003). The Ecology and Evolution of Seed Dispersal: A Theoretical Perspective. *Annual Review of Ecology, Evolution, and Systematics*, 34(1), 575–604. Retrieved 2023-05-15, from <https://doi.org/10.1146/annurev.ecolsys.34.011802.132428> (_eprint: <https://doi.org/10.1146/annurev.ecolsys.34.011802.132428>) doi: 10

- .1146/annurev.ecolsys.34.011802.132428
- Lloyd, D. G., & Webb, C. J. (1977). Secondary Sex Characters in Plants. *Botanical Review*, 43(2), 177–216. Retrieved 2023-05-15, from <https://www.jstor.org/stable/4353917> (Publisher: New York Botanical Garden Press)
- McDaniel, S. F. (2005, November). Genetic correlations do not constrain the evolution of sexual dimorphism in the moss *Ceratodon purpureus*. *Evolution; International Journal of Organic Evolution*, 59(11), 2353–2361.
- Meagher, T. R. (1992, April). THE QUANTITATIVE GENETICS OF SEXUAL DIMORPHISM IN *SILENE LATIFOLIA* (CARYOPHYLLACEAE). I. GENETIC VARIATION. *Evolution; International Journal of Organic Evolution*, 46(2), 445–457. doi: 10.1111/j.1558-5646.1992.tb02050.x
- Ming, R., Bendahmane, A., & Renner, S. S. (2011). Sex chromosomes in land plants. *Annual Review of Plant Biology*, 62, 485–514. doi: 10.1146/annurev-arplant-042110-103914
- Moore, J. C., & Pannell, J. R. (2011, March). Sexual selection in plants. *Current biology: CB*, 21(5), R176–182. doi: 10.1016/j.cub.2010.12.035
- Navajas-Pérez, R., de la Herrán, R., López González, G., JAMILENA, M., Lozano, R., Ruiz Rejón, C., . . . Garrido-Ramos, M. A. (2005, September). The evolution of reproductive systems and sex-determining mechanisms within rumex (polygonaceae) inferred from nuclear and chloroplastidial sequence data. *Molecular Biology and Evolution*, 22(9), 1929–1939. doi: 10.1093/molbev/msi186
- Niklas, K. J. (1985). The Aerodynamics of Wind Pollination. *Botanical Review*, 51(3), 328–386. Retrieved 2023-05-15, from <https://www.jstor.org/stable/4354060> (Publisher: New York Botanical Garden Press)
- Obeso, J. R. (2002, September). The costs of reproduction in plants. *The New Phytologist*, 155(3), 321–348. doi: 10.1046/j.1469-8137.2002.00477.x
- Okubo, A., & Levin, S. A. (1989). A Theoretical Framework for Data Analysis of Wind Dispersal of Seeds and Pollen. *Ecology*, 70(2), 329–338. Retrieved 2023-05-15, from <https://www.jstor.org/stable/1937537> (Publisher: Ecological Society of America) doi: 10.2307/1937537
- Pickup, M., & Barrett, S. C. H. (2012, April). Reversal of height dimorphism promotes pollen and seed dispersal in a wind-pollinated dioecious plant. *Biology Letters*, 8(2), 245–248. doi: 10.1098/rsbl.2011.0950
- Pickup, M., & Barrett, S. C. H. (2013, March). The influence of demography and local mating environment on sex ratios in a wind-pollinated dioecious plant.

- Ecology and Evolution*, 3(3), 629–639. doi: 10.1002/ece3.465
- Poissant, J., Wilson, A. J., & Coltman, D. W. (2010, January). Sex-specific genetic variance and the evolution of sexual dimorphism: a systematic review of cross-sex genetic correlations. *Evolution; International Journal of Organic Evolution*, 64(1), 97–107. doi: 10.1111/j.1558-5646.2009.00793.x
- Rice, W. R. (1984, July). SEX CHROMOSOMES AND THE EVOLUTION OF SEXUAL DIMORPHISM. *Evolution; International Journal of Organic Evolution*, 38(4), 735–742. doi: 10.1111/j.1558-5646.1984.tb00346.x
- Smith, B. W. (1963, October). The Mechanism of Sex Determination in *Rumex Hastatulus*. *Genetics*, 48(10), 1265–1288. doi: 10.1093/genetics/48.10.1265
- Soons, M. B., Heil, G. W., Nathan, R., & Katul, G. G. (2004). Determinants of Long-Distance Seed Dispersal by Wind in Grasslands. *Ecology*, 85(11), 3056–3068. Retrieved 2023-05-15, from <https://www.jstor.org/stable/3450545> (Publisher: Ecological Society of America)
- Stehlik, I., & Barrett, S. C. H. (2006, June). Pollination intensity influences sex ratios in dioecious *Rumex nivalis*, a wind-pollinated plant. *Evolution; International Journal of Organic Evolution*, 60(6), 1207–1214.
- Stehlik, I., Friedman, J., & Barrett, S. C. H. (2008, August). Environmental influence on primary sex ratio in a dioecious plant. *Proceedings of the National Academy of Sciences of the United States of America*, 105(31), 10847–10852. doi: 10.1073/pnas.0801964105
- Steven, J. C., Delph, L. F., & Brodie, E. D. (2007, January). Sexual dimorphism in the quantitative-genetic architecture of floral, leaf, and allocation traits in *Silene latifolia*. *Evolution; International Journal of Organic Evolution*, 61(1), 42–57. doi: 10.1111/j.1558-5646.2007.00004.x
- Steven, J. C., & Waller, D. M. (2007). Isolation Affects Reproductive Success in Low-Density but Not High-Density Populations of Two Wind-Pollinated *Thalictrum* Species. *Plant Ecology*, 190(1), 131–141. Retrieved 2023-05-15, from <https://www.jstor.org/stable/40212904> (Publisher: Springer)
- Sánchez Vilas, J., & Pannell, J. R. (2011, January). Sexual dimorphism in resource acquisition and deployment: both size and timing matter. *Annals of Botany*, 107(1), 119–126. doi: 10.1093/aob/mcq209
- Tackenberg, O., Poschlod, P., & Bonn, S. (2003). Assessment of Wind Dispersal Potential in Plant Species. *Ecological Monographs*, 73(2), 191–205. Retrieved 2023-05-15, from <https://www.jstor.org/stable/3100013> (Publisher: Ecological Society of America)

- Team, R. C. (2022). R: A Language and Environment for Statistical Computing, Vienna, Austria. Retrieved from <https://CRAN.R-project.org/package=here>
- Teitel, Z., Pickup, M., Field, D. L., & Barrett, S. C. H. (2016, January). The dynamics of resource allocation and costs of reproduction in a sexually dimorphic, wind-pollinated dioecious plant. *Plant Biology (Stuttgart, Germany)*, *18*(1), 98–103. doi: 10.1111/plb.12336
- Thomson, F. J., Moles, A. T., Auld, T. D., & Kingsford, R. T. (2011). Seed dispersal distance is more strongly correlated with plant height than with seed mass. *Journal of Ecology*, *99*(6), 1299–1307. Retrieved 2023-05-15, from <https://onlinelibrary.wiley.com/doi/abs/10.1111/j.1365-2745.2011.01867.x> (_eprint: <https://onlinelibrary.wiley.com/doi/pdf/10.1111/j.1365-2745.2011.01867.x>) doi: 10.1111/j.1365-2745.2011.01867.x
- Tonnabel, J., David, P., Klein, E. K., & Pannell, J. R. (2019, May). Sex-specific selection on plant architecture through "budget" and "direct" effects in experimental populations of the wind-pollinated herb, *Mercurialis annua*. *Evolution; International Journal of Organic Evolution*, *73*(5), 897–912. doi: 10.1111/evo.13714
- Weller, S. G., Sakai, A. K., Culley, T. M., Campbell, D. R., & Dunbar-Wallis, A. K. (2006, March). Predicting the pathway to wind pollination: heritabilities and genetic correlations of inflorescence traits associated with wind pollination in *Schiedea salicaria* (Caryophyllaceae). *Journal of Evolutionary Biology*, *19*(2), 331–342. doi: 10.1111/j.1420-9101.2005.01038.x

CHAPTER 2

Sex-specific estimation of *cis* and *trans* regulation of gene expression in heads and gonads of *Drosophila melanogaster*¹

Gemma Puixeu, Ariana Macon and Beatriz Vicoso

Abstract

The regulatory architecture of gene expression is known to differ substantially between the sexes in *Drosophila*, but most studies performed so far used whole body data, and only single crosses, which may have limited their scope to detect patterns that are robust across tissues and biological replicates. Here we use allele-specific gene expression of parental and reciprocal hybrid crosses between 6 *Drosophila melanogaster* inbred lines to quantify *cis*- and *trans*-regulatory variation in heads and gonads of both sexes separately, across three replicate crosses.

Our results suggest that female and male heads, as well as ovaries, have a similar regulatory architecture. On the other hand, testes display more and substantially different *cis*-regulatory effects, suggesting that the sex differences in regulatory architecture that have been previously observed may largely derive from testes-specific effects. We also examine the difference in *cis*-regulatory variation of genes across different levels of sex bias in gonads and heads. Consistent with the idea that intersex correlations constrain expression and can lead to sexual antagonism, we find more *cis* variation in unbiased and moderately-biased genes in heads. In ovaries, reduced *cis* variation is observed for male-biased genes, suggesting that the *cis* variants acting on these genes in males do not lead to changes in ovary expression. Finally, we examine the dominance patterns of gene expression, and find that sex- and tissue-specific patterns of inheritance as well as *trans*-regulatory variation are highly variable across biological crosses, although these were performed in highly controlled experimental conditions. This highlights the importance of using various genetic backgrounds to infer generalizable patterns.

¹This work has been published at <https://doi.org/10.1093/g3journal/jkad121>

Introduction

Variation in gene expression has been shown to underlie human disease and contribute to trait evolution between closely related species, and understanding the mutational and selective processes driving it has been a key goal in evolutionary biology (Emerson et al., 2010; Signor & Nuzhdin, 2018). The genetic variants that contribute to the inheritable component of this variation can modulate gene expression either in *cis* or in *trans*. *Cis* variants only affect the expression of a linked allele (e.g. mutations at a gene promoter or enhancer), whereas *trans*-acting variants can affect the expression of both copies of close or distant genes (e.g. mutations that change the activity or expression of a transcription factor, reviewed in Signor & Nuzhdin, 2018).

Two main approaches have been employed for studying the evolution of gene regulation within and between species, and the contribution of *cis* and *trans* variants. Expression quantitative trait loci (eQTLs) can uncover the local and distal regulatory architecture of gene expression variation, which are typically assigned as acting in *cis* and *trans* based on a distance cutoff (e.g. Bhasin et al., 2008; Massouras et al., 2012). A more mechanistic assessment of *cis* and *trans* effects has come from comparisons of parental lines or species and allele-specific expression in heterozygous hybrid crosses, as *trans* regulators should modulate the expression of both gene copies in the hybrid, whereas *cis* regulators lead to allelic imbalances in the hybrids (e.g. Wittkopp et al., 2004; Graze et al., 2009). While unable to pinpoint specific genetic variants underlying the regulation, these hybrid studies provide an estimate of the total *cis* and *trans* regulation affecting individual genes, with both types of regulation being common (Hughes et al., 2006; Wittkopp et al., 2008; Metzger et al., 2016). This approach also provides information on the level of dominance of regulatory variants, and has shown that *cis*-acting variants are typically closer to additivity than *trans*-acting variants (Lemos et al., 2008; McManus et al., 2010; Meiklejohn et al., 2014).

Comparisons of estimates of *cis* and *trans* effects over various distances between the parental lines show that while *trans* variants control most of the variation within species, *cis* variants appear to disproportionately contribute to differences between species (Wittkopp et al., 2008; Coolon et al., 2014; Metzger et al., 2017), either because they are less pleiotropic, or because their increased additivity (Lemos et al., 2008; McManus et al., 2010; Zhang et al., 2011; Gruber et al., 2012; Meiklejohn et al., 2014) and larger effect sizes (Brem et al., 2002; Schadt et al., 2003; Hughes et

al., 2006; Gruber et al., 2012; Metzger et al., 2016) give them a selective advantage over *trans* variants. Importantly, the regulatory architecture and contribution of *cis* and *trans* variants vary depending on the population under study (Martin et al., 2014), the sampled tissue (GTEx Consortium et al., 2017; Glaser-Schmitt et al., 2018; Benowitz et al., 2020) and sex (Meiklejohn et al., 2014; Oliva et al., 2020), and on the environment (Chen et al., 2015; Fear et al., 2016; Buchberger et al., 2019), and this has potentially important consequences for how selection acts on genes expressed in these different contexts (Chen et al., 2015; Buchberger et al., 2019).

Genes which are expressed exclusively or preferably in one sex have been of particular interest, as they show unusual patterns of divergence of gene expression (Ellegren & Parsch, 2007). Genes that are primarily expressed in the testis often evolve unusually quickly in arthropods both at the sequence and expression level (Meiklejohn et al., 2003; Whittle et al., 2021). This is thought to be due to sexual selection (Ellegren & Parsch, 2007), as well as to the low pleiotropy of many genes expressed in the testis (Meisel, 2011). Ovary-biased genes, on the other hand, tend to show either no or small increases in divergence rates compared with unbiased genes (Ellegren & Parsch, 2007; Sackton et al., 2014; Whittle & Extavour, 2019; Whittle et al., 2021; but see Whittle & Extavour, 2017 for an exception in mosquitoes). In the soma, the relationship between sex-biased expression and rates of evolution has been mostly studied in heads and brain tissue (Khodursky et al., 2020; Whittle et al., 2021). In that case, both female and male-biased genes appear to have faster expression divergence than unbiased genes (Khodursky et al., 2020; Whittle et al., 2021). Consistent with these unusual evolutionary patterns, gene regulation also appears to vary between females and males. In *Drosophila*, variants with a sexually dimorphic effect on expression often act in *cis* (Meiklejohn et al., 2014), and genes with female-biased expression carry more *cis* variants (Mishra et al., 2022). The dominance of regulatory variants can also differ between the sexes, with deviations from additivity of *cis* variants acting in opposite directions in the two sexes in *Drosophila* hybrids (Meiklejohn et al., 2014), and males generally showing more additive effects than females in nematode hybrids (Sánchez-Ramírez et al., 2021). Despite this long standing interest in the regulation and evolution of sex-biased genes, direct comparisons of estimates of *cis* and *trans* effects in gonads and somatic tissues are rare. It is therefore unclear if these differences relate to germline-specific regulatory architecture or to more general differences in how males and females control gene expression. Mishra et al. (2022) recently found that sex-specific *cis*

effects were more common in the gonad, but total *cis* effects were not.

The prevalence of *cis* and *trans* effects found in different categories of genes also has the potential to shed some light on what selective pressures are acting on gene expression (Emerson & Li, 2010; Coolon et al., 2014). For instance, genes known to be under strong selective constraint show less *cis*- and *trans*-driven expression variation than other genes, consistent with stabilizing selection on gene expression (Emerson et al., 2010). Mishra et al. (2022) recently predicted an excess of *cis* effects for genes for which gene expression is evolving under sexual antagonism, as mutations that increase or decrease expression may be under balancing selection. Contrary to their expectations, genes with intermediate levels of sex-bias, which are thought to be more often under sexual conflict (Cheng & Kirkpatrick, 2016), did not harbour an excess of *cis* variants. Instead, the prevalence of *cis* effects increased with increasing female-bias, but why this occurred was unclear. More generally, both positive and negative selection should decrease the amount of polymorphic *cis* and *trans* variants within a population, while balancing selection should lead to their maintenance.

Here, we systematically estimate *cis* and *trans* effects, as well as dominance, acting on gene expression in the soma and germline of *Drosophila melanogaster*. We performed pairwise crosses between 6 inbred lines of the *Drosophila* Genetic Reference Panel (DGRP; Mackay et al., 2012; Huang et al., 2014), such that we had 3 hybrid crosses as independent biological replicates, and obtained RNA-seq reads for both heads and gonads of females and males. Our results highlight the unusual regulatory architecture of the testis, and suggest that the expression of genes that are sex-biased is under different levels of *cis* regulation compared with unbiased genes. Finally, despite the highly correlated patterns of expression across samples in our dataset, results varied substantially between crosses, highlighting the limitations of studying these patterns in a single genetic context.

Materials and Methods

Sample preparation and sequencing

We obtained sex-specific replicated gene expression for heads and gonads from crosses within and between *Drosophila melanogaster* inbred lines. Specifically, we randomly selected 6 lines from the DGRP without *Wolbachia* infection and main inversions (Huang et al., 2014) and matched them into three pairs: DGRP-757 x

DGRP-392, DGRP-208 x DGRP-808 and DGRP-83 x DGRP-332. Crosses within and between lines were set up in vials containing 40 males and 40 virgin females (between 1 and 5 vials depending on the number of individuals that could be obtained), at 23°C under a 12 hours light / 12 hours dark cycle. For each cross, we then dissected two replicate samples of heads and gonads of 20 4-day-old virgin females and virgin males for each within-line and reciprocal between-line cross, obtaining a total of 96 samples (experimental design outlined in Figure S1). Both replicates contained individuals pooled across vials so as to avoid biases due to variation across micro-environments.

Samples were flash frozen in liquid nitrogen and kept at -80°C until further processing. RNA was then extracted with a Maxwell® RSC Simply RNA Tissue Kit (Promega). Two Smart-seq2 RNA-seq libraries were produced from the tagged and pooled samples at the Vienna Biocenter Sequencing Facility (one for each replicate), and sequenced on an Illumina Novaseq machine (single end 100bp reads).

Data processing and (allele-specific) expression estimation

We obtained demultiplexed data for each of the two libraries, each containing 48 samples, and corresponding respectively to the replicates R1 and R2 of each tissue/-sex. We trimmed the data using Trimmomatic (Bolger et al., 2014) and performed UMI-based deduplication using UMI-tools (Smith et al., 2017). The final dataset consisted of 5.7 to 10.6 million reads per sample, except for sample 808M x 208F male testes R2, which had only about 15,000 reads and was removed from the analysis. We estimated overall count and TPM (transcripts per million) gene expression using Kallisto (Bray et al., 2016), reported in Supplementary Datasets S1 and S2 respectively. Two further samples were removed because of their low correlation to other samples of the same tissue: 392M x 392F male testes R2 and 392F x 757M male heads R2 (Spearman correlation < 0.8). All subsequent analyses were done without these three samples.

To estimate allele-specific expression we followed the pipeline described in Takada et al. (2017). In short, we reconstructed the genotypes of the six parental lines using VCFtools (Danecek et al., 2011), from a VCF file containing information of all the DGRP lines, and the corresponding dm3 reference genome sequence, eliminating indels and only keeping SNPs. We then estimated allele-specific expression by mapping the RNA-seq reads to transcriptomes reconstructed from the parental genomes. The line-specific transcriptomes were generated from the reconstructed genotypes using the Ensembl GTF file (version dm3, obtained from

<https://hgdownload.soe.ucsc.edu>). We mapped the RNA-seq on the transcripts using bowtie2 (Langmead & Salzberg, 2012) and estimated allele-specific expression using ASE-Tigar (Nariai et al., 2016). Because allele-specific expression data cannot be accurately estimated for genes with minimal variation between the parental lines, we only used transcripts with at least three exonic SNVs between the parental lines. We then summed estimated FPKM (fragments per kilobase of transcript per million mapped reads) and counts per transcript across isoforms to obtain expression levels per gene. To avoid biases in males and for consistency in females, X-linked genes were removed, so only autosomal data was used for all the subsequent analyses. This same pipeline was used to estimate overall parental expression between pairs of parental lines from a file containing the reads of both parents pooled together, so that the hybrid allelic and overall parental expression estimates are comparable to one another.

Hybrid allelic and overall parental expression are in Supplementary Datasets S3 and S4 as count and FPKM estimates, respectively. Count hybrid allelic expression data were used to estimate *cis*-regulatory (CR), parent-of-origin (PO) and maternal genotype (MG) effects via Takada et al. (2017) pipeline, and both hybrid allelic and overall parental expression to estimate *cis*- and *trans*-regulatory effects via the McManus et al. (2010) pipeline.

Estimation of *cis*-regulatory (CR), parent-of-origin (PO) and maternal genotype (MG) effects

We adapted a pipeline developed by Takada et al. (2017) to estimate CR, PO and MG effects by modeling the allele-specific gene expression as count data as a function of the three binary fixed effects: $E \sim \mu + CR + PO + MG + \epsilon$. We defined separate models per sex, tissue and cross leading to a total of 12 models, each (except for those with some missing samples, see above) including eight data points: expression for alleles A and B in two replicates of each reciprocal cross. For CR we assigned 0 (1) for A (B); for PO, 0 (1) was assigned if the chromosome was inherited from the mother (father); for MG, 0 (1) was assigned to samples from cross AxB (BxA; see Takada et al., 2017 for more details on the models). We included in the analyses all genes with TPM > 1 in at least four of the eight samples. We defined negative binomial generalized linear models (GLMs), modeling the RNA-seq as count data using EdgeR library (McCarthy et al., 2012) in the R statistical package (R Core Team, 2022). Significance was determined at Benjamini-Hochberg false discovery

rate (FDR)-corrected p-values of < 0.05 . We also computed the deviance explained by CR, as the difference of the total deviance in allele-specific expression explained by the full model without the CR (only with PO and MG) and the full model including CR. The data used for this analysis can be found in Dataset S3.

Sex- and tissue-dependent CR effects

We extended the models above by including tissue-specific (sex-specific) samples of both sexes (tissues) to examine how CR interacts with sex (tissue). Sex-differences in CR effects can be due to differences in magnitude or direction, the first being variation that affects gene expression more strongly in one sex than the other and the second mutations that lead to increase in gene expression in one sex and decrease in the other (i.e. sex reversal). To be able to disentangle between the two, we defined two types of models. First, we modelled allelic-specific expression as $E \sim \mu + CR + sex + CR \times sex + \epsilon$. Second, we modeled allelic-specific expression as $E \sim \mu + CRsex + \epsilon$, CRsex being CR recoded to explicitly be contrary in the two sexes: A (B) being 0 (1) in females and 1 (0) in males. While the first strategy captures significant interactions between CR and sex, which would include both sex-differences of different magnitude and direction, the second only looks for differences in direction, explicitly giving an idea of the extent of sex reversal in CR.

The exact same strategy was applied to examine tissue differences in CR.

Extent of CR effects across sex bias levels

To examine whether the extent of CR effects differs with sex bias we compared the deviance in allele-specific gene expression explained by CR effects across genes (estimated using the negative binomial GLMs) belonging to different sex bias categories. Sex bias was determined as $SB = \log_2[(\exp_f + 1)/(\exp_m + 1)]$ for each cross and tissue separately. Genes were split into five sex bias categories: strongly male-biased (MS), $SB < -1$; male-biased (MB), $-1 < SB < -0.3$; unbiased (UB), $-0.3 < SB < 0.3$; female-biased (FB), $0.3 < SB < 1$; strongly female-biased (FS), $SB > 1$. Within-sex statistical comparisons of deviances explained across sex bias categories were done with Mann-Whitney U test in Python.

Overlap of CR effects between samples

We next examined whether the genes showing CR are the same across samples by testing the significance in the overlap between CR hits across all pairs of samples. Concretely, we defined contingency tables by determining which genes have equal CR categorization in the two samples considered: CR in both (shared CR), CR in one or the other, and non-CR in both, at $FDR < 0.05$. Next, we applied Chi-squared tests to determine the significance of the under- or over-representation of the shared CR category.

Cis- and *trans*-regulatory divergence assignment

We classified genes into various *cis*- and *trans*-regulatory categories by following the pipeline described in [McManus et al. \(2010\)](#). For this, we used allele-specific count expression data in the hybrids, and overall expression in the parentals, both of which were estimated using the ASE-Tigar pipeline described above. We made the classification separately for each sex, tissue and cross, pooling the reciprocals together (so that for each parental and hybrid we have a total of 2 and 4 samples, respectively, except for those crosses with missing data), and only using genes where the sum of estimated reads in the two parental lines was at least 20. The data used for this analysis can be found in Dataset S3. We determined whether there was a significant difference in expression between parentals (P), between the two alleles in hybrids (H) and a *trans* (T) effect for each particular gene. P and H effects were determined via statistical tests (DEseq2; [Love et al., 2014](#)). P expression was considered differential if the FDR for differential expression between the two parentals was less than 0.05. The same threshold was used to determine differential expression between the two alleles in H samples. T effects were determined by comparing allelic-specific mRNA abundance difference between the P and H samples using Fisher's exact test followed by FDR analysis, and considered significant at $FDR < 0.05$. Using a custom Python script, we classified genes into the following seven categories by comparing the significance classifications from all the three tests:

- Conserved: no significant differential expression in P or H. No significant T.
- *Cis* only: significant differential expression in P and H. No significant T.
- *Trans* only: significant differential expression in P, but not in H. Significant T.

- *Cis + trans*: significant differential expression in P and H. Significant T. $\log_2(P_1/P_2)/\log_2(A_1/A_2) > 1$. *Cis*- and *trans*-regulatory effects favor expression of the same allele.
- *Cis × trans*: significant differential expression in P and H. Significant T. $\log_2(P_1/P_2)/\log_2(A_1/A_2) < 1$. *Cis*- and *trans*-regulatory effects favor expression of the opposite allele.
- Compensatory: significant differential expression in H, but not in P. Significant T. Expression difference caused by *cis*- and *trans*-regulatory components have an opposite direction and perfectly compensate each other such that there is no expression difference in P.
- Ambiguous: significant in only one of differential expression tests in P, H or T. Thus, no explicit *cis/trans* effect can be detected.

Inheritance patterns classification

The mode of inheritance was determined for genes that are differentially-expressed across the two parental lines (with fold-difference between the two parents of at least 1.5) and where the sum of estimated reads in the two parental lines was at least 20, separately for each sex, tissue and cross, by averaging across reciprocals.

We adapted the pipeline developed by [Gibson et al. \(2004\)](#) to classify the genes into the various inheritance categories using a 1.25-fold change TPM expression cut-off between overall expression estimated by Kallisto (ignoring allele-specific expression) in parentals vs hybrids. We considered that genes whose expression in hybrids deviated from that of either parent have nonconserved inheritance, and classified them into the following categories: additive genes are those where hybrid expression was 1.25-fold greater than one parent and less than the other; overdominant (underdominant) genes were 1.25-fold greater (less) than both parents; dominant genes were only different from one of the two parents. The data used for this analysis can be found in Dataset S2.

Results

We randomly chose six *Drosophila melanogaster* inbred lines from the *Drosophila* Genetic Reference Panel ([Mackay et al., 2012](#); [Huang et al., 2014](#)) without *Wolbachia* infection and major inversions ([Huang et al., 2014](#)), and matched them pairwise:

DGRP-757 x DGRP-392, DGRP-208 x DGRP-808 and DGRP-83 x DGRP-332. For each pair, we performed both within-line crosses as well as the two between-line reciprocals, and obtained two replicated measures of sex-specific gene expression in heads and gonads for each of the four crosses per pair (see Figure S1 for a schematic representation of the experimental design).

More *cis*-variation in the testes than in ovaries and heads

We took two complementary approaches to evaluate the extent of *cis* regulatory variation in female and male heads and gonads. First, we implemented the generalized linear model of Takada et al. (2017), which models replicated allele-specific expression data in reciprocal crosses (E) as a function of *cis*-regulatory (CR) effects on expression. This method also considers potential parent-of-origin effects (PO , e.g. imprinting) and maternal genotype effects (MG , e.g. due to mitochondria or maternal RNAs deposited in the egg), which are thought to be rare in *Drosophila* (Wittkopp et al., 2006; Coolon et al., 2012; Chen et al., 2015; Takada et al., 2017), but can potentially bias estimates of *cis* variation and so are included in the model as covariates: $E \sim \mu + CR + PO + MG + \epsilon$, where μ and ϵ are the estimated average and error term. Since X-chromosomes are hemizygous in males, we focus on autosomal genes. Table S1 confirms the near absence of PO or MG effects. The detection of MG effects almost exclusively in males indicates that those might reflect X-downstream effects. In line with previous results, we found widespread CR effects, with 7.7-10.3, 7.7-8.4, 7.8-13.6 and 13.9-16.5% of genes showing significant *cis* effects in female heads, male heads, female ovary and male testis across replicate crosses. The proportion of genes that are *cis*-regulated is higher in the testis than in the other three tissues for all crosses (Figure 1, p-value < 0.05 for all Fisher's exact comparisons), showing that differences between the sexes are largely driven by the testis.

The second approach follows the pipeline developed by McManus et al. (2010), which uses allele-specific expression estimates in the hybrids together with overall expression in both parental lines to estimate both *cis*- and *trans*-regulatory effects. Specifically, genes that have the same ratio of expression between the two parental alleles in the hybrids as between the parentals themselves are likely under *cis* regulation, while genes without allelic imbalances in the hybrids given differences in expression between parentals are likely under *trans* regulation. We applied this approach to each of the tissues, sexes and crosses, using differential expression tests (DEseq2) to call differences between allelic expression in the parents and hybrids (Figure 2A,

Materials and Methods). We again found evidence of increased *cis*-regulatory variation in the testes (p-value < 0.05 for all comparisons, two-proportions z-test), while the extent of *trans* regulation was highly variable across sexes, tissues and crosses (Figure 2B). We only had two replicates per sample, which limited the power to detect differentially expressed genes. Since we found little evidence of PO and MG effects in the previous analysis (Table S1), which indicates that the reciprocal crosses behave largely as biological replicates, we used hybrids derived from reciprocal crosses as replicates for the main analysis. Importantly, we find that the main patterns hold when looking at reciprocals separately (Figure S3). The CR effects identified using both [McManus et al. \(2010\)](#) and [Takada et al. \(2017\)](#) pipelines are also highly concordant, with p-values p-value $< 1e - 16$ for all comparisons between the two (Chi-square on contingency tables as CR vs non-CR using the two methods).

The excess of *cis* variation in testis could be due to testis-specific genes harboring more genetic variants, or to genetic variants on broadly expressed genes causing more variation in gene expression in the testis. To investigate this, we inferred the extent of testis-specificity of each gene as the proportion of its total expression in the Fly Atlas 2 database ([Leader et al., 2018](#)) that came from testis. We then checked if the excess of *cis* effects (inferred using the generalized linear model) was driven by testis-specific genes. A lack of correlation between testes-specificity and CR FDR-corrected p-values (Spearman rank correlation of -0.002, 0.001 and -0.024 for each of the three crosses, and corresponding p-values of 0.881, 0.974 and 0.053) suggests that the enrichment for *cis* effects in testes is at least partly a consequence of testes-specific regulation of broadly expressed genes rather than a property of testes-specific genes. It should be noted that other tissue-specific properties, such differences in mean or variance in expression, may also contribute to the detection of an excess of CR variation in the testis.

Finally, we looked at the overlap of genes that are under CR effects across sexes, tissues and crosses (Figure S4). We find a significant overlap of CR effects between heads of the two sexes and ovaries, indicating that the standing CR genetic variation is similarly used between these tissues. However, significantly fewer genes than expected have shared CR effects in the testes and the other tissues, which presents further evidence that this tissue has its own CR landscape.

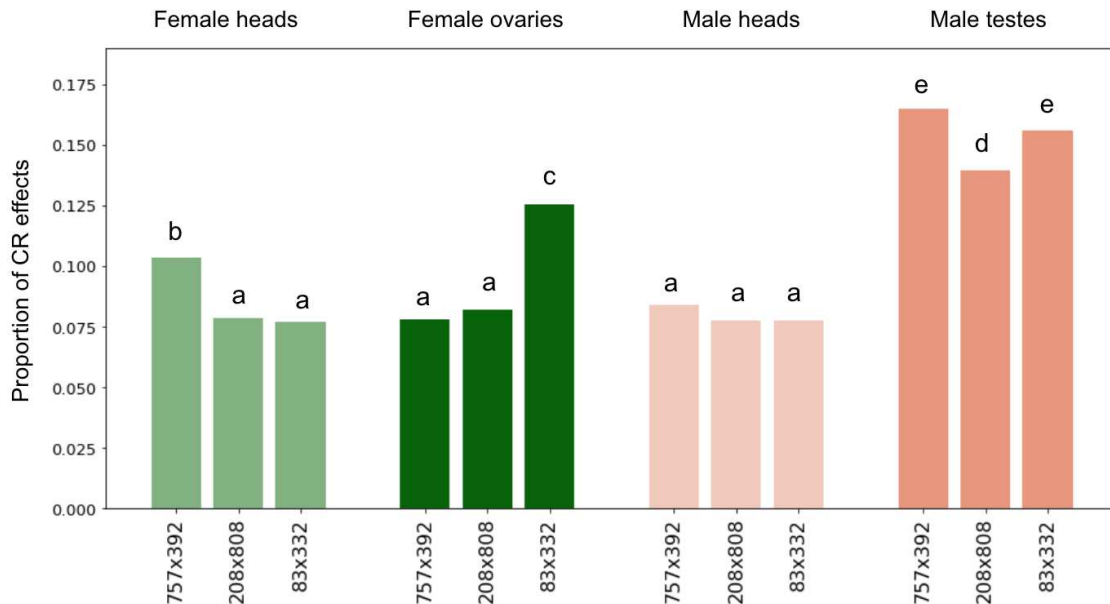


Figure 1: Sex-, tissue- and cross-specific proportion of *cis*-regulatory (CR) effects. CR effects have been determined by modeling allele-specific expression (E) as a function of CR, parent-of-origin (PO) and maternal genotype (MG) effects as $E \sim \mu + CR + PO + MG + \epsilon$, as described in Materials and Methods. Significance groups revealing differences between proportions of genes with significant CR effects across all samples (Fisher’s exact test at p-value < 0.05) are denoted by different letters (a–e).

Extensive sex-specific CR effects in the gonads

We next investigated whether there are sex differences in CR effects, i.e. if the same genetic variants affect male and female expression differently. Such “sex-by-*cis* effects” are evidence of a sex-specific regulatory architecture, and are thought to contribute to the decoupling of the genotype-to-phenotype relationship between sexes, allowing sex-specific (expression) traits to evolve independently towards their optima (e.g. [Stewart et al., 2010](#)). We detected sex differences in *cis*-regulation by modelling the sex-by-CR effect interaction on gene expression: $E \sim \mu + CR + \text{sex} + CR \times \text{sex} + \epsilon$. We detected between 7.5 and 11.1% of genes across crosses having a significant sex-by-CR effect interaction in gonads, while only a 0.3-1.1% were significant in heads, suggesting that regulatory architecture is highly shared between sexes in heads, but substantially sex-specific in gonads. This is consistent with sex differences in allelic usage being an important genetic mechanism contributing to sexual dimorphism.

Sex differences in CR effects can be of different magnitude or direction, the latter consisting of a sex-reversal in allelic-specific expression. This extreme case of

differential allelic imbalances between the sexes might be maintained by sexually-antagonistic balancing selection (Kidwell et al., 1977; Connallon & Chenoweth, 2019). We detected sex-reversal in allelic imbalance by explicitly modeling a scenario where allelic usage is opposite across sexes (see Materials and Methods). We find that sex reversal in CR effects is rare in gonads (0.1-1%) and almost absent in heads (0.0-0.1%).

We used a similar strategy to detect tissue differences in CR effects. We modelled sex-specific tissue-by-*cis* effect interaction to detect tissue differences in allelic usage and opposite allele-specific usages across tissues to detect tissue-reversal. We find a significant tissue-by-CR effect in between 4.6-7.0% of genes in females and in

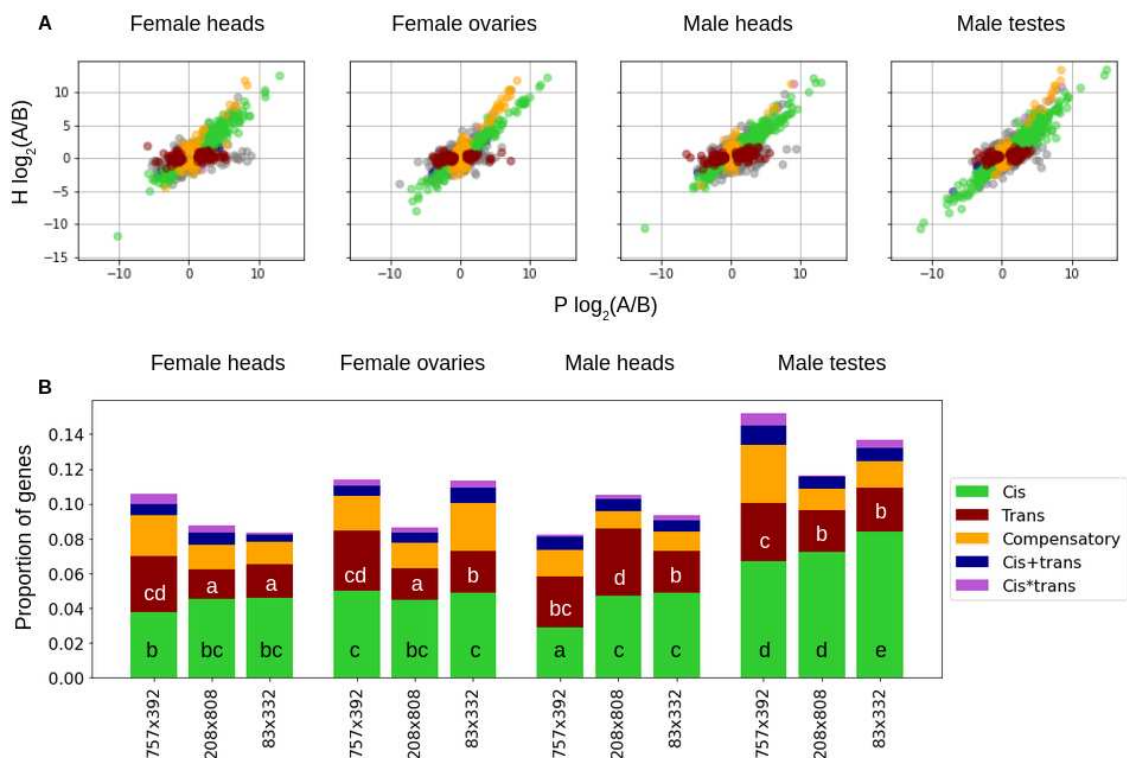


Figure 2: Patterns of *cis* and *trans* regulatory variation. (A) Scatter plots of the relative allele-specific expression levels in parental (P) vs hybrid (H, averaged across reciprocals) datasets in each sex and tissue for the cross 83x332 as a representative example (but see Figure S2 for all the plots). Each dot is a different gene and is color-coded according to the mechanism of expression regulation, inferred via hierarchical classifications based on significant expression differences in allelic expression between P and H. (B) Proportion of genes displaying each of the expression regulation mechanisms in each sex, tissue and cross. Significance groups revealing differences in proportions of genes displaying *cis* and *trans* regulation (in black and white, respectively) across all samples (two-proportions z-test at p-value < 0.05) are denoted by different letters (a-e and a-d).

10.2-13.0% of genes in males across replicate crosses. The higher extent of tissue differences in allelic usage in males is further evidence of the testes-specific CR architecture.

Sex-specific CR effects across sex bias categories

To test the hypothesis that genes of intermediate sex bias, likely under strongest sexual conflict (Cheng & Kirkpatrick, 2016) have more CR variation (Mishra et al., 2022), we determined, for each gene, how much of the deviance in their expression was explained by CR effects in our generalized linear model in both tissues and sexes separately. We then compared the distribution of the deviation explained by *cis* effects across genes of different sex bias categories in heads and gonads separately.

Figure 3 shows that, in heads, the deviance explained by CR effects forms an inverted U-shape along categories of sex bias: strongly female- and male-biased genes have very low CR variation in both female and male heads, while unbiased

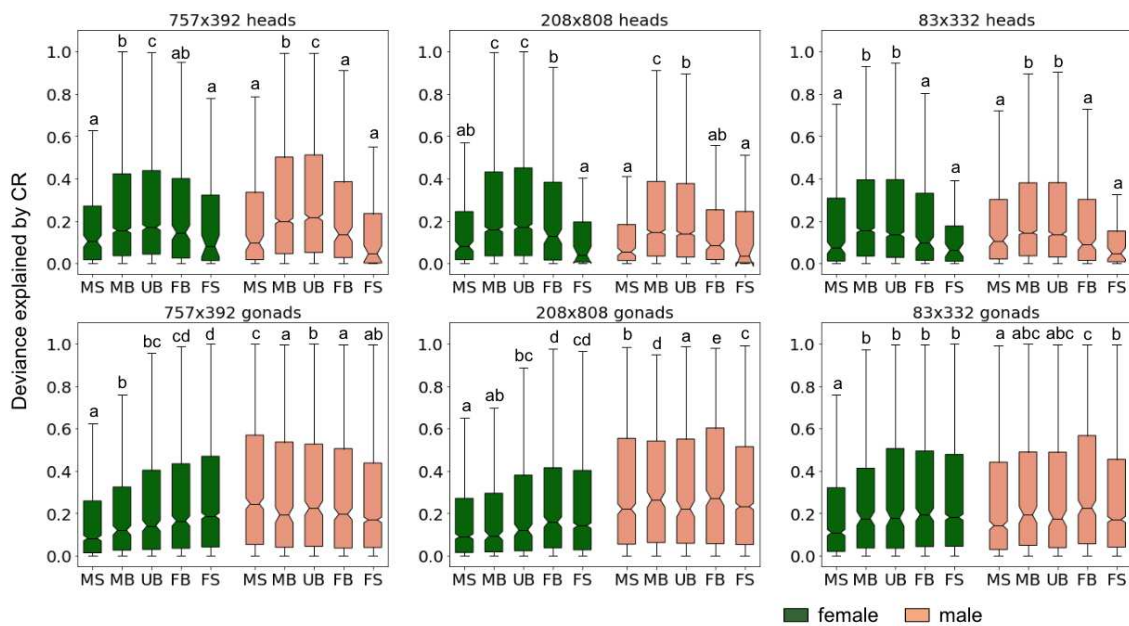


Figure 3: Deviance in allelic gene expression explained by *cis*-regulatory effects (CR) in each sex bias category for each tissue and cross in females (green) and males (orange). Each gene was classified into five sex bias categories: strongly male-biased (MS), male-biased (MB), unbiased (UB), female-biased (FB), strongly female-biased (FS). CR deviances were calculated for each sex as the deviance in allele-specific expression explained by CR while correcting for the other effects considered (see Materials and Methods). Significance groups revealing differences between sex bias groups within each cross, tissue and sex (Mann-Whitney U tests at p -value < 0.05) are denoted by different letters (a–e).

or moderately male-biased genes show the most variation. In gonads, the picture is less consistent across sexes and crosses. In the ovary, there is a decrease in CR variation in strongly male-biased genes relative to unbiased and female-biased genes. In testes, we find a symmetric pattern to that of ovaries in one of the replicate crosses (less testes *cis* variation in (strongly) female-biased genes, although this is not significant). In the other two crosses, we find the expected enrichment in *cis* variation for genes with intermediate levels of sex bias (Figure 3), but this difference is only significant for one cross.

Additive genes have more CR effects

Lastly, we tested whether there is a relationship between the molecular mechanisms of regulatory divergence and the degree of additivity of expression. We determined the degree of additivity of expression of each gene by comparing overall expression between parental and hybrid lines for each sex, tissue, and cross independently, averaging across reciprocals. Genes whose expression in hybrids deviated more than 1.25 fold from that of either parent were considered to have nonconserved inheritance and were classified in the following categories (Gibson et al., 2004; McManus et al., 2010): additive, if hybrid expression was greater than one parental and less than the other; dominant, if hybrid expression was similar to one of the two parents; and over- (under-)dominant, if hybrid expression was greater (less) than both parents.

Overall, we found that between 20.5-41.2% of genes have additive effects, 50.6-65.1% have dominance effects in both directions and between 1.0-14.0% (1.0-18.8%) have under- (over-)dominance effects (Figure S5). In agreement with previous results, we found that additive genes have more CR variation than non-additive genes, consistently in all tissues, sexes and crosses (Figure 4), although this is only significant for a subset of these. However, we did not observe an enrichment for any inheritance pattern in any sex or tissue across different types of analyses (when analyzing both reciprocals together or separately, or by using a statistical test rather than fold differences, Figures S5-7). In particular, we did not find an overall enrichment of additive effects in the testes (Figure S5), as might be expected from the observed enrichment in CR effects in this tissue. On the other hand, we did find that testes display the highest proportion of CR variation amongst additive genes (Figure 4).

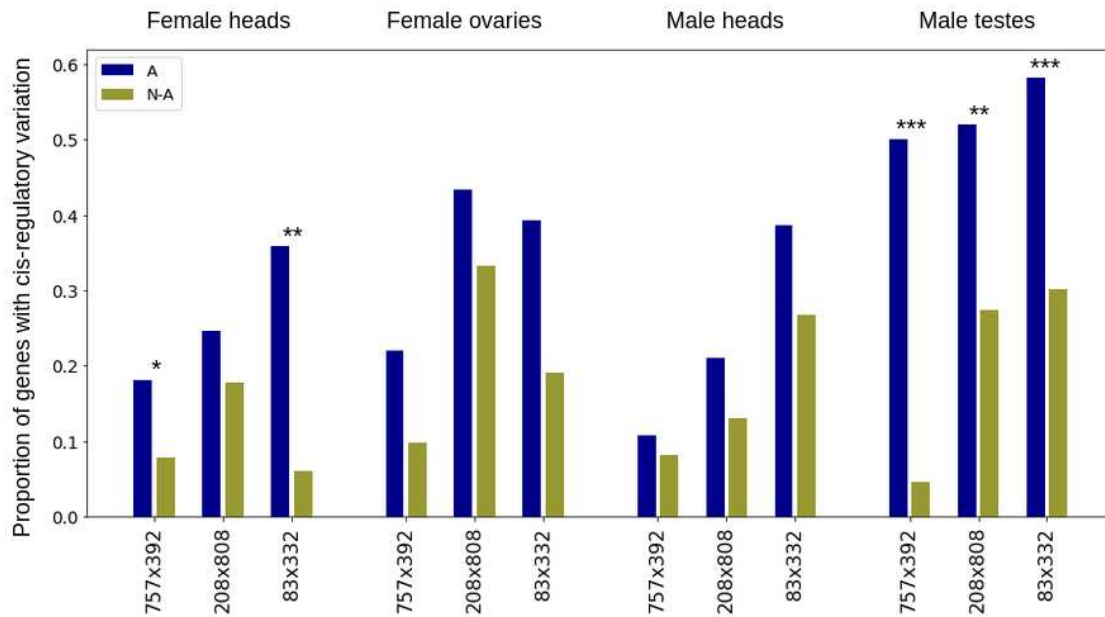


Figure 4: Proportion of additive and non-additive genes with CR divergence. Blue and ochre bars display the proportion of genes showing CR variation of those additive (A) and non-additive (N-A) for each sex, tissue and cross. Stars indicate significance in the proportion of CR effects between A and N-A genes within sample: *** (p-value > 0.001), ** (p-value < 0.01), * (p-value < 0.05) and non-significant otherwise (two-proportions z-test).

Discussion

Absence of PO and MG effects, and inconsistent *trans* regulatory effects between crosses and tissues

We estimated *cis* and *trans* effects acting on gene expression by comparing allelic expression between parental and hybrid lines in heads and gonads of *D. melanogaster* using three separate crosses between lines from the DGRP. Contrary to what has been found in other within-species studies of *cis* and *trans* regulation (Signor & Nuzhdin, 2018), we find more *cis*- than *trans*-regulatory effects. This may simply be due to our choice of threshold to call one versus the other, which is necessarily arbitrary and may introduce biases. However, this should not be an issue here, since we apply the same approach to all samples and are primarily interested in comparing the different types of regulatory effects across sexes, tissues and replicate crosses rather than providing direct quantifications of these effects. Since no clear differences between samples were found for *trans* effects, and the method of Takada

et al. (2017) applies linear modeling rather than simple cutoffs to infer *cis* effects, we focused on the results of the latter approach for the rest of the study. Their strategy detects CR together with parent-of-origin (PO) and maternal genotype (MG) effects on gene expression. In agreement with previous results (Wittkopp et al., 2006; Coolon et al., 2012; Chen et al., 2015; Takada et al., 2017) we found no PO and minimal MG effects only in males (Table S1), which suggests that the latter might reflect X-downstream effects. Overall, this confirms the fact that hybrids derived from reciprocal crosses have almost exactly the same patterns of expression in *D. melanogaster*, which is why we pooled them for the rest of the analyses.

Testis-specific regulatory architecture of gene expression

Most of the sex-specific analyses of regulatory architecture in *Drosophila* have been performed on whole bodies, which can mask the true extent of expression variation. Despite this, ample evidence was found for independent effects of *cis* variants on male and female gene expression, even when the genes involved were sex-biased in expression (Gibson et al., 2004; Coolon et al., 2013, 2015; Meiklejohn et al., 2014). Here we show that, at least for *cis* variants, these differences were most likely driven by testis-specific CR mechanisms of gene expression. Since we only sampled one somatic organ as a control (heads), it is possible that other sexually dimorphic tissues also display sex differences in allelic expression, and that sex-specific CR interactions are a more general mechanism contributing to sex-specific expression and overall sexual dimorphism. However, this effect is likely to be strongest in the testis, since, in *Drosophila*, this tissue is known to have a different regulatory architecture compared to ovary and somatic tissues (Landeem et al., 2016; Witt et al., 2021). While in the ovary expression is primarily driven by a combination of transcription factors, the more broadly open chromatin of the testis contributes greatly to expression in this tissue (Witt et al., 2021). Polymorphic SNPs have been shown to lead to substantial changes in chromatin state in various *Drosophila* tissues (Huynh et al., 2023), which potentially explains why we observe that *cis* variation in the testis is both more abundant but also affects different genes than in other tissues.

Surprisingly given the limited role of transcription factors in driving expression in the testis, we did not find a systematic reduction in *trans* effects for this tissue compared to heads or ovaries. Instead, inconsistencies in *trans* effects were detected between crosses and tissues, highlighting the limited power to draw conclusions from just a single comparison. Similarly, no clear difference was detected for the inheri-

tance patterns across the different tissues, a somewhat unexpected result given two observations: first, in crosses between *D. mauritania* and *D. simulans*, *cis* variants are more likely to have different effects in males and females (Meiklejohn et al., 2014). Second, additive changes are more likely to be controlled in *cis* (Lemos et al., 2008; McManus et al., 2010; Meiklejohn et al., 2014), a pattern which also holds for all of our crosses, such that an excess of additive variation might have been expected in the testes. While this is not the case, we do find that the relative enrichment in *cis* regulatory effects in additive genes with respect to non-additive genes is strongest in testes relative to the other tissues (Figure 4).

Selective pressures acting on sex biased expression

Following Mishra et al. (2022), we divided genes according to their level of sex bias to try to gain new insights into what selective pressures are shaping gene expression with different levels of dimorphism. Analyses within one species are limited for this purpose, as both stronger stabilizing and directional selection on expression can lead to fewer polymorphic *cis* variants, while only the latter would lead to large numbers of fixed differences between more distant populations and species. Similarly, without a clear neutral control, more frequent detection of *cis* effects for one class of genes can be diagnostic of either balancing selection (e.g. due to intralocus sexual conflict over expression levels) or decreased selective constraint. Despite these caveats, and based on our knowledge of expression divergence for different tissues, some selective scenarios appear more likely. For instance, in heads, all but the most sex-biased genes are frequently under *cis* effects in both females and males. Given the rapid turnover of sex-biased genes in heads of *Drosophila* species (Khodursky et al., 2020), one possibility is that very sex-biased genes are under stronger directional selection. However, a recent study comparing within and between species divergence of *Drosophila* head expression found no evidence of positive selection acting on sex-biased genes, and some support for balancing selection acting on the expression of female-biased genes (Khodursky et al., 2020). Furthermore, they found evidence of strong genetic correlations between male and female expression in this tissue (Khodursky et al., 2020), consistent with the near-absence of sex-by-*cis* effects in our head data. Taken together, these patterns may suggest that sexual antagonism over expression leads to the maintenance of more *cis* variants in unbiased and moderately biased genes, generally in line with the predictions of Mishra et al. (2022). Interestingly, in that study no such effect was found, with strongly female-biased genes showing more *cis* effects than other categories of sexual dimorphism. One

difference may be the distance between the parental lines used, since ours were derived from the same North American population, and theirs compared one North American and one South African. Over substantial periods of reproductive isolation, balancing selection due to sexual conflict will act to reduce divergence, and this may contribute to the difference observed here.

The patterns we obtain for gonads are more complex, and differ when we estimate *cis* effects in ovary versus testis, consistent with the prevalence of *cis*-by-sex effects in this tissue. In ovary, strongly male-biased genes harbor weaker or fewer *cis* effects than other genes. In the testis, no clear pattern emerges, with different categories of sex-biased genes harboring the highest strength of *cis* effects in the different crosses. Two hypotheses could explain why male-biased genes behave differently in the two sexes. First, testis-biased genes may be depleted of regulatory variants (leading to reduced *cis* effects in the ovary), but with each variant having a disproportionately large effect on gene expression in the testis (restoring them in the testis). Second, testis-biased genes may have normal levels of diversity at regulatory sites, but these regulatory variants do not lead to detectable changes in expression in the ovary. While the approaches used here do not infer where *cis* variants are located relative to the genes they regulate, diversity data at 5' UTRs in *D. melanogaster* and *D. simulans* does not support reduced diversity upstream of male-biased genes (if anything there may be a slight excess of variants; [Lawniczak et al., 2008](#); [Campos et al., 2018](#)). It therefore seems more likely that *cis* variants at testis-biased genes do not lead to changes in ovary expression. Whether this represents a true biological difference, or a limitation of the method to detect *cis* effects when gene expression is low, as is the case of testis-biased genes in the ovary, is currently unclear. However, it is in line with the observation that many *cis*-eQTLs that modulate male expression in *D. melanogaster* do not do so in females even if they affect genes that are expressed in both sexes ([Massouras et al., 2012](#)). In any case, we find no substantial evidence of increased *cis* variation for genes at intermediate sex-bias in the gonad, suggesting that sex differences in allelic usage in this organ may be sufficient to avoid widespread sexual conflict over expression. Furthermore, the fact that many *cis* regulatory interactions shaping testis expression do not affect expression in ovaries may partly explain why male-biased gene expression is subject to few constraints and can therefore evolve fast, in line with what is often observed. More generally, these results highlight the need for approaches that incorporate the identification of *cis* variants with their cumulative regulatory effects on genes, as well as diversity and divergence estimates, in order to fully understand the muta-

tion to *cis* effect relationship, and the selective pressures acting on expression and their regulatory variants.

Data Availability

All RNA-seq reads have been deposited to the NCBI short reads archive under bio-project number PRJNA945803. The tables of overall allele expression in parentals and hybrids as counts and TPM estimated using Kallisto are in Supplementary Datasets S1-S2, and the allele-specific parental and hybrid expression data estimated using ASE-Tigar are in Datasets S3-S4 as counts and FPKM respectively. Supplementary Datasets can be found in this link: <https://doi.org/10.15479/AT:ISTA:12933>

Acknowledgments

We thank members of the Vicoso group for comments on the manuscript, the Scientific Computing unit at ISTA for technical support and two anonymous reviewers for useful feedback.

GP is the recipient of a DOC Fellowship of the Austrian Academy of Sciences at the Institute of Science and Technology Austria (DOC 25817) and received funding from the European Union's Horizon 2020 research and innovation program under the Marie Skłodowska-Curie Grant (agreement no. 665385).

Author Contributions

GP and BV conceived the study and designed the research experiment; GP and AM obtained the experimental dataset; GP performed the data analysis; GP and BV wrote the manuscript.

References

Benowitz, K. M., Coleman, J. M., Allan, C. W., & Matzkin, L. M. (2020, July). Contributions of *cis*- and *trans*-Regulatory Evolution to Transcriptional Divergence across Populations in the *Drosophila mojavensis* Larval

- Brain. *Genome Biology and Evolution*, *12*(8), 1407–1418. Retrieved 2023-05-14, from <https://www.ncbi.nlm.nih.gov/pmc/articles/PMC7495911/> doi: 10.1093/gbe/evaa145
- Bhasin, J. M., Chakrabarti, E., Peng, D.-Q., Kulkarni, A., Chen, X., & Smith, J. D. (2008, January). Sex specific gene regulation and expression QTLs in mouse macrophages from a strain intercross. *PloS One*, *3*(1), e1435. doi: 10.1371/journal.pone.0001435
- Bolger, A. M., Lohse, M., & Usadel, B. (2014, August). Trimmomatic: a flexible trimmer for Illumina sequence data. *Bioinformatics*, *30*(15), 2114–2120. Retrieved 2023-05-15, from <https://www.ncbi.nlm.nih.gov/pmc/articles/PMC4103590/> doi: 10.1093/bioinformatics/btu170
- Bray, N. L., Pimentel, H., Melsted, P., & Pachter, L. (2016, May). Near-optimal probabilistic RNA-seq quantification. *Nature Biotechnology*, *34*(5), 525–527. doi: 10.1038/nbt.3519
- Brem, R. B., Yvert, G., Clinton, R., & Kruglyak, L. (2002, April). Genetic dissection of transcriptional regulation in budding yeast. *Science (New York, N.Y.)*, *296*(5568), 752–755. doi: 10.1126/science.1069516
- Buchberger, E., Reis, M., Lu, T.-H., & Posnien, N. (2019, June). Cloudy with a Chance of Insights: Context Dependent Gene Regulation and Implications for Evolutionary Studies. *Genes*, *10*(7), 492. Retrieved 2023-05-14, from <https://www.ncbi.nlm.nih.gov/pmc/articles/PMC6678813/> doi: 10.3390/genes10070492
- Campos, J. L., Johnston, K. J. A., & Charlesworth, B. (2018, March). The Effects of Sex-Biased Gene Expression and X-Linkage on Rates of Sequence Evolution in *Drosophila*. *Molecular Biology and Evolution*, *35*(3), 655–665. doi: 10.1093/molbev/msx317
- Chen, J., Nolte, V., & Schlötterer, C. (2015, February). Temperature Stress Mediates Decanalization and Dominance of Gene Expression in *Drosophila melanogaster*. *PLOS Genetics*, *11*(2), e1004883. Retrieved 2023-05-14, from <https://journals.plos.org/plosgenetics/article?id=10.1371/journal.pgen.1004883> (Publisher: Public Library of Science) doi: 10.1371/journal.pgen.1004883
- Cheng, C., & Kirkpatrick, M. (2016, September). Sex-Specific Selection and Sex-Biased Gene Expression in Humans and Flies. *PLOS Genetics*, *12*(9), e1006170. Retrieved 2023-05-14, from <https://journals.plos.org/plosgenetics/article?id=10.1371/journal.pgen.1006170> (Publisher:

- Public Library of Science) doi: 10.1371/journal.pgen.1006170
- Connallon, T., & Chenoweth, S. F. (2019). Dominance reversals and the maintenance of genetic variation for fitness. *PLOS Biology*, *17*(1), e3000118. Retrieved 2023-05-14, from <https://journals.plos.org/plosbiology/article?id=10.1371/journal.pbio.3000118> (Publisher: Public Library of Science) doi: 10.1371/journal.pbio.3000118
- Coolon, J. D., McManus, C. J., Stevenson, K. R., Graveley, B. R., & Wittkopp, P. J. (2014, May). Tempo and mode of regulatory evolution in *Drosophila*. *Genome Research*, *24*(5), 797–808. Retrieved 2023-05-14, from <https://www.ncbi.nlm.nih.gov/pmc/articles/PMC4009609/> doi: 10.1101/gr.163014.113
- Coolon, J. D., Stevenson, K. R., McManus, C. J., Graveley, B. R., & Wittkopp, P. J. (2012, July). Genomic imprinting absent in *Drosophila melanogaster* adult females. *Cell Reports*, *2*(1), 69–75. doi: 10.1016/j.celrep.2012.06.013
- Coolon, J. D., Stevenson, K. R., McManus, C. J., Yang, B., Graveley, B. R., & Wittkopp, P. J. (2015, October). Molecular Mechanisms and Evolutionary Processes Contributing to Accelerated Divergence of Gene Expression on the *Drosophila* X Chromosome. *Molecular Biology and Evolution*, *32*(10), 2605–2615. Retrieved 2023-05-14, from <https://www.ncbi.nlm.nih.gov/pmc/articles/PMC4592344/> doi: 10.1093/molbev/msv135
- Coolon, J. D., Webb, W., & Wittkopp, P. J. (2013, December). Sex-Specific Effects of Cis-Regulatory Variants in *Drosophila melanogaster*. *Genetics*, *195*(4), 1419–1422. Retrieved 2023-05-14, from <https://www.ncbi.nlm.nih.gov/pmc/articles/PMC3832283/> doi: 10.1534/genetics.113.156331
- Danecek, P., Auton, A., Abecasis, G., Albers, C. A., Banks, E., DePristo, M. A., ... 1000 Genomes Project Analysis Group (2011, August). The variant call format and VCFtools. *Bioinformatics*, *27*(15), 2156–2158. Retrieved 2023-05-15, from <https://doi.org/10.1093/bioinformatics/btr330> doi: 10.1093/bioinformatics/btr330
- Ellegren, H., & Parsch, J. (2007, September). The evolution of sex-biased genes and sex-biased gene expression. *Nature Reviews. Genetics*, *8*(9), 689–698. doi: 10.1038/nrg2167
- Emerson, J. J., Hsieh, L.-C., Sung, H.-M., Wang, T.-Y., Huang, C.-J., Lu, H. H.-S., ... Li, W.-H. (2010, June). Natural selection on cis and trans regulation in yeasts. *Genome Research*, *20*(6), 826–836. Retrieved 2023-05-14, from <https://www.ncbi.nlm.nih.gov/pmc/articles/PMC2877579/> doi: 10.1101/gr.101576.109

- Emerson, J. J., & Li, W.-H. (2010, August). The genetic basis of evolutionary change in gene expression levels. *Philosophical Transactions of the Royal Society B: Biological Sciences*, *365*(1552), 2581–2590. Retrieved 2023-05-14, from <https://www.ncbi.nlm.nih.gov/pmc/articles/PMC2935095/> doi: 10.1098/rstb.2010.0005
- Fear, J. M., León-Novelo, L. G., Morse, A. M., Gerken, A. R., Van Lehmann, K., Tower, J., ... McIntyre, L. M. (2016, July). Buffering of Genetic Regulatory Networks in *Drosophila melanogaster*. *Genetics*, *203*(3), 1177–1190. Retrieved 2023-05-14, from <https://www.ncbi.nlm.nih.gov/pmc/articles/PMC4937466/> doi: 10.1534/genetics.116.188797
- Gibson, G., Riley-Berger, R., Harshman, L., Kopp, A., Vacha, S., Nuzhdin, S., & Wayne, M. (2004, August). Extensive sex-specific nonadditivity of gene expression in *Drosophila melanogaster*. *Genetics*, *167*(4), 1791–1799. Retrieved 2023-05-14, from <https://www.ncbi.nlm.nih.gov/pmc/articles/PMC1471026/> doi: 10.1534/genetics.104.026583
- Glaser-Schmitt, A., Zečić, A., & Parsch, J. (2018, September). Gene Regulatory Variation in *Drosophila melanogaster* Renal Tissue. *Genetics*, *210*(1), 287–301. doi: 10.1534/genetics.118.301073
- Graze, R. M., McIntyre, L. M., Main, B. J., Wayne, M. L., & Nuzhdin, S. V. (2009, October). Regulatory divergence in *Drosophila melanogaster* and *D. simulans*, a genomewide analysis of allele-specific expression. *Genetics*, *183*(2), 547–561, 1SI–21SI. doi: 10.1534/genetics.109.105957
- Gruber, J. D., Vogel, K., Kalay, G., & Wittkopp, P. J. (2012, February). Contrasting properties of gene-specific regulatory, coding, and copy number mutations in *Saccharomyces cerevisiae*: frequency, effects, and dominance. *PLoS genetics*, *8*(2), e1002497. doi: 10.1371/journal.pgen.1002497
- GTEX Consortium, Laboratory, Data Analysis & Coordinating Center (LDACC)—Analysis Working Group, Statistical Methods groups—Analysis Working Group, Enhancing GTEX (eGTEX) groups, NIH Common Fund, NIH/NCI, ... Montgomery, S. B. (2017, October). Genetic effects on gene expression across human tissues. *Nature*, *550*(7675), 204–213. doi: 10.1038/nature24277
- Huang, W., Massouras, A., Inoue, Y., Peiffer, J., Ràmia, M., Tarone, A. M., ... Mackay, T. F. C. (2014, July). Natural variation in genome architecture among 205 *Drosophila melanogaster* Genetic Reference Panel lines. *Genome Research*, *24*(7), 1193–1208. doi: 10.1101/gr.171546.113

- Hughes, K. A., Ayroles, J. F., Reedy, M. M., Drnevich, J. M., Rowe, K. C., Ruedi, E. A., ... Paige, K. N. (2006, July). Segregating variation in the transcriptome: cis regulation and additivity of effects. *Genetics*, *173*(3), 1347–1355. doi: 10.1534/genetics.105.051474
- Huynh, K., Smith, B. R., Macdonald, S. J., & Long, A. D. (2023, May). Genetic variation in chromatin state across multiple tissues in *Drosophila melanogaster*. *PLOS Genetics*, *19*(5), e1010439. Retrieved 2023-05-14, from <https://journals.plos.org/plosgenetics/article?id=10.1371/journal.pgen.1010439> (Publisher: Public Library of Science) doi: 10.1371/journal.pgen.1010439
- Khodursky, S., Svetec, N., Durkin, S. M., & Zhao, L. (2020, June). The evolution of sex-biased gene expression in the *Drosophila* brain. *Genome Research*, *30*(6), 874–884. doi: 10.1101/gr.259069.119
- Kidwell, J. F., Clegg, M. T., Stewart, F. M., & Prout, T. (1977, January). Regions of stable equilibria for models of differential selection in the two sexes under random mating. *Genetics*, *85*(1), 171–183. doi: 10.1093/genetics/85.1.171
- Landeem, E. L., Muirhead, C. A., Wright, L., Meiklejohn, C. D., & Presgraves, D. C. (2016, July). Sex Chromosome-wide Transcriptional Suppression and Compensatory Cis-Regulatory Evolution Mediate Gene Expression in the *Drosophila* Male Germline. *PLoS biology*, *14*(7), e1002499. doi: 10.1371/journal.pbio.1002499
- Langmead, B., & Salzberg, S. L. (2012, March). Fast gapped-read alignment with Bowtie 2. *Nature Methods*, *9*(4), 357–359. doi: 10.1038/nmeth.1923
- Lawniczak, M. K. N., Holloway, A. K., Begun, D. J., & Jones, C. D. (2008). Genomic analysis of the relationship between gene expression variation and DNA polymorphism in *Drosophila simulans*. *Genome Biology*, *9*(8), R125. doi: 10.1186/gb-2008-9-8-r125
- Leader, D. P., Krause, S. A., Pandit, A., Davies, S. A., & Dow, J. A. T. (2018, January). FlyAtlas 2: a new version of the *Drosophila melanogaster* expression atlas with RNA-Seq, miRNA-Seq and sex-specific data. *Nucleic Acids Research*, *46*(D1), D809–D815. doi: 10.1093/nar/gkx976
- Lemos, B., Araripe, L. O., Fontanillas, P., & Hartl, D. L. (2008, September). Dominance and the evolutionary accumulation of cis- and trans-effects on gene expression. *Proceedings of the National Academy of Sciences of the United States of America*, *105*(38), 14471–14476. doi: 10.1073/pnas.0805160105
- Love, M. I., Huber, W., & Anders, S. (2014). Moderated estimation of fold change

- and dispersion for RNA-seq data with DESeq2. *Genome Biology*, *15*(12), 550. doi: 10.1186/s13059-014-0550-8
- Mackay, T. F. C., Richards, S., Stone, E. A., Barbadilla, A., Ayroles, J. F., Zhu, D., ... Gibbs, R. A. (2012, February). The *Drosophila melanogaster* Genetic Reference Panel. *Nature*, *482*(7384), 173–178. doi: 10.1038/nature10811
- Martin, A. R., Costa, H. A., Lappalainen, T., Henn, B. M., Kidd, J. M., Yee, M.-C., ... Bustamante, C. D. (2014, August). Transcriptome sequencing from diverse human populations reveals differentiated regulatory architecture. *PLoS genetics*, *10*(8), e1004549. doi: 10.1371/journal.pgen.1004549
- Massouras, A., Waszak, S. M., Albarca-Aguilera, M., Hens, K., Holcombe, W., Ayroles, J. F., ... Deplancke, B. (2012). Genomic variation and its impact on gene expression in *Drosophila melanogaster*. *PLoS genetics*, *8*(11), e1003055. doi: 10.1371/journal.pgen.1003055
- McCarthy, D. J., Chen, Y., & Smyth, G. K. (2012, May). Differential expression analysis of multifactor RNA-Seq experiments with respect to biological variation. *Nucleic Acids Research*, *40*(10), 4288–4297. doi: 10.1093/nar/gks042
- McManus, C. J., Coolon, J. D., Duff, M. O., Eipper-Mains, J., Graveley, B. R., & Wittkopp, P. J. (2010, June). Regulatory divergence in *Drosophila* revealed by mRNA-seq. *Genome Research*, *20*(6), 816–825. doi: 10.1101/gr.102491.109
- Meiklejohn, C. D., Coolon, J. D., Hartl, D. L., & Wittkopp, P. J. (2014, January). The roles of cis- and trans-regulation in the evolution of regulatory incompatibilities and sexually dimorphic gene expression. *Genome Research*, *24*(1), 84–95. doi: 10.1101/gr.156414.113
- Meiklejohn, C. D., Parsch, J., Ranz, J. M., & Hartl, D. L. (2003, August). Rapid evolution of male-biased gene expression in *Drosophila*. *Proceedings of the National Academy of Sciences of the United States of America*, *100*(17), 9894–9899. doi: 10.1073/pnas.1630690100
- Meisel, R. P. (2011, June). Towards a more nuanced understanding of the relationship between sex-biased gene expression and rates of protein-coding sequence evolution. *Molecular Biology and Evolution*, *28*(6), 1893–1900. doi: 10.1093/molbev/msr010
- Metzger, B. P. H., Dubeau, F., Yuan, D. C., Tryban, S., Yang, B., & Wittkopp, P. J. (2016, May). Contrasting Frequencies and Effects of cis- and trans-Regulatory Mutations Affecting Gene Expression. *Molecular Biology and Evolution*, *33*(5), 1131–1146. doi: 10.1093/molbev/msw011
- Metzger, B. P. H., Wittkopp, P. J., & Coolon, J. D. (2017, April). Evolutionary Dy-

- namics of Regulatory Changes Underlying Gene Expression Divergence among Saccharomyces Species. *Genome Biology and Evolution*, 9(4), 843–854. doi: 10.1093/gbe/evx035
- Mishra, P., Barrera, T. S., Grieshop, K., & Agrawal, A. F. (2022, September). *Cis-regulatory variation in relation to sex and sexual dimorphism in Drosophila melanogaster*. bioRxiv. Retrieved 2023-05-14, from <https://www.biorxiv.org/content/10.1101/2022.09.20.508724v1> (Pages: 2022.09.20.508724 Section: New Results) doi: 10.1101/2022.09.20.508724
- Nariai, N., Kojima, K., Mimori, T., Kawai, Y., & Nagasaki, M. (2016, January). A Bayesian approach for estimating allele-specific expression from RNA-Seq data with diploid genomes. *BMC genomics*, 17 Suppl 1(Suppl 1), 2. doi: 10.1186/s12864-015-2295-5
- Oliva, M., Muñoz-Aguirre, M., Kim-Hellmuth, S., Wucher, V., Gewirtz, A. D. H., Cotter, D. J., ... Stranger, B. E. (2020, September). The impact of sex on gene expression across human tissues. *Science (New York, N.Y.)*, 369(6509), eaba3066. doi: 10.1126/science.aba3066
- Sackton, T. B., Corbett-Detig, R. B., Nagaraju, J., Vaishna, L., Arunkumar, K. P., & Hartl, D. L. (2014, August). Positive selection drives faster-Z evolution in silkmoths. *Evolution; International Journal of Organic Evolution*, 68(8), 2331–2342. doi: 10.1111/evo.12449
- Schadt, E. E., Monks, S. A., Drake, T. A., Lusk, A. J., Che, N., Colinayo, V., ... Friend, S. H. (2003, March). Genetics of gene expression surveyed in maize, mouse and man. *Nature*, 422(6929), 297–302. doi: 10.1038/nature01434
- Signor, S. A., & Nuzhdin, S. V. (2018, July). The Evolution of Gene Expression in cis and trans. *Trends in genetics: TIG*, 34(7), 532–544. doi: 10.1016/j.tig.2018.03.007
- Smith, T., Heger, A., & Sudbery, I. (2017, March). UMI-tools: modeling sequencing errors in Unique Molecular Identifiers to improve quantification accuracy. *Genome Research*, 27(3), 491–499. Retrieved 2023-05-15, from <https://www.ncbi.nlm.nih.gov/pmc/articles/PMC5340976/> doi: 10.1101/gr.209601.116
- Stewart, A. D., Pischedda, A., & Rice, W. R. (2010). Resolving intralocus sexual conflict: genetic mechanisms and time frame. *The Journal of Heredity*, 101 Suppl 1(Suppl 1), S94–99. doi: 10.1093/jhered/esq011
- Sánchez-Ramírez, S., Weiss, J. G., Thomas, C. G., & Cutter, A. D. (2021, March). Widespread misregulation of inter-species hybrid transcriptomes due to sex-

- specific and sex-chromosome regulatory evolution. *PLoS genetics*, *17*(3), e1009409. doi: 10.1371/journal.pgen.1009409
- Takada, Y., Miyagi, R., Takahashi, A., Endo, T., & Osada, N. (2017, July). A Generalized Linear Model for Decomposing Cis-regulatory, Parent-of-Origin, and Maternal Effects on Allele-Specific Gene Expression. *G3 (Bethesda, Md.)*, *7*(7), 2227–2234. doi: 10.1534/g3.117.042895
- Team, R. C. (2022). R: A Language and Environment for Statistical Computing, Vienna, Austria. Retrieved from <https://CRAN.R-project.org/package=here>
- Whittle, C. A., & Extavour, C. G. (2017, August). Rapid Evolution of Ovarian-Biased Genes in the Yellow Fever Mosquito (*Aedes aegypti*). *Genetics*, *206*(4), 2119–2137. doi: 10.1534/genetics.117.201343
- Whittle, C. A., & Extavour, C. G. (2019, February). Selection shapes turnover and magnitude of sex-biased expression in *Drosophila* gonads. *BMC evolutionary biology*, *19*(1), 60. doi: 10.1186/s12862-019-1377-4
- Whittle, C. A., Kulkarni, A., & Extavour, C. G. (2021, August). Evolutionary dynamics of sex-biased genes expressed in cricket brains and gonads. *Journal of Evolutionary Biology*, *34*(8), 1188–1211. doi: 10.1111/jeb.13889
- Witt, E., Svetec, N., Benjamin, S., & Zhao, L. (2021, May). Transcription Factors Drive Opposite Relationships between Gene Age and Tissue Specificity in Male and Female *Drosophila* Gonads. *Molecular Biology and Evolution*, *38*(5), 2104–2115. doi: 10.1093/molbev/msab011
- Wittkopp, P. J., Haerum, B. K., & Clark, A. G. (2004, July). Evolutionary changes in cis and trans gene regulation. *Nature*, *430*(6995), 85–88. doi: 10.1038/nature02698
- Wittkopp, P. J., Haerum, B. K., & Clark, A. G. (2006, July). Parent-of-origin effects on mRNA expression in *Drosophila melanogaster* not caused by genomic imprinting. *Genetics*, *173*(3), 1817–1821. doi: 10.1534/genetics.105.054684
- Wittkopp, P. J., Haerum, B. K., & Clark, A. G. (2008, March). Regulatory changes underlying expression differences within and between *Drosophila* species. *Nature Genetics*, *40*(3), 346–350. doi: 10.1038/ng.77
- Zhang, X., Cal, A. J., & Borevitz, J. O. (2011, May). Genetic architecture of regulatory variation in *Arabidopsis thaliana*. *Genome Research*, *21*(5), 725–733. doi: 10.1101/gr.115337.110

CHAPTER 3

Characterizing the regulatory architecture of sex differences in expression via sex bias eQTL analysis in heads and gonads of *Drosophila melanogaster*

Gemma Puixeu, Christine Syrowatka, Ariana Macon, Luísa Scolari,
Nick Barton and Beatriz Vicoso

Abstract

Sex-specific selective forces acting on a shared genome lead to a sexual conflict of interests. Resolution of sexual conflict relies on sex linkage and sex-specific expression of shared genomic regions. Since most of the genome is shared between sexes, sex bias in gene expression is thought to be the main mechanism underlying sex differences, so the study of its molecular basis is key to understanding the selective forces as well as evolutionary dynamics of phenotypic dimorphism.

So far, most of our understanding of the molecular basis of sex differences in expression, particularly in *Drosophila*, has relied on the comparison of sex-specific eQTL analyses using whole body data, which is suboptimal. On the one hand, because gene expression, as well as its regulatory variation is highly tissue-dependent. On the other hand, because the comparison of sex-specific eQTL analyses, revealing sex differences in regulatory architecture, is not directly informative of the genetic basis of sex differences in expression.

In this study we propose an alternative approach, exactly to this end: sex bias eQTL analyses, whereby we find genetic variation associated with expression differences across sexes explicitly in F1 crosses between *Drosophila melanogaster* inbred lines, separately for heads and gonads. Consistently with its higher phenotypic dimorphism, we find that gonads have more sex biased gene expression, as well as more sex-specific regulatory variation than heads. We find that most variation underlying sex differences in expression acts in a male-specific manner, and scarce evidence of sex-biased and sexually-antagonistic associations underlying sex biased expression. Finally, we detect evidence that intersex correlation acts to constrain sexual dimorphism evolution.

Introduction

Females and males are often subject to different selective pressures arising from divergent ecological niches and reproductive interests. This can lead to both sex-specific natural and sexual selection on traits that have a shared genetic basis between them, causing a genetic “tug of war” known as intralocus sexual antagonism (Bonduriansky & Chenoweth, 2009). The resolution of this conflict occurs via mechanisms that allow phenotypic decoupling of a single genome in a sex-specific manner (i.e. the evolution of sexual dimorphism) which, broadly, involve sex-linkage and sex-biased expression (Griffin et al., 2013; Mank, 2017). The first implies genetic linkage of sexually-antagonistic alleles to sex-determining regions (Dean & Mank, 2014; A. E. Wright et al., 2017); the second refers to differential expression of shared regions under conflict, which encompasses sex-specific expression both at the transcriptional and post-transcriptional level, sex-specific splicing and expression of gene duplicates or imprinting (Williams & Carroll, 2009; Stewart et al., 2010; Singh & Agrawal, 2023). While sex linkage is limited to loci with differential representation in both sexes (e.g. sex chromosomes or mitochondrial and chloroplast DNA), sex-specific expression of the shared genes is likely the main mechanism for resolving sexual conflict across the vast majority of the genome and, so, thought to be responsible for most sex differences (Jiang & Machado, 2009; Stewart et al., 2010; Mank, 2017). Therefore, the study of the molecular basis of sexual dimorphism, of which we still lack thorough understanding, can help us gain insights into the selective forces and evolutionary dynamics underlying sex-specific adaptation.

Several studies have shown that the expression of a large proportion of genes is sex-biased across a range of taxa (reviewed in Ellegren & Parsch, 2007; eg. Jin et al., 2001; Gibson et al., 2004 in *Drosophila*; Rinn & Snyder, 2005 in mammals; Mank et al., 2008 in birds; Hartman et al., 2021 in humans), and a few others have characterized the genetic basis of such differences (eg. Massouras et al., 2012; Huang et al., 2015, 2020; Pallares et al., 2023 in *Drosophila*; Stranger et al., 2007; Dimas et al., 2012; GTEx Consortium, 2020; Oliva et al., 2020 in humans; Bhasin et al., 2008; Gonzales et al., 2018 in mice). Outside of vertebrates, particularly in the model *Drosophila* (Massouras et al., 2012; Huang et al., 2015, 2020; Everett et al., 2020), most sex-specific eQTL analyses, aimed at the discovery of genetic variants that are associated with sex-specific gene expression variation, were performed on whole bodies. However, the resolution achievable and the scope of questions that can be answered with this type of data are very limited because each tissue has different

(sex-specific) expression patterns (Stamboliyska & Parsch, 2011; Leader et al., 2018; Urbut et al., 2019; Oliva et al., 2020) and regulatory mechanisms (Urbut et al., 2019; Oliva et al., 2020). Also, studies of the genetic variation underlying sexual dimorphism across tissues can provide information about molecular mechanisms driving sexually-dimorphic development and their evolutionary dynamics. For instance, it has been suggested that the speed of sexual conflict resolution via evolution of sex bias in gene expression is faster in tissues with pre-existing sexually-dimorphic regulatory elements (driven by, for example, sex hormone receptors or sex-linked –in Y/W chromosomes– transcription factors; D. B. Wright, 1993; Bonduriansky & Rowe, 2005; Stewart et al., 2010). Across *Drosophila* species, there is evidence that the persistent expression of genes in the sex determination cascade leads to the development of sexually-dimorphic structures (Williams & Carroll, 2009; Rice et al., 2018). Joint analyses of the molecular patterns of sex and tissue dimorphism are needed to understand whether the regulatory variation driving phenotypic plasticity is reused across sexes and tissues, or whether the mechanisms leading to sex and tissue expression differences are different, as currently suggested (Gordon & Ruvinsky, 2012; Oliva et al., 2020).

Whether or not sexual conflict plays a role in shaping the long-term evolution of sex-biased genes depends on how easy it is to decouple expression between the two sexes, which relies on the genetic architecture underlying (sex-specific) gene expression. Specifically, several studies have shown that the potential for sexually-dimorphic adaptation depends on the variance-covariance (G) matrix between traits and across sexes underlying phenotypic expression. Concretely, we have theoretical evidence that intersex correlation quantitatively constrains sexual dimorphism evolution by determining its evolutionary rate (Lande, 1980, 1987; Chapter 4 of this thesis). This idea is supported by a general negative correlation between intersex correlation and sex differences observed across traits and species (Delph et al., 2004, 2010; Bonduriansky & Rowe, 2005; McDaniel, 2005; Poissant et al., 2010), including gene expression in *Drosophila* (Griffin et al., 2013). More mechanistically, it is generally assumed that traits with a high (low) intersex correlation will hardly (easily) evolve to be dimorphic (Stewart et al., 2010), which is consistent with the hypothesis that intersex correlation for gene expression should be lower in gonads than in heads, where it has already been observed to be high (Khodursky et al., 2020).

Another aspect of the genetic architecture that is expected to influence the ability

for the two sexes to diverge is the amount of mutations underlying gene expression variation. For infinitesimal or highly polygenic traits with imperfect intersex correlation, sexual conflict is always expected to be resolved given enough time (Lande, 1980, 1987; Chapter 4 of this thesis). On the other hand, oligogenic traits underlied by very few mutations are more constrained and gene expression is expected to remain unbiased for longer (Haldane, 1962; Rhen, 2000), generating potential for longer-term sexual conflict (Cheng & Kirkpatrick, 2016; Ruzicka et al., 2019).

eQTL analyses are a powerful tool to study the genetic architecture underlying gene expression variation, because they allow the characterization of particular mutations affecting (sex-specific) gene expression. Analyzing which types of genes are more likely to be sex biased, and which mutations account for variation in sex differences in expression, can also shed light on the selective forces that are acting on sex biased gene expression and its regulatory variation (eg. Simons et al., 2018). Generally, positive and negative selection should decrease the amount of polymorphic variation within a population, while balancing selection should lead to their maintenance. So, while it is often assumed that genes with sexually dimorphic expression should be associated with most sex-specific eQTL variation, it is unclear whether this prediction should hold: if sex bias resolves sexual conflict, genes with intermediate sex bias levels should be subject to stronger balancing selection (Cheng & Kirkpatrick, 2016) and therefore may present more genetic variation than sex biased genes. This is consistent with theoretical models of stabilizing selection showing that mutations accounting for most sexual dimorphism should be fixed and therefore not contribute to variation at steady state (Reeve & Fairbairn, 2001; Chapter 4 of this thesis), and also with the observation that the degree of sex bias in gene expression does not substantially differ between genes with and without sex differences in regulatory architecture (Dimas et al., 2012; Oliva et al., 2020).

The mode of action and respective frequency of eQTLs associated with sex bias are also key parameters for understanding the evolution of dimorphism: mutations that generate variation for sex bias can be sex-specific, sex-biased (affecting both sexes in the same direction but different magnitudes) and sexually-antagonistic (affecting expression in both sexes in opposite directions). The prevalence of each type of mutation depends on how likely they are to arise as well as their persistence times after selection operates. We predict that sex-specific mutations should account for most variation underlying sex differences in expression, since newly arising mutations with sex-specific effects are predicted to be common, particularly for

sexually-dimorphic tissues (Stewart et al., 2010). They are further expected to account for twice as much genetic variation in the respective sex as mutations affecting both sexes would because they are under selection only half of the time, assuming directional selection (Morrow & Connallon, 2013). On the other hand, sexually-antagonistic mutations are expected to arise only rarely, and become fixed (lost) very fast if they generate sex bias in (against) the direction of selection (Muralidhar & Coop, 2023). This is consistent with only rare evidence of sexually-antagonistic mutations for gene expression variation (Dimas et al., 2012; Meiklejohn et al., 2014; Oliva et al., 2020), although theoretical work suggests that they might have an important contribution to sex-specific phenotypic variation (e.g. Connallon & Clark, 2014).

The genetic variants that explain variation for sex bias and sex-specific gene expression can act in *cis* or in *trans*. While *cis* variants act by affecting the expression of linked genes (e.g. mutations at promoters or enhancers), *trans*-acting variants can affect the expression of both copies of close or distant genes by, for example, changing the activity or expression of a transcription factor (Signor & Nuzhdin, 2018). The estimated prevalence of *cis*- vs *trans*-acting mutations depends on the scope of the analysis. Concretely, *cis*-acting eQTLs seem to disproportionately contribute to differences between species (Wittkopp et al., 2008; Coolon et al., 2014; Metzger et al., 2017), and tend to have more differential effects between sexes when introgressed from another species (Meiklejohn et al., 2014), while *trans*-acting eQTLs account for most variation within species, including variation across tissues (Grundberg et al., 2012; GTEx Consortium et al., 2017) and sexes (Bhasin et al., 2008; Meiklejohn et al., 2014; Porcu et al., 2022). Further characterization of the genetic variation for sex differences in expression into *cis*- and *trans*-acting can provide useful insights into its mode of action as well as evolutionary processes shaping it, and how this might differ between more or less sexually-dimorphic tissues.

So far, most of our understanding of the genetic basis of sex differences in expression has derived from sex-specific eQTL analyses, i.e. by comparing male- and female-specific eQTL associations, which reveal significant decoupling of the regulatory architecture between the two sexes (e.g. Bhasin et al., 2008; Dimas et al., 2012; Massouras et al., 2012; Huang et al., 2015). However, while this widely-used approach can shed light on the differences in regulatory variation across sexes, it is not directly informative about the genetic variation leading to sex differences in expression. First, because independent sets of analyses with different statistical

specifications are run for each sex, leading to results that are not directly comparable. Second, because this approach lacks the power to discover subtle but potentially functionally relevant variants. For example, it cannot detect QTLs that generate variation for sex differences in expression by affecting gene expression weakly in absolute terms but by a significantly different amount across sexes. Third and most crucially, because previous studies reported evidence that genes with sex-specific eQTL regulation (genes whose expression is regulated by different eQTLs in the two sexes) are not more sex-biased than genes with shared regulatory variation between sexes (Dimas et al., 2012; Oliva et al., 2020), which suggests that sex differences in expression regulation do not primarily lead to sex differences in expression levels.

A more statistically-correct and powerful alternative to characterize the genetic variation in sex differences in expression would involve detecting sex bias eQTLs, i.e. by running eQTL analysis using sex bias in gene expression (measured as the binary logarithm of the ratio between female and male gene expression, referred to throughout as sex bias), as a direct measure of sex differences in expression, as our phenotype. This is a strategy that has not been used before, likely because it ideally relies on having sex-specific expression values per genotype, which can only be obtained for homozygous lines in inbred populations. This is suboptimal: first because this is unavailable for wild, outbred populations; second, because inbred lines present reduced genetic variation and might display patterns of (sex-specific) gene expression and overall phenotypic variation that are not representative of those of wild populations (Charlesworth & Willis, 2009; Zhao et al., 2019).

In this study, we characterize various aspects of the genetic basis of sex differences in expression using a newly-generated expression dataset specifically tailored to circumvent some of these caveats. Specifically, we obtained replicate sex-specific gene expression data in heads and gonads of 95 F1 crosses between inbred lines of the *Drosophila* Genetic Reference Panel (DGRP, Mackay et al., 2012; Huang et al., 2014). The DGRP contains around 200 *Drosophila melanogaster* lines that have been generated by successive inbreeding of individuals sampled from an originally outbred population from Raleigh, USA, over 20 generations. These lines have been genotyped for around 6 million genome-wide SNPs and phenotyped for multiple traits, including gene expression. Their patterns of genetic (Mackay et al., 2012; Huang et al., 2014) as well as their association with phenotypic variation (e.g. Hoffman et al., 2014; Lecheta et al., 2020; Wilson et al., 2020, reviewed in Mackay & Huang, 2018), including gene expression (Huang et al., 2015), have been described,

which makes them a great tool for further characterization of genetic variation. However, they are highly inbred. By using first-generation crosses between lines, we make sure that the F1 individuals are heterozygous themselves, and thus free from inbreeding depression and its potential effects on phenotypic as well as gene expression variation, but still genetically identical within each line, allowing us to obtain a measure of sex bias per genotype, as is essential for our analysis. Also, while other studies of eQTL variation in the DGRP have used expression in whole bodies (Huang et al., 2015, 2020; Everett et al., 2020), we obtain tissue-specific expression data, allowing us to compare patterns of sex bias as well as its regulatory variation in heads and gonads. Other work has looked at eQTL variation in *Drosophila* heads (King et al., 2014; Pallares et al., 2023) but, to our knowledge no study to date has examined the regulatory variation of gene expression in the gonads of this species. Importantly, our approach relies on an absence of maternal genotypic (MG) and parent-of-origin (PO) effects in gene expression, as each line is crossed only once either as maternal or paternal. Although an absence of MG and PO effects has been reported by previous studies in *Drosophila* (Wittkopp et al., 2006; Coolon et al., 2012; Chen et al., 2015; Takada et al., 2017), we explicitly confirmed this pattern using within- and reciprocal between-line crosses across a subset of the DGRP lines in a previous study (Chapter 2 of this thesis).

By comparing the results obtained via sex bias eQTL analyses with traditional sex-specific eQTL analysis, we present a comprehensive study addressing various open questions on the tissue-specific genetic basis of sex differences in expression.

Materials and methods

Sample preparation and sequencing

We obtained sex-specific replicated gene expression for heads and gonads from F1 crosses between *Drosophila melanogaster* inbred lines. Specifically, we randomly paired 190 lines from the DGRP into 95 crosses, each line being crossed just once to another line, either as maternal or paternal. About 53% of the DGRP lines are infected with *Wolbachia pipientis* (Huang et al., 2014), which is a maternally-transmitted endosymbiotic bacterium which infects 20% of insects. Although the full range of *Wolbachia* effects on physiology and generally quantitative trait expression is unknown, it has been shown to manipulate host biology to increase production of infected females (Hoffmann et al., 1986), and it is expected to affect gene expression

patterns (Huang et al., 2015). We ensured that the F1 lines are free from *Wolbachia* infection by pairing the infected lines as paternal. All the maternal lines were PCR-tested to ensure absence of infection, after treating the few *Wolbachia*-positive lines to be crossed as maternal with Tetracycline.

Crosses were set up in vials containing 40 males and 40 virgin females (between 1 and 5 vials depending on the number of individuals that could be obtained), at 23°C under a 12 hours light / 12 hours dark cycle. For each cross, we then dissected two replicate samples of heads and gonads of 20 4-day-old virgin females and virgin males for each cross, obtaining a total of 760 samples. The experimental design is outlined in Figure 1A. Samples were flash frozen in liquid nitrogen and kept at -80°C until further processing. RNA was then extracted with a Maxwell® RSC Simply RNA Tissue Kit (Promega). The whole array of samples was divided into three Smart-seq2 RNA-seq libraries, which were produced from the tagged and pooled samples at the Vienna Biocenter Sequencing Facility, and sequenced on an Illumina Novaseq machine (single end 100bp reads).

Data processing and gene expression estimation

We obtained demultiplexed data for each of the three libraries, each containing 268, 246 and 244 samples (for a total of 758 samples; two were missing at the moment of the plating: 392F x 176M female heads R2 and 392F x 176M female ovaries R2). We trimmed the data using Trimmomatic (Bolger et al., 2014) and performed UMI-based deduplication using UMI-tools (Smith et al., 2017). We estimated overall count and TPM (transcripts per million) expression for each transcript using Kallisto (Bray et al., 2016). Three further samples were removed because of their low correlation to other samples of the same tissue after processing: 195F x 730M male head R1, 373F x 513M male testes R2 and 195F x 730M female heads R2 (Spearman correlation < 0.8). All subsequent analyses were done without these five samples.

We summed TPM per transcript across isoforms to obtain expression levels per gene, and averaged expression across the two replicates. To avoid biases in males and for consistency in females, X-linked genes were removed, so only autosomal data was used for all the analyses. We quantile-normalized the final dataset across samples of both tissues and sexes together.

eQTL analyses

We ran eQTL analyses using sex-specific as well as sex bias in expression per tissue as phenotypes using our newly-generated gene expression dataset. The tissue- and sex-specific phenotypic files correspond to the binary logarithm of expression averaged across replicates, for those genes with $\text{TPM} > 1$ across all lines per tissue. Sex bias was computed per tissue as the binary logarithm of female over male expression, $\log_2(\text{exp}_f/\text{exp}_m)$, for those genes with $\text{TPM} > 1$ across all lines in both sexes. Thus, we are eliminating sex-specific genes and only considering genes expressed in both sexes per tissue for our analyses of sex bias (see Figure 1B,C for the tissue-specific sex bias distribution). We combined the genotypic data (BED, BIM and FAM files downloaded from the DGRP website) of the two parents by taking the maternal and paternal genotype at each position to obtain the genotype files of the heterozygous F1 crosses. We considered only autosomal SNPs with a minor allele frequency (MAF) > 0.05 across haplotypes.

We used PLINK (Purcell et al., 2007) to run eQTL analyses for six conditions: female head, male head, sex bias head, female ovaries, male testes and sex bias gonad. Concretely, we linearly regress \log_2 expression on SNP status in each sex (and the difference between sex-specific \log_2 expression for sex bias), separately for every gene and SNP. For each association, we obtain its direction (regression coefficient), effect size (coefficient of determination) and significance (p-value). We compute false discovery rate (FDR) using the Benjamini-Hochberg correction method, and select significant associations between SNPs and genes at $\text{FDR} < 0.05$.

Results

We obtained sex-specific gene expression data in heads and gonads of 95 F1 crosses between 190 *Drosophila melanogaster* inbred lines from the DGRP (see Figure 1A for a schematic representation of the experimental design). We used this newly-generated dataset to run eQTL analyses on female and male expression as well as on sex bias, computed as $\log_2(\text{exp}_f/\text{exp}_m)$, for heads and gonads separately. We compare the results of eQTL analyses across the various conditions to characterize the tissue-specific patterns of sex differences in expression, as well as its regulatory variation.

More sex bias in gonads than in heads

We first assessed sex-specificity of gene expression in heads and gonads. We define genes as female (male)-specific if they are expressed at $\text{TPM} > 1$ in females (males) and $\text{TPM} < 1$ in males (females), and shared if they are expressed at $\text{TPM} > 1$ in both sexes. We find more sex-specific genes in gonads (1,591 female-specific, 1,708 male-specific and 3,992 shared genes) than in heads (219 female-specific, 255 male-specific and 5,616 shared genes). A higher degree of sex-specific expression in the gonads is expected given the higher levels of phenotypic sexual dimorphism in gonads than in heads.

We examine the sex bias of those genes that are shared between sexes per tissue ($\text{TPM} > 1$ in both, thus excluding genes previously determined as sex-specific), computed as the binary logarithm of female over male expression. Concretely, we determined that genes are sex biased if they show a twofold expression in one of the two sexes over the other. As also expected, we observe more sex biased genes in the gonads (2,683) than in heads (54), as is illustrated by a wider sex bias distribution in gonads than in heads (Figure 1B,C). While this distribution is relatively symmetrical in the heads (34 and 20 female- and male-biased genes), there are more female-biased (2,174) than male-biased (509) genes in the gonads. This indicates that of the genes that are expressed in gonads of both sexes, more have higher ovary than testes expression.

The regulatory variation underlying sex-specific and sex bias in head and gonad gene expression in *D. melanogaster*

We next characterized the genetic variation underlying sex-specific and sex bias in gene expression. To do so, we defined linear models regressing gene expression on SNP status, independently for each SNP and gene using PLINK, and selected significant associations at a Benjamini-Hochberg $\text{FDR} < 0.05$. A separate analysis was run in each of the following conditions: female heads, male heads, female ovaries, male testes, sex bias heads (i.e. using $\log_2(\text{female/male})$ head expression as the phenotype), and sex bias gonads.

Only a small subset of all the autosomal 1,394,283 SNPs considered act as eQTLs (are associated with expression of at least one gene) in each condition, with eQTLs underlying sex bias in heads yielding the lowest count (7,636, representing 0.55% of all SNPs, while for the other analyses between 4.61-9.16% of SNPs act as eQTLs; Table 1). The percentage of eQTL-genes (genes with at least one associated eQTL)

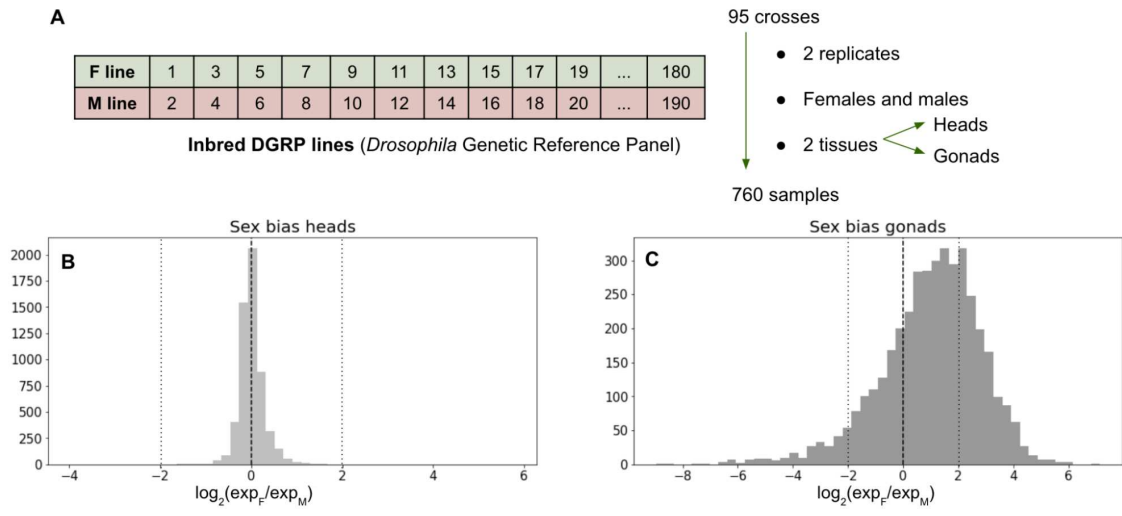


Figure 1: On the expression dataset. A: Experimental outline: we obtained replicate expression for heads and gonads in females and males of 95 F1 crosses between 190 inbred *Drosophila melanogaster* lines from the DGRP. B and C: Distribution of sex bias ($SB = \log_2(\bar{e}_f/\bar{e}_m)$, where \bar{e}_f and \bar{e}_m are sex-specific averages across lines for each gene) in heads and gonads for genes expressed at $TPM > 1$ in both sexes (thus excluding sex-specific genes, see main text). The dashed vertical lines indicate the threshold at which we are classifying genes as female- ($SB > 2$) and male-biased ($SB < -2$).

ranges between 9.29-25.14%, with sex bias heads and male testes respectively having the lowest and highest percentages (Table 1. When we consider specific eQTL-gene associations (associations between particular eQTL and gene pairs) we find that, while we have a similar number of associations in the two sexes in heads (116,167 in females and 99,894 in males), there are almost twice as many associations in testes (260,597) than ovaries (140,640; Table 1, Figure 2). While the total number of associations for sex bias in gonads is similar to the number of sex-specific associations in both tissues, the counts are much lower for sex bias heads (12,966 vs 89,341-260,966 in the rest of the conditions; Table 1) which, again, reflects the lower sex bias in this tissue, as well as a similar regulatory architecture across sexes.

We consider associations in *cis* if SNPs are located within 10kb of the genes that they regulate, and in *trans* otherwise. Using this threshold, we find that the vast majority of associations acts in *trans*, with a percentage of *cis* associations of around 2% consistently across analyses (with the exception of sex bias associations in heads, for which the proportion of *cis*-associations is only 0.48% (Table 1).

We detect evidence of high pleiotropy in sex-specific and sex bias regulatory architecture. Concretely, we find that the distribution of eQTLs associated with each

	N genes	N (%) eQTLs	N (%) eQTL-genes	N associations	N (%) <i>cis</i> associations
Female heads	5,836	80,997 (5.81)	1,231 (21.10)	116,167	2,215 (1.91)
Male heads	5,871	76,645 (5.50)	1,259 (21.44)	99,894	2,600 (2.60)
Female ovaries	5,583	101,192 (7.26)	914 (16.37)	140,640	1,934 (1.38)
Male testes	5,700	127,744 (9.16)	1,433 (25.14)	260,597	5,209 (2.00)
Sex bias heads	5,616	7,636 (0.55)	522 (9.29)	12,966	62 (0.48)
Sex bias gonads	3,992	64,297 (4.61)	655 (16.41)	89,341	1,790 (2.00)

Table 1: Summary of eQTL results for each analysis. N genes are the total amount of genes analyzed per sample (autosomal with TPM > 1 across all lines); N (%) eQTLs are the amount (percentage) of SNPs associated with expression of at least one gene; N (%) eQTL-genes are the amount (percentage) of genes whose expression is associated with at least one eQTL; N associations are the amount of associations between specific eQTL-gene pairs; N (%) *cis* associations are the amount (percentage) of associations acting in *cis* (eQTLs located within 10kb of the gene). We report significant results at an FDR < 0.05.

eQTL-gene is very right-skewed: while the expression of most genes is affected only by a few eQTLs, some genes have thousands of associated eQTLs, for all analyses (Figure S1). Similarly, we find that some eQTLs affect the expression of multiple genes (Figure S2). Here, we find a substantial difference in the distribution of the number of genes associated with *cis* and *trans*-acting associations: eQTLs can affect the expression of dozens of genes in *trans*, while when acting in *cis* they only affect expression of the gene(s) they are on (Figure S2), consistently with previous studies across species (Brem et al., 2002; Hughes et al., 2006; Gruber et al., 2012). Also the effect size distribution differs between *cis* and *trans* eQTLs, with average effect size ranging between 0.30-0.32 and 0.18-0.22 across analyses, respectively (Figure S3), also consistently with previous results (Brem et al., 2002; Hughes et al., 2006; Bhasin et al., 2008; Gruber et al., 2012; Metzger et al., 2016).

The modus operandi of sex bias eQTLs

By comparing the eQTL variation detected in sex-specific as well as sex bias analyses we can get a better picture of the mode of action of the regulatory architecture generating sex differences in expression. We therefore looked at the overlap between the different kinds of eQTL-gene associations (those identified in the female- and male-specific analyses, and those identified in the sex bias analysis) in each tissue separately (Figure 2A).

First, we find that only few associations are shared between the sexes (fm and s-fm categories in Figure 2A) in gonads (6,756, being 4.80 and 2.60% of total associations in females and males), while many are shared in heads (43,572, representing 37.51 and 43.62% of total female- and male-acting associations). This, together with the result that there are many more sex bias eQTLs as well as eQTL-gene associations in gonads than in heads (Table 1, Figure 2A), supports the idea that the greater extent of sex-biased expression observed in gonads is associated with decoupled regulatory architectures between the sexes.

Second, we examine the modus operandi of eQTL-gene associations that affect sex bias to quantify the proportion of sex-specific, sex-biased and sexually-antagonistic associations generating variation for sex bias (referred to as sex bias associations), as well as the amount of sex bias associations that are not found in sex-specific analyses (Figure 2B). Associations generating variation in sex bias by affecting expression in only one sex (corresponding to categories s-f and s-m in Figure 2A and to “sex-specific” in Figure 2B; illustrated for one example in Figure S4) account for about a third of sex bias associations in heads, and two thirds in gonads. Interestingly, most of those are male-specific, suggesting that much of the variation for sex differences in expression acts in a male-specific manner. While this holds for both tissues, it is most pronounced in gonads. Generally, we find that only a relatively small proportion of the associations that are only found in one of the two sexes are also associated with sex bias, representing 1.49 and 2.85% of female and male associations in heads and 7.96% in ovaries, while these are substantially larger for testes (20.09%). This overall suggests that most sex differences in regulatory architecture are not associated with sex differences in expression.

Associations generating variation for sex bias by affecting expression in the two sexes in the same direction but with different magnitudes (corresponding to a subset of s-fm category in Figure 2A and to “sex-biased” associations in Figure 2B; illustrated in Figure S5) are rare both in heads (10) and gonads (16). We detect few

associations generating variation for sex bias by increasing expression in one sex and decreasing it in the other (corresponding to the rest in the s-fm category in Figure 2A and to “antagonistic” associations in Figure 2B; see Figure S6 for an example), exclusively in gonads, indicating that those are generally very rare. We looked at the sexually-antagonistic associations generating variation for sex bias in gonads in more detail. Of those 21 associations, 17 affect expression in one particular gene, all in *cis* (see Figure S6 for the respective Manhattan plot). This gene is Threonyl-carbamoyl synthesis 5 (Tcs5, FBgn0035590) which encodes an atypical Ser/Thr kinase part of the KEOPS/EKC complex. It phosphorylates the product of p53 and is regulated by the products of Akt and Rab35. It is involved in tRNAs modification, telomere and chromatin dynamics (from Flybase, Gramates et al., 2022).

We also find a significant amount of sex bias eQTLs which are not detected in sex-specific analyses, these representing a higher percentage of the total amount of sex bias eQTLs in heads (64.6%) than in gonads (28.8%; category s in Figure 2A,B). This suggests that comparing the results of sex-specific analyses provides only a partial picture of the variation underlying sex differences in expression.

Last, we find very little overlap between associations across tissues in each sex, with only 2.68-7.32% of associations being shared between heads and gonads in each sex, and no overlap in sex bias associations between tissues (Figure 1C). This suggests that the regulatory architecture is highly tissue-specific.

Enrichment of *cis*-acting associations among those shared between sexes

We test a few predictions on the regulatory basis of the various categories of associations based on their sharing between conditions. Based on previous results (Bhasin et al., 2008; Meiklejohn et al., 2014; Porcu et al., 2022), we expect that associations that are shared between sexes typically act in *cis*. Consistently, we find that the few associations that are shared between the three analyses (s-fm; 10 and 37 in heads and gonads) almost always (100% in heads and 85.50% in gonads) act in *cis*. While the % *cis* is very slow for the rest of the categories, we find that associations that are shared between the sexes but not with sex bias (category fm) have the next highest proportion of *cis* action both in heads (3.34%) and gonads (4.21%; Figure 3A,B). It is also worth noting that sex bias eQTL associations that are not detected in sex-specific analyses (category s) have the lowest percentage of *cis* both in heads (0.04%) and gonads (1.13%; Figure 3A,B).

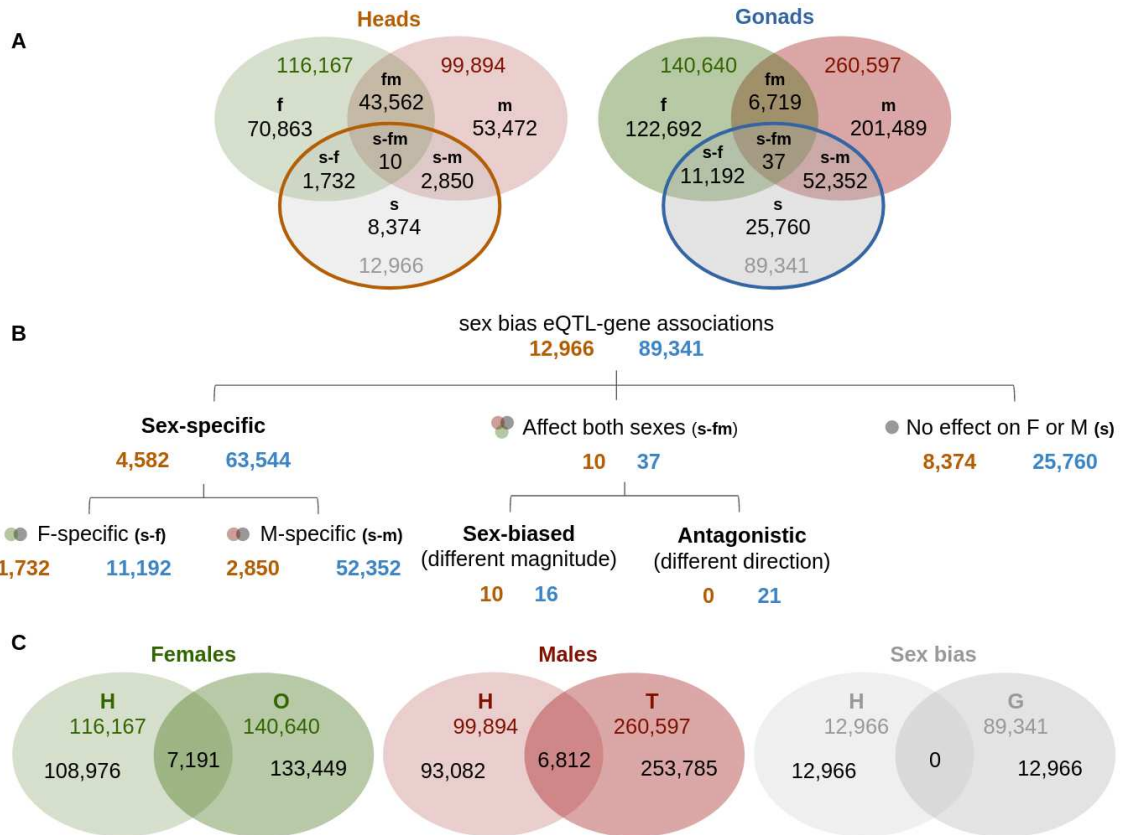


Figure 2: Sharing of eQTL-gene associations between analyses. A: Number of shared associations between female, male and sex bias analyses in heads and gonads. These include: sex-specific (f, m) and shared (fm) associations not generating variation for sex bias; associations generating variation for sex bias also detected in one sex (s-f, s-m), in both (s-fm) or in none (s). B: Closer examination of the modus operandi of sex bias associations in heads (brown) and gonads (blue). Sex-specific (sex bias) associations (s-f, s-m) correspond to those generating variation for sex bias by affecting expression in one sex but not the other. Sex-biased and antagonistic (sex bias) associations (s-fm) generate variation for sex bias by affecting expression in both sexes in different magnitudes and directions, respectively. C: Number of shared associations between heads and gonads in females, males and sex bias. Significance of the results has been determined at $FDR < 0.05$.

Similarly, we expect that eQTLs that are shared between analyses have stronger effect sizes (Bhasin et al., 2008; Dimas et al., 2012; Massouras et al., 2012). We find that the effect sizes of associations detected in the three analyses (s-fm category) are consistently higher, potentially reflecting the generally higher effect sizes of *cis*-acting mutations (Figure S3), while the rest have similarly low distributions of effect sizes, centered at around 0.2 in both heads and gonads (Figure 3C,D). We also expected that sex bias eQTLs that are not detected in sex-specific analyses

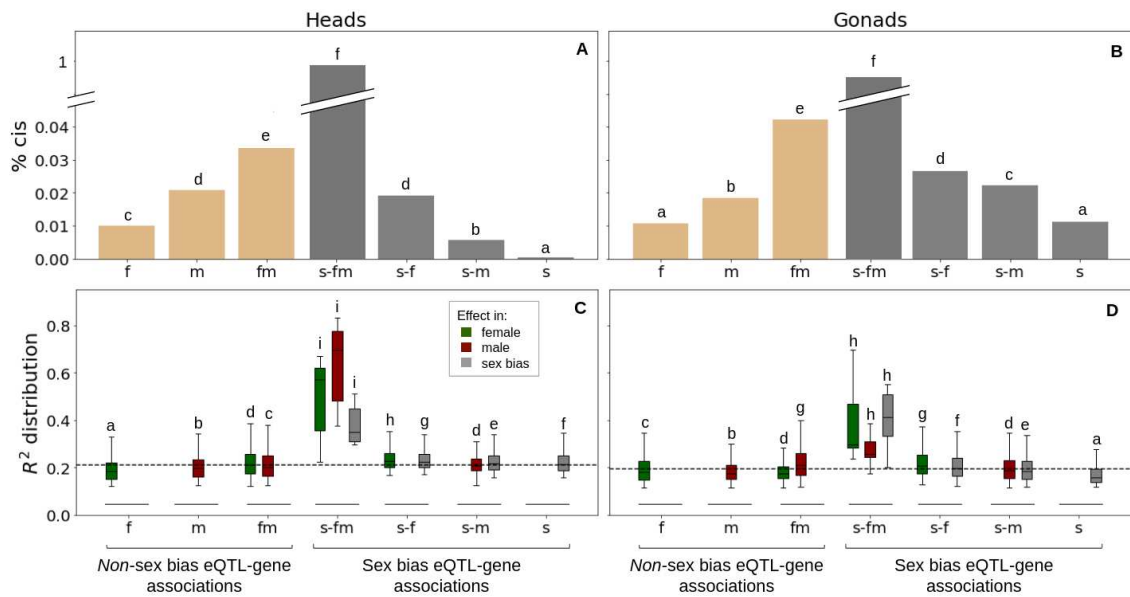


Figure 3: The regulatory basis of the various categories of associations. A (B): Percentage of significant associations acting in *cis* in heads (gonads). C (D): Effect size distribution in heads (gonads). The various categories of associations correspond to their sharing across the various analyses (see Figure 2A): sex-specific (f, m) and shared (fm) associations not generating variation for sex bias (in ocre in A,B); sex bias associations (in grey in A,B) also detected in one sex (s-f, s-m), in both (s-fm) and in none (s). In C-D the boxes in green, red and grey correspond to female, male and sex bias distributions for mutations of each category (when applying), and the dashed horizontal lines are at average effect size distribution in heads and gonads. Significance groups revealing differences between categories within tissue per analysis, calculated as two-proportions z-test at p-value < 0.05 for A-B and Mann-Whitney U test at p-value < 0.05 for C-D, are denoted by different letters, sorted by ascending means.

(s category) have particularly low effect sizes, which holds for gonads but not for heads.

Genes with shared genetic architecture between sexes have higher intersex correlation in expression

Next, we test some predictions on the genetic architecture underlying sex differences in expression. First, we expect intersex correlation (r_{fm}) to be negatively associated with the extent of sexual dimorphism (e.g. Poissant et al., 2010; Griffin et al., 2013). Consistent with this prediction, we find that intersex correlation (computed as between-sex covariance divided by the geometric mean of sex-specific variances, calculated per gene across lines) is significantly higher for heads than for gonads,

with means of 0.50 and 0.19, respectively (Mann-Whitney U test, p-value < 0.001; Figure 4A), and a significant negative correlation between r_{fm} and sex bias in heads (linear regression coefficient=-0.11, p-value < 1e-16, Figure 4B). However, r_{fm} and sex bias are positively correlated in gonads (linear regression coefficient=1.07, p-value < 1e-16, Figure 4C). We also expected that intersex correlation should be higher for genes with a shared regulatory architecture between sexes, and lower for those with associated sex bias eQTLs. Indeed, we find higher intersex correlation for genes with associated regulatory associations that are shared between the sexes (fm category, Figure 4D,E). Also, although only significant for some comparisons, we find that r_{fm} for genes with associated sex bias eQTLs (categories s-fm, s-f, s-m, s; grey boxes) is generally lower than for those genes without associated sex bias eQTLs (categories f, m, fm; brown boxes, Figure 4D,E).

Second, we checked whether genes with associated sex-specific and sex bias eQTLs are more sex biased than genes with shared genetic architecture. Consistently with previous results (Dimas et al., 2012; Oliva et al., 2020), we did not find any pattern in the distribution of sex bias across categories of genes, with genes with shared genetic architecture (category fm in Figure 4F,G) and genes with associated sex bias eQTLs (grey boxes in Figure 4F,G) all having similar sex bias. Third, we expect that more polygenic traits are able to more easily diverge between the sexes, while those underlain by very few mutations are more constrained (discussed in e.g. Rhen, 2000), so we predict that the extent of sex bias is positively correlated with the amount of associated eQTLs. This was however not observed. Instead, we found a non-significant correlation between the amount of eQTLs and sex bias both in heads and in gonads (linear regression p-values of 0.34 and 0.49).

Discussion and work in progress

Sex-specific expression of a shared genome is thought to be one of the main molecular mechanisms underlying phenotypic sexual dimorphism (Jiang & Machado, 2009; Stewart et al., 2010; Mank, 2017), so studying its regulatory basis is key to understanding the evolutionary dynamics underlying sexually-dimorphic adaptation.

Most previous studies looking at sex differences in the regulatory variation in gene expression rely on the comparison of sex-specific eQTL analyses. However, we argue that, while this approach provides insights into sex differences in the regulatory variation of gene expression, it is not directly informative of the genetic basis of sex differences in expression, since previous studies provided evidence that genes

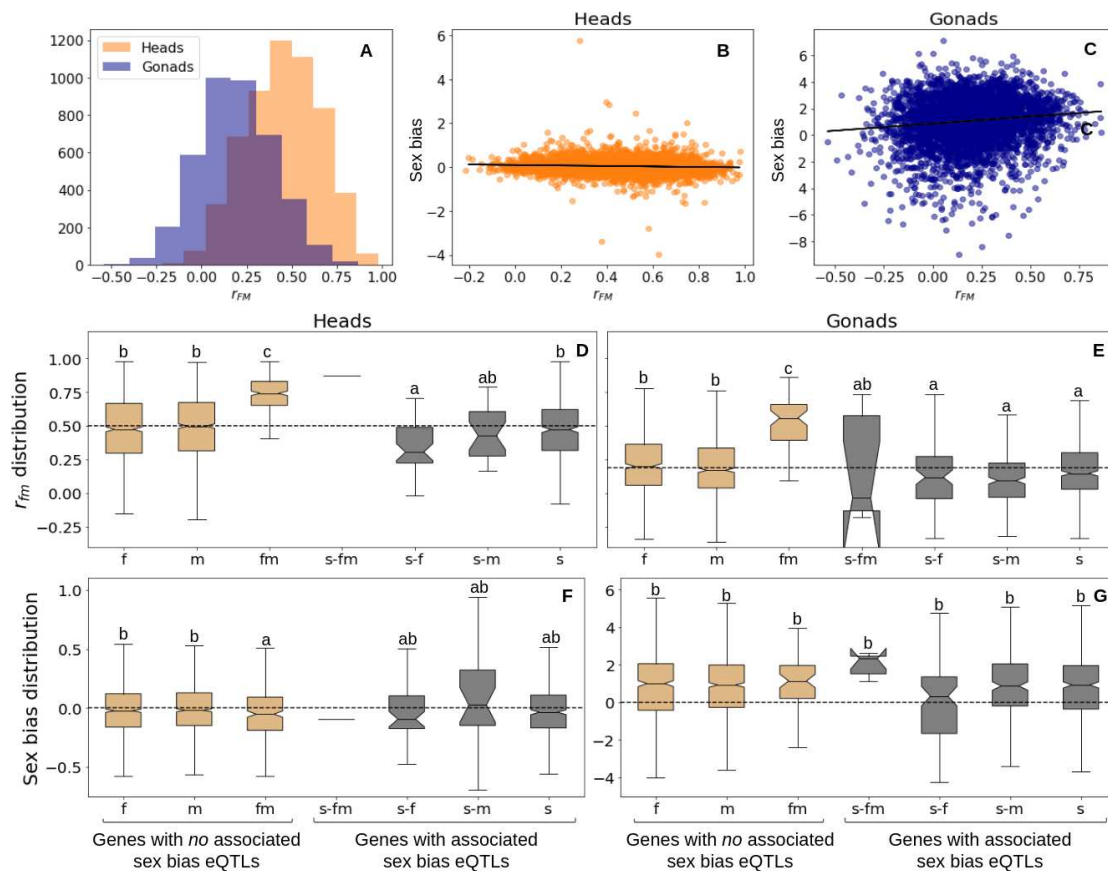


Figure 4: Intersex correlation (r_{fm}) and sex bias. A: Distribution of r_{fm} values across genes in heads (orange) and gonads (blue). B (C): Scatter plot of r_{fm} and sex bias, $SB = \log_2(\bar{e}_f/\bar{e}_m)$, in heads (gonads), where \bar{e}_f and \bar{e}_m are sex-specific averages across lines for each gene. The black solid lines display the least-squares regression, corresponding to $-0.11x + 0.10$ (p-value $< 1e-16$) in heads and $1.07x + 0.87$ (p-value $< 1e-16$) in gonads. D (E): r_{fm} distribution across genes associated with various categories of eQTLs in heads (gonads). F (G): Sex bias distribution across genes associated with various categories of eQTLs in heads (gonads). The various categories of associated eQTLs correspond to their sharing across the various analyses (see Figure 2A): sex-specific (f, m) and shared (fm) associations not generating variation for sex bias (in ocre in A,B); sex bias associations (in grey in A,B) also detected in one sex (s-f, s-m), in both (s-fm) and in none (s). In D-E (F-G), the dashed horizontal lines are at average r_{fm} (sex bias) in heads and gonads. In D-G, significance groups revealing differences between categories, calculated Mann-Whitney U test with p-value threshold < 0.05 , are denoted by different letters, sorted by ascending means.

associated with sex-specific eQTL variation are not more sex biased than genes with shared regulatory variation across sexes (Dimas et al., 2012; Oliva et al., 2020), suggesting that sex differences in regulatory architecture do not necessarily lead to sex differences in expression levels. Instead, looking for genetic variation underlying sex

bias, computed as $\log_2(\text{exp}_f/\text{exp}_m)$, as a measure of sex differences in expression, is a more appropriate approach to the characterization of the regulatory landscape of sex differences in expression. However, this method relies on sex-specific gene expression of single genotypes, which is not available for wild, outbred populations. Also, most eQTL studies in *Drosophila* have analyzed whole body data (Massouras et al., 2012; Huang et al., 2015, 2020; Everett et al., 2020), which is suboptimal because gene expression patterns as well as their regulatory variation are highly tissue-specific (Urbut et al., 2019; Oliva et al., 2020).

In this study, we obtain a gene expression dataset specifically tailored to characterize the tissue-specific genetic variation of sex differences. We crossed 190 inbred lines of the DGRP into 95 crosses, obtaining F1 individuals that are heterozygous themselves but all genetically identical within each cross, allowing us to obtain sex-specific gene expression per each genotype, as required to detect sex bias eQTLs, separately for heads and gonads. We use this dataset to run sex-specific eQTL analyses, as well as eQTL analyses using sex bias as a phenotype to characterize the tissue-specific patterns of sex bias in gene expression as well its regulatory variation. While a few studies have characterized the eQTL variation underlying *Drosophila* head expression (King et al., 2014; Pallares et al., 2023), to our knowledge, no study to date has characterized the regulatory variation for gene expression in ovaries and testes in *Drosophila*, which seems of particular importance given that this is the most sexually-dimorphic tissue and that most sex expression differences in this species are driven by the gonads (Parisi et al., 2003; Arbeitman et al., 2004; Lebo et al., 2009; Catalán et al., 2012; Perry et al., 2014).

We find clear molecular signals of the difference in sexual dimorphism between heads and gonads in terms of gene expression and its regulatory variation. On the one hand, heads have lower sex bias in gene expression than gonads. Also, while the sex bias distribution looks symmetrical in the heads, it is female-skewed in the gonads (Figure 1B,C), indicating higher female-expression for those genes expressed in gonads of both sexes. A higher female-bias in expression, although it has been found by some studies analyzing whole-body (Jiang & Machado, 2009) and head data (Arbeitman et al., 2016) of *Drosophila*, is in contrast with higher male-biased gene expression generally reported for this species (Ranz et al., 2003; Ellegren & Parsch, 2007; Pallares et al., 2023), mainly driven by testes. This qualitative difference in the direction of sex bias that we observe might be due to the fact that we are only

considering genes that are shared between ovaries and testes, a subset that is likely enriched for constitutive genes. Indeed, there is evidence for female-overexpression among genes with intermediate sex bias, while those with extreme sex bias tend to be male-biased (Ranz et al., 2003), and likely drive the otherwise generally-observed higher extent of male bias in *Drosophila* expression. In our analyses, we indeed find more male- than female- strongly sex biased genes, but we consider them sex-specific and disregard them for our analysis of the genetic variation underlying sex bias.

On the other hand, we find that heads have a more similar regulatory architecture across sexes, reflected in a higher sharing of eQTL associations between sexes, as well as less associations for sex bias, relative to gonads (Figure 2A,B). We characterize the modus operandi of eQTL associations generating variation for sex bias and find evidence of sex-specific, sex-biased and sexually-antagonistic mutations significantly associated with sex differences in expression. Associations generating variation for sex bias by affecting expression in a sex-specific manner account for about a third of sex bias associations in heads, and two thirds in gonads. Of those, particularly in gonads, most are male-specific. This suggests that, although we find more female- than male-biased genes in this tissue, much of the genetic variation for sex differences in expression acts in a testes-specific manner. This is surprising, since one would expect more power to detect regulatory associations with higher phenotypic variation, and suggests real biological effects. An excess of male-specific associations generating variation for sex bias in gonads suggests more positive selection acting on testes expression while ovaries have a more constrained regulatory architecture. This is consistent with previous observations of a higher turnover of male-biased genes across species (Jiang & Machado, 2009), but also with increased regulatory variation in the testes (Chapter 2 of this thesis), and with general evidence for male-biased fitness effects of new mutations in *Drosophila* (Mallet et al., 2011; Sharp & Agrawal, 2013).

We also detect some sex-biased and sexually-antagonistic associations leading to variation for sex bias by affecting expression in the two sexes at different magnitudes and directions, respectively, although those are very rare, as previous evidence suggested (Meiklejohn et al., 2014; Oliva et al., 2020). Interestingly, we find that most sexually-antagonistic associations we detect in gonads affect sex bias in one particular gene (FBgn0035590). A quick search for this gene indicates that it encodes Tcs5, an atypical kinase involved in tRNAs modification, telomere and chromatin dynamics (Flybase, Gramates et al., 2022). Apart from an association with longer duration of greenness and photosynthetic capacity during grain-filling of its paralog

in rice (Fu et al., 2011), not much is known about Tcs5.

Generally, we find that only a small proportion of the detected sex-specific associations are associated with sex bias (Figure 2A), and that genes associated with sex differences in regulatory architecture are not more sex biased than genes with shared regulatory architecture between sexes (Figure 4F,G), which is in line with previous results that sex differences in regulatory architecture do not necessarily lead to sex differences in expression (Dimas et al., 2012; Oliva et al., 2020), and further motivates the explicit analysis of the variation underlying sex bias, in comparison with sex-specific eQTL analyses.

In this regard, we detect a high proportion (64.6% in heads and 28.8% in gonads) of sex bias associations that are missed in sex-specific analysis, indicating that a high proportion of the genetic variation underlying sex differences in expression consists of mutations with effect sizes that are subtle overall, but sufficiently different between sexes to generate variation for sex differences in expression. We are still working on a proper characterization of these ‘missed’ associations for sex bias. Some predictions include that they have weaker effect sizes, for which we find inconsistent preliminary evidence (Figure 3C,D), and that they might harbor more sexually-antagonistic mutations, since those are expected to have low effect sizes and potentially be missed in sex-specific analyses.

Also agreeing with previous results (Bhasin et al., 2008; Meiklejohn et al., 2014; Porcu et al., 2022), we find that the proportion of *cis*-eQTL associations is higher for those that are shared between sexes than for those that are not (Figure 3A,B). This suggests a substantial role of *trans*-regulatory mechanisms driving most differences in expression within species, and particularly in sex differences in gene expression, as has previously been suggested (Williams & Carroll, 2009). However, our classification of eQTLs into *cis*- and *trans*-acting relies on a distance cutoff, assuming that eQTLs that are physically close to the respective genes are enriched for *cis*-acting mutations on promoters. The mechanistic definition of *cis* and *trans*-eQTLs, however, relies on their mode of action: while *cis*-eQTLs affect the allele they are linked with, *trans*-eQTLs modulate the expression of both gene copies in heterozygous individuals (Wittkopp et al., 2004; Graze et al., 2009; Chapter 2 of this thesis). The detection of mechanistic *cis* and *trans* mode of eQTL action thus relies on the characterization of allelic imbalances in hybrid expression. We implemented this approach using crosses between a subset of DGRP lines in the Chapter 2 of this

thesis to find substantial *cis* and *trans* regulatory variation in heads and gonads of both sexes. We are currently working on obtaining allele-specific expression data to mechanistically validate that allele-specific bias in expression is higher amongst transcripts we predict to be regulated by *cis*-eQTLs, as other studies have reported (e.g. [Massouras et al., 2012](#)).

It is generally expected that the regulatory variation for sex bias in gene expression is fundamentally different between monomorphic and dimorphic tissues ([Williams & Carroll, 2009](#); [Stewart et al., 2010](#)). Concretely in *Drosophila*, there is evidence for sex-specific development of sexually-dimorphic tissues to be downstream of the sex-determination cascade ([Williams & Carroll, 2009](#); [Rice et al., 2018](#)), an aspect that we will characterize in follow-up analyses. These results are in line with our observation that regulatory architecture is tissue-specific (Figure 2C). Also, while there is some evidence that the genetic variation generating differences in expression between sexes is different from that generating variation for gene expression differences across tissues ([Gordon & Ruvinsky, 2012](#); [Oliva et al., 2020](#)), this is yet not well understood. We are working on testing this prediction with our data. Concretely, we are characterizing the regulatory architecture underlying tissue differences in expression via ‘tissue bias eQTLs’, where we run eQTL analyses using tissue bias, as $\log_2(\text{gonad/head})$ gene expression per sex as phenotype. By comparing tissue bias with sex bias eQTL associations we can get an idea of whether the associations generating variation in gene expression differences between tissues are the same generating variation in expression differences between tissues.

Also, we will compare our eQTL associations in heads and gonads to those found for whole bodies in other DGRP studies ([Huang et al., 2015, 2020](#); [Everett et al., 2020](#)) to determine whether whole-body regulatory associations are enriched for those identified in somatic or germline tissues.

We tested predictions on the general genetic architecture of sex biased gene expression. Concretely, a large body of literature on sex-specific adaptation generally assumes that intersex correlation should constrain sexually-dimorphic evolution, and that both should negatively correlate with one another, which is supported by general empirical evidence of a negative covariance between intersex correlation and sex differences across traits and species (e.g. [Delph et al., 2004, 2010](#); [Bonduriansky & Rowe, 2005](#); [McDaniel, 2005](#); [Poissant et al., 2010](#)), including gene expression in *Drosophila* ([Griffin et al., 2013](#)), a pattern which, however, other studies failed to

find (Cowley & Atchley, 1988; Chenoweth & Blows, 2003; Ashman & Majetic, 2006; Leinonen et al., 2011, Chapter 1 of this thesis). Our results reflect this mixed evidence (Figure 4): on the one hand, consistently with the predictions, we find that 1) intersex correlation in expression is lower in heads than in gonads, reflecting a larger between-sex decoupling in gene expression in the latter, and 2) a significant negative correlation between intersex correlation and sex bias in heads. On the other hand, we find that intersex correlation and sex bias significantly positively correlate with one another in gonads, which is contrary to the general intuition and for which we so far do not have a good explanation. However, we do generally find that intersex correlation in expression is higher for genes with a shared regulatory architecture between sexes, providing further evidence that the evolution of sex-specific gene expression regulatory variation is one of the mechanisms to decouple genotype-to-phenotype relationships between sexes (Williams & Carroll, 2009; Stewart et al., 2010).

For the current version of this study we did not examine the genetic vs environmental contribution to sex-specific variances and intersex covariance. We hope for minimal environmental contribution to gene expression variation, as we performed all crosses in very controlled experimental conditions. However, we are currently working on the characterization of the heritable variation for gene expression across lines, since it determines our ability to detect associated eQTLs, as well as the extent of genetic and non-genetic expression covariance between sexes. Also, detecting the amount of sex-specific genetic variance for gene expression will provide important information on the selective forces acting on sex- and tissue-specific expression, as well as its evolutionary potential.

We also characterized the pleiotropy of the variation underlying sex-specific as well as sex bias in gene expression. We find evidence of pleiotropic associations, both in terms of genes with many associated eQTLs (Figure S1), as well as *trans*-eQTLs associated with expression of many genes (Figure S2). We are still working on the detection of potential regulatory and functional clusters within genes with similar eQTL regulation, as well as the characterization of those “super” *trans*-eQTLs.

Three other aspects are still ongoing work. The first one is conceptually relevant, and involves running eQTL analyses detecting sex-by-genotype interactions. While this is a better approach to the comparison between sex-specific analyses, it has not been extensively used in the characterization of sex differences in the regulatory variation underlying gene expression or phenotypic variation in general (but see

e.g. [Dimas et al., 2012](#); [Shen et al., 2019](#); [Oliva et al., 2020](#) for gene expression and [Hoffman et al., 2014](#); [Winkler et al., 2015](#); [Awotoye et al., 2022](#); [Eissman et al., 2022](#)). This might be due to the fact that this approach, similarly to the detection of sex bias eQTLs that we propose, ideally requires sex-specific expression of each genotype which, as discussed, is generally only available for inbred lines. Studies using this approach with data from outbred populations require accounting for the fact that female and male data points have different genetic backgrounds and reduces their power to detect relevant variation within populations, limiting their scope to analyses across populations or clusters of genetically-related individuals (e.g. [Dimas et al., 2012](#)). Our dataset of sex-specific gene expression in single genotypes circumvents these caveats and therefore offers a good opportunity to explore this approach to study sex-by-genotype interactions within a population. We are currently working on running sex-by-genotype interaction models, which we will compare to our sex bias eQTL analyses. We expect that both types of analyses will detect similar signals of the regulatory variation underlying sex differences in expression – but an explicit test of this prediction is still to come.

The second aspect is more technical, and involves correcting the expression data for a series of covariates. Indeed, GWAS are sensitive to any type of structure in the data ([Price et al., 2006, 2010](#)), and so eliminating variation driven by confounding covariates is a necessary step prior to the analysis, which we have not implemented yet. Previous studies have characterized the genetic structure within the DGRP lines ([Huang et al., 2014](#)). Concretely, they report some sort of population structure (systematic ancestry differences between groups of lines, potentially associated with expression phenotypes) among DGRP lines. Also, these lines present 16 major segregating inversions (Figures S4-S6), which have been shown to correlate with genome size, be the major drivers of population structure and, long-range linkage disequilibrium and be associated with various traits, including gene expression ([Huang et al., 2014, 2015](#)). Besides these biological covariates, PCA on the expression data suggests that it might present some stratification based on experimental variables, most notably sequencing library and replicate. We are currently working on finding the best strategy to correct our expression data for these covariates and for now analyzing their patterns of variation with a grain of salt, aware that some of these might change after the correction step has been incorporated.

Third, we have so far jointly analyzed sex-specific and sex bias eQTL results by comparing the significant associations across analyses, where significance has been

determined following an arbitrary threshold of $FDR < 0.05$. While this is the most commonly-used strategy, it is suboptimal because significance thresholds depend on power, which differs across analyses, and ignores more subtle effects. Instead, a better approach consists on directly comparing the effect sizes of each association, together with their significance, across analyses, a strategy that has been implemented in softwares like mash (Urbut et al., 2019). We are going to use this approach to jointly analyze the eQTL associations for sex-specific gene expression, sex bias and sex-by-genotype interactions to get a more accurate picture of the regulatory variation underlying sex differences in expression, and how it operates by affecting gene expression in the two sexes, also considering subtle effects.

In general, our current results, together with the ongoing analyses, will provide an in-depth characterization of the regulatory variation underlying sex differences in gene expression by comparing the outcomes of sex-specific as well as sex bias in gene expression, in heads and gonads, two tissues with marked differences in phenotypic sexual dimorphism. Overall, this provides important insight into the genetic architecture of phenotypic sex differences (Porcu et al., 2022), which is the first step towards a deeper understanding of the selective forces and evolutionary dynamics driving sexual dimorphism evolution.

Acknowledgments

We thank members of the Vicoso and Barton groups for comments on the manuscript and the Scientific Computing unit at ISTA for technical support.

GP is the recipient of a DOC Fellowship of the Austrian Academy of Sciences at the Institute of Science and Technology Austria (DOC 25817) and received funding from the European Union’s Horizon 2020 research and innovation program under the Marie Skłodowska-Curie Grant (agreement no. 665385).

Author Contributions

GP, NB and BV conceived the study; GP, AM and BV designed the research experiment; GP, AM, LS obtained the experimental dataset; GP and CS performed the data analyses; GP wrote the manuscript.

References

- Arbeitman, M. N., Fleming, A. A., Siegal, M. L., Null, B. H., & Baker, B. S. (2004, May). A genomic analysis of *Drosophila* somatic sexual differentiation and its regulation. *Development (Cambridge, England)*, *131*(9), 2007–2021. doi: 10.1242/dev.01077
- Arbeitman, M. N., New, F. N., Fear, J. M., Howard, T. S., Dalton, J. E., & Graze, R. M. (2016, April). Sex Differences in *Drosophila* Somatic Gene Expression: Variation and Regulation by doublesex. *G3: Genes|Genomes|Genetics*, *6*(7), 1799–1808. Retrieved 2023-06-06, from <https://www.ncbi.nlm.nih.gov/pmc/articles/PMC4938635/> doi: 10.1534/g3.116.027961
- Ashman, T.-L., & Majetic, C. J. (2006, May). Genetic constraints on floral evolution: a review and evaluation of patterns. *Heredity*, *96*(5), 343–352. doi: 10.1038/sj.hdy.6800815
- Awotoye, W., Connick, C., Pendleton, C., Zeng, E., Alade, A., Mossey, P., ... Butali, A. (2022, April). Genome-wide Gene-by-Sex Interaction Studies Identify Novel Nonsyndromic Orofacial Clefts Risk Locus. *Journal of Dental Research*, *101*(4), 465–472. Retrieved 2023-06-06, from <https://www.ncbi.nlm.nih.gov/pmc/articles/PMC8935575/> doi: 10.1177/00220345211046614
- Bhasin, J. M., Chakrabarti, E., Peng, D.-Q., Kulkarni, A., Chen, X., & Smith, J. D. (2008, January). Sex specific gene regulation and expression QTLs in mouse macrophages from a strain intercross. *PloS One*, *3*(1), e1435. doi: 10.1371/journal.pone.0001435
- Bolger, A. M., Lohse, M., & Usadel, B. (2014, August). Trimmomatic: a flexible trimmer for Illumina sequence data. *Bioinformatics*, *30*(15), 2114–2120. Retrieved 2023-06-06, from <https://www.ncbi.nlm.nih.gov/pmc/articles/PMC4103590/> doi: 10.1093/bioinformatics/btu170
- Bonduriansky, R., & Chenoweth, S. F. (2009, May). Intralocus sexual conflict. *Trends in Ecology & Evolution*, *24*(5), 280–288. Retrieved 2023-05-23, from [https://www.cell.com/trends/ecology-evolution/abstract/S0169-5347\(09\)00075-5](https://www.cell.com/trends/ecology-evolution/abstract/S0169-5347(09)00075-5) (Publisher: Elsevier) doi: 10.1016/j.tree.2008.12.005
- Bonduriansky, R., & Rowe, L. (2005, September). Intralocus sexual conflict and the genetic architecture of sexually dimorphic traits in *Prochyliza xanthostoma* (Diptera: Piophilidae). *Evolution; International Journal of Organic Evolution*, *59*(9), 1965–1975.
- Bray, N. L., Pimentel, H., Melsted, P., & Pachter, L. (2016, May). Near-optimal probabilistic RNA-seq quantification. *Nature Biotechnology*, *34*(5), 525–527.

doi: 10.1038/nbt.3519

- Brem, R. B., Yvert, G., Clinton, R., & Kruglyak, L. (2002, April). Genetic dissection of transcriptional regulation in budding yeast. *Science (New York, N.Y.)*, *296*(5568), 752–755. doi: 10.1126/science.1069516
- Catalán, A., Hutter, S., & Parsch, J. (2012, November). Population and sex differences in *Drosophila melanogaster* brain gene expression. *BMC genomics*, *13*, 654. doi: 10.1186/1471-2164-13-654
- Charlesworth, D., & Willis, J. H. (2009, November). The genetics of inbreeding depression. *Nature Reviews. Genetics*, *10*(11), 783–796. doi: 10.1038/nrg2664
- Chen, J., Nolte, V., & Schlotterer, C. (2015, February). Temperature Stress Mediates Decanalization and Dominance of Gene Expression in *Drosophila melanogaster*. *PLOS Genetics*, *11*(2), e1004883. Retrieved 2023-05-14, from <https://journals.plos.org/plosgenetics/article?id=10.1371/journal.pgen.1004883> (Publisher: Public Library of Science) doi: 10.1371/journal.pgen.1004883
- Cheng, C., & Kirkpatrick, M. (2016, September). Sex-Specific Selection and Sex-Biased Gene Expression in Humans and Flies. *PLoS genetics*, *12*(9), e1006170. doi: 10.1371/journal.pgen.1006170
- Chenoweth, S. F., & Blows, M. W. (2003). Signal Trait Sexual Dimorphism and Mutual Sexual Selection in *Drosophila Serrata*. *Evolution*, *57*(10), 2326–2334. Retrieved 2023-04-27, from <https://onlinelibrary.wiley.com/doi/abs/10.1111/j.0014-3820.2003.tb00244.x> (_eprint: <https://onlinelibrary.wiley.com/doi/pdf/10.1111/j.0014-3820.2003.tb00244.x>) doi: 10.1111/j.0014-3820.2003.tb00244.x
- Connallon, T., & Clark, A. G. (2014, July). Balancing selection in species with separate sexes: insights from Fisher’s geometric model. *Genetics*, *197*(3), 991–1006. doi: 10.1534/genetics.114.165605
- Coolon, J. D., McManus, C. J., Stevenson, K. R., Graveley, B. R., & Wittkopp, P. J. (2014, May). Tempo and mode of regulatory evolution in *Drosophila*. *Genome Research*, *24*(5), 797–808. Retrieved 2023-05-14, from <https://www.ncbi.nlm.nih.gov/pmc/articles/PMC4009609/> doi: 10.1101/gr.163014.113
- Coolon, J. D., Stevenson, K. R., McManus, C. J., Graveley, B. R., & Wittkopp, P. J. (2012, July). Genomic imprinting absent in *Drosophila melanogaster* adult females. *Cell Reports*, *2*(1), 69–75. doi: 10.1016/j.celrep.2012.06.013
- Cowley, D. E., & Atchley, W. R. (1988, June). Quantitative Genetics of *Drosophila Melanogaster*. II. Heritabilities and Genetic Correlations between Sexes for

- Head and Thorax Traits. *Genetics*, 119(2), 421–433. doi: 10.1093/genetics/119.2.421
- Dean, R., & Mank, J. E. (2014). The role of sex chromosomes in sexual dimorphism: discordance between molecular and phenotypic data. *Journal of Evolutionary Biology*, 27(7), 1443–1453. Retrieved 2023-05-23, from <https://onlinelibrary.wiley.com/doi/abs/10.1111/jeb.12345> (eprint: <https://onlinelibrary.wiley.com/doi/pdf/10.1111/jeb.12345>) doi: 10.1111/jeb.12345
- Delph, L. F., Arntz, A. M., Scotti-Saintagne, C., & Scotti, I. (2010, October). The genomic architecture of sexual dimorphism in the dioecious plant *Silene latifolia*. *Evolution; International Journal of Organic Evolution*, 64(10), 2873–2886. doi: 10.1111/j.1558-5646.2010.01048.x
- Delph, L. F., Frey, F. M., Steven, J. C., & Gehring, J. L. (2004). Investigating the independent evolution of the size of floral organs via G-matrix estimation and artificial selection. *Evolution & Development*, 6(6), 438–448. doi: 10.1111/j.1525-142X.2004.04052.x
- Dimas, A. S., Nica, A. C., Montgomery, S. B., Stranger, B. E., Raj, T., Buil, A., ... Dermitzakis, E. T. (2012, December). Sex-biased genetic effects on gene regulation in humans. *Genome Research*, 22(12), 2368–2375. doi: 10.1101/gr.134981.111
- Eissman, J. M., Dumitrescu, L., Mahoney, E. R., Smith, A. N., Mukherjee, S., Lee, M. L., ... Hohman, T. J. (2022, May). Sex differences in the genetic architecture of cognitive resilience to Alzheimer’s disease. *Brain*, 145(7), 2541–2554. Retrieved 2023-06-09, from <https://www.ncbi.nlm.nih.gov/pmc/articles/PMC9337804/> doi: 10.1093/brain/awac177
- Ellegren, H., & Parsch, J. (2007, September). The evolution of sex-biased genes and sex-biased gene expression. *Nature Reviews. Genetics*, 8(9), 689–698. doi: 10.1038/nrg2167
- Everett, L. J., Huang, W., Zhou, S., Carbone, M. A., Lyman, R. F., Arya, G. H., ... Mackay, T. F. C. (2020, March). Gene expression networks in the *Drosophila* Genetic Reference Panel. *Genome Research*, 30(3), 485–496. doi: 10.1101/gr.257592.119
- Fu, J.-D., Yan, Y.-F., Kim, M. Y., Lee, S.-H., & Lee, B.-W. (2011, March). Population-specific quantitative trait loci mapping for functional stay-green trait in rice (*Oryza sativa* L.). *Genome*, 54(3), 235–243. doi: 10.1139/G10-113

- Gibson, G., Riley-Berger, R., Harshman, L., Kopp, A., Vacha, S., Nuzhdin, S., & Wayne, M. (2004, August). Extensive sex-specific nonadditivity of gene expression in *Drosophila melanogaster*. *Genetics*, *167*(4), 1791–1799. doi: 10.1534/genetics.104.026583
- Gonzales, N. M., Seo, J., Hernandez Cordero, A. I., St Pierre, C. L., Gregory, J. S., Distler, M. G., ... Palmer, A. A. (2018, December). Genome wide association analysis in a mouse advanced intercross line. *Nature Communications*, *9*(1), 5162. doi: 10.1038/s41467-018-07642-8
- Gordon, K. L., & Ruvinsky, I. (2012, January). Tempo and mode in evolution of transcriptional regulation. *PLoS genetics*, *8*(1), e1002432. doi: 10.1371/journal.pgen.1002432
- Gramates, L. S., Agapite, J., Attrill, H., Calvi, B. R., Crosby, M. A., Dos Santos, G., ... the FlyBase Consortium (2022, April). FlyBase: a guided tour of highlighted features. *Genetics*, *220*(4), iyac035. doi: 10.1093/genetics/iyac035
- Graze, R. M., McIntyre, L. M., Main, B. J., Wayne, M. L., & Nuzhdin, S. V. (2009, October). Regulatory divergence in *Drosophila melanogaster* and *D. simulans*, a genomewide analysis of allele-specific expression. *Genetics*, *183*(2), 547–561, 1SI–21SI. doi: 10.1534/genetics.109.105957
- Griffin, R. M., Dean, R., Grace, J. L., Rydén, P., & Friberg, U. (2013, September). The shared genome is a pervasive constraint on the evolution of sex-biased gene expression. *Molecular Biology and Evolution*, *30*(9), 2168–2176. doi: 10.1093/molbev/mst121
- Gruber, J. D., Vogel, K., Kalay, G., & Wittkopp, P. J. (2012, February). Contrasting properties of gene-specific regulatory, coding, and copy number mutations in *Saccharomyces cerevisiae*: frequency, effects, and dominance. *PLoS genetics*, *8*(2), e1002497. doi: 10.1371/journal.pgen.1002497
- Grundberg, E., Small, K. S., Hedman, K., Nica, A. C., Buil, A., Keildson, S., ... Spector, T. D. (2012, October). Mapping cis- and trans-regulatory effects across multiple tissues in twins. *Nature Genetics*, *44*(10), 1084–1089. Retrieved 2023-05-26, from <https://www.nature.com/articles/ng.2394> (Number: 10 Publisher: Nature Publishing Group) doi: 10.1038/ng.2394
- GTEX Consortium. (2020, September). The GTEx Consortium atlas of genetic regulatory effects across human tissues. *Science (New York, N.Y.)*, *369*(6509), 1318–1330. doi: 10.1126/science.aaz1776
- GTEx Consortium, Laboratory, Data Analysis & Coordinating Center

- (LDACC)—Analysis Working Group, Statistical Methods groups—Analysis Working Group, Enhancing GTEx (eGTEx) groups, NIH Common Fund, NIH/NCI, ... Montgomery, S. B. (2017, October). Genetic effects on gene expression across human tissues. *Nature*, *550*(7675), 204–213. doi: 10.1038/nature24277
- Haldane, J. B. S. (1962, March). Conditions for Stable Polymorphism at an Autosomal Locus. *Nature*, *193*(4820), 1108–1108. Retrieved 2023-05-23, from <https://www.nature.com/articles/1931108a0> (Number: 4820 Publisher: Nature Publishing Group) doi: 10.1038/1931108a0
- Hartman, R. J. G., Mokry, M., Pasterkamp, G., & den Ruijter, H. M. (2021, September). Sex-dependent gene co-expression in the human body. *Scientific Reports*, *11*(1), 18758. Retrieved 2023-05-23, from <https://www.nature.com/articles/s41598-021-98059-9> (Number: 1 Publisher: Nature Publishing Group) doi: 10.1038/s41598-021-98059-9
- Hoffman, J. M., Soltow, Q. A., Li, S., Sidik, A., Jones, D. P., & Promislow, D. E. L. (2014, August). Effects of age, sex, and genotype on high-sensitivity metabolomic profiles in the fruit fly, *Drosophila melanogaster*. *Aging Cell*, *13*(4), 596–604. Retrieved 2023-05-26, from <https://www.ncbi.nlm.nih.gov/pmc/articles/PMC4116462/> doi: 10.1111/accel.12215
- Hoffmann, A. A., Turelli, M., & Simmons, G. M. (1986, July). UNIDIRECTIONAL INCOMPATIBILITY BETWEEN POPULATIONS OF DROSOPHILA SIMULANS. *Evolution; International Journal of Organic Evolution*, *40*(4), 692–701. doi: 10.1111/j.1558-5646.1986.tb00531.x
- Huang, W., Campbell, T., Carbone, M. A., Jones, W. E., Unsel, D., Anholt, R. R. H., & Mackay, T. F. C. (2020, March). Context-dependent genetic architecture of *Drosophila* life span. *PLoS biology*, *18*(3), e3000645. doi: 10.1371/journal.pbio.3000645
- Huang, W., Carbone, M. A., Magwire, M. M., Peiffer, J. A., Lyman, R. F., Stone, E. A., ... Mackay, T. F. C. (2015, November). Genetic basis of transcriptome diversity in *Drosophila melanogaster*. *Proceedings of the National Academy of Sciences of the United States of America*, *112*(44), E6010–6019. doi: 10.1073/pnas.1519159112
- Huang, W., Massouras, A., Inoue, Y., Peiffer, J., Ràmia, M., Tarone, A. M., ... Mackay, T. F. C. (2014, July). Natural variation in genome architecture among 205 *Drosophila melanogaster* Genetic Reference Panel lines. *Genome Research*, *24*(7), 1193–1208. doi: 10.1101/gr.171546.113

- Hughes, K. A., Ayroles, J. F., Reedy, M. M., Drnevich, J. M., Rowe, K. C., Ruedi, E. A., ... Paige, K. N. (2006, July). Segregating variation in the transcriptome: cis regulation and additivity of effects. *Genetics*, *173*(3), 1347–1355. doi: 10.1534/genetics.105.051474
- Jiang, Z.-F., & Machado, C. A. (2009, November). Evolution of sex-dependent gene expression in three recently diverged species of *Drosophila*. *Genetics*, *183*(3), 1175–1185. doi: 10.1534/genetics.109.105775
- Jin, W., Riley, R. M., Wolfinger, R. D., White, K. P., Passador-Gurgel, G., & Gibson, G. (2001, December). The contributions of sex, genotype and age to transcriptional variance in *Drosophila melanogaster*. *Nature Genetics*, *29*(4), 389–395. doi: 10.1038/ng766
- Khodursky, S., Svetec, N., Durkin, S. M., & Zhao, L. (2020, June). The evolution of sex-biased gene expression in the *Drosophila* brain. *Genome Research*, *30*(6), 874–884. doi: 10.1101/gr.259069.119
- King, E. G., Sanderson, B. J., McNeil, C. L., Long, A. D., & Macdonald, S. J. (2014, May). Genetic Dissection of the *Drosophila melanogaster* Female Head Transcriptome Reveals Widespread Allelic Heterogeneity. *PLOS Genetics*, *10*(5), e1004322. Retrieved 2023-06-06, from <https://journals.plos.org/plosgenetics/article?id=10.1371/journal.pgen.1004322> (Publisher: Public Library of Science) doi: 10.1371/journal.pgen.1004322
- Lande, R. (1980, March). SEXUAL DIMORPHISM, SEXUAL SELECTION, AND ADAPTATION IN POLYGENIC CHARACTERS. *Evolution; International Journal of Organic Evolution*, *34*(2), 292–305. doi: 10.1111/j.1558-5646.1980.tb04817.x
- Lande, R. (1987). Genetic correlations between the sexes in the evolution of sexual dimorphism and mating preferences. In J. W. Bardbury & M. B. Andersson (Eds.), *Sexual Selection: Testing the Alternatives : Report of the Dahlem Workshop on Sexual Selection: Testing the Alternatives, Berlin 1986, August 31-September 5*. Wiley. (Google-Books-ID: Z9lqAAAAMAAJ)
- Leader, D. P., Krause, S. A., Pandit, A., Davies, S. A., & Dow, J. A. (2018, January). FlyAtlas 2: a new version of the *Drosophila melanogaster* expression atlas with RNA-Seq, miRNA-Seq and sex-specific data. *Nucleic Acids Research*, *46*(Database issue), D809–D815. Retrieved 2023-06-06, from <https://www.ncbi.nlm.nih.gov/pmc/articles/PMC5753349/> doi: 10.1093/nar/gkx976
- Lebo, M. S., Sanders, L. E., Sun, F., & Arbeitman, M. N. (2009, February). Somatic, germline and sex hierarchy regulated gene expression during *Drosophila*

- metamorphosis. *BMC genomics*, *10*, 80. doi: 10.1186/1471-2164-10-80
- Lecheta, M. C., Awde, D. N., O’Leary, T. S., Unfried, L. N., Jacobs, N. A., Whitlock, M. H., ... Cahan, S. H. (2020). Integrating GWAS and Transcriptomics to Identify the Molecular Underpinnings of Thermal Stress Responses in *Drosophila melanogaster*. *Frontiers in Genetics*, *11*, 658. doi: 10.3389/fgene.2020.00658
- Leinonen, T., Cano, J. M., & Merilä, J. (2011, February). Genetic basis of sexual dimorphism in the threespine stickleback *Gasterosteus aculeatus*. *Heredity*, *106*(2), 218–227. doi: 10.1038/hdy.2010.104
- Mackay, T. F. C., & Huang, W. (2018, January). Charting the Genotype-Phenotype Map: Lessons from the *Drosophila melanogaster* Genetic Reference Panel. *Wiley interdisciplinary reviews. Developmental biology*, *7*(1), 10.1002/wdev.289. Retrieved 2023-05-26, from <https://www.ncbi.nlm.nih.gov/pmc/articles/PMC5746472/> doi: 10.1002/wdev.289
- Mackay, T. F. C., Richards, S., Stone, E. A., Barbadilla, A., Ayroles, J. F., Zhu, D., ... Gibbs, R. A. (2012, February). The *Drosophila melanogaster* Genetic Reference Panel. *Nature*, *482*(7384), 173–178. doi: 10.1038/nature10811
- Mallet, M. A., Bouchard, J. M., Kimber, C. M., & Chippindale, A. K. (2011, June). Experimental mutation-accumulation on the X chromosome of *Drosophila melanogaster* reveals stronger selection on males than females. *BMC Evolutionary Biology*, *11*(1), 156. Retrieved 2023-05-10, from <https://doi.org/10.1186/1471-2148-11-156> doi: 10.1186/1471-2148-11-156
- Mank, J. E. (2017, January). The transcriptional architecture of phenotypic dimorphism. *Nature Ecology & Evolution*, *1*(1), 6. doi: 10.1038/s41559-016-0006
- Mank, J. E., Hultin-Rosenberg, L., Webster, M. T., & Ellegren, H. (2008, March). The unique genomic properties of sex-biased genes: insights from avian microarray data. *BMC genomics*, *9*, 148. doi: 10.1186/1471-2164-9-148
- Massouras, A., Waszak, S. M., Albarca-Aguilera, M., Hens, K., Holcombe, W., Ayroles, J. F., ... Deplancke, B. (2012). Genomic variation and its impact on gene expression in *Drosophila melanogaster*. *PLoS genetics*, *8*(11), e1003055. doi: 10.1371/journal.pgen.1003055
- McDaniel, S. F. (2005, November). Genetic correlations do not constrain the evolution of sexual dimorphism in the moss *Ceratodon purpureus*. *Evolution; International Journal of Organic Evolution*, *59*(11), 2353–2361.
- Meiklejohn, C. D., Coolon, J. D., Hartl, D. L., & Wittkopp, P. J. (2014, January). The roles of cis- and trans-regulation in the evolution of regulatory incom-

- patibilities and sexually dimorphic gene expression. *Genome Research*, *24*(1), 84–95. doi: 10.1101/gr.156414.113
- Metzger, B. P. H., Duveau, F., Yuan, D. C., Tryban, S., Yang, B., & Wittkopp, P. J. (2016, May). Contrasting Frequencies and Effects of cis- and trans-Regulatory Mutations Affecting Gene Expression. *Molecular Biology and Evolution*, *33*(5), 1131–1146. doi: 10.1093/molbev/msw011
- Metzger, B. P. H., Wittkopp, P. J., & Coolon, J. D. (2017, April). Evolutionary Dynamics of Regulatory Changes Underlying Gene Expression Divergence among *Saccharomyces* Species. *Genome Biology and Evolution*, *9*(4), 843–854. doi: 10.1093/gbe/evx035
- Morrow, E. H., & Connallon, T. (2013, December). Implications of sex-specific selection for the genetic basis of disease. *Evolutionary Applications*, *6*(8), 1208–1217. doi: 10.1111/eva.12097
- Muralidhar, P., & Coop, G. (2023, March). *Polygenic outcomes of sexually antagonistic selection*. bioRxiv. Retrieved 2023-05-10, from <https://www.biorxiv.org/content/10.1101/2023.03.02.530911v1> (Pages: 2023.03.02.530911 Section: New Results) doi: 10.1101/2023.03.02.530911
- Oliva, M., Muñoz-Aguirre, M., Kim-Hellmuth, S., Wucher, V., Gewirtz, A. D. H., Cotter, D. J., ... Stranger, B. E. (2020, September). The impact of sex on gene expression across human tissues. *Science (New York, N.Y.)*, *369*(6509), eaba3066. doi: 10.1126/science.aba3066
- Pallares, L. F., Melo, D., Wolf, S., Cofer, E. M., Abhyankar, V., Peng, J., & Ayroles, J. F. (2023, May). *Saturating the eQTL map in *Drosophila melanogaster*: genome-wide patterns of cis and trans regulation of transcriptional variation in outbred populations*. bioRxiv. Retrieved 2023-06-09, from <https://www.biorxiv.org/content/10.1101/2023.05.20.541576v2> (Pages: 2023.05.20.541576 Section: New Results) doi: 10.1101/2023.05.20.541576
- Parisi, M., Nuttall, R., Naiman, D., Bouffard, G., Malley, J., Andrews, J., ... Oliver, B. (2003, January). Paucity of genes on the *Drosophila* X chromosome showing male-biased expression. *Science (New York, N.Y.)*, *299*(5607), 697–700. doi: 10.1126/science.1079190
- Perry, J. C., Harrison, P. W., & Mank, J. E. (2014, May). The ontogeny and evolution of sex-biased gene expression in *Drosophila melanogaster*. *Molecular Biology and Evolution*, *31*(5), 1206–1219. doi: 10.1093/molbev/msu072
- Poissant, J., Wilson, A. J., & Coltman, D. W. (2010, January). Sex-specific ge-

- netic variance and the evolution of sexual dimorphism: a systematic review of cross-sex genetic correlations. *Evolution; International Journal of Organic Evolution*, *64*(1), 97–107. doi: 10.1111/j.1558-5646.2009.00793.x
- Porcu, E., Claringbould, A., Weihs, A., Lepik, K., Richardson, T. G., Völker, U., ... BIOS Consortium (2022, August). Limited evidence for blood eQTLs in human sexual dimorphism. *Genome Medicine*, *14*(1), 89. Retrieved 2023-05-26, from <https://doi.org/10.1186/s13073-022-01088-w> doi: 10.1186/s13073-022-01088-w
- Price, A. L., Patterson, N. J., Plenge, R. M., Weinblatt, M. E., Shadick, N. A., & Reich, D. (2006, August). Principal components analysis corrects for stratification in genome-wide association studies. *Nature Genetics*, *38*(8), 904–909. doi: 10.1038/ng1847
- Price, A. L., Zaitlen, N. A., Reich, D., & Patterson, N. (2010, July). New approaches to population stratification in genome-wide association studies. *Nature Reviews. Genetics*, *11*(7), 459–463. doi: 10.1038/nrg2813
- Purcell, S., Neale, B., Todd-Brown, K., Thomas, L., Ferreira, M. A. R., Bender, D., ... Sham, P. C. (2007, September). PLINK: a tool set for whole-genome association and population-based linkage analyses. *American Journal of Human Genetics*, *81*(3), 559–575. doi: 10.1086/519795
- Ranz, J. M., Castillo-Davis, C. I., Meiklejohn, C. D., & Hartl, D. L. (2003, June). Sex-dependent gene expression and evolution of the *Drosophila* transcriptome. *Science (New York, N.Y.)*, *300*(5626), 1742–1745. doi: 10.1126/science.1085881
- Reeve, J. P., & Fairbairn, D. J. (2001). Predicting the evolution of sexual size dimorphism. *Journal of Evolutionary Biology*, *14*(2), 244–254. Retrieved 2023-04-27, from <https://onlinelibrary.wiley.com/doi/abs/10.1046/j.1420-9101.2001.00276.x> (eprint: <https://onlinelibrary.wiley.com/doi/pdf/10.1046/j.1420-9101.2001.00276.x>) doi: 10.1046/j.1420-9101.2001.00276.x
- Rhen, T. (2000, February). Sex-limited mutations and the evolution of sexual dimorphism. *Evolution; International Journal of Organic Evolution*, *54*(1), 37–43. doi: 10.1111/j.0014-3820.2000.tb00005.x
- Rice, G., Barmina, O., Hu, K., & Kopp, A. (2018, March). Evolving doublesex expression correlates with the origin and diversification of male sexual ornaments in the *Drosophila* immigrans species group. *Evolution & Development*, *20*(2), 78–88. doi: 10.1111/ede.12249

- Rinn, J. L., & Snyder, M. (2005, May). Sexual dimorphism in mammalian gene expression. *Trends in genetics: TIG*, *21*(5), 298–305. doi: 10.1016/j.tig.2005.03.005
- Ruzicka, F., Hill, M. S., Pennell, T. M., Flis, I., Ingleby, F. C., Mott, R., . . . Reuter, M. (2019, April). Genome-wide sexually antagonistic variants reveal long-standing constraints on sexual dimorphism in fruit flies. *PLoS biology*, *17*(4), e3000244. doi: 10.1371/journal.pbio.3000244
- Sharp, N. P., & Agrawal, A. F. (2013, April). Male-biased fitness effects of spontaneous mutations in *Drosophila melanogaster*. *Evolution; International Journal of Organic Evolution*, *67*(4), 1189–1195. doi: 10.1111/j.1558-5646.2012.01834.x
- Shen, J. J., Wang, Y.-F., & Yang, W. (2019). Sex-Interacting mRNA- and miRNA-eQTLs and Their Implications in Gene Expression Regulation and Disease. *Frontiers in Genetics*, *10*. Retrieved 2023-06-06, from <https://www.frontiersin.org/articles/10.3389/fgene.2019.00313>
- Signor, S. A., & Nuzhdin, S. V. (2018, July). The Evolution of Gene Expression in cis and trans. *Trends in genetics: TIG*, *34*(7), 532–544. doi: 10.1016/j.tig.2018.03.007
- Simons, Y. B., Bullaughey, K., Hudson, R. R., & Sella, G. (2018, March). A population genetic interpretation of GWAS findings for human quantitative traits. *PLoS biology*, *16*(3), e2002985. doi: 10.1371/journal.pbio.2002985
- Singh, A., & Agrawal, A. F. (2023, May). Two Forms of Sexual Dimorphism in Gene Expression in *Drosophila melanogaster*: Their Coincidence and Evolutionary Genetics. *Molecular Biology and Evolution*, *40*(5), msad091. doi: 10.1093/molbev/msad091
- Smith, T., Heger, A., & Sudbery, I. (2017, March). UMI-tools: modeling sequencing errors in Unique Molecular Identifiers to improve quantification accuracy. *Genome Research*, *27*(3), 491–499. Retrieved 2023-06-06, from <https://www.ncbi.nlm.nih.gov/pmc/articles/PMC5340976/> doi: 10.1101/gr.209601.116
- Stamboliyska, R., & Parsch, J. (2011, June). Dissecting gene expression in mosquito. *BMC genomics*, *12*(1), 297. doi: 10.1186/1471-2164-12-297
- Stewart, A. D., Pischedda, A., & Rice, W. R. (2010). Resolving intralocus sexual conflict: genetic mechanisms and time frame. *The Journal of Heredity*, *101* Suppl 1(Suppl 1), S94–99. doi: 10.1093/jhered/esq011
- Stranger, B. E., Nica, A. C., Forrest, M. S., Dimas, A., Bird, C. P., Beazley, C.,

- ... Dermitzakis, E. T. (2007, October). Population genomics of human gene expression. *Nature Genetics*, *39*(10), 1217–1224. doi: 10.1038/ng2142
- Takada, Y., Miyagi, R., Takahashi, A., Endo, T., & Osada, N. (2017, July). A Generalized Linear Model for Decomposing Cis-regulatory, Parent-of-Origin, and Maternal Effects on Allele-Specific Gene Expression. *G3 (Bethesda, Md.)*, *7*(7), 2227–2234. doi: 10.1534/g3.117.042895
- Urbut, S. M., Wang, G., Carbonetto, P., & Stephens, M. (2019, January). Flexible statistical methods for estimating and testing effects in genomic studies with multiple conditions. *Nature Genetics*, *51*(1), 187–195. doi: 10.1038/s41588-018-0268-8
- Williams, T. M., & Carroll, S. B. (2009, November). Genetic and molecular insights into the development and evolution of sexual dimorphism. *Nature Reviews. Genetics*, *10*(11), 797–804. doi: 10.1038/nrg2687
- Wilson, K. A., Beck, J. N., Nelson, C. S., Hilsabeck, T. A., Promislow, D., Brem, R. B., & Kapahi, P. (2020, July). GWAS for Lifespan and Decline in Climbing Ability in Flies upon Dietary Restriction Reveal decima as a Mediator of Insulin-like Peptide Production. *Current biology: CB*, *30*(14), 2749–2760.e3. doi: 10.1016/j.cub.2020.05.020
- Winkler, T. W., Justice, A. E., Graff, M., Barata, L., Feitosa, M. F., Chu, S., ... Loos, R. J. F. (2015, October). The Influence of Age and Sex on Genetic Associations with Adult Body Size and Shape: A Large-Scale Genome-Wide Interaction Study. *PLoS genetics*, *11*(10), e1005378. doi: 10.1371/journal.pgen.1005378
- Wittkopp, P. J., Haerum, B. K., & Clark, A. G. (2004, July). Evolutionary changes in cis and trans gene regulation. *Nature*, *430*(6995), 85–88. doi: 10.1038/nature02698
- Wittkopp, P. J., Haerum, B. K., & Clark, A. G. (2006, July). Parent-of-origin effects on mRNA expression in *Drosophila melanogaster* not caused by genomic imprinting. *Genetics*, *173*(3), 1817–1821. doi: 10.1534/genetics.105.054684
- Wittkopp, P. J., Haerum, B. K., & Clark, A. G. (2008, March). Regulatory changes underlying expression differences within and between *Drosophila* species. *Nature Genetics*, *40*(3), 346–350. doi: 10.1038/ng.77
- Wright, A. E., Darolti, I., Bloch, N. I., Oostra, V., Sandkam, B., Buechel, S. D., ... Mank, J. E. (2017, January). Convergent recombination suppression suggests role of sexual selection in guppy sex chromosome formation. *Nature Communications*, *8*, 14251. doi: 10.1038/ncomms14251

- Wright, D. B. (1993). Evolution of sexually dimorphic characters in peccaries (Mammalia, Tayassuidae). *Paleobiology*, 19(1), 52–70. Retrieved 2023-05-10, from https://www.cambridge.org/core/product/identifier/S0094837300012318/type/journal_article doi: 10.1017/S0094837300012318
- Zhao, L., Li, Y., Lou, J., Yang, Z., Liao, H., Fu, Q., . . . Bao, Z. (2019, October). Transcriptomic Profiling Provides Insights into Inbreeding Depression in Yesso Scallop *Patinopecten yessoensis*. *Marine Biotechnology (New York, N.Y.)*, 21(5), 623–633. doi: 10.1007/s10126-019-09907-9

CHAPTER 4

When and why should we expect a negative correlation between intersex correlation and sexual dimorphism?

Gemma Puixeu and Laura Hayward

Abstract

That a high genetic correlation between the sexes (r_{fm}) constrains the evolution of sexual dimorphism and that they should negatively correlate with one another are assumptions commonly made in the field of sex-specific adaptation. While these assumptions are supported by some empirical observations of a general negative relationship between the two, we lack mechanistic understanding of why and when this should occur. Concretely, two hypotheses are often proposed to explain this pattern: first, that traits with ancestrally low r_{fm} are less constrained in their ability to respond to sex-specific selection and thus evolve to be more dimorphic; second, that sex-specific selection acts to reduce the r_{fm} . However, no model to date has formalized these hypotheses and tested the conditions in which they should hold. Here, we define models of sex-specific stabilizing selection, mutation and drift to explore various scenarios potentially leading to a negative correlation between intersex correlation and sexual dimorphism, with special focus on testing the common hypotheses.

We recover the classical result that r_{fm} and expected sexual dimorphism are independent at equilibrium. However, we also put forward and demonstrate the novel hypothesis that, even at equilibrium, genetic drift can generate a negative association between the two. In addition, we illustrate that these two common hypotheses only imply a negative association if three additional assumptions are made. Specifically, that 1) some traits are sex-specifically adapting under directional selection, 2) that this sex-specific adaptation is more commonly divergent than convergent and 3) that some subset of traits have a non-infinitesimal genetic architecture.

These results provide, to our knowledge, the first mechanistic account of various scenarios potentially leading to a negative correlation between intersex correlation and sexual dimorphism. Also, they give intuition for why this pattern is found only inconsistently in nature.

1 Introduction

That a high correlation between the sexes (r_{fm}) constrains the evolution of sexual dimorphism and that both should negatively correlate with one another are common assumptions in the field of sex-specific adaptation (Fisher, 1958, Chapter 6), (Lande, 1980, 1987; Bonduriansky & Rowe, 2005; Stewart et al., 2010). These assumptions are supported by general evidence that traits that are more sexually dimorphic have lower r_{fm} values which, although far from universal (Cowley & Atchley, 1988; Chenoweth & Blows, 2003; Ashman & Majetic, 2006; Leinonen et al., 2011; Puixeu et al., 2019 – Chapter 1 of this thesis), has been described across traits and species (e.g. Preziosi & Roff, 1998; Delph et al., 2004, 2010; Bonduriansky & Rowe, 2005; McDaniel, 2005; Poissant et al., 2010).

Two hypotheses are most commonly proposed as potential explanations for this pattern (stated in e.g. Bonduriansky & Rowe, 2005; Griffin et al., 2013; Stewart & Rice, 2018; McGlothlin et al., 2019): first, that traits with ancestrally low r_{fm} are less constrained in their ability to respond to sex-specific selection and thus evolve to be more dimorphic (as discussed in, for example, Bolnick & Doebeli, 2003; Poissant et al., 2010; Stewart et al., 2010); second, that sex-specific selection acts to reduce the r_{fm} (Lande, 1980; Bonduriansky & Rowe, 2005; Bonduriansky & Chenoweth, 2009; McGlothlin et al., 2019).

In line with the first hypothesis is the idea that sexual dimorphism will easily (hardly) evolve for traits with a low (high) intersex correlation (Stewart et al., 2010; Stewart & Rice, 2018). The potential for a high intersex correlation to pose a long-term constraint on the evolution of sex differences has been illustrated by some artificial selection experiments (Harrison, 1953; Reeve & Fairbairn, 1996; Stewart & Rice, 2018). Most notably, Stewart and Rice (2018) observe a minimal change in sexual dimorphism in fly body size after as many as 250 generations of selection for sexual dimorphism. However, multiple studies have also provided evidence for fast, seemingly unconstrained, sexual dimorphism evolution (Frankham, 1968a, 1968b; Bird & Schaffer, 1972; Eisen & Hanrahan, 1972; Zwaan et al., 2008; Delph et al., 2011). For example, Bird and Schaffer (1972) selected fruit flies for sexual dimorphism on wing size and found a significant change in sex differences after only 15 generations. Such qualitative differences in outcomes are usually attributed to differences in genetic architecture: traits with a high (low) intersex correlation will easily (hardly) decouple between the sexes (Stewart et al., 2010).

This prediction is well-supported by models of sex-specific adaptation of quanti-

tative traits, first formulated by Lande (1980), who showed that intersex correlation determines the rate of sexually-dimorphic adaptation. Nevertheless, from the same models, it follows that as long as intersex correlation is imperfect ($r_{fm} < 1$) and given enough time, sexual conflict will be fully resolved. This suggests that, while r_{fm} poses a quantitative constraint on sex-specific adaptation, it is not predictive of the extent of sexual dimorphism eventually achieved. Most 2-sex models of this process (e.g. Lande, 1980; Cheverud et al., 1985) have assumed an infinitesimal genetic architecture, which ignores individual loci and assumes that genic (co)variances remain constant over time (Lande, 1976; Barton et al., 2017). However, we know that considering different genetic architectures can lead to qualitatively different results (as discussed in e.g. Rhen, 2000; Reeve & Fairbairn, 2001). For example, in single-locus (or generally genetic variance-limited) models of sexual antagonism, sexual conflict is not resolved (Kidwell et al., 1977; Rice, 1984; Rhen, 2000; Morrow & Connallon, 2013), and more realistic models considering polygenic genetic architectures (Reeve & Fairbairn, 2001; Muralidhar & Coop, 2023) involve changes in genetic (co)variances over time, and thus display phenotypic dynamics that deviate from the infinitesimal predictions.

The second hypothesis states that a negative relationship between intersex correlation and sex differences arises because sex-specific selection favors genetic modifications that reduce the intersex covariance, which allow sex-specific adaptation (Lande, 1980, 1987; Bonduriansky & Rowe, 2005; Bonduriansky & Chenoweth, 2009; McGlothlin et al., 2019). Indeed, according to the standard picture of sexual dimorphism evolution (as discussed in e.g. Rice & Chippindale, 2001; Bonduriansky & Rowe, 2005; Cox & Calsbeek, 2009; Morrow, 2015), an initially monomorphic trait that becomes subject to sex-specific selection will decouple between sexes, allowing sex-specific means to approach their optima and resolve sexual conflict. The idea that this process involves a decrease in intersex correlation traces back to Lande (1980), who, as had Fisher (1958, Chapter 6), suggested that genes with sex-limited effects would accumulate over time leading to the prediction that r_{fm} will decrease as sexual dimorphism evolves. However, neither author presented a mathematical justification for this suggestion. Instead, it seems to be based on an intuition of how the intersex correlations should evolve, potentially implying the evolution of sex-specific modifiers, and generally an evolving genetic architecture (Bonduriansky & Rowe, 2005), allowing for a stable, long-term reduction in intersex correlation (Bonduriansky & Rowe, 2005; Williams & Carroll, 2009; Stewart et al., 2010). Nev-

ertheless, the evolution of genetic architecture, in general and particularly for sexual dimorphism, is likely to be a very slow process (Williams & Carroll, 2009; Stewart et al., 2010), and is probably not occurring within the scope of shorter-term evolutionary processes, including most artificial selection experiments cited above, where phenotypes evolve without major changes in the genetic architecture.

In spite of these predictions for scenarios leading to a negative correlation between intersex correlation and sexual dimorphism, we have no good understanding of the underlying mechanisms and the assumptions they require – which defines the main motivation of the current study.

We formulate a model of sex-specific stabilizing selection, mutation and drift (a 2-sex extension of Hayward & Sella, 2022), which is a common regime in sex-specific adaptation (Prasad et al., 2007; Abbott et al., 2010; Stulp et al., 2012; Sanjak et al., 2018), and analyze the dynamics of sexually-concordant and sexually-dimorphic evolution after a shift in sex-specific optima, while keeping track of intersex correlation over time. Given that the dynamics seem to strongly depend on the assumptions on the genetic architecture, we compare the predictions of the deterministic infinitesimal model with the evolutionary outcomes of simulations considering two types of highly polygenic architectures, which we consider non-evolving (i.e. we are not considering modifier loci leading to stable decreases in intersex covariances): an approximately infinitesimal architecture, where all contributing alleles have small effect sizes and do not experience substantial changes in frequency under directional selection, and a less infinitesimal architecture with a significant proportion of large-effect mutations, which seems to be the genetic architecture underlying most complex traits, as suggested by numerous GWAS (e.g. Wood et al., 2014; Locke et al., 2015; Simons et al., 2018).

We find that, consistent with Lande (1980)’s classical result, at equilibrium under stabilizing selection intersex correlation is independent of expected sexual dimorphism. However, we also show that drift can generate a negative covariance between intersex correlation at equilibrium, which represents a novel mechanism with the potential to generate this pattern.

By considering the transient phase of adaptation to new sex-specific optima (during which directional selection acts), we test the two hypotheses commonly used to explain the existence of a negative association between r_{fm} and sexual dimorphism. In line with the first hypothesis, that an initially low intersex correlation allows for

more dimorphism evolution, is the previously-obtained result that intersex correlation determines the rate of sexually-dimorphic adaptation. Supporting the second hypothesis that evolution of sex differences drives a decrease in intersex correlation and agreeing with results by [Reeve and Fairbairn \(2001\)](#), we find that, when genetic architecture is not approximately infinitesimal, there is a transient decrease in sex-specific variances leading to a temporary decrease in intersex correlation with sexually-dimorphic evolution under directional selection. However, since the results for both hypotheses hold for divergent as well as convergent evolution (adaptation to a shift in sex-specific trait optima where they move further apart and closer together, respectively), their contribution to the generation of a qualitative negative association between intersex correlation and sexual dimorphism requires the additional assumption that sex-specific adaptation is more commonly divergent than convergent.

Altogether, our results provide, to our knowledge, the first account of various mechanisms which can contribute to generating a negative correlation between intersex correlation and sexual dimorphism. They allow us to formalize and contextualize common intuitions in the field, as well as clearly state the assumptions and mechanisms that underlie common hypotheses, thereby providing a better understanding of the mechanisms potentially leading to empirical observations.

2 Methods

2.1 The model

We define a 2-sex extension of the standard model for the evolution of a highly polygenic, quantitative trait under stabilizing selection ([S. Wright, 1935](#); [Simons et al., 2018](#); [Hayward & Sella, 2022](#)). Assuming an additive model, an individual's phenotypic value follows from its genotype ([Lynch & Walsh, 1998](#)), and is given, for females (z_f) and males (z_m), by

$$z_f = \sum_{i=1}^L 2a_{i,f} + \epsilon_f; \quad z_m = \sum_{i=1}^L 2a_{i,m} + \epsilon_m. \quad (1)$$

The first term is the genetic contribution, given by the sum of the sex-specific phenotypic effects ($a_{i,f}$ and $a_{i,m}$) inherited from both parents across L sites. The second term is the sex-specific environmental contribution, which we take to be normally distributed and independent of the genetic contribution ($\epsilon_\alpha \sim N(0, V_{E\alpha})$)

for $\alpha = f, m$).

Stabilizing selection is modelled via sex-specific Gaussian fitness functions, where fitness declines with distance from sex-specific optima (O_f, O_m):

$$W_f(z_f) = \text{Exp} \left[-\frac{\gamma_f^2(z_f - O_f)^2}{V_S} \right]; \quad W_m(z_m) = \text{Exp} \left[-\frac{\gamma_m^2(z_m - O_m)^2}{V_S} \right]. \quad (2)$$

Here, $1/V_S$ determines the overall strength of stabilizing selection; γ_f and γ_m modulate the proportion of selection that acts on each sex, and satisfy $\gamma_f^2 + \gamma_m^2 = 1$. We assume that neither sex is evolving neutrally, so the sex-specific selection strengths, $1/V_{S,f} \equiv 2\gamma_f^2/V_S$ and $1/V_{S,m} \equiv 2\gamma_m^2/V_S$, are nonzero (ie., $\gamma_f, \gamma_m > 0$). We choose to parametrize the problem in terms of γ_f, γ_m and V_S instead of $V_{S,f}, V_{S,m}$ because it allows us to separate the overall strength of selection and the proportion that acts on each sex; however, replacing them with $V_{S,f}, V_{S,m}$ recovers the parametrization used in previous studies (e.g. Lande, 1980). Since the sex-specific additive environmental contributions to phenotypic variation can be absorbed into $V_{S,f}, V_{S,m}$ (by replacing them with $V'_{S,f} = V_{S,f} + V_{\epsilon,f}$; $V'_{S,m} = V_{S,m} + V_{\epsilon,m}$, Turelli, 1984), we consider only the genetic contributions.

The population evolves according to the standard model of a diploid, panmictic population of constant size N , with non-overlapping generations. Exactly half of individuals are female and half male and, each generation, mothers and fathers are randomly chosen to reproduce with probabilities proportional to their fitness (via Wright-Fisher sampling with fertility selection). This is followed by mutation, free recombination and Mendelian segregation. We use the infinite sites approximation, which is accurate provided that the per site mutation rate, u , is sufficiently low so that very few sites are hit by mutation more than once over relevant timescales ($Nu \ll 1$), so loci are only rarely more than bi-allelic. Consequently, we sample the number of new mutations per gamete per generation from a Poisson distribution with mean $U = Lu$.

The sex-specific effect sizes of incoming mutations, a_f and a_m , are obtained as follows: we draw the overall scaled strength of stabilizing selection of the allele ($2Ns_e$) from an exponential distribution with different averages (see below), and we determine the fraction of stabilizing selection that acts on the allele via females from a second distribution (details will be provided in Section 3.1.1.1). The sex-specific effect sizes follow from these two quantities (using Equation 16 in Section 3.1.1.1).

For each mutation, we assume there is an equal probability of its being positive or negative (increasing or decreasing the trait value). In Table 1 we provide a summary of all notation used.

2.2 Parameter ranges and choice of units

We examine the genetic and phenotypic dynamics of a 2-sex population adapting to changes in sex-specific optima. We follow previous studies (Simons et al., 2018; Hayward & Sella, 2022) in defining the working parameter ranges to ensure that the conditions assumed by the analytic framework hold.

We assume that the trait is highly polygenic ($2NU \gg 1$) and subject to substantial but not catastrophically strong stabilizing selection. We further assume that the distance between the optimum phenotype in females (O_f) and that in males (O_m) is not massive relative the width of the fitness function ($|O_f - O_m| \lesssim 0.5\sqrt{V_S}$; see Section 3 in Supplementary Material). Under these assumptions, the phenotypic distribution at stabilizing selection-mutation-drift balance is symmetric, with sex-specific mean phenotypes exhibiting small, rapid fluctuations around the respective optima with variance $\delta^2 = \frac{V_S}{2N}$ (Bürger & Lande, 1994); the phenotypic variance is greater than these fluctuations $V_A \gg \delta^2$, but substantially smaller than the width of the fitness function $V_A \ll V_S$.

After ensuring that the population is at equilibrium under mutation-selection-drift balance, we sometimes apply a shift in sex-specific optima Λ_f, Λ_m . We assume that the magnitude of the shift is larger than the random fluctuations of the sex-specific trait means ($|\Lambda_f|, |\Lambda_m| > \delta$), but smaller than, or on the order of, the width of the fitness function ($|\Lambda_f|, |\Lambda_m| \lesssim \sqrt{V_S}$). We tested the limits to the shift size: for $\Lambda_f, \Lambda_m \lesssim 0.5\sqrt{V_S}$ the above assumption is attained and the analytics approximate well the phenotypic variation after the shift in the extreme case with symmetric sex-specific selection and completely shared genetic architecture between the sexes (see Section 3 in Supplementary Material).

We work in units of δ , the typical deviation of the population mean from the optimum at equilibration. Working in these units (by setting $V_S = 2N$ so that $\delta^2 = \frac{V_S}{2N} = 1$) makes our results invariant with respect to changing the population size, N , stabilizing selection parameter, V_S , mutational input per generation, $2NU$, and distributions of incoming effects, $g(a)$.

2.3 Simulations

In order to simulate the model efficiently, we make two additional simplifying assumptions. First, we assume that alleles are in linkage equilibrium, which allows us to simulate the evolution of the population by tracking only the list of segregating alleles in the population, rather than individuals. Second, we assume that allele frequency differences between sexes after selection are negligible (i.e., $x_f = x_m = x$ so alleles are at Hardy-Weinberg equilibrium). This assumption allows us to track only average frequencies of alleles, rather than sex-specific frequencies, as does our analytical framework, and holds because we consider that selection is weak. Previous studies have shown that sexually-antagonistic selection can lead to considerable differences in allele frequencies between the sexes, where balancing selection contributes to the maintenance of substantial genetic variation (Kidwell et al., 1977; Rice, 1984; Morrow & Connallon, 2013; Connallon & Clark, 2014a). However, this requires very strong selection, beyond the range we consider in this study, and also beyond what is likely to apply to most traits. Besides the Wright-Fisher Hardy-Weinberg simulations, we however wrote various other types of simulations with different simplifying assumptions and computational tractability to explicitly test that all assumptions required by the analytical framework are met by our simulations.¹ In all simulations, unless explicitly stated otherwise, we let populations burn in for a period of $10N$ generations to ensure they attain mutation-selection-drift balance, before applying the shift in optima. We display averages and standard errors of the means (SEM) across 200 replicates.²

Throughout we run simulations assuming a highly polygenic trait ($2NU \gg 1$), but in two different parameter regimes, with genetic architectures that differ in such a way as to affect simulation results qualitatively. In the first parameter regime, simulation results are well-approximated by the infinitesimal model, which assumes

¹These include: first, exact simulations, where we keep track of all individuals and the mutations they carry along time. We defined two types of exact simulations: i) with fertility selection, where parents of the new generation are selected based on their fitness, realizing the full model described above, and ii) with viability selection, where we accept or reject offspring generated from randomly-selected parents based on their fitness. In the second type of simulations, we track sex-specific allele frequencies rather than individuals, and update them according to the Wright-Fisher process, assuming linkage equilibrium. The third type of simulations, used for the results, additionally assumes Hardy-Weinberg equilibrium, meaning that the allele frequency differences between sexes after selection are negligible ($x_f = x_m = x$), so we only track overall allele frequencies. Besides the 2-sex simulations, we also defined 1-sex versions of each type of simulations, to make sure that our results match those of previous studies using a 1-sex version of our framework (Hayward & Sella, 2022).

²This is the default scheme for all simulations presented in the results; variations to this are clearly stated in reference to the relevant figure.

that the trait is underlied by an infinite number of alleles, each with an infinitesimal effect size (Barton et al., 2017). For our modest shifts in optima, this will be the case when most mutations have fairly small effect sizes ($2N s_e < 4$; corresponding to the *Lande case* in Hayward & Sella, 2022). The second parameter regime, while still highly polygenic, has a significant contribution to trait variation from larger effect alleles (with $2N s_e > 4$) and displays deviations from infinitesimal behaviour when subject to directional selection (the *Non-Lande case* in Hayward & Sella, 2022). We henceforth refer to these two types of genetic architecture as ‘approximately infinitesimal’ and ‘multigenic’, respectively.

To simulate traits with different degrees of intersex correlation, we relied on previous studies, which typically reduce the very complex regulatory genetic architecture of sex-specific trait expression into the consideration of shared and sex-specific mutations (Rhen, 2000; Reeve & Fairbairn, 2001; Bolnick & Doebeli, 2003). In this case, we assume there is a proportion, $p \equiv r \cdot 2 / (1 + r)$ (where we specify $0 \leq r \leq 1$), of shared mutations with equal effect sizes in males and females ($a_f = a_m$), and the remaining $1 - p$ are sex-specific, out of which half are female-specific ($a_m = 0$) and half are male-specific ($a_f = 0$). For each mutation, there is an equal probability of its increasing the trait or decreasing the trait. This choice of trait architecture is extremely convenient because it gives us direct control over r_{fm} , as the intersex correlation exactly corresponds to the parameter r ($E[r_{fm}] = r$; see Section 3.1.1.2 for details). It is worth noting, however, that our analytic results do not rely on this simplification.

Below we provide a summary of the parameter values used in the simulations:

- In all simulations the population size is $N = 1,000$ and we take $\gamma_f^2 = \gamma_m^2 = 1/2$, so that the strength of stabilizing selection is the same in both sexes ($V_{S,f} = V_{S,m} = V_S$).
- In all simulations (except for Figure 1) we consider an overall genetic variance of $V_A = 40$.
- In order to illustrate the approximately infinitesimal and multigenic architectures, we consider different combinations of mutation rate U and average effect size $E(a^2)$, sampled from an exponential distribution, yielding the same overall variance at equilibrium before the shift:
 - Approximately infinitesimal architecture: $E(a^2) = 1$ and $U = 0.0134$
 - Multigenic architecture: $E(a^2) = 16$ and $U = 0.0047$

- We run simulations with various $E[r_{fm}]$ values (parametrized by r), to illustrate the evolutionary outcomes with various genetic correlations between sexes. These correspond to $r = 0.33, 0.67$ and 0.90 .
- We implement shifts in sex-specific means of concrete sizes. These correspond to $0.15\sqrt{V_S}$ (small), $0.25\sqrt{V_S}$ (medium) and $0.5\sqrt{V_S}$ (large). These magnitudes are within the limits of the shift size for our analytical approximations to work (tested in Section 3 of the Supplementary Material). Relative to standard error of the phenotypic distribution (considering $V_A = 40$), the three shift sizes correspond to: $1.06\sqrt{V_A}$ (small), $1.77\sqrt{V_A}$ (medium) and $3.54\sqrt{V_A}$ (large).

2.4 Empirical calculation of sex-specific variances, intersex covariance and intersex correlation

Empirical sex-specific variances ($V_{A,f}^e$ and $V_{A,m}^e$) can easily be computed as the variance across all individuals of each sex in the population. Under our assumptions of linkage equilibrium and an additive trait with no environmental contribution, they should correspond to the sex-specific genic variances, which are sum of the contributions to variance of all alleles in each sex:

$$V_{A,f} = \sum_i^L 2a_{i,f}^2 x_i(1 - x_i); \quad V_{A,m} = \sum_i^L 2a_{i,m}^2 x_i(1 - x_i). \quad (3)$$

Similarly, under our assumptions, the intersex covariance, B , is given by the contributions to covariance of all alleles

$$B = \sum_i^L 2a_{i,f}a_{i,m}x_i(1 - x_i); \quad (4)$$

and the intersex correlation is given by

$$r_{fm} = \frac{B}{\sqrt{V_{A,f}V_{A,m}}}. \quad (5)$$

Technically, the intersex covariance, B , and correlation, r_{fm} , are defined as the covariance and correlation between allelic effects if they were to be expressed in both sexes at the same time. Since genotypes are never expressed simultaneously in both a female and male (except in the case of heavily inbred populations), the empirical

calculations of intersex covariance and correlation relies on phenotypic similarity between relatives. In this study, we use a parent-to-offspring regression to calculate empirical intersex correlation (Lynch & Walsh, 1998; as in e.g. Bonduriansky & Rowe, 2005) as:

$$r_{fm}^e = \sqrt{\frac{h_{MS}^2 h_{FD}^2}{h_{MD}^2 h_{FS}^2}}, \quad (6)$$

where h^2 represents heritability, calculated as twice the offspring-to-parent phenotypic regression coefficient, for mother-son (MS), father-daughter (FD), mother-daughter (MD) and father-son (FS). We compute empirical between-sex covariance from empirical sex-specific variances and empirical intersex correlation as

$$B^e = \frac{\sqrt{V_{A,f}^e V_{A,m}^e}}{r_{fm}^e}. \quad (7)$$

As we are tracking allele frequencies we can use Equations 3, 4 and 5 to compute sex-specific variances, intersex covariance and intersex correlation for our results; however, the empirical estimates would be required to compute such quantities from genotypes and phenotypic values for individuals in a population rather than allele frequencies, which would be the case for natural populations as well as from exact simulations, where we are tracking all mutations carried by each individual.

3 Results

In the present study, we examine the relationship between intersex correlation (defined in Section 2.4 above) and sexual dimorphism, defined as the difference between sex-specific trait means: $SD = \bar{z}_f - \bar{z}_m$ (where sex-specific trait means can be calculated by summing the allelic contributions to the mean $\bar{z}_f = \sum_i^L 2a_{i,f}x_i$ and $\bar{z}_m = \sum_i^L 2a_{i,m}x_i$). We predict the circumstances under which one should expect a negative correlation between the two, a pattern which, although often observed in empirical studies, we currently lack a mechanistic understanding of. To this end, we characterize the phenotypic and allelic dynamics of a population at equilibrium under sex-specific stabilizing selection, mutation and drift. In section 3.1, we describe the implications for the equilibrium relationship between intersex correlation and sexual dimorphism. Then, in Section 3.2, we examine two common hypotheses for the relationship between intersex correlation and sexual dimorphism. In order to do so, we explore the allelic and phenotypic response of a population (initially at

equilibrium) to a change in sex-specific optima. We consider how these two common hypotheses are affected by assumptions made regarding 1) the genetic architecture of the trait (i.e. if the trait is approximately infinitesimal or multigenic), which we consider non-evolving, and 2) whether adaptation is sexually-concordant (i.e. the mean trait optimum across both sexes changes) or sexually-antagonistic (i.e. the distance between sex-specific optima changes).

Throughout our analysis we rely on the fact that allele dynamics, both in and out of equilibrium (and under the continuous time approximation), can be described in terms of the first two moments of change in frequency in a single generation. The first moment, which, for an allele segregating at frequency x with effect sizes a_f and a_m in females and males, respectively, is calculated by averaging the fitness of the three genotypes over genetic backgrounds, and is given by

$$E[\Delta x] = \underbrace{\left(\frac{a_f D_f \gamma_f^2}{V_S} + \frac{a_m D_m \gamma_m^2}{V_S} \right) x(1-x)}_{\text{Directional selection}} - \underbrace{\left(\frac{a_f^2 \gamma_f^2}{V_S} + \frac{a_m^2 \gamma_m^2}{V_S} \right) x(1-x)(1/2-x)}_{\text{Stabilizing selection}}, \quad (8)$$

where $D_f \equiv O_f - \bar{z}_f$ and $D_m \equiv O_m - \bar{z}_m$ are the distances of sex-specific trait means from their respective optima (Equation 8 is derived in Section 1 of Supplementary Material). The second moment is the standard drift term

$$V[\Delta x] \approx \frac{x(1-x)}{2N}. \quad (9)$$

The two terms in Equation 8 reflect two selection modes. The first corresponds to directional selection which, within each sex, acts to increase (decrease) the frequency of those alleles which move the mean phenotype of that sex closer to (further away from) its optimum; its effect becomes weaker as the sex-specific distance to the optima, D_f, D_m , decrease. The second term corresponds to stabilizing selection, which acts to decrease alleles' contributions to phenotypic variance by reducing minor allele frequencies (MAFs); it weakens as the MAF approaches 1/2. Replacing, $V_{S,f} = V_S/(2\gamma_f^2)$ and $V_{S,m} = V_S/(2\gamma_m^2)$ gives the sex-specific strengths of stabilizing selection.

3.1 The relationship between r_{fm} and sexual dimorphism at equilibrium

3.1.1 At equilibrium, expected sexual dimorphism and intersex correlation are independent of each other

Under our assumption of an infinite sites model, and provided that at least some incoming mutations have different effects in the two sexes (i.e. $a_f \neq a_m$ for some alleles), directional selection will eventually drive the expected sex-specific means to their respective optima (Figure 1A). Thus at equilibrium

$$E[SD] = E[\bar{z}_f] - E[\bar{z}_m] = O_f - O_m. \quad (10)$$

Clearly, the expression for $E[SD]$ does not depend on intersex correlation. To establish that expected equilibrium intersex correlation and expected sexual dimorphism are independent, it remains to derive an expression for expected r_{fm} at equilibrium and show that it does not depend on trait optima or trait means. In order to do this, we introduce a useful way to parameterize sex-specific allele effects.

3.1.1.1 Parameritization of sex-specific allele effects At equilibrium, $D_f = D_m = 0$ in expectation and only the stabilizing selection term in Equation 8 is relevant:

$$E_{eq}[\Delta x] = -\frac{a^2}{V_S}x(1-x)(1/2-x), \quad (11)$$

where we define $a > 0$ to be the *total* phenotypic magnitude with

$$a^2 \equiv a_f^2\gamma_f^2 + a_m^2\gamma_m^2. \quad (12)$$

It follows from Equation 11, that allele dynamics at equilibrium depend only on the scaled selection coefficient given by

$$2Ns_e \equiv 2Na^2/V_S = a^2/\delta^2 = a^2, \quad (13)$$

where the last equality follows from the fact that we are working in units of δ ($V_S = 2N$). Consequently, dynamics at equilibrium are independent of mean trait values and therefore of the level of sexual dimorphism.

Although allele frequency distributions at equilibrium depend only on the overall strength of selection on alleles (captured by a^2), the intersex correlation depends on whether stabilizing selection is stronger when the allele is present in a female or

when it is present in a male; which we parametrize in terms of an angle, ϕ_a . This angle directly determines the fraction of stabilizing selection on an allele that acts via females ($\cos^2(\phi_a)$) and via males ($\sin^2(\phi_a)$) and corresponds to:

$$\cos^2(\phi_a) = \frac{a_f^2 \gamma_f^2}{a^2} \quad \text{and} \quad \sin^2(\phi_a) = \frac{a_m^2 \gamma_m^2}{a^2} \quad (\text{with } \cos^2(\phi_a) + \sin^2(\phi_a) = 1). \quad (14)$$

Parameterizing allele effects in terms of the allele magnitude a , and the angle, ϕ_a (rather than the sex specific effects a_f and a_m), we can re-write the expected change in frequency at equilibrium under stabilizing selection (Equation 11) as

$$E_{eq}[\Delta x] = - \underbrace{\frac{a^2}{V_s}}_{\text{total strength of selection}} \left[\underbrace{\cos^2(\phi_a)}_{\text{fraction selection via females}} + \underbrace{\sin^2(\phi_a)}_{\text{fraction selection via males}} \right] x(1-x)(1/2-x). \quad (15)$$

We have chosen this parameterization because the distribution of allele magnitudes, $g(a)$, directly determines whether the genetic architecture is approximately infinitesimal or multigenic and, as we will soon demonstrate, the distribution of angles, $h(\phi_a)$, determines the intersex correlation. However, (using γ_f and γ_m) it is easy to recover the sex-specific effects from a and ϕ_a :

$$a_f = \frac{a \cos(\phi_a)}{\gamma_f} \quad \text{and} \quad a_m = \frac{a \sin(\phi_a)}{\gamma_m}. \quad (16)$$

Crucially, our analysis relies on the assumption that a and ϕ_a are independent, meaning that large-effect mutations are as likely to be female-biased as male-biased.

3.1.1.2 The intersex correlation at equilibrium In order to characterize the intersex correlation we need to calculate the 2nd central moments of the phenotypic distribution ($V_{A,f}$, $V_{A,m}$ and B defined in Equations 3 and 4). To do so, it is useful to define a total genetic variance which depends on alleles' total magnitudes (as defined in Equation 12):

$$V_{A,T} \equiv \sum_i^L 2a_i^2 x_i (1 - x_i). \quad (17)$$

Since Equation 11 for the expected change in frequency is identical to the single-sex case for an allele with magnitude a , the total variance is equal to the genic variance

in the single-sex case and is given by

$$V_{A,T} = 2NU \cdot \int_0^\infty v(a)g(a)da, \quad (18)$$

where $g(a)$ is the distribution of incoming effect magnitudes, $v(a) = 4a \cdot D_+(a/2)$ and D_+ is the Dawson function (Hayward & Sella, 2022).

In Supplementary Section 2, we show that one can compute the expressions for sex-specific variances and covariance (relative to $V_{A,T}$) at equilibrium under stabilizing selection-mutation-drift balance as integrals over the distribution of angles, $h(\phi_a)$,

$$\begin{aligned} \frac{V_{A,f}}{V_{A,T}} &= \frac{1}{\gamma_f^2} \int_0^{2\pi} \cos(\phi_a)^2 h(\phi_a) d\phi_a; & \frac{V_{A,m}}{V_{A,T}} &= \frac{1}{\gamma_m^2} \int_0^{2\pi} \sin(\phi_a)^2 h(\phi_a) d\phi_a \\ \frac{B}{V_{A,T}} &= \frac{1}{\gamma_f \gamma_m} \int_0^{2\pi} \cos(\phi_a) \sin(\phi_a) h(\phi_a) d\phi_a. \end{aligned} \quad (19)$$

The expressions in Equation 19 can be combined to obtain the intersex correlation, yielding

$$r_{fm} = \frac{\int \cos(\phi_a) \sin(\phi_a) h(\phi_a) d\phi_a}{\sqrt{\int \cos(\phi_a)^2 h(\phi_a) d\phi_a \cdot \int \sin(\phi_a)^2 h(\phi_a) d\phi_a}}. \quad (20)$$

It is immediate from Equation 20, that the intersex correlation at equilibrium is independent of trait means and trait optima and therefore does not depend on the expected level of sexual dimorphism, a classical result first discussed by Lande (1980). In addition, Equation 20 shows that r_{fm} at equilibrium depends only on the fraction of stabilizing selection acting on alleles via females (or males), which is determined by the distribution of angles $h(\phi_a)$. Since

$$\tan(\phi_a) = \frac{a_m}{a_f} \cdot \frac{\gamma_f}{\gamma_m}, \quad (21)$$

it is apparent that the parameter ϕ_a depends both on the ratio of alleles' sex-specific mutational effects (i.e., a_f/a_m) and on the ratio of the strength of stabilizing selection in the two sexes (i.e. γ_f/γ_m). Thus Equation 20 demonstrates that the presence of sexually-antagonistic variation (i.e., $r_{fm} < 1$) can arise from both sex-specific mutation ($a_f \neq a_m$) and sex-specific stabilizing selection ($\gamma_f \neq \gamma_m$), confirming the findings of other studies (e.g. Connallon & Clark, 2014b).

As mentioned in Section 2.3, in simulations we use a specific, highly simplified distribution of angles, $h_r(\phi_a)$ parameterized by $0 \leq r \leq 1$. In particular, we assumed

a proportion, $p \equiv r \cdot 2/(1+r)$ of mutations have equal effect sizes in the two sexes ($a_f = a_m$ and $\phi_a = \pi/4$ or $5\pi/4$), and a proportion $1-p$ of mutations are sex-specific, out of which half are female-specific ($a_m = 0$ and $\phi_a = 0$ or π) and half are male-specific ($a_f = 0$ and $\phi_a = \pi/2$ or $3\pi/2$). For each mutation, there is an equal probability of its increasing the trait (i.e., $\phi_a = 0, \pi/4$ or $\pi/2$) or decreasing the trait (i.e., $\phi_a = \pi, 5\pi/4$ or $3\pi/2$). This choice of $h(\phi_a)$ is convenient because it provides a simple way to control r_{fm} : direct computation using Equation 20 yields $E[r_{fm}] = r$. Nevertheless, our analytical results are derived for general distributions h , provided alleles are equally likely to be positive or negative (i.e., $h(\phi_a) = h(\phi_a + \pi)$, e.g. Equation 20).

In simulations, in addition to using $h_r(\phi_a)$, we also typically assume that the overall strength of stabilizing selection is the same in both sexes ($\gamma_f = \gamma_m = 1/\sqrt{2}$). In this case, sex-specific variances are equal and we can drop the subscripts f and m in referencing them, i.e.

$$V_A \equiv V_{A,f} = V_{A,m} = V_{A,T}. \quad (22)$$

In addition, the intersex covariance is given by $B = rV_{A,T}$.

It is important to note that our expressions for V_A , $V_{A,T}$, $V_{A,f}$, $V_{A,m}$, B and r_{fm} (Equations 18, 19, 20 and 22) are actually expressions for the expected values of these quantities. Since, in this study, we only consider the expected values of the phenotypic variances, covariance and correlations, we suppress the $E[\dots]$ when referring to these quantities, for ease of reading.

3.1.2 At equilibrium, drift can generate a negative correlation between r_{fm} and sexual dimorphism

In the previous section we saw that, in expectation, between-sex correlation, r_{fm} , and sexual dimorphism, $SD = \bar{z}_f - \bar{z}_m$, are independent of each other at equilibrium. In particular, we saw that $E[SD] = O_f - O_m$ and that consequently, when sex-specific optima coincide, irrespective of intersex correlation, we expect no sexual dimorphism. Here, we show that genetic drift can generate a nonzero sexual dimorphism even when sex-specific optima are equal ($O_f = O_m$); and, importantly, that the amount of dimorphism generated depends on the intersex correlation.

The nonzero dimorphism arises from the fact that—although, in expectation, at equilibrium trait means are equal to trait optima—genetic drift leads them to undergo rapid fluctuations around their expected values (Bürger & Lande, 1994).

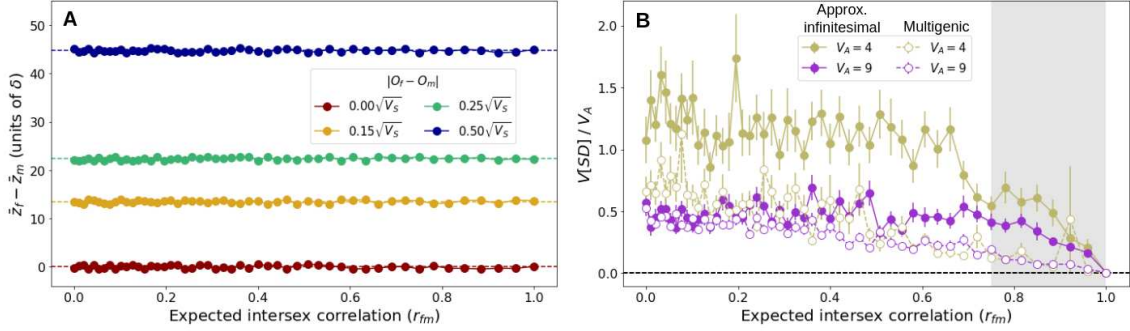


Figure 1: Relationship between expected intersex correlation (r_{fm}) and sexual dimorphism at equilibrium. A: Sexual dimorphism, as difference between sex-specific trait means ($\bar{z}_f - \bar{z}_m$) corresponds to the difference between sex-specific optima $|O_f - O_m|$ for $r_{fm} < 1$. This result is consistent across overall genetic variances (V_A) for approximately infinitesimal and multigenic genetic architectures, so we show results just for approximately infinitesimal genetic architecture with $V_A = 9$. B: Sexual dimorphism, as variance-normalized squared difference between sex-specific means ($\frac{(\bar{z}_f - \bar{z}_m)^2}{V_A}$), over various levels of r_{fm} , variances ($V_A = 4, 9$) and for approximately infinitesimal and multigenic genetic architectures ($E(a^2) = 1$ and 16 , respectively), for $O_f = O_m = 0$. All simulations were run for $10N$ generations (except for $r_{fm} > 0.95$, which needed longer to reach equilibrium and were run for $100N$ generations). For both, error bars indicate SEM across 200 replicates.

When trait values in the two sexes are uncorrelated ($r_{fm} = 0$), female and male trait means will fluctuate independently. Consequently, most of the time, sex-specific trait means will not be equal, implying a nonzero sexual dimorphism ($SD \neq 0$). In contrast, if the intersex correlation is 1, with all incoming mutations having the same effect in both sexes ($a_f = a_m$), then the mean trait value in females and males must always coincide, and sexual dimorphism will be zero at all times. For intermediate intersex correlations, the two trait means will fluctuate in a somewhat correlated fashion that depends on the intersex correlation.

The magnitude of the typical distance between the two trait means, generated by genetic drift, is captured by the variance in sexual dimorphism,

$$V[SD] = V[\bar{z}_f] + V[\bar{z}_m] - 2Cov[\bar{z}_f, \bar{z}_m]. \quad (23)$$

The significance of the fluctuations depends on how their magnitude compares to the genetic variance in the trait value, i.e. $\sqrt{V_A}/\delta$. Thus, in Figure 1B we plot $V[SD]/V_A$ for different values of intersex correlation, and for $\sqrt{V_A}/\delta = 2$ and 3 , which correspond to fluctuations of the means around the optima of typical magnitude half and a third of the standard deviation in the trait distribution, respectively.

From the figure we see that, for both an approximately infinitesimal and a multi-genic genetic architecture, the average magnitude of fluctuations in SD decrease with increasing intersex correlation, with a particularly steep drop off once r_{fm} exceeds ≈ 0.75 (the shaded area in the figure). The fluctuations can be highly significant when the genetic variance is low. For example when $V_A/\delta^2 = 4$ and the trait architecture is approximately infinitesimal, $V[SD]/V_A \approx 1$ for $r_{fm} < 0.75$, implying that, just by chance, trait means in the two sexes could frequently differ by a full phenotypic standard deviation.

3.2 A negative relationship between r_{fm} and sexual dimorphism out of equilibrium – exploring common hypotheses

In the previous section we describe how, while intersex correlation and sex differences at equilibrium are independent *in expectation*, drift can generate a negative correlation between them. This represents a novel mechanism which, to our knowledge, has never previously been considered in discussions of mechanisms that could lead to the empirically-observed negative correlation between intersex correlation and sex differences. Instead, two hypotheses, both of which require deviations from equilibrium dynamics, are most commonly discussed to explain the observed pattern (Bonduriansky & Rowe, 2005; Griffin et al., 2013; Stewart & Rice, 2018; McGlothlin et al., 2019): first, that traits with ancestrally low r_{fm} are less constrained to respond to sex-specific selection and therefore evolve to be more dimorphic (H1: low r_{fm} precedes); second, that sex-specific selection acts to reduce the intersex correlation (H2: low r_{fm} follows).

In this section, we explore the validity of these two hypotheses in the context of a population, initially at equilibrium under sex-specific stabilizing selection, mutation and drift, that is subject to a sudden environmental change leading to a shift in sex-specific optima. In our analysis, we rely on the following equation describing how the per generation change in distances between sex-specific means and their optima ($D_f \equiv O_f - \bar{z}_f$ and $D_m \equiv O_m - \bar{z}_m$) depend on the second and third order

central moments of the joint female and male phenotype distribution:

$$E \begin{bmatrix} \Delta D_f \\ \Delta D_m \end{bmatrix} = \underbrace{-\frac{V_S^{-1}}{2} \cdot \begin{bmatrix} 2\gamma_f^2 & 0 \\ 0 & 2\gamma_m^2 \end{bmatrix} \cdot \begin{bmatrix} V_{A,f} & B \\ B & V_{A,m} \end{bmatrix} \cdot \begin{bmatrix} D_f \\ D_m \end{bmatrix}}_{\text{Directional selection}} + \underbrace{\frac{V_S^{-1}}{2} \cdot \begin{bmatrix} 2\gamma_f^2 & 0 \\ 0 & 2\gamma_m^2 \end{bmatrix} \cdot \begin{bmatrix} \mu_{3,f} \\ \mu_{3,m} \end{bmatrix}}_{\text{Stabilizing selection}}. \quad (24)$$

Here, $\mu_{3,f} \equiv \frac{1}{2}(\mu_{3,fff} + \mu_{3,mmm})$ and $\mu_{3,m} \equiv \frac{1}{2}(\mu_{3,mmm} + \mu_{3,fff})$, where $\mu_{3,\alpha\beta\gamma}$ ($\alpha, \beta, \gamma = f$ or m), are the third order central moments given by $\mu_{3,\alpha\beta\gamma} = \sum_i 2a_{i,\alpha}a_{i,\beta}a_{i,\gamma}x_i(1-x_i)(1-2x_i)$. Equation 24 is derived by adding up the contributions to the change in mean phenotype coming from all segregating variants. Just like in the equation for alleles' expected change in frequency (Equation 8), the two terms correspond to the two modes of selection underlying the dynamics: the first describes directional selection acting to reduce distances between means and respective optima at a rate that depends on sex-specific variances and covariance, while the second reflects the effect of stabilizing selection on an asymmetric (skewed) phenotypic distribution.

3.2.1 Exploring H1 (low r_{fm} precedes): lower intersex correlation leads to more sexual dimorphism – after a given period of time

This hypothesis relies on the idea that traits that initially have a low intersex correlation respond faster to novel sex-specific selection, eventually achieving higher levels of sexual dimorphism. As we saw in Section 3.1.1 and in agreement with previous results assuming a polygenic or infinitesimal genetic architecture (Lande, 1980), so long as there is variation for sexual dimorphism (in other words, if $r_{fm} < 1$), the two sexes will eventually evolve to diverge until sexual conflict is resolved – regardless of the intersex correlation (Figure 1A). However, while expected sexual dimorphism at equilibrium is independent of r_{fm} , the *rate* at which it evolves, and therefore the time frame for sexually-dimorphic evolution, is not. Consequently, in this section we characterize the time frame of adaptation to new sex-specific optima.

As in the single-sex case, this time frame can roughly be split into two phases. An initial, rapid phase dominated by directional selection, where small changes in allele frequencies at many loci move the sex-specific means close to the new optima; and a longer stabilizing selection-dominated equilibration phase, during which the small frequency differences translate into a slight increase in the fixation of alleles with effects that align with the shifts in optima, relative to those with effects that oppose

the shifts in optima. We examine the impact of intersex correlation on the time frame of both phases for sexually-concordant and sexually-dimorphic adaptation of traits with approximately infinitesimal and multigenic architectures, and discuss the implications of our findings for the hypothesis that lower intersex correlation leads to increased sexual dimorphism. We find that, in agreement with H1, because a high intersex correlation delays sexually-dimorphic evolution, intersex correlation might be correlated with the degree of sexual dimorphism. However, we also conclude that in order to show that this correlation is negative (as expected from empirical observations), an additional assumption is required.

3.2.1.1 Adaptation in the infinitesimal limit: r_{fm} determines the relative rate of sexually-concordant vs sexually-dimorphic evolution

We first explore the rate of response to a change in sex-specific optima assuming an approximately infinitesimal genetic architecture. We also make the simplifying assumption that the strength of stabilizing selection is equal in the two sexes (i.e., $V_{S,f} = V_{S,m} = V_S$) so that the γ^2 matrix in Equation 24 is equal to the identity matrix. When the genetic architecture is approximately infinitesimal, phenotypic variances and covariance remain almost unchanged after the shift in optima, and the trait distribution remains approximately symmetric ($\mu_{3,\alpha\beta\gamma} = 0$ for $\alpha, \beta, \gamma = f$ or m). Consequently, Equation 24 for the expected change in the distances of the sex-specific means from the optima reduces to

$$E \begin{bmatrix} \Delta D_f(t) \\ \Delta D_m(t) \end{bmatrix} = -\frac{V_S^{-1}}{2} \cdot \overbrace{\begin{bmatrix} V_{A,f}(0) & B(0) \\ B(0) & V_{A,m}(0) \end{bmatrix}}^{G \text{ matrix}} \cdot \begin{bmatrix} D_f(t) \\ D_m(t) \end{bmatrix}, \quad (25)$$

which is the 2-sex extension of the breeder's equation, as formulated by Lande (1980). If assuming that (co)variances remain constant along time ($V_{A,f}(0)$, $V_{A,m}(0)$, $B(0)$) it describes well the phenotypic evolution in the infinitesimal limit, where individual alleles do not change in frequency under directional selection and the moments of the phenotypic distribution remain unchanged. From Equation 25, we see that after the shift in optima, directional selection acts directly on each sex to decrease the distance between the sex-specific trait mean and its optimum ($D_f(t)$ or $D_m(t)$) at a rate proportional to the distance itself, as well as to the initial phenotypic variance within that sex ($V_{A,f}(0)$ or $V_{A,m}(0)$). Directional selection within the opposite sex, however, can act to either increase or decrease the rate of adaptation to the new

optimum at a rate proportional to the distance of the opposite sex from its new optimum, and to the intersex covariance, $B(0)$.

To better understand the role played by intersex covariance, we follow Lande (1980) in proposing a change of variables: instead of tracking sex-specific means (\bar{z}_f and \bar{z}_m), we track the ‘average’ and ‘average distance’ of their means, given by

$$\bar{z}_a \equiv \frac{1}{2}(\bar{z}_f + \bar{z}_m) \text{ and } \bar{z}_d \equiv \frac{1}{2}(\bar{z}_f - \bar{z}_m), \quad (26)$$

respectively. Notice that changes in \bar{z}_a capture the evolution of the population as a whole (in fact, \bar{z}_a is the population mean for the trait) and changes in \bar{z}_d over time capture the evolution of sexual dimorphism (in fact, $\bar{z}_d = 1/2 \cdot SD$). Similarly, we define an ‘average’ and ‘average distance’ version of every variable k that has both a female and male counterpart, as

$$k_a \equiv \frac{1}{2}(k_f + k_m); \quad k_d \equiv \frac{1}{2}(k_f - k_m). \quad (27)$$

So, for example, $O_a = (O_f + O_m)/2$ and $O_d = (O_f - O_m)/2$ are the average and average distance optima. With this change of variables, we can use Equation 25 to obtain an expression for the expected per generation change in $D_a \equiv O_a - \bar{z}_a$ and $D_d \equiv O_d - \bar{z}_d$:

$$E \begin{bmatrix} \Delta D_a(t) \\ \Delta D_d(t) \end{bmatrix} = -\frac{V_S^{-1}}{2} \cdot \overbrace{\begin{bmatrix} V_{A,a}(0) + B(0) & V_{A,d}(0) \\ V_{A,d}(0) & V_{A,a}(0) - B(0) \end{bmatrix}}^{G' \text{ matrix}} \cdot \begin{bmatrix} D_a(t) \\ D_d(t) \end{bmatrix}. \quad (28)$$

From Equation 28 it follows 1) that a high overall phenotypic variance, $V_{A,a}(0)$, helps drive the evolution of both the overall trait mean (to the new mean optimum) and sexual dimorphism (to the new difference in optima); 2) a large, positive intersex covariance, $B(0)$, helps move the population mean to the new mean optimum, but delays the evolution of sexual dimorphism; and 3) that differences in phenotypic variance between the two sexes generate interactions in the evolution of the overall trait mean, and sexual dimorphism.

If the initial phenotypic variance is the same in the two sexes, so that $V_{A,d}(0) = 0$, then the population mean and sexual dimorphism evolve independently and Equa-

tion 28 above reduces to

$$E[\Delta D_a(t)] = -\frac{(V_{A,a}(0) + B(0))}{2V_S} D_a(t); \quad E[\Delta D_d] = -\frac{(V_{A,a}(0) - B(0))}{2V_S} D_d(t). \quad (29)$$

In continuous time this is solved by

$$D_a(t) = \Delta_a e^{-t \frac{V_{A,a}(0) + B(0)}{2V_S}}; \quad D_d(t) = \Delta_d e^{-t \frac{V_{A,a}(0) - B(0)}{2V_S}}. \quad (30)$$

where Λ_a and Λ_d are the sizes of the shifts in O_a and O_d . Defining the length of the initial rapid phase of sexually concordant (t_a) and sexually dimorphic (t_d) adaptation to be the time that it takes for D_a and D_d to equal the typical deviation of the population mean from the optima at equilibrium, $\delta = \sqrt{V_S/2N}$, respectively, it follows that

$$t_a = \frac{2V_S}{V_{A,a}(0) + B(0)} \ln \left[\frac{\Lambda_a}{\delta} \right]; \quad t_d = \frac{2V_S}{V_{A,a}(0) - B(0)} \ln \left[\frac{\Lambda_d}{\delta} \right]. \quad (31)$$

Thus the length of the initial phase of sexually-dimorphic adaptation relative to sexually-concordant adaptation is

$$\frac{t_d}{t_a} = \frac{V_{A,a}(0) + B(0)}{V_{A,a}(0) - B(0)} = \frac{1 + r_{fm}}{1 - r_{fm}}. \quad (32)$$

This result, initially obtained by Lande (1980), illustrates the quantitative constraint that intersex correlation places on the evolution of sex differences. In particular, when intersex correlation is close to 1, the denominator in Equation 32, $1 - r_{fm}$, will be very small, and sexually-dimorphic adaptation in the directional-selection dominated rapid phase could take orders of magnitude longer than sexually-concordant adaptation ($t_d \gg t_a$), corresponding to the two phases of 2-sex phenotypic evolution discussed by Lande (1980).

These dynamics are illustrated in Figure 2. Concretely, we implement sexually-concordant selection by applying sex-specific shifts in optima of the same magnitude and direction ($\Lambda_d = 0$), and sexually-divergent selection by applying sex-specific shifts in optima of the same magnitude but in opposite directions ($\Lambda_a = 0$), for low, intermediate and high values of intersex correlation (Figure 2A,B). We see that the lower r_{fm} , the faster (slower) the reduction in D_a (D_d) (Figure 2C,D). This result holds qualitatively for both the approximately infinitesimal and the multigenic genetic architectures. However, the latter shows some quantitative differences, as

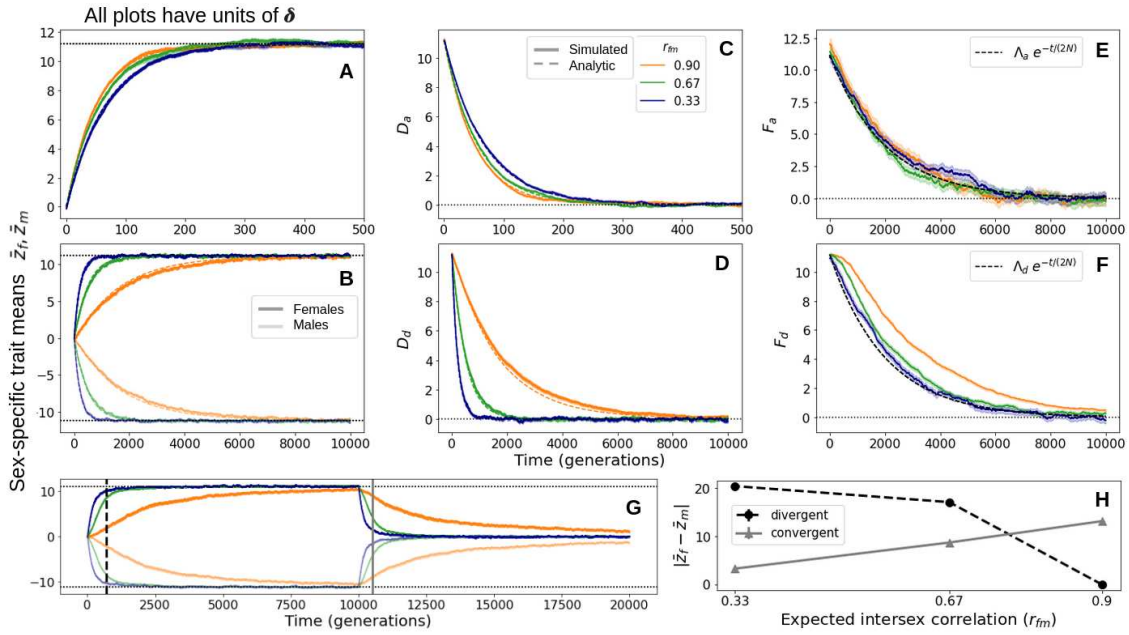


Figure 2: Phenotypic evolution with an approximately infinitesimal genetic architecture. A: Sex-specific trait means adapting to a shift in sex-specific optima of equal magnitude and direction, which implies only sexually-concordant adaptation ($\Lambda_a = 0.25\sqrt{V_S}$ and $\Lambda_d = 0$). B: Sex-specific trait means adapting to a shift in sex-specific optima of equal magnitude and opposite direction, which implies only sexually-dimorphic adaptation ($\Lambda_a = 0$ and $\Lambda_d = 0.25\sqrt{V_S}$). Sex-specific optima before the shift are both at zero, and after the shift are indicated as dashed lines. Thicker solid lines are simulations, and thin dashed lines are predictions using Equation 25. C (D): D_a (D_d) along time in simulations (thick solid lines) and predicted using equation 28 (thin dashed lines) for the sex-specific shifts in means in A (B). E (F): F_a (F_d) along time for the optima shifts in A (B). Coloured lines correspond to simulations and the dashed black line corresponds to the prediction according to Equation 37 (38). G: Sex-specific trait means adapting to first divergent and then convergent shifts in optima of magnitude $0.25\sqrt{V_S}$. H: Sexual dimorphism, as absolute difference between sex-specific means for different levels of r_{fm} at a given point of sexually-dimorphic divergent (black dashed, corresponding to the black dashed vertical line in G) and convergent (grey solid, corresponding to the grey solid vertical line in G) adaptation.

All simulations correspond to an approximately infinitesimal genetic architecture with $V_A = 40$, $E(a^2) = 1$ and for various levels of r_{fm} : 0.90 (orange), 0.67 (green) and 0.33 (blue). Simulations have been run for $10N$ generations before the shift in optima. Results display averages and SEM across 200 replicates. Results for A and C have been zoomed in to appreciate the relevant evolutionary dynamics. All quantities displayed in the figure are in units of δ .

we outline in the next section.

3.2.1.2 Adaptation with a multigenic genetic architecture: transient changes in the 2nd and 3rd order moments of the phenotype distribution alter the dynamics of phenotypic adaptation The accuracy of the predictions for the evolution of phenotypic means in Equations 25 and 28 relies on the assumption that the respective G and G' matrices remain constant over time. This will be approximately true when the genetic architecture is approximately infinitesimal. However, when considering a less infinitesimal trait architecture, with a significant proportion of mutations with larger effect sizes ($a^2 > 4$) as exemplified by our multigenic trait architecture, the approximations in Equations 25 and 28 are no longer accurate. This is because directional selection on effect alleles with larger effects can generate a significant increase in the 2nd central moments of the joint phenotype distribution, as well as the establishment of nonzero third central moments (Figure S2). To accurately predict phenotypic evolution with a multigenic genetic architecture we therefore need the full expression for the expected change in the distances of the sex-specific means from their respective optima (Equation 24), with generation-wise updated 2nd and 3rd central moments (i.e. $V_{A,f}(t)$, $V_{A,m}(t)$, $B(t)$, $\mu_{3,f}(t)$, $\mu_{3,m}(t)$). Assuming, as we did for the approximately infinitesimal architecture, that the strength of stabilizing selection is equal in the two sexes (i.e., $V_{S,f} = V_{S,m} = V_S$) Equation 24 simplifies to:

$$E \begin{bmatrix} \Delta D_f(t) \\ \Delta D_m(t) \end{bmatrix} = -\frac{V_S^{-1}}{2} \cdot \overbrace{\begin{bmatrix} V_{A,f}(t) & B(t) \\ B(t) & V_{A,m}(t) \end{bmatrix}}^{G \text{ matrix}} \cdot \begin{bmatrix} D_f(t) \\ D_m(t) \end{bmatrix} + \frac{V_S^{-1}}{2} \cdot \overbrace{\begin{bmatrix} \mu_{3,f}(t) \\ \mu_{3,m}(t) \end{bmatrix}}^{\mu_3 \text{ matrix}}. \quad (33)$$

As before, a simple change of variables (Equation 27) yields an expression for the evolution of the overall trait mean (captured by D_a) and the level of sexual dimorphism (captured by D_d):

$$E \begin{bmatrix} \Delta D_a(t) \\ \Delta D_d(t) \end{bmatrix} = -\frac{V_S^{-1}}{2} \cdot \overbrace{\begin{bmatrix} V_{A,a}(t) + B(t) & V_{A,d}(t) \\ V_{A,d}(t) & V_{A,a}(t) - B(t) \end{bmatrix}}^{G' \text{ matrix}} \cdot \begin{bmatrix} D_a(t) \\ D_d(t) \end{bmatrix} + \frac{V_S^{-1}}{2} \cdot \overbrace{\begin{bmatrix} \mu_{3,a}(t) \\ \mu_{3,d}(t) \end{bmatrix}}^{\mu'_3 \text{ matrix}}. \quad (34)$$

By updating (co)variances and 3rd central moments, we can use Equation 34 to accurately predict the mean trajectories of D_a and D_d (see Section 4 in Supplementary material and Figure S3).

In cases where the trait has a multigenic genetic architecture, changes in the 2nd and 3rd central moments of the phenotypic distribution *do* affect the trajectories of D_a and D_d (Figure S3). During the initial, rapid phase these effects are subtle and Equations 30, 31 and 32, derived for an approximately infinitesimal trait, provide reasonable approximations. However, changes in 2nd and 3rd central moments act to respectively speed up and slow down phenotypic evolution, as is shown in Figure S3.

After the rapid phase, the average trajectories of D_a and D_d can deviate significantly from the exponential decrease predicted by Equation 30. Once the mean phenotype nears the new optimum, the decreasing distance and increasing 3rd central moments reach the point at which the two terms on the right-hand side of Equation 34 approximately cancel out and the changes in D_a and D_d come almost to a stop. The rates of approaching the new optima are then largely determined by the rate at which the 3rd central moments decay. This roughly corresponds to the rate at which the allele frequency distribution equilibrates (changes in frequency generated by directional selection translate into fixed differences, as described below) and mutation-selection-drift balance is restored around the new optima.

In Section 5 of the Supplementary Material we discuss the equilibration phase with a multigenic genetic architecture. We derive a quasi-static approximation for D_a and D_d similar to that derived for a single sex in [Hayward and Sella \(2022\)](#). We find that, while intersex correlation determines the time it takes to reach the equilibration phase (given approximately by Equation 32), it does not seem to make a qualitative difference in the initial phase of the quasi-static approximation of means towards their optima during the equilibration phase. However, as we demonstrate in the next section, a higher intersex correlation does imply a longer equilibration phase.

3.2.1.3 Higher intersex correlation delays equilibration for sex differences

In section 3.2.1.1 we described how the time required for the average and average distance of the sex-specific trait means to approach their new optima depends on r_{fm} (Equations 31 and 32). These timepoints correspond to the length of the initial, directional selection-dominated phases of sexually-concordant and sexually-dimorphic adaptation, which are driven by small changes in allele frequencies at many loci. In this section, we analyze the timeframe associated with equilibration, during which stabilizing selection translates the allele frequency differences (generated by directional selection) between alleles with phenotypic effects that are aligned

and opposed to the phenotypic shift into differences in fixation probabilities. This process restores the equilibrium phenotypic distributions with means at the new optima.

To examine the dynamics of equilibration we track the female and male fixed backgrounds (\tilde{F}_f and \tilde{F}_m), defined as the trait value of a female or male that is homozygous for the derived allele at every segregating site:

$$\tilde{F}_f = \sum_j 2a_{j,f}; \quad \tilde{F}_m = \sum_j 2a_{j,m}. \quad (35)$$

As before, we distinguish between sexually-concordant and sexually-dimorphic adaptation by performing a change of variables (Equation 27). Using Equation 27, we define the average fixed background and the fixed background difference ($\tilde{F}_a \equiv (\tilde{F}_f + \tilde{F}_m)/2$ and $\tilde{F}_d \equiv (\tilde{F}_f - \tilde{F}_m)/2$) and their distances

$$F_a = \Lambda_a - \tilde{F}_a; \quad F_d = \Lambda_d - \tilde{F}_d. \quad (36)$$

At equilibrium, we expect the fixed distances, F_a and F_d , to be 0; the rate at which F_a approaches 0 gives the timescale over which sexually-concordant adaptation occurs and the rate at which F_d approaches 0 gives the timescale over which sexually-dimorphic adaptation occurs over the second, stabilizing-selection dominated phase of phenotypic adaptation.

Not unexpectedly, we find that sexually-concordant adaptation takes place at much the same rate as when there is just a single-sex, and thus the trajectory of F_a is well-approximated by

$$F_a(t) \approx \Lambda_a e^{-\frac{t}{2N}}. \quad (37)$$

(Hayward & Sella, 2022; Figure 2E). Sexually-concordant adaptation thus occurs over a time period on the order of $2N$ generations. Somewhat surprisingly, we find that when the intersex correlation is fairly low, F_d also decays approximately exponentially at a rate $1/(2N)$

$$F_d(t) \approx \Lambda_d e^{-\frac{t}{2N}}. \quad (38)$$

(Figure 2F). When intersex correlation is high, however, the approximation in Equation 38 becomes quite inaccurate since the decay of F_d can be significantly delayed (Figure 2E). Thus high intersex correlation increases the time period over which

sexually-divergent adaption occurs.

Simulation results suggest that, for traits with an approximately infinitesimal architecture, the approximation for F_a (Equation 37) is highly accurate and, provided intersex correlation is not too high, the approximation for F_d (Equation 38) is also highly accurate (Figure 2E,F); when the trait architecture is multigenic we observe slight deviations from exponential decay in F_a and F_d (even when intersex correlation is low). In particular, the decay is initially slower and later faster than predicted by the approximations in Equations 37 and 38 (Figure S5). However, the time taken for the fixed backgrounds to reach the new optima, and therefore for the various moments of the phenotypic distribution to be restored to equilibrium values, is nevertheless on the order of $2N$ generations. We are still exploring potential interactions between the effects of high intersex correlation and genetic architecture on the length of time taken for equilibration.

3.2.1.4 H1 holds – given an additional assumption We have shown that, while intersex correlation does not predict the overall realized sexual dimorphism, it does determine the rate at which it evolves. First, it directly determines the rate of sexually-concordant vs dimorphic phenotypic adaptation in the rapid phase; second, a high intersex correlation can delay sexually-dimorphic equilibration. When considering non-equilibrium dynamics of adaptation, these aspects might contribute to generate an overall, negative relationship between r_{fm} and sexual dimorphism, consistent with the first common hypothesis that initially lower intersex correlation allows for faster decoupling between sexes and more sexual dimorphism evolution. However, this only holds given the extra assumption that traits are more likely to be selected to diverge (i.e., trait optima move further apart) than to converge (i.e., trait optima move closer together) between sexes.

This extra assumption is required because a lower intersex correlation allows for a faster sexually-dimorphic evolution, both after a divergent as well as *convergent* shift in sex-specific optima (Figure 2G). Concretely, after a divergent shift in sex-specific optima (i.e. keeping O_a constant and increasing the absolute value of O_d), traits with a higher intersex correlation will take longer to diverge between sexes, leading to a negative relationship between intersex correlation and sex differences at a given time during divergent evolution (black dashed line in Figure 2H, corresponding to the timepoint of the black vertical dashed line in Figure 2G). However, this is also true for adaptation after a convergent shift in optima (i.e. keeping O_a constant and decreasing the absolute value of O_d): traits with a higher intersex correlation will

take longer to adapt to a convergent shift than traits with an initially lower r_{fm} , potentially leading to the opposite pattern, i.e. to a positive relationship between intersex correlation and sex differences at a given time during convergent evolution (grey solid line in Figure 2H, corresponding to the timepoint of the grey vertical solid line in Figure 2G).

3.2.2 Exploring H2 (low r_{fm} follows): sex-specific directional selection acts to *transiently* reduce intersex correlation

In this section we explore the hypothesis, often stated as an alternative to H1, that a negative correlation between r_{fm} and sexual dimorphism arises as a consequence of sex-specific adaptation driving a reduction in intersex correlation. To do so, we examine how intersex correlation evolves with sexually dimorphic adaptation. Intersex correlation depends both on the variances within a single sex, $V_{A,f}$ and $V_{A,m}$, and on the covariance, B (Equation 5). In Section 3.2.1.1, we established that for traits with approximately infinitesimal genetic architectures, the 2nd order central moments remain approximately unchanged by directional selection (Figure S2, Figure 3A,C,D). Consequently, when the trait has an approximately infinitesimal architecture, intersex correlation does not evolve at all (Figure 3A,E). In contrast, as we discussed in Section 3.2.1.2, for traits with multigenic architectures directional selection generates transient changes in 2nd central moments of the phenotypic distributions (Figure S2, Figure 3B,C,D). These changes *can* result in a temporary decrease in intersex correlation (Figure 3B,E).

This decrease in intersex correlation (for traits with a multigenic architecture) is specific to sexually-dimorphic adaptation (i.e., the distance between sex-specific trait optima changes). With sexually-concordant adaptation (i.e., the mean optimum trait value changes), there is an increase in sex-specific variances proportional to the increase in between-sex covariance. Consequently, intersex correlation remains constant over time regardless of the magnitude of the shift (scenarios $\Lambda_{a,S}$, $\Lambda_{a,M}$ and $\Lambda_{a,L}$ in Figure 3C,D,E). However, with sexually-dimorphic adaptation, there is a transient increase in sex-specific variances, while the covariance remains constant, which leads to a transient decrease in r_{fm} (scenarios $\Lambda_{d,S}$, $\Lambda_{d,M}$ and $\Lambda_{d,L}$ in Figure 3C,D,E). This occurs because a subset of sex-specific mutations are favoured by sexually-dimorphic directional selection, while shared mutations are not. Concretely, directional selection will generate increases in frequency of those sex-specific mutations which drive phenotypic change in the direction of the shift, leading to an increase in sex-specific variances. Nevertheless, it will not on average increase

the frequency of shared mutations (which generate covariance). With sexually-concordant adaptation, however, there is selection for phenotypic change along the main axis of the G matrix (under our assumption that $V_{A,f} = V_{A,m}$), so both sex-specific variances as well as between-sex covariance will increase equally. This is only a transient phenomenon; as described in Section 3.2.1.3, (co)variances, as well as r_{fm} will be restored to their equilibrium values during the equilibration phase, over a time period on the order $2N$ (Figure 2E,F).

The potential transient decrease in sexual dimorphism described above could generate an association between intersex correlation and sexual dimorphism. However, the direction of this association depends on whether sexually-dimorphic adaptation is divergent (i.e., sex-specific optima move further apart) or convergent (i.e., sex-specific optima move closer together). For some intuition, let us consider a set of monomorphic (dimorphic) traits with similar r_{fm} values at equilibrium, a subset of which becomes sex-specifically selected after a divergent (convergent) shift in sex-specific optima. Those traits in the process of diverging (converging) will experience a temporary decrease in intersex correlation, which would generate a negative (positive) correlation between r_{fm} and sexual dimorphism. The negative (positive) association between intersex correlation and sexual dimorphism that might arise as a consequence of divergent (convergent) sexually-dimorphic adaptation is illustrated in Figure 3F.

These results indicate that, in accordance with H2, a negative correlation between intersex correlation and sexual dimorphism could arise from sex-specific adaptation leading to a reduction in r_{fm} . However, this phenomenon is only transient. In addition, it only applies when some additional conditions are met. First, at least some traits must have a non-infinitesimal genetic architecture, where (co)variances change under directional selection; second, traits must be adapting to (partially) non-concordant directional selection between sexes, where (a subset of) sex-specific mutations are more beneficial than shared mutations; third, this sexually-dimorphic adaptation must be divergent more frequently than it is convergent.

4 Discussion

Based on the quantitative constraint that a high intersex correlation r_{fm} poses on the evolution of sexual dimorphism (Lande, 1980, 1987; Stewart & Rice, 2018) is the general idea that they should negatively correlate with one another, either be-

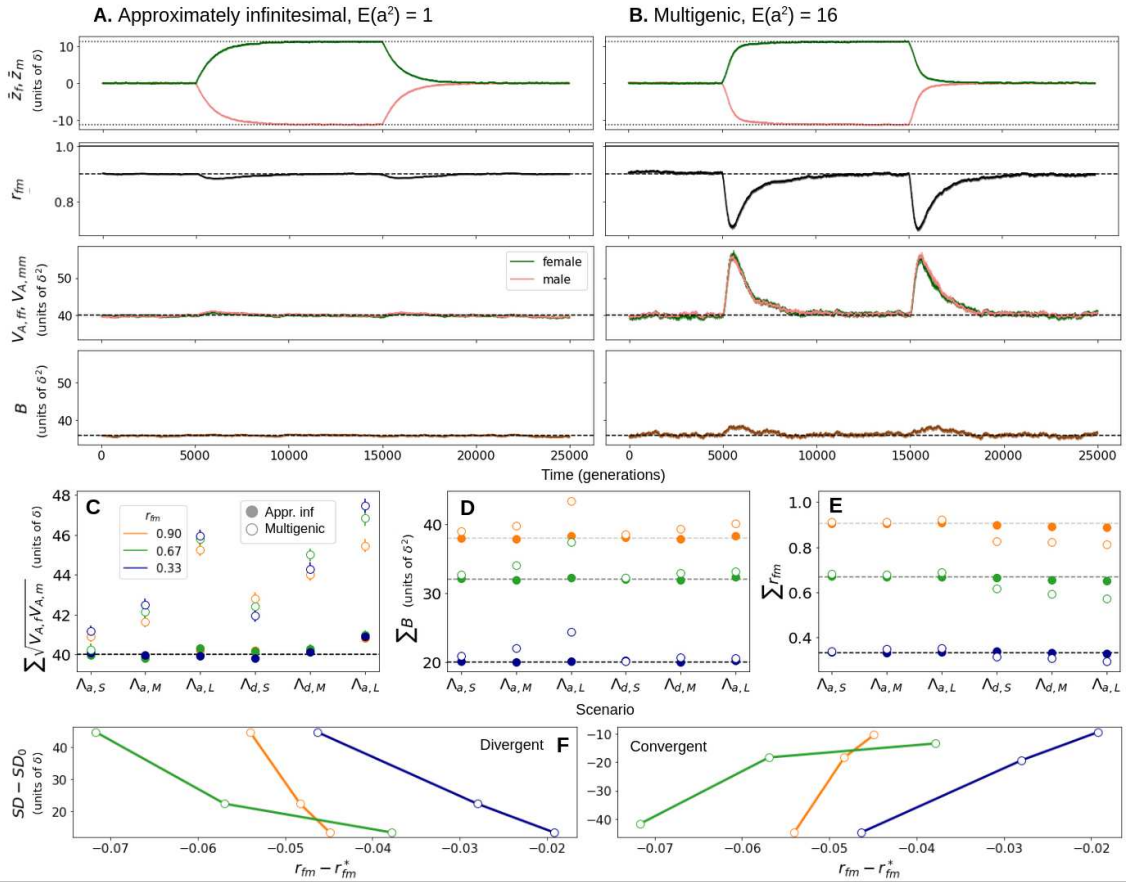


Figure 3: Transient decrease in r_{fm} during sexually-dimorphic (divergent and convergent) evolution. A, B: Evolution of sex-specific trait means, intersex correlation, sex-specific variances and covariance along time with an approximately infinitesimal (A, $E(a^2) = 1$) and multigenic (B, $E(a^2) = 16$) genetic architecture. We let the population evolve for $10N$ generations before and after applying a shift in sex-specific optima of magnitude $\Lambda = 0.25\sqrt{V_S}$ inducing divergent (optima move apart), and then convergent (optima move together) evolution between the sexes. C, D, E: Average of the geometric mean of sex-specific variances (C), covariance (D) and intersex correlations (E) for $5N$ generations after the shift in optima, for approximately infinitesimal (solid circles) and multigenic (open circles) genetic architecture and across different scenarios indicating different types of shifts: $\Lambda_{a,-}$ are shifts of same magnitude and direction in both sexes, leading to sexually-concordant adaptation (similar to scenario depicted in Figure 2A, in which $\Lambda_{d,-} = 0$); $\Lambda_{d,-}$ are shifts of same magnitude and different direction in both sexes, leading to sexually-dimorphic adaptation (similar to scenario in Figure 2B, in which $\Lambda_{a,-} = 0$). $\Lambda_{-,S}$, $\Lambda_{-,M}$ and $\Lambda_{-,L}$ indicate small, medium and large shifts, with magnitudes $0.15\sqrt{V_S}$, $0.25\sqrt{V_S}$ and $0.5\sqrt{V_S}$. F: Negative (positive) relationship between intersex correlation and sexual dimorphism with divergent –left– (convergent, right) sexually-dimorphic selection. The y axis corresponds to the difference between sexual dimorphism before and after the shift, for the three considered magnitudes ($0.15\sqrt{V_S}$, $0.25\sqrt{V_S}$ and $0.5\sqrt{V_S}$); on the x axis is the difference between the average r_{fm} across $5N$ generations after the shift, corresponding to the dots in $\Lambda_{d,S}$, $\Lambda_{d,M}$ and $\Lambda_{d,L}$ in E for a multigenic genetic architecture, and the equilibrium r_{fm} values (dashed horizontal lines in E), for the three r_{fm} (0.9, 0.67 and 0.33 in orange, green and blue).

cause traits will evolve to be more dimorphic if they are less correlated between the sexes (hypothesis H1, ‘low r_{fm} precedes’; Bolnick & Doebeli, 2003; Poissant et al., 2010; Stewart & Rice, 2018) or because sexually dimorphic evolution requires that intersex correlation decreases with time, to allow independent adaptation of both sexes (hypothesis H2, ‘low r_{fm} follows’; Lande, 1980; Bonduriansky & Rowe, 2005; Bonduriansky & Chenoweth, 2009; McGlothlin et al., 2019). Although these are common assumptions in the sexual dimorphism literature, partially based on the empirical observation of a general negative correlation between r_{fm} and sexual dimorphism (Ashman, 2003; Delph et al., 2004; Bonduriansky & Rowe, 2005; McDaniel, 2005; Poissant et al., 2010; Griffin et al., 2013), we lack mechanistic understanding for them, which poses the main motivation of the present study: we use theory to explore the relationship between intersex correlation and sexual dimorphism, and outline the conditions under which a negative correlation between the two is expected, with a special focus on testing these common hypotheses.

Concretely, we model a population that is at equilibrium under sex-specific stabilizing selection, mutation and drift and observe how it adapts to a sudden environmental change that brings about a shift in sex-specific optima. We obtain predictions for both sexually-concordant and sexually-dimorphic adaptation, and explore how these predictions depend on intersex correlation. We obtain results for traits with both (approximately) infinitesimal and multigenic genetic architectures, assuming that the genetic architecture remains unchanged over time.

First, we reproduce the well-known result (first obtained by Lande, 1980) that, for a highly polygenic or quantitative trait with enough sex-specific genetic variation (either because there is enough standing variation or we have substantial sex-specific mutational input) sexual conflict will be resolved, in the sense that, given enough time, sex-specific means will eventually align with their optima. We derive explicit expressions to illustrate that the stabilizing selection-dominated dynamics of the system at equilibrium are independent of phenotypic values (Equation 11); instead, they depend on the overall strength of stabilizing selection (Equations 13). We show that the G matrix at equilibrium depends only on the overall and sex-specific mutational pleiotropy and selection strength, which has also been shown for correlated traits in the 1-sex literature (Lande & Arnold, 1983; Turelli, 1985; Jones et al., 2003; Chantepie & Chevin, 2020). This implies that, at equilibrium, expected intersex correlation and sexual dimorphism are independent of each other (Figure 1A).

Our results indicate that a negative correlation between intersex correlation and sexual dimorphism can arise at equilibrium due to drift, however. This follows from the fact that the fluctuations of the mean phenotypes around the optima at equilibrium under stabilizing selection are expected to be more divergent between the sexes with lower intersex correlation, potentially generating substantial sexual dimorphism (Figure 1B). The significance of the drift-dependent sexual dimorphism at equilibrium depends on the magnitude of the fluctuations around the optima relative to the genetic variance of the trait. We show that when fluctuations are relatively large (of magnitude 1/3 or 1/2 of the genetic standard deviation of the trait distribution) then, just by chance, trait means in the two sexes could differ by a full and a half phenotypic standard deviation, respectively. The effect is expected to be smaller for traits with smaller fluctuation in means relative to phenotypic variance (i.e. higher $\sqrt{V_A}/\delta$). We do not know the empirical values of this quantity, so it is hard to predict the empirical relevance of the effect of drift on SD at equilibrium. However, we could test whether empirical results are consistent with the drift hypothesis by looking at the variance-normalized variance in sexual dimorphism as a function of r_{fm} (as in Figure 1B) for empirical data, like gene expression. Thus, drift represents a novel and possibly testable mechanism with the potential to generate a negative correlation between sexual dimorphism and intersex correlation which has not been modeled before, nor discussed as a possibly contributing factor in the observed general negative correlation between r_{fm} and sex differences.

The hypotheses most commonly discussed in the literature with the potential to explain this pattern involve dynamic properties of the system, so we explored them by looking at the out-of-equilibrium dynamics of sex-specific adaptation under directional selection. The first hypothesis, discussed in Section 3.2.1, predicts higher levels of sexual dimorphism if intersex correlation is initially lower. We find that this holds – transiently and, importantly, given some additional assumptions. This is because, while intersex correlation does not determine the ultimate realized sexual dimorphism, it does determine the rate at which it evolves. Concretely, as Lande (1980) described, the rates of sexually-concordant vs sexually-dimorphic evolution are proportional to $1 + r_{fm}$ and $1 - r_{fm}$ (Equations 31 and 32, Figure 2B,C), both evolving in two very different timescales for high intersex correlation. This result illustrates the quantitative constraint that r_{fm} imposes on the evolution of sex differences, and supports the idea that, after a limited time, the expected realized sexual dimorphism negatively correlates with intersex correlation (Bolnick

& Doebeli, 2003), partially validating this first hypothesis. However, as we show, a higher intersex correlation not only constrains *divergent* but also *convergent* evolution between the sexes, and the latter has the potential to generate the opposite pattern of a positive relationship between intersex correlation and sexual dimorphism (Figure 2G). So the hypothesis that a negative correlation between intersex correlation and sexual dimorphism arises because sexually-dimorphic evolution is less constrained with lower r_{fm} requires some additional assumptions: i) that traits are sexually-dimorphically adapting under directional selection (since at equilibrium sexual dimorphism is independent of r_{fm}); and ii) that sexually-dimorphic adaptation is more commonly divergent than convergent. The plausibility of these assumptions is discussed below.

The second hypothesis, discussed in Section 3.2.2, supports the idea that a negative correlation between intersex correlation and extent of sex differences arises as a consequence of sexually-dimorphic adaptation involving an accumulation of sex-specific mutations leading to a decrease in r_{fm} over time. This idea traces back to D. B. Wright (1993) and Lande (1980, 1987) and, since neither author provides a mathematical justification for it, seems rather based on an intuition of how such a process should evolve. Indeed, we find that intersex correlation decreases due to an increase in sex-specific variances, but not covariance, during sexually-dimorphic adaptation under directional selection, for a trait with a non-infinitesimal genetic architecture.

These changes in the (co)variance matrix are only transient; stabilizing selection translates the allele frequency changes between alleles with effects that are aligned and opposed to the phenotypic shift generated by directional selection into differences in fixation probabilities. After this equilibration phase, the transient increase in (co)variances ceases, and their equilibrium values are restored. Also, the same transient decrease in intersex correlation is expected for divergent as well as convergent evolution.

This result suggests that sexual dimorphism can evolve without long-term changes in r_{fm} , as already discussed by Reeve and Fairbairn (2001), who also illustrate how this transient increase in second order moments speeds up adaptation with a non-infinitesimal genetic architecture with respect to the infinitesimal predictions. We recapitulate this result, and additionally show that transient increases in third central moments have the opposite effect, in that they act to slow down phenotypic adaptation both in the rapid (Figure S3) as well as equilibration phases (Figure

S5), which was shown for the 1-sex case before (Hayward & Sella, 2022). We are still on the process of characterizing how the transient increases in 2nd and 3rd order moments interact with r_{fm} to influence the dynamics of sexually-concordant vs dimorphic adaptation.

We also obtain predictions for the equilibration timescale. Hayward and Sella (2022) showed that phenotypic distributions are reestablished over a time frame of the order of $2N$ generations, which we find to hold well for equilibration under sexually-concordant adaptation regardless of the r_{fm} (Figure 2E). However, we find that higher intersex correlation delays equilibration when the population is sexually-dimorphically adapting (Figure 2F). However, we find the effect of r_{fm} on equilibration time to be surprisingly small, given the constraint it poses on phenotypic evolution. This suggests some compensatory process: while, with high r_{fm} , the amount of mutations contributing to sexually-dimorphic adaptation is less than those contributing to sexually-concordant adaptation, they might individually be subject to stronger directional selection and fix faster, leading to an similar rate of equilibration for the two types of adaptation.

Our model predicts a transient reduction in r_{fm} due to a temporary increase in sex-specific variances, and not a permanent reduction due to a decrease in between-sex covariance, as the common intuition seems to suggest (verbal arguments tracing back to Fisher, 1958 and Lande, 1980). These two results seem easy to reconcile by noting that, while we assumed that genetic architecture remains stable, as do most models of sex-specific adaptation (Reeve & Fairbairn, 2001; Bolnick & Doebeli, 2003; Connallon & Clark, 2014a, 2014b; Muralidhar & Coop, 2023), the general intuition seems to suggest an evolving genetic architecture (Lande, 1980; D. B. Wright, 1993; Bonduriansky & Rowe, 2005). Indeed, there are many different mechanisms that can lead to sexual conflict resolution: sex-specific expression of autosomal loci, via sex-linked modifiers or alternative splicing mechanisms (McIntyre et al., 2006; Stewart et al., 2010; Pennell & Morrow, 2013; Singh & Agrawal, 2023) gene duplication followed by sex-specific regulation of the paralogues (Rice & Chippindale, 2002; Proulx & Phillips, 2006; Sison-Mangus et al., 2006; Connallon & Clark, 2011), genomic imprinting (Day & Bonduriansky, 2004) and sex-dependent dominance of antagonistic alleles (Kidwell et al., 1977; Barson et al., 2015). The evolution of some of these mechanisms (e.g. a target for sex-hormone regulation or moving to a sex chromosome) would involve changes in the genetic architecture, i.e. leading to a higher proportion of sex-specific mutations underlying its expression – which

we assume to be constant through time in our model. Some of those sex-specific changes in genetic architecture are expected to accelerate the rate of sexual dimorphism evolution and would likely drive more permanent reduction in r_{fm} as sexual dimorphism evolves (D. B. Wright, 1993; Bonduriansky & Rowe, 2005), contributing to a more stable negative correlation between sexual dimorphism and r_{fm} (Williams & Carroll, 2009; Stewart et al., 2010). However, they are likely to be slow (Williams & Carroll, 2009; Stewart et al., 2010; Bonduriansky & Chenoweth, 2009), probably occurring at an extra phase to the two described by Lande (1980, 1987) (and that we reproduce here) for sexually-concordant and -dimorphic adaptation with a constant genetic architecture, as suggested by D. B. Wright (1993). Looking at the dynamics with a non-changing genetic architecture is a useful first step that likely reflects the most likely genetic changes over the timescale of most experimental studies (e.g. Bird & Schaffer, 1972; Reeve & Fairbairn, 1996; Stewart & Rice, 2018). However, incorporating the option for an evolving genetic architecture in our model, involving changes in $h(\phi_\alpha)$ leading to a higher (lower) proportion of sex-specific vs shared mutations, would be an easy and logical next step which would allow us to explore questions such as the conditions in which a slower pace in sexual dimorphism evolution could somehow ‘incentivize’ a more permanent reduction in r_{fm} involving changes in the genetic architecture, and whether these changes are expected to be partially restored after sexual conflict has been resolved.

Data can help shed light into whether sexually-dimorphic evolution typically implies changes in the genetic architecture leading to a permanent reduction in r_{fm} , or whether it often relies on the current genetic architecture. Empirical studies report a general negative association between both (e.g. Poissant et al., 2010; Griffin et al., 2013), but this is far from universal, with many studies finding only weak or even absent associations (e.g. Cowley & Atchley, 1988; Ashman & Majetic, 2006). The inconsistency in the pattern suggests that, although we have evidence of sexual conflict resolution having relied on various types of changes in the genetic architecture (Delph et al., 2011; A. E. Wright et al., 2018), it might in many cases more likely reflect the condition-dependent transient dynamics under constant genetic architecture we illustrate, which only lead to this prediction in certain conditions, given certain assumptions.

The main assumptions to consider are three. First, that a good fraction of traits are out-of-equilibrium adapting under (at least partially) sex-specific selection. This is because, at equilibrium we only predict a drift-driven negative correlation between

r_{fm} and sexual dimorphism, which is expected to be low and unlikely to account for all sexually-dimorphic variation for most complex traits. However, it might help explain sex differences in traits where drift might be substantial, like gene expression patterns. Besides this mechanism operating at equilibrium, the predictions for a negative association between r_{fm} and sexual dimorphism following the two common hypotheses respond to transient dynamics of sexually-antagonistic adaptation to sex-specific directional selection. Given the high prevalence of sex-specific selection (Cox & Calsbeek, 2009) and the long timeframe for sexual dimorphism evolution, specially for traits with high r_{fm} (Equations 31, Figure 2C,D), it seems likely that most traits are subject to (sex-specific) directional selection.

The second assumption implies that this sex-specific directional selection is more often divergent than convergent. This is because under both hypothesis we predict that the correlation between r_{fm} and sex differences is negative with divergent but positive with convergent sex-specific adaptation (Figure 2G,H, Figure 3A,B,F). However, selection for convergent evolution has also been reported for some traits and species (Owens & Hartley, 1998; Bonduriansky, 2006; Chursina, 2019; Lassek & Gaulin, 2022), indicating that this assumption might not generally hold. Generally, we expect that both occur similarly frequently.

The third assumption implies that many traits have a non-infinitesimal genetic architecture. This is not required for the first hypothesis to hold, where intersex correlation determines the rate of sexually-dimorphic adaptation with infinitesimal (Figure 2D) as well as multigenic (Figure S3) genetic architecture. However, the transient reduction in r_{fm} with sexually-dimorphic adaptation illustrated in H2 only occurs with non-infinitesimal traits, since with an infinitesimal genetic architecture the phenotypic distribution remains unchanged under directional selection. The presence of high-effect mutations seems to be the rule for most complex traits, as suggested by GWAS (e.g. Wood et al., 2014; Locke et al., 2015; Simons et al., 2018), so this assumption seems plausibly fulfilled.

Other aspects of the genetic architecture are important to consider in the dynamics of (sex-specific) adaptation. The specific choice of sex-specificity of individual mutations can impact the evolutionary outcome (Rhen, 2000). In this case, we are sampling overall effect sizes from an exponential distribution, which seems to be a popular option (e.g. Connallon & Clark, 2014b), and define them as shared or sex-specific, with equal probabilities of being female- or male-specific. This choice is common in similar studies (Rhen, 2000; Reeve & Fairbairn, 2001; Bolnick & Doe-

beli, 2003) and is partially based on empirical evidence that sex-biased and sexually antagonistic mutations, with phenotypic effects of different sizes and magnitudes across sexes, respectively, should be rare (Dimas et al., 2012; Oliva et al., 2020; Chapter 3 of this thesis). However, their consideration is likely to be a relevant extension to our work, since theoretical studies suggest that they can have a substantial contribution to phenotypic adaptation (Connallon & Clark, 2014a; Muralidhar & Coop, 2023). Also, we assume that the effect size distribution of new mutations is symmetric across sexes, and that this is independent of the effect size, meaning that large-effect mutations are equally likely to be female- and male-biased. Nevertheless, there is empirical evidence of a male bias in fitness effects of spontaneous mutations in *Drosophila* (Mallet et al., 2011; Sharp & Agrawal, 2013), which is consistent with the larger amount of male- rather than female-specific eQTL interactions we detect in Chapter 3 of this thesis.

Also importantly, previous work has shown that even with perfect intersex correlation and sexually concordant selection, sexual dimorphism can evolve if sex-specific genetic variances are unequal (Lynch & Walsh, 1998; Connallon & Clark, 2014b; Houle & Cheng, 2021). This suggests that interpreting r_{fm} as a constraint, which is the narrative employed in this manuscript, as well as many others cited throughout, relies on the assumptions that all genetic variance is additive, and that variances do not differ between the sexes (Lynch & Walsh, 1998; Bonduriansky & Chenoweth, 2009). These aspects illustrate the importance of clearly stating the assumptions underlying the chosen models, as they may lead to qualitatively different results, and support the idea that differences in genetic architecture are likely to account for a big part of the differences in the evolutionary dynamics of sexual dimorphism that have been observed across species and traits.

In summary, our work provides an in-depth examination of the relationship between intersex correlation and sex differences as well as their joint evolutionary dynamics in a population adapting to a sex-specific shift in optima under sex-specific stabilizing selection, mutation and drift, assuming non-evolving genetic architecture. It represents, to our knowledge, the first comprehensive account of various mechanisms that can generate a negative association between intersex correlation and sexual dimorphism, formalizing common intuition in the field. Also, it stresses the importance of revisiting commonly-used verbal arguments and illustrates how contextualizing their underlying assumptions can provide insightful information of the evolutionary forces shaping empirical patterns.

Table 1: Summary of notation

Symbol	Definition
General parameters	
N	Population size
U	Expected number of mutations per generation per gamete
V_S	Width of the Gaussian fitness function ($1/V_S$ measures the strength of stabilizing selection)
δ	Typical squared magnitude of fluctuations around the optimum at equilibrium ($\delta = V_S/(2N)$)
ϕ_a	Angle determining the fraction of stabilizing selection on an allele that acts via each sex
$h(\phi_a)$	Mutational distribution of ϕ_a
a^2	Squared total phenotypic magnitude, corresponding to the scaled stabilizing selection coefficient ($a^2 \equiv 2Ns_e$)
$g(a)$	Mutational distribution of phenotypic magnitudes
$V_{A,T}$	Total additive genetic variance (defined in terms of the total phenotypic magnitude)
Sex-specific parameters	
γ_f, γ_m	Modulators of the relative strength of selection acting on females or males ($\gamma_f, \gamma_m > 0$ and $\gamma_f^2 + \gamma_m^2 = 1$)
$V_{S,f}, V_{S,m}$	Widths of the sex-specific fitness functions, with $V_{S,f} \equiv 2V_S/(2\gamma_f^2)$ and $V_{S,m} \equiv 2V_S/(2\gamma_m^2)$ ($1/V_{S,f}$ and $1/V_{S,m}$ being the strengths of sex-specific stabilizing selection)
a_f, a_m	Allele's sex-specific effects on the phenotype
\bar{z}_f, \bar{z}_m	Sex-specific trait means
O_f, O_m	Sex-specific optima
D_f, D_m	Sex-specific distances of the mean phenotypes from their respective optima
Λ_f, Λ_m	Sex-specific shifts in trait optima
$V_{A,f}, V_{A,m}$	Sex-specific additive genetic variances
B	Between-sex covariance in the trait
r_{fm}	Intersex correlation in the trait
$\mu_{3,f}, \mu_{3,m}$	$\mu_{3,f} \equiv \frac{1}{2}(\mu_{3,fff} + \mu_{3,fmm})$ and $\mu_{3,m} \equiv \frac{1}{2}(\mu_{3,mmm} + \mu_{3,ffm})$, where $\mu_{3,\alpha\beta\gamma}$ ($\alpha, \beta, \gamma = f$ or m), are the third order central moments given by $\mu_{3,\alpha\beta\gamma} = \sum_i 2a_{i,\alpha}a_{i,\beta}a_{i,\gamma}x_i(1-x_i)(1-2x_i)$
'Average' and 'average distance' parameters: $k_a \equiv \frac{1}{2}(k_f + k_m)$; $k_d \equiv \frac{1}{2}(k_f - k_m)$	
\bar{z}_a, \bar{z}_d	Average and average distance of the mean phenotypes
O_a, O_d	Average and average distance of the phenotypic optima
D_a, D_d	Distance between average and average distance of the mean phenotypes and their optima
Λ_a, Λ_d	Shifts in average and average distance optima
$V_{A,a}, V_{A,d}$	Average and average distance of the additive genetic variance
$\mu_{3,a}, \mu_{3,d}$	$\mu_{3,a} = (\mu_{3,fff} + \mu_{3,fmm} + \mu_{3,ffm} + \mu_{3,mmm})/4$; $\mu_{3,d} = (\mu_{3,fff} + \mu_{3,fmm} - \mu_{3,ffm} - \mu_{3,mmm})/4$

Acknowledgments

We thank Tim Connallon for useful discussions on the topic, Himani Sachdeva and Nick Barton for comments on the manuscript and the Scientific Computing unit at ISTA for technical support.

GP is the recipient of a DOC Fellowship of the Austrian Academy of Sciences at the Institute of Science and Technology Austria (DOC 25817) and received funding from the European Union's Horizon 2020 research and innovation program under the Marie Skłodowska-Curie Grant (agreement no. 665385).

Author Contributions

GP and LH conceived the study, performed the analyses and wrote the manuscript.

References

- Abbott, J. K., Bedhomme, S., & Chippindale, A. K. (2010, September). Sexual conflict in wing size and shape in *Drosophila melanogaster*. *Journal of Evolutionary Biology*, *23*(9), 1989–1997. doi: 10.1111/j.1420-9101.2010.02064.x
- Ashman, T.-L. (2003, September). Constraints on the evolution of males and sexual dimorphism: field estimates of genetic architecture of reproductive traits in three populations of gynodioecious *Fragaria virginiana*. *Evolution; International Journal of Organic Evolution*, *57*(9), 2012–2025. doi: 10.1111/j.0014-3820.2003.tb00381.x
- Ashman, T.-L., & Majetic, C. J. (2006, May). Genetic constraints on floral evolution: a review and evaluation of patterns. *Heredity*, *96*(5), 343–352. doi: 10.1038/sj.hdy.6800815
- Barson, N. J., Aykanat, T., Hindar, K., Baranski, M., Bolstad, G. H., Fiske, P., ... Primmer, C. R. (2015, December). Sex-dependent dominance at a single locus maintains variation in age at maturity in salmon. *Nature*, *528*(7582), 405–408. Retrieved 2023-05-10, from <https://www.nature.com/articles/nature16062> (Number: 7582 Publisher: Nature Publishing Group) doi: 10.1038/nature16062
- Barton, N. H., Etheridge, A. M., & Véber, A. (2017, December). The infinitesimal model: Definition, derivation, and implications. *Theoretical Population Biology*, *118*, 50–73. doi: 10.1016/j.tpb.2017.06.001

- Bird, M. A., & Schaffer, H. E. (1972, November). A study of the genetic basis of the sexual dimorphism for wing length in *Drosophila melanogaster*. *Genetics*, *72*(3), 475–487. doi: 10.1093/genetics/72.3.475
- Bolnick, D. I., & Doebeli, M. (2003, November). Sexual dimorphism and adaptive speciation: two sides of the same ecological coin. *Evolution; International Journal of Organic Evolution*, *57*(11), 2433–2449. doi: 10.1111/j.0014-3820.2003.tb01489.x
- Bonduriansky, R. (2006, May). Convergent evolution of sexual shape dimorphism in Diptera. *Journal of Morphology*, *267*(5), 602–611. doi: 10.1002/jmor.10426
- Bonduriansky, R., & Chenoweth, S. F. (2009, May). Intralocus sexual conflict. *Trends in Ecology & Evolution*, *24*(5), 280–288. doi: 10.1016/j.tree.2008.12.005
- Bonduriansky, R., & Rowe, L. (2005, September). Intralocus sexual conflict and the genetic architecture of sexually dimorphic traits in *Prochyliza xanthostoma* (Diptera: Piophilidae). *Evolution; International Journal of Organic Evolution*, *59*(9), 1965–1975.
- Bürger, R., & Lande, R. (1994, November). On the Distribution of the Mean and Variance of a Quantitative Trait under Mutation-Selection-Drift Balance. *Genetics*, *138*(3), 901–912. Retrieved 2023-05-28, from <https://www.ncbi.nlm.nih.gov/pmc/articles/PMC1206237/>
- Chantepie, S., & Chevin, L.-M. (2020, December). How does the strength of selection influence genetic correlations? *Evolution Letters*, *4*(6), 468–478. doi: 10.1002/evl3.201
- Chenoweth, S. F., & Blows, M. W. (2003). Signal Trait Sexual Dimorphism and Mutual Sexual Selection in *Drosophila Serrata*. *Evolution*, *57*(10), 2326–2334. Retrieved 2023-04-27, from <https://onlinelibrary.wiley.com/doi/abs/10.1111/j.0014-3820.2003.tb00244.x> (eprint: <https://onlinelibrary.wiley.com/doi/pdf/10.1111/j.0014-3820.2003.tb00244.x>) doi: 10.1111/j.0014-3820.2003.tb00244.x
- Cheverud, J. M., Dow, M. M., & Leutenegger, W. (1985). The Quantitative Assessment of Phylogenetic Constraints in Comparative Analyses: Sexual Dimorphism in Body Weight Among Primates. *Evolution*, *39*(6), 1335–1351. Retrieved 2023-05-05, from <https://onlinelibrary.wiley.com/doi/abs/10.1111/j.1558-5646.1985.tb05699.x> (eprint: <https://onlinelibrary.wiley.com/doi/pdf/10.1111/j.1558-5646.1985.tb05699.x>) doi: 10.1111/j.1558-5646.1985.tb05699.x

- Chursina, M. A. (2019, August). Convergent evolution of sexual dimorphism in species of the family Dolichopodidae (Diptera). *Biodiversitas Journal of Biological Diversity*, 20(9). Retrieved 2023-05-10, from <https://smujo.id/biodiv/article/view/4066> (Number: 9) doi: 10.13057/biodiv/d200908
- Connallon, T., & Clark, A. G. (2011, March). The Resolution of Sexual Antagonism by Gene Duplication. *Genetics*, 187(3), 919–937. Retrieved 2023-05-10, from <https://www.ncbi.nlm.nih.gov/pmc/articles/PMC3063682/> doi: 10.1534/genetics.110.123729
- Connallon, T., & Clark, A. G. (2014a, July). Balancing selection in species with separate sexes: insights from Fisher’s geometric model. *Genetics*, 197(3), 991–1006. doi: 10.1534/genetics.114.165605
- Connallon, T., & Clark, A. G. (2014b, February). Evolutionary inevitability of sexual antagonism. *Proceedings. Biological Sciences*, 281(1776), 20132123. doi: 10.1098/rspb.2013.2123
- Cowley, D. E., & Atchley, W. R. (1988, June). Quantitative Genetics of *Drosophila Melanogaster*. II. Heritabilities and Genetic Correlations between Sexes for Head and Thorax Traits. *Genetics*, 119(2), 421–433. doi: 10.1093/genetics/119.2.421
- Cox, R. M., & Calsbeek, R. (2009, February). Sexually antagonistic selection, sexual dimorphism, and the resolution of intralocus sexual conflict. *The American Naturalist*, 173(2), 176–187. doi: 10.1086/595841
- Day, T., & Bonduriansky, R. (2004, August). Intralocus sexual conflict can drive the evolution of genomic imprinting. *Genetics*, 167(4), 1537–1546. doi: 10.1534/genetics.103.026211
- Delph, L. F., Arntz, A. M., Scotti-Saintagne, C., & Scotti, I. (2010, October). The genomic architecture of sexual dimorphism in the dioecious plant *Silene latifolia*. *Evolution; International Journal of Organic Evolution*, 64(10), 2873–2886. doi: 10.1111/j.1558-5646.2010.01048.x
- Delph, L. F., Frey, F. M., Steven, J. C., & Gehring, J. L. (2004). Investigating the independent evolution of the size of floral organs via G-matrix estimation and artificial selection. *Evolution & Development*, 6(6), 438–448. doi: 10.1111/j.1525-142X.2004.04052.x
- Delph, L. F., Steven, J. C., Anderson, I. A., Herlihy, C. R., & Brodie, E. D. (2011, October). Elimination of a genetic correlation between the sexes via artificial correlational selection. *Evolution; International Journal of Organic Evolution*, 65(10), 2872–2880. doi: 10.1111/j.1558-5646.2011.01350.x

- Dimas, A. S., Nica, A. C., Montgomery, S. B., Stranger, B. E., Raj, T., Buil, A., ... Dermitzakis, E. T. (2012, December). Sex-biased genetic effects on gene regulation in humans. *Genome Research*, *22*(12), 2368–2375. doi: 10.1101/gr.134981.111
- Eisen, E. J., & Hanrahan, J. P. (1972, October). Selection for sexual dimorphism in body weight of mice. *Australian Journal of Biological Sciences*, *25*(5), 1015–1024. doi: 10.1071/bi9721015
- Fisher, R. (1958). *The Genetical Theory of Natural Selection* (Second edition ed.). New York: dover.
- Frankham, R. (1968a, December). Sex and selection for a quantitative character in *Drosophila*. II. The sex dimorphism. *Australian Journal of Biological Sciences*, *21*(6), 1225–1237. doi: 10.1071/bi9681225
- Frankham, R. (1968b, December). Sex and selection for a quantitative character in *Drosophila*. I. Single-sex selection. *Australian Journal of Biological Sciences*, *21*(6), 1215–1223. doi: 10.1071/bi9681215
- Griffin, R. M., Dean, R., Grace, J. L., Rydén, P., & Friberg, U. (2013, September). The shared genome is a pervasive constraint on the evolution of sex-biased gene expression. *Molecular Biology and Evolution*, *30*(9), 2168–2176. doi: 10.1093/molbev/mst121
- Harrison, B. J. (1953, August). Reversal of a secondary sex character by selection. *Heredity*, *7*(2), 153–164. Retrieved 2023-04-27, from <https://www.nature.com/articles/hdy195324> (Number: 2 Publisher: Nature Publishing Group) doi: 10.1038/hdy.1953.24
- Hayward, L. K., & Sella, G. (2022, September). Polygenic adaptation after a sudden change in environment. *eLife*, *11*, e66697. doi: 10.7554/eLife.66697
- Houle, D., & Cheng, C. (2021, May). Predicting the Evolution of Sexual Dimorphism in Gene Expression. *Molecular Biology and Evolution*, *38*(5), 1847–1859. doi: 10.1093/molbev/msaa329
- Jones, A. G., Arnold, S. J., & Bürger, R. (2003). Stability of the G-Matrix in a Population Experiencing Pleiotropic Mutation, Stabilizing Selection, and Genetic Drift. *Evolution*, *57*(8), 1747–1760. Retrieved 2023-05-10, from <https://www.jstor.org/stable/3448700> (Publisher: [Society for the Study of Evolution, Wiley])
- Kidwell, J. F., Clegg, M. T., Stewart, F. M., & Prout, T. (1977, January). Regions of stable equilibria for models of differential selection in the two sexes under random mating. *Genetics*, *85*(1), 171–183. doi: 10.1093/genetics/85.1.171

- Lande, R. (1976, June). NATURAL SELECTION AND RANDOM GENETIC DRIFT IN PHENOTYPIC EVOLUTION. *Evolution; International Journal of Organic Evolution*, *30*(2), 314–334. doi: 10.1111/j.1558-5646.1976.tb00911.x
- Lande, R. (1980, March). SEXUAL DIMORPHISM, SEXUAL SELECTION, AND ADAPTATION IN POLYGENIC CHARACTERS. *Evolution; International Journal of Organic Evolution*, *34*(2), 292–305. doi: 10.1111/j.1558-5646.1980.tb04817.x
- Lande, R. (1987). Genetic correlations between the sexes in the evolution of sexual dimorphism and mating preferences. In J. W. Bardbury & M. B. Andersson (Eds.), *Sexual Selection: Testing the Alternatives : Report of the Dahlem Workshop on Sexual Selection: Testing the Alternatives, Berlin 1986, August 31-September 5*. Wiley. (Google-Books-ID: Z9lqAAAAMAAJ)
- Lande, R., & Arnold, S. J. (1983). The Measurement of Selection on Correlated Characters. *Evolution*, *37*(6), 1210–1226. Retrieved 2023-05-10, from <https://www.jstor.org/stable/2408842> (Publisher: [Society for the Study of Evolution, Wiley]) doi: 10.2307/2408842
- Lassek, W. D., & Gaulin, S. J. C. (2022). Substantial but Misunderstood Human Sexual Dimorphism Results Mainly From Sexual Selection on Males and Natural Selection on Females. *Frontiers in Psychology*, *13*. Retrieved 2023-05-10, from <https://www.frontiersin.org/articles/10.3389/fpsyg.2022.859931>
- Leinonen, T., Cano, J. M., & Merilä, J. (2011, February). Genetic basis of sexual dimorphism in the threespine stickleback *Gasterosteus aculeatus*. *Heredity*, *106*(2), 218–227. doi: 10.1038/hdy.2010.104
- Locke, A. E., Kahali, B., Berndt, S. I., Justice, A. E., Pers, T. H., Day, F. R., ... Speliotes, E. K. (2015, February). Genetic studies of body mass index yield new insights for obesity biology. *Nature*, *518*(7538), 197–206. Retrieved 2023-05-10, from <https://www.nature.com/articles/nature14177> (Number: 7538 Publisher: Nature Publishing Group) doi: 10.1038/nature14177
- Lynch, M., & Walsh, B. (1998). *Genetics and Analysis of Quantitative Traits* (1st edition ed.). Sunderland, Mass: Sinauer Associates is an imprint of Oxford University Press.
- Mallet, M. A., Bouchard, J. M., Kimber, C. M., & Chippindale, A. K. (2011, June). Experimental mutation-accumulation on the X chromosome of *Drosophila melanogaster* reveals stronger selection on males than females. *BMC Evolutionary Biology*, *11*(1), 156. Retrieved 2023-05-10, from <https://doi.org/>

- [10.1186/1471-2148-11-156](https://doi.org/10.1186/1471-2148-11-156) doi: 10.1186/1471-2148-11-156
- McDaniel, S. F. (2005, November). Genetic correlations do not constrain the evolution of sexual dimorphism in the moss *Ceratodon purpureus*. *Evolution; International Journal of Organic Evolution*, *59*(11), 2353–2361.
- McGlothlin, J. W., Cox, R. M., & Brodie, E. D. (2019, July). Sex-Specific Selection and the Evolution of Between-Sex Genetic Covariance. *The Journal of Heredity*, *110*(4), 422–432. doi: 10.1093/jhered/esz031
- McIntyre, L. M., Bono, L. M., Genissel, A., Westerman, R., Junk, D., Telonis-Scott, M., ... Nuzhdin, S. V. (2006, August). Sex-specific expression of alternative transcripts in *Drosophila*. *Genome Biology*, *7*(8), R79. Retrieved 2023-05-10, from <https://doi.org/10.1186/gb-2006-7-8-r79> doi: 10.1186/gb-2006-7-8-r79
- Morrow, E. H. (2015). The evolution of sex differences in disease. *Biology of Sex Differences*, *6*, 5. doi: 10.1186/s13293-015-0023-0
- Morrow, E. H., & Connallon, T. (2013, December). Implications of sex-specific selection for the genetic basis of disease. *Evolutionary Applications*, *6*(8), 1208–1217. doi: 10.1111/eva.12097
- Muralidhar, P., & Coop, G. (2023, March). *Polygenic outcomes of sexually antagonistic selection*. bioRxiv. Retrieved 2023-05-10, from <https://www.biorxiv.org/content/10.1101/2023.03.02.530911v1> (Pages: 2023.03.02.530911 Section: New Results) doi: 10.1101/2023.03.02.530911
- Oliva, M., Muñoz-Aguirre, M., Kim-Hellmuth, S., Wucher, V., Gewirtz, A. D. H., Cotter, D. J., ... Stranger, B. E. (2020, September). The impact of sex on gene expression across human tissues. *Science (New York, N.Y.)*, *369*(6509), eaba3066. doi: 10.1126/science.aba3066
- Owens, I. P. F., & Hartley, I. R. (1998, March). Sexual dimorphism in birds: why are there so many different forms of dimorphism? *Proceedings of the Royal Society of London. Series B: Biological Sciences*, *265*(1394), 397–407. Retrieved 2023-05-10, from <https://royalsocietypublishing.org/doi/10.1098/rspb.1998.0308> doi: 10.1098/rspb.1998.0308
- Pennell, T. M., & Morrow, E. H. (2013). Two sexes, one genome: the evolutionary dynamics of intralocus sexual conflict. *Ecology and Evolution*, *3*(6), 1819–1834. Retrieved 2023-05-10, from <https://onlinelibrary.wiley.com/doi/abs/10.1002/ece3.540> (eprint: <https://onlinelibrary.wiley.com/doi/pdf/10.1002/ece3.540>) doi: 10.1002/ece3.540

- Poissant, J., Wilson, A. J., & Coltman, D. W. (2010, January). Sex-specific genetic variance and the evolution of sexual dimorphism: a systematic review of cross-sex genetic correlations. *Evolution; International Journal of Organic Evolution*, *64*(1), 97–107. doi: 10.1111/j.1558-5646.2009.00793.x
- Prasad, N. G., Bedhomme, S., Day, T., & Chippindale, A. K. (2007, January). An evolutionary cost of separate genders revealed by male-limited evolution. *The American Naturalist*, *169*(1), 29–37. doi: 10.1086/509941
- Preziosi, R. F., & Roff, D. A. (1998, July). Evidence of genetic isolation between sexually monomorphic and sexually dimorphic traits in the water strider *Aquarius remigis*. *Heredity*, *81*(1), 92–99. Retrieved 2023-04-27, from <https://www.nature.com/articles/6883800> (Number: 1 Publisher: Nature Publishing Group) doi: 10.1046/j.1365-2540.1998.00380.x
- Proulx, S. R., & Phillips, P. C. (2006). Allelic Divergence Precedes and Promotes Gene Duplication. *Evolution*, *60*(5), 881–892. Retrieved 2023-05-10, from <https://www.jstor.org/stable/4095392> (Publisher: [Society for the Study of Evolution, Wiley])
- Puixeu, G., Pickup, M., Field, D. L., & Barrett, S. C. H. (2019, November). Variation in sexual dimorphism in a wind-pollinated plant: the influence of geographical context and life-cycle dynamics. *The New Phytologist*, *224*(3), 1108–1120. doi: 10.1111/nph.16050
- Reeve, J. P., & Fairbairn, D. J. (1996, October). SEXUAL SIZE DIMORPHISM AS A CORRELATED RESPONSE TO SELECTION ON BODY SIZE: AN EMPIRICAL TEST OF THE QUANTITATIVE GENETIC MODEL. *Evolution; International Journal of Organic Evolution*, *50*(5), 1927–1938. doi: 10.1111/j.1558-5646.1996.tb03580.x
- Reeve, J. P., & Fairbairn, D. J. (2001). Predicting the evolution of sexual size dimorphism. *Journal of Evolutionary Biology*, *14*(2), 244–254. Retrieved 2023-04-27, from <https://onlinelibrary.wiley.com/doi/abs/10.1046/j.1420-9101.2001.00276.x> (_eprint: <https://onlinelibrary.wiley.com/doi/pdf/10.1046/j.1420-9101.2001.00276.x>) doi: 10.1046/j.1420-9101.2001.00276.x
- Rhen, T. (2000, February). Sex-limited mutations and the evolution of sexual dimorphism. *Evolution; International Journal of Organic Evolution*, *54*(1), 37–43. doi: 10.1111/j.0014-3820.2000.tb00005.x
- Rice, W. R. (1984, July). SEX CHROMOSOMES AND THE EVOLUTION OF SEXUAL DIMORPHISM. *Evolution; International Journal of Organic Evo-*

- lution*, 38(4), 735–742. doi: 10.1111/j.1558-5646.1984.tb00346.x
- Rice, W. R., & Chippindale, A. K. (2001). Intersexual ontogenetic conflict. *Journal of Evolutionary Biology*, 14(5), 685–693. Retrieved 2023-04-27, from <https://onlinelibrary.wiley.com/doi/abs/10.1046/j.1420-9101.2001.00319.x> (_eprint: <https://onlinelibrary.wiley.com/doi/pdf/10.1046/j.1420-9101.2001.00319.x>) doi: 10.1046/j.1420-9101.2001.00319.x
- Rice, W. R., & Chippindale, A. K. (2002, November). The Evolution of Hybrid Infer-
tility: Perpetual Coevolution between Gender-Specific and Sexually Antago-
nistic Genes. *Genetica*, 116(2), 179–188. Retrieved 2023-05-10, from <https://doi.org/10.1023/A:1021205130926> doi: 10.1023/A:1021205130926
- Sanjak, J. S., Sidorenko, J., Robinson, M. R., Thornton, K. R., & Visscher, P. M. (2018, January). Evidence of directional and stabilizing selection in contempo-
rary humans. *Proceedings of the National Academy of Sciences of the United States of America*, 115(1), 151–156. doi: 10.1073/pnas.1707227114
- Sharp, N. P., & Agrawal, A. F. (2013, April). Male-biased fitness effects of sponta-
neous mutations in *Drosophila melanogaster*. *Evolution; International Journal of Organic Evolution*, 67(4), 1189–1195. doi: 10.1111/j.1558-5646.2012.01834.x
- Simons, Y. B., Bullaughey, K., Hudson, R. R., & Sella, G. (2018, March). A
population genetic interpretation of GWAS findings for human quantitative
traits. *PLoS biology*, 16(3), e2002985. doi: 10.1371/journal.pbio.2002985
- Singh, A., & Agrawal, A. F. (2023, May). Two Forms of Sexual Dimorphism in
Gene Expression in *Drosophila melanogaster*: Their Coincidence and Evo-
lutionary Genetics. *Molecular Biology and Evolution*, 40(5), msad091. Re-
trieved 2023-05-10, from <https://doi.org/10.1093/molbev/msad091> doi:
10.1093/molbev/msad091
- Sison-Mangus, M. P., Bernard, G. D., Lampel, J., & Briscoe, A. D. (2006, August).
Beauty in the eye of the beholder: the two blue opsins of lycaenid butterflies
and the opsin gene-driven evolution of sexually dimorphic eyes. *The Journal of Experimental Biology*, 209(Pt 16), 3079–3090. doi: 10.1242/jeb.02360
- Stewart, A. D., Pischedda, A., & Rice, W. R. (2010). Resolving intralocus sexual
conflict: genetic mechanisms and time frame. *The Journal of Heredity*, 101
Suppl 1(Suppl 1), S94–99. doi: 10.1093/jhered/esq011
- Stewart, A. D., & Rice, W. R. (2018, September). Arrest of sex-specific adaptation
during the evolution of sexual dimorphism in *Drosophila*. *Nature Ecology &
Evolution*, 2(9), 1507–1513. doi: 10.1038/s41559-018-0613-4

- Stulp, G., Kuijper, B., Buunk, A. P., Pollet, T. V., & Verhulst, S. (2012, December). Intralocus sexual conflict over human height. *Biology Letters*, *8*(6), 976–978. doi: 10.1098/rsbl.2012.0590
- Turelli, M. (1984, April). Heritable genetic variation via mutation-selection balance: Lerch's zeta meets the abdominal bristle. *Theoretical Population Biology*, *25*(2), 138–193. doi: 10.1016/0040-5809(84)90017-0
- Turelli, M. (1985, September). Effects of pleiotropy on predictions concerning mutation-selection balance for polygenic traits. *Genetics*, *111*(1), 165–195. doi: 10.1093/genetics/111.1.165
- Williams, T. M., & Carroll, S. B. (2009, November). Genetic and molecular insights into the development and evolution of sexual dimorphism. *Nature Reviews. Genetics*, *10*(11), 797–804. doi: 10.1038/nrg2687
- Wood, A. R., Esko, T., Yang, J., Vedantam, S., Pers, T. H., Gustafsson, S., ... Frayling, T. M. (2014, November). Defining the role of common variation in the genomic and biological architecture of adult human height. *Nature Genetics*, *46*(11), 1173–1186. Retrieved 2023-05-10, from <https://www.nature.com/articles/ng.3097> (Number: 11 Publisher: Nature Publishing Group) doi: 10.1038/ng.3097
- Wright, A. E., Fumagalli, M., Cooney, C. R., Bloch, N. I., Vieira, F. G., Buechel, S. D., ... Mank, J. E. (2018, April). Male-biased gene expression resolves sexual conflict through the evolution of sex-specific genetic architecture. *Evolution Letters*, *2*(2), 52–61. doi: 10.1002/evl3.39
- Wright, D. B. (1993). Evolution of sexually dimorphic characters in peccaries (Mammalia, Tayassuidae). *Paleobiology*, *19*(1), 52–70. Retrieved 2023-05-10, from https://www.cambridge.org/core/product/identifier/S0094837300012318/type/journal_article doi: 10.1017/S0094837300012318
- Wright, S. (1935, March). The analysis of variance and the correlations between relatives with respect to deviations from an optimum. *Journal of Genetics*, *30*(2), 243–256. Retrieved 2023-05-10, from <https://doi.org/10.1007/BF02982239> doi: 10.1007/BF02982239
- Zwaan, B. J., Zijlstra, W. G., Keller, M., Pijpe, J., & Brakefield, P. M. (2008, December). Potential constraints on evolution: sexual dimorphism and the problem of protandry in the butterfly *Bicyclus anynana*. *Journal of Genetics*, *87*(4), 395–405. doi: 10.1007/s12041-008-0062-y

Joint discussion across thesis chapters

Connecting the dots

Gemma Puixeu

In the various projects of this thesis I have characterized variation in sexual dimorphism across species, phenotypic levels, traits and tissues, and have obtained predictions for its evolutionary dynamics under various selective forces, levels of intersex correlation and genetic architectures.

Each project has used different methodology and data from different species to tackle different questions, leading to a general understanding of genetic, transcriptional and phenotypic sexual dimorphism: first, how phenotypic sexual dimorphism varies across time and space, but also across traits and tissues; second, how sex differences in gene expression are likely to underlie most patterns of complex sexual dimorphism, and how testes show evidence of a unique regulatory architecture; third, how individual mutations operate to generate sex differences in gene expression; fourth, how the evolutionary dynamics of sexual dimorphism depend on assumptions about the patterns of (co)variance between the sexes, the genetic architecture of the considered trait(s) and the selective regimes they are subject to.

I will now proceed to a comparison between projects in particular points.

Sexual dimorphism, as well as its regulatory variation, varies in time, space and across genetic backgrounds

In the first Chapter, we examined patterns of genetically-based sexual dimorphism, measured in standardized greenhouse conditions, across life stages and populations spanning the whole geographic range and including two sex chromosome races of *Rumex hastatulus*, a wind-pollinated dioecious plant. We found that males are taller at peak flowering to facilitate wind-mediated pollen dispersal, while females are taller at peak maturity to facilitate wind-mediated seed dispersal, leading to a temporal change in sexual dimorphism for height.

We did not find evidence of differences in sexual dimorphism between the two chromosome races, in spite of their different sex chromosomes. Although it is predicted that sex chromosomes are enriched for genetic variation driving phenotypic differentiation between sexes (Rice, 1984), in our they account for a small amount of variation in sexual dimorphism, unsurprisingly. On the one hand, because the genetic content of the sex chromosomes is expected to be similar in the two chromosome races. This is because these karyotypic differences can be explained by a fusion between an autosome and the X chromosome in an ancestor with the XY karyotype, a rearrangement has resulted in one fewer autosome, a cytologically larger X and an extra Y chromosome in individuals of the North Carolina race with respect to those of the Texas race (Smith, 1963). Although there is some indication of this neo-sex chromosomes contributing to reproductive isolation between the two races (Beaudry et al., 2022), the rearrangement is expected to be recent and thus not have accumulated many mutations contributing to sex-specific adaptation. On the other hand, there are all sorts of other factors that differ between the two races (geographic, climatic or even autosomal genetic variation) which are expected to account for larger proportion of variation in sexual dimorphism.

In line with this, we found substantial variation in sexual dimorphism among populations distributed across a wide geographical range. We illustrate how these local adaptations are encoded in the genome, since we were able to recover correlations between sexual dimorphism patterns measured in a glasshouse experiment and demographic and climatic variables of the source populations. For example, we found that variation in sexual dimorphism for various traits was larger for individuals derived from less dense source populations. This is surprising given that density is expected to largely vary across seasons, particularly for such a largely annual plant, and provides indirect evidence that, for this species, density in each population likely remains fairly constant across the years, so that adaptations to such an effect are encoded in the genome. Also, we find that bioclimatic variables of the source populations explain up to a third of the (genetically-driven) variation for sexual dimorphism across various reproductive and vegetative traits, largely due to both sexes differently responding to changes in climatic conditions. We have not examined the genetic-geographic distance correlations between populations, but their detection would have provided more direct evidence of the genetic basis underlying local adaptation across the geographical range of the species.

That (sex-specific) phenotypic variation differs between population with differ-

ent genetic backgrounds leads to the prediction that sex-specific regulatory interactions underlying these phenotypic sex differences are likely to differ between genetic backgrounds. We provide direct evidence for this in the second thesis Chapter. Concretely, we find that overall patterns of regulatory variation, particularly those *trans*-acting, as well as the inheritance patterns of gene expression, vary greatly between biological replicates with different genetic backgrounds, even though the data across replicates was obtained in very controlled lab conditions.

These results suggest that sex-specific variation also reflects patterns of local adaptation to disruptive selection (Bolnick & Doebeli, 2003), which can generate stratification in sexual dimorphism in non-panmictic populations with marked population structure, such as plants. Also, this confirms that patterns of phenotypic sexual dimorphism strongly depend on genetic variation, and so can only be generalized when they are analyzed across genetic backgrounds.

Two complementary approaches to the study of the regulatory basis of sex- and tissue-specific gene expression

In the second and third Chapters we employed two different methods for the characterization of the regulatory architecture underlying sex- and tissue-specific gene expression in *Drosophila melanogaster*. In the second, we analyzed the overall extent of *cis*- and *trans*-regulatory variation, as well as inheritance patterns of gene expression, by comparing allele-specific expression between reciprocal and parental crosses; in the third, we performed eQTL analyses of sex-specific as well as sex bias in gene expression, calculated as $\log_2(\text{exp}_f/\text{exp}_m)$, to characterize the regulatory variation underlying sex differences in expression.

The data we used for these analyses were newly-generated datasets of sex-specific gene expression in heads and gonads of F1 crosses between inbred *Drosophila* Genetic Reference Panel (DGRP; Mackay et al., 2012; Huang et al., 2014) lines. The generation of these data, particularly for the third Chapter, was very challenging. It involved amplification of 190 *Drosophila melanogaster* lines, crossing them into 95 F1 lines from which we dissected over 10,000 individuals into 760 samples, which we sequenced using a multiplexing method that was new to the lab. Therefore, before starting this process, we produced a dataset using the same experimental conditions but at a smaller scale, which allowed us to test and tune the experimental setup, as well as the sequencing and bioinformatic pipelines. This was the dataset used in

Chapter 2, where we performed within- and reciprocal between-line crosses between a small subset of DGRP lines.

Moreover, the design of this “pilot experiment” was planned to allow us to explore complementary questions. Most importantly, by comparing gene expression patterns between reciprocal crosses, it allowed us to explicitly corroborate the result obtained by previous studies (Wittkopp et al., 2006; Coolon et al., 2012; Chen et al., 2015; Takada et al., 2017), some of which also analyzed reciprocal F1 crosses between DGRP lines, that maternal genotype and parent-of-origin effects should be absent in *Drosophila*. This was crucial for the generation of the big dataset used for the eQTL analyses, since every line was crossed just once as maternal or paternal, and maternal genotypic as well parent-of-origin effects, if present, would have been confounded with genetic effects in the GWAS. Also, besides obtaining tissue-specific gene expression, which allowed us to compare patterns of regulatory variation between heads and gonads, two tissues with marked differences in sexual dimorphism, using data collected in controlled conditions, one of the main goals of generating our own gene expression dataset instead of using already-published data (eg. using DGRP expression data directly) was that our F1 individuals are outbred. Although inbreeding depression is thought to impact patterns of genetic and phenotypic variation (Charlesworth & Willis, 2009), surprisingly little is known about the effects of inbreeding on gene expression. Some studies have not detected systematic differences in gene expression caused by inbreeding across species (Kristensen et al., 2005; Hansson et al., 2014), as they seem to be inconsistent between replicate inbred populations (Menzel et al., 2015), while others have reported evidence for changes in gene expression in inbred lines potentially protecting against inbreeding depression (García et al., 2012), or involving metabolism-related genes (Kristensen et al., 2006; Zhao et al., 2019), suggesting their decreased metabolic efficiency. While this was far from our focus in this study, we failed to find any effects of inbreeding on gene expression (by looking at broad statistics such as mean and average) between inbred and outbred lines. However, we believe that our dataset, consisting of sex- and tissue-specific expression of within- and reciprocal between-line crosses among 3 pairs of inbred lines, can be a useful resource in the study of the transcriptomic impact of inbreeding.

Our focus was, instead, the characterization of the sex- and tissue-specific regulatory variation underlying gene expression, which we examined using the two complementary approaches outlined above. We found that *cis*-regulatory effects are

more consistent across biological replicates, as reported in the second Chapter, and enriched for interactions shared between sexes, as shown in the third. Also, in both studies we detected evidence of a testis-specific regulatory variation. In Chapter 2, we find that *cis*-regulatory effects are overall more prevalent and different than those in heads and ovaries, which are largely shared; in Chapter 3, we show that testes have more eQTLs than the rest of the tissues and that most of the regulatory variation generating sex differences in expression in the gonads acts in a testis-specific manner. This points to a differential regulatory architecture of the testis, and is consistent with previous observations that, while in ovaries gene expression levels positively correlate with gene age and are largely determined by a combination of transcription factors, the testis is uniquely able to express younger genes controlled by relatively few TFs (Witt et al., 2021), allowing widespread baseline expression that is relatively unresponsive to regulatory changes (Witt et al., 2021). A more open chromatine that allows for higher exposure of promoters is consistent with two of our observations: on the one hand, that testes have more *cis*-regulatory variation, which is also different from that used in other tissues, which instead are potentially more responsive to *trans* effects; on the other hand, that these effects are not specific to testis-specific genes, and rather are an effect of testis-specific regulation of potentially widely-spread genes. This result is in line with the observation, consistent across species, that testis-expressed genes have higher evolutionary rates, both at the expression as well as sequence levels (Meiklejohn et al., 2003; Whittle et al., 2021): a more open chromatine that allows higher baseline expression increases the effective genetic variation, which allows testis-expressed genes for a faster response to directional selection.

In both analyses we detected substantial differences in the regulatory variation between heads and gonads, the latter showing substantially higher sexual dimorphism in expression and sex differences in regulatory variation, as is expected (Williams & Carroll, 2009; Stewart et al., 2010). This supports the general idea that sex-specific expression of shared regions should be responsible for most phenotypic differences between sexes, and that its regulatory variation should also be associated with phenotypic variation between sexes. However, evidence for this is still scarce (Porcu et al., 2022).

How data can inform the theory: on the distribution of mutations underlying sexual dimorphism

In the fourth project we defined models of sex-specific stabilizing selection, mutation and drift to examine sex-specific evolutionary dynamics under different selection regimes and genetic architectures.

For this, we relied on some assumptions about the genetic architecture underlying (sex-specific) phenotypic variation, since not much is known about the degree of sexual dimorphism among new mutations affecting phenotypic variation. Concretely, we sampled the overall effect sizes from an exponential distribution, which generally is in agreement with the empirical effect size distribution we find for mutations affecting sex-specific as well as sex bias in gene expression in Chapter 3. Also, we assumed that a fraction of mutations are sex-specific, whilst the rest are shared (with the same effect sizes in both sexes), therefore ignoring mutations that affect the two sexes in different magnitudes or directions.

This choice is well supported by our results on the modus operandi of the mutations generating variation for sex differences in expression in Chapter 3: on the one hand and according with previous results (Dimas et al., 2012; Meiklejohn et al., 2014; Oliva et al., 2020), we find that sex-biased and sexually-antagonistic mutations are rare; on the other hand, we find that a large proportion of the variation associated with sex differences in expression acts in a sex-specific manner.

In our model we also assume symmetrical distributions of incoming mutations across sexes. Specifically, we consider 1) the same amount of female- as male-specific mutations, with the same average effect size across sexes, and 2) that this is independent of the overall effect size (i.e. that stronger effect mutations are as likely to be female- as they are to be male-specific).

However, this is not fully supported by empirical data. Concretely, in Chapter 3 we find more standing variation underlying gene expression in males than females, particularly in gonads, which is consistent with other studies reporting male-biased fitness effects of new mutations (Mallet et al., 2011; Sharp & Agrawal, 2013). Considering data-informed sex-specific effect size distributions of incoming mutations is an upcoming extension of our theoretical project.

How theory can inform the data: on the relationship between intersex correlation and sexual dimorphism

An aspect that has been examined throughout all my PhD projects is the relationship between intersex correlation (r_{fm}) and sexual dimorphism. As outlined in Chapter 4, inconsistent experimental evidence fails to fully support the general prediction of a negative association between intersex correlation and sexual dimorphism, which is also true across our empirical studies. In Chapter 1, we found no significant correlation between r_{fm} and the extent of sexual dimorphism across traits, populations and life stages in *Rumex hastatulus*. In Chapter 3, we found that intersex correlation is higher for heads than for gonads and a negative association between intersex correlation and sex bias in heads, consistently with the general prediction. However, this was significantly positive in gonads, which is contrary to expectation.

Motivated by such inconsistent empirical results (despite a clear longstanding expectation in the field that intersex correlation should negatively covary with intersex correlation, for which no theoretical evidence was so far provided), in the last project we set out to formally test the conditions in which this pattern is expected to arise. Concretely, we use models of sex-specific stabilizing selection with mutation and drift to examine the relationship between intersex correlation and sexual dimorphism both at steady state and as the population adapts to a shift in sex-specific optima, for different selection regimes and genetic architectures of the considered trait. Our results suggest that a negative correlation between the two is generally not predicted at equilibrium, except when drift is considered. Generally, we find that a negative association between r_{fm} and sexual dimorphism is a far from universal pattern, only expected qualitatively and under particular conditions, given that some assumptions are fulfilled: 1) that a subset of traits has a non-infinitesimal genetic architecture, 2) that traits are sex-specifically adapting under directional selection, and 3) that this sex-specific adaptation is more commonly divergent than convergent (i.e. the two sexes are more commonly evolving to differ than to resemble). Related to this last assumption, we actually find that a *positive* relationship between intersex correlation and sexual dimorphism can arise in traits that adapt to converge between sexes, which provides, to our knowledge, the first mechanistic explanation for the conditions in which this pattern, which opposes the common expectation, might arise. This may help explain some empirical observations, such

as the positive relationship we observe between intersex correlation and sexual dimorphism in gonads of *Drosophila melanogaster*. It is unclear how likely it is that convergent selection is acting on gene expression in gonads of this species, but this offers a potential explanation for this observation.

References

- Beaudry, F. E. G., Rifkin, J. L., Peake, A. L., Kim, D., Jarvis-Cross, M., Barrett, S. C. H., & Wright, S. I. (2022). Effects of the neo-X chromosome on genomic signatures of hybridization in *Rumex hastatulus*. *Molecular Ecology*, *31*(13), 3708–3721. Retrieved 2023-08-02, from <https://onlinelibrary.wiley.com/doi/abs/10.1111/mec.16496> (eprint: <https://onlinelibrary.wiley.com/doi/pdf/10.1111/mec.16496>) doi: 10.1111/mec.16496
- Bolnick, D. I., & Doebeli, M. (2003, November). Sexual dimorphism and adaptive speciation: two sides of the same ecological coin. *Evolution; International Journal of Organic Evolution*, *57*(11), 2433–2449. doi: 10.1111/j.0014-3820.2003.tb01489.x
- Charlesworth, D., & Willis, J. H. (2009, November). The genetics of inbreeding depression. *Nature Reviews. Genetics*, *10*(11), 783–796. doi: 10.1038/nrg2664
- Chen, J., Nolte, V., & Schlötterer, C. (2015, February). Temperature Stress Mediates Decanalization and Dominance of Gene Expression in *Drosophila melanogaster*. *PLOS Genetics*, *11*(2), e1004883. Retrieved 2023-05-14, from <https://journals.plos.org/plosgenetics/article?id=10.1371/journal.pgen.1004883> (Publisher: Public Library of Science) doi: 10.1371/journal.pgen.1004883
- Coolon, J. D., Stevenson, K. R., McManus, C. J., Graveley, B. R., & Wittkopp, P. J. (2012, July). Genomic imprinting absent in *Drosophila melanogaster* adult females. *Cell Reports*, *2*(1), 69–75. doi: 10.1016/j.celrep.2012.06.013
- Dimas, A. S., Nica, A. C., Montgomery, S. B., Stranger, B. E., Raj, T., Buil, A., ... Dermitzakis, E. T. (2012, December). Sex-biased genetic effects on gene regulation in humans. *Genome Research*, *22*(12), 2368–2375. doi: 10.1101/gr.134981.111
- García, C., Avila, V., Quesada, H., & Caballero, A. (2012, September). Gene-expression changes caused by inbreeding protect against inbreeding depression in *Drosophila*. *Genetics*, *192*(1), 161–172. doi: 10.1534/genetics.112.142687

- Hansson, B., Naurin, S., & Hasselquist, D. (2014, September). Does inbreeding affect gene expression in birds? *Biology Letters*, *10*(9), 20140648. doi: 10.1098/rsbl.2014.0648
- Huang, W., Massouras, A., Inoue, Y., Peiffer, J., Ràmia, M., Tarone, A. M., ... Mackay, T. F. C. (2014, July). Natural variation in genome architecture among 205 *Drosophila melanogaster* Genetic Reference Panel lines. *Genome Research*, *24*(7), 1193–1208. doi: 10.1101/gr.171546.113
- Kristensen, T. N., Sørensen, P., Kruhøffer, M., Pedersen, K. S., & Loeschcke, V. (2005, September). Genome-wide analysis on inbreeding effects on gene expression in *Drosophila melanogaster*. *Genetics*, *171*(1), 157–167. doi: 10.1534/genetics.104.039610
- Kristensen, T. N., Sørensen, P., Pedersen, K. S., Kruhøffer, M., & Loeschcke, V. (2006, July). Inbreeding by environmental interactions affect gene expression in *Drosophila melanogaster*. *Genetics*, *173*(3), 1329–1336. doi: 10.1534/genetics.105.054486
- Mackay, T. F. C., Richards, S., Stone, E. A., Barbadilla, A., Ayroles, J. F., Zhu, D., ... Gibbs, R. A. (2012, February). The *Drosophila melanogaster* Genetic Reference Panel. *Nature*, *482*(7384), 173–178. doi: 10.1038/nature10811
- Mallet, M. A., Bouchard, J. M., Kimber, C. M., & Chippindale, A. K. (2011, June). Experimental mutation-accumulation on the X chromosome of *Drosophila melanogaster* reveals stronger selection on males than females. *BMC Evolutionary Biology*, *11*(1), 156. Retrieved 2023-05-10, from <https://doi.org/10.1186/1471-2148-11-156> doi: 10.1186/1471-2148-11-156
- Meiklejohn, C. D., Coolon, J. D., Hartl, D. L., & Wittkopp, P. J. (2014, January). The roles of cis- and trans-regulation in the evolution of regulatory incompatibilities and sexually dimorphic gene expression. *Genome Research*, *24*(1), 84–95. doi: 10.1101/gr.156414.113
- Meiklejohn, C. D., Parsch, J., Ranz, J. M., & Hartl, D. L. (2003, August). Rapid evolution of male-biased gene expression in *Drosophila*. *Proceedings of the National Academy of Sciences of the United States of America*, *100*(17), 9894–9899. doi: 10.1073/pnas.1630690100
- Menzel, M., Sletvold, N., Ågren, J., & Hansson, B. (2015, August). Inbreeding Affects Gene Expression Differently in Two Self-Incompatible *Arabidopsis lyrata* Populations with Similar Levels of Inbreeding Depression. *Molecular Biology and Evolution*, *32*(8), 2036–2047. doi: 10.1093/molbev/msv086
- Oliva, M., Muñoz-Aguirre, M., Kim-Hellmuth, S., Wucher, V., Gewirtz, A. D. H.,

- Cotter, D. J., ... Stranger, B. E. (2020, September). The impact of sex on gene expression across human tissues. *Science (New York, N.Y.)*, *369*(6509), eaba3066. doi: 10.1126/science.aba3066
- Porcu, E., Claringbould, A., Weihs, A., Lepik, K., Richardson, T. G., Völker, U., ... BIOS Consortium (2022, August). Limited evidence for blood eQTLs in human sexual dimorphism. *Genome Medicine*, *14*(1), 89. Retrieved 2023-05-26, from <https://doi.org/10.1186/s13073-022-01088-w> doi: 10.1186/s13073-022-01088-w
- Rice, W. R. (1984, July). SEX CHROMOSOMES AND THE EVOLUTION OF SEXUAL DIMORPHISM. *Evolution; International Journal of Organic Evolution*, *38*(4), 735–742. doi: 10.1111/j.1558-5646.1984.tb00346.x
- Sharp, N. P., & Agrawal, A. F. (2013, April). Male-biased fitness effects of spontaneous mutations in *Drosophila melanogaster*. *Evolution; International Journal of Organic Evolution*, *67*(4), 1189–1195. doi: 10.1111/j.1558-5646.2012.01834.x
- Smith, B. W. (1963, October). The Mechanism of Sex Determination in *Rumex Hastatulus*. *Genetics*, *48*(10), 1265–1288. doi: 10.1093/genetics/48.10.1265
- Stewart, A. D., Pischedda, A., & Rice, W. R. (2010). Resolving intralocus sexual conflict: genetic mechanisms and time frame. *The Journal of Heredity*, *101 Suppl 1*(Suppl 1), S94–99. doi: 10.1093/jhered/esq011
- Takada, Y., Miyagi, R., Takahashi, A., Endo, T., & Osada, N. (2017, July). A Generalized Linear Model for Decomposing Cis-regulatory, Parent-of-Origin, and Maternal Effects on Allele-Specific Gene Expression. *G3 (Bethesda, Md.)*, *7*(7), 2227–2234. doi: 10.1534/g3.117.042895
- Whittle, C. A., Kulkarni, A., & Extavour, C. G. (2021, August). Evolutionary dynamics of sex-biased genes expressed in cricket brains and gonads. *Journal of Evolutionary Biology*, *34*(8), 1188–1211. doi: 10.1111/jeb.13889
- Williams, T. M., & Carroll, S. B. (2009, November). Genetic and molecular insights into the development and evolution of sexual dimorphism. *Nature Reviews. Genetics*, *10*(11), 797–804. doi: 10.1038/nrg2687
- Witt, E., Svetec, N., Benjamin, S., & Zhao, L. (2021, May). Transcription Factors Drive Opposite Relationships between Gene Age and Tissue Specificity in Male and Female *Drosophila* Gonads. *Molecular Biology and Evolution*, *38*(5), 2104–2115. doi: 10.1093/molbev/msab011
- Wittkopp, P. J., Haerum, B. K., & Clark, A. G. (2006, July). Parent-of-origin effects on mRNA expression in *Drosophila melanogaster* not caused by genomic

imprinting. *Genetics*, *173*(3), 1817–1821. doi: 10.1534/genetics.105.054684
Zhao, L., Li, Y., Lou, J., Yang, Z., Liao, H., Fu, Q., . . . Bao, Z. (2019, October).
Transcriptomic Profiling Provides Insights into Inbreeding Depression in Yesso
Scallop *Patinopecten yessoensis*. *Marine Biotechnology (New York, N.Y.)*,
21(5), 623–633. doi: 10.1007/s10126-019-09907-9

CHAPTER 1

Variation in sexual dimorphism in a wind-pollinated plant: the influence of geographical context and life-cycle dynamics

Supplementary Material

Gemma Puixeu*, Melinda Pickup*, David L. Field
and Spencer C.H. Barrett

* These authors contributed equally to this work.

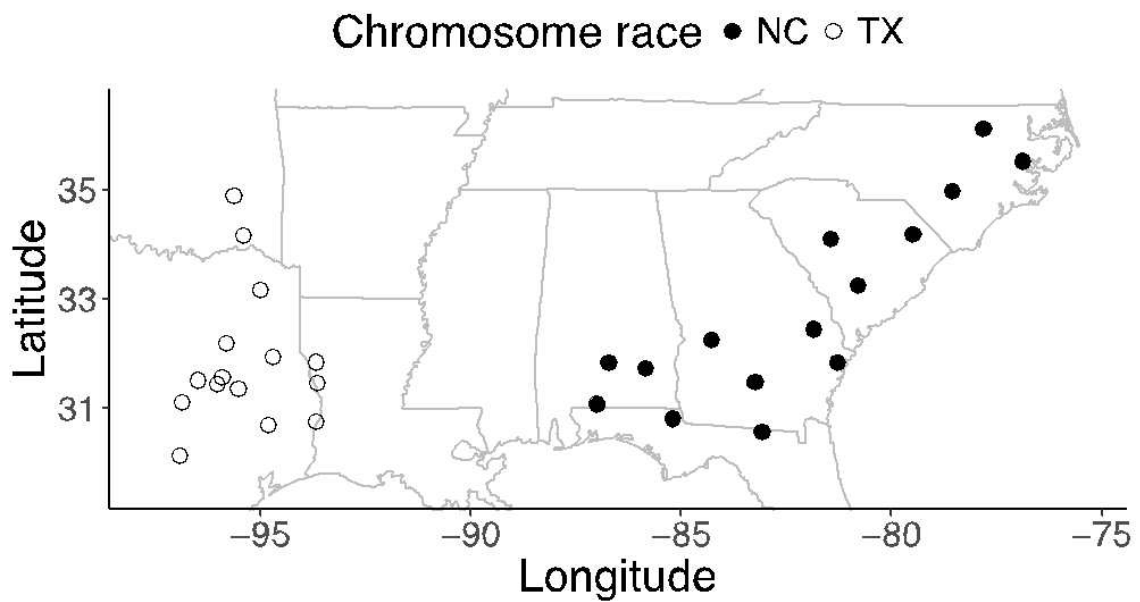


Figure S1: The geographic distribution of the 30 sampled populations of *Rumex hastatulus* representing the Texas (open circles) and North Carolina (closed circles) chromosome races.

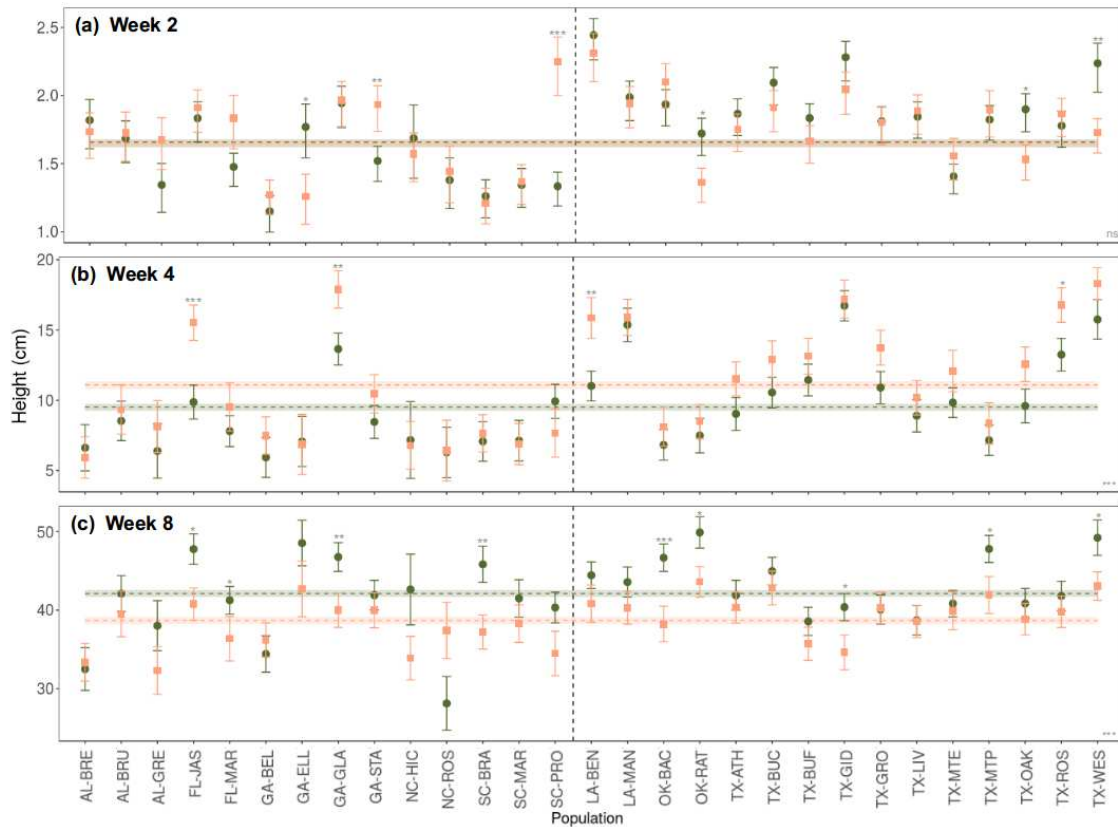


Figure S2: Plant height across life-cycle stages and populations of *Rumex hastatulus*. Predicted means and 95% confidence intervals for males (orange squares) and females (green circles) across populations and life-cycle stages. Significance of sex differences per population and overall is indicated with stars above individual bars and at the lower right corner, respectively. *: $0.01 < P < 0.05$, **: $0.001 < P < 0.01$, ***: $P < 0.001$, ns (or absence of asterisks on individual points): not statistically significant

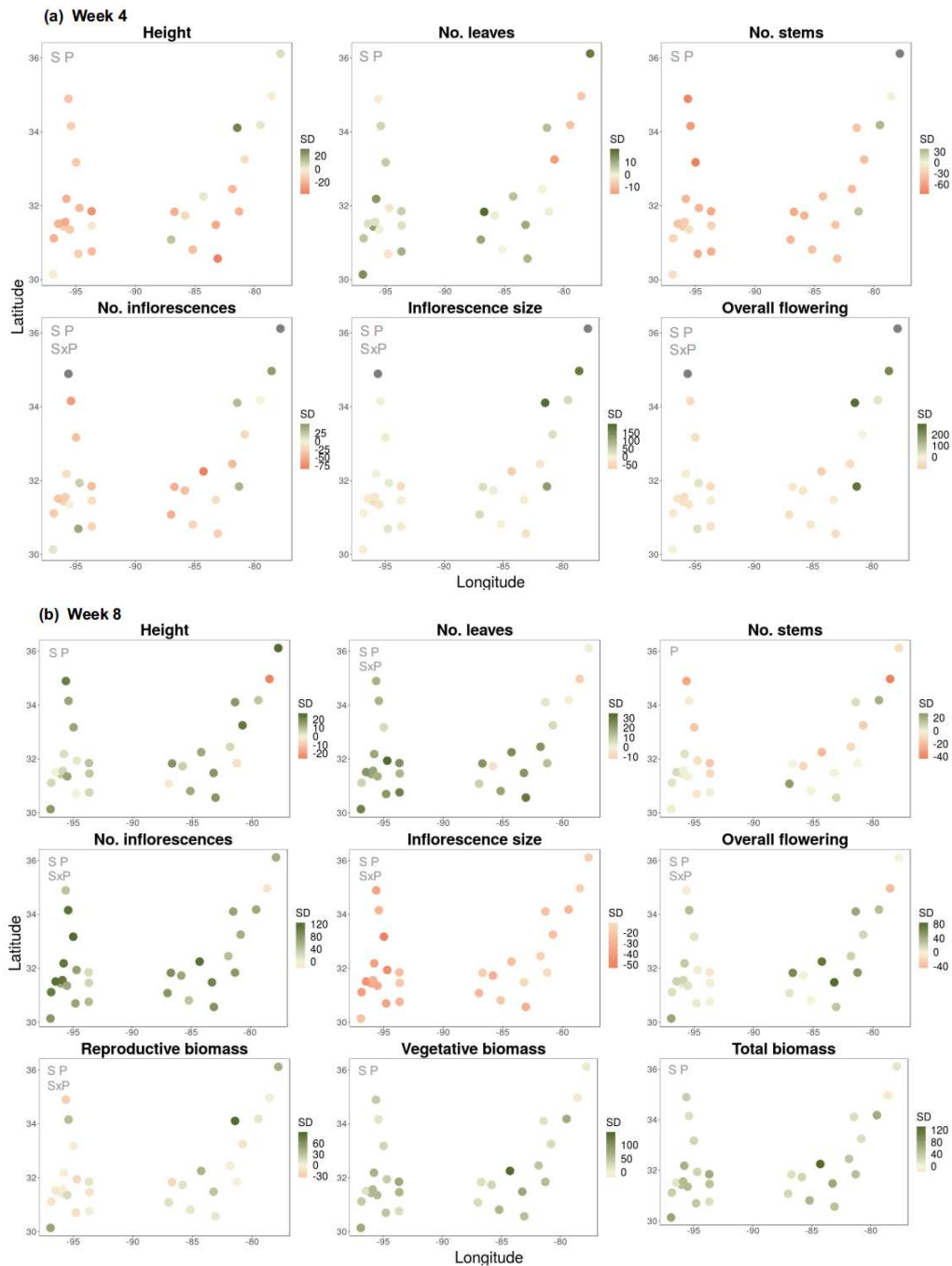


Figure S3: Sexual dimorphism (%SD) among populations at (A) week 4 and (B) week 8 in *Rumex hastatulus*. Percent sexual dimorphism (see the Materials and Methods section) for each population plotted according to its geographical location (longitude and latitude). Green (orange) indicates female (male) bias. Significant variation between sexes and among populations and their interaction obtained from GLMM (see Materials and Methods section) is indicated as “S”, “P” and “SxP” in the upper left corner, respectively.

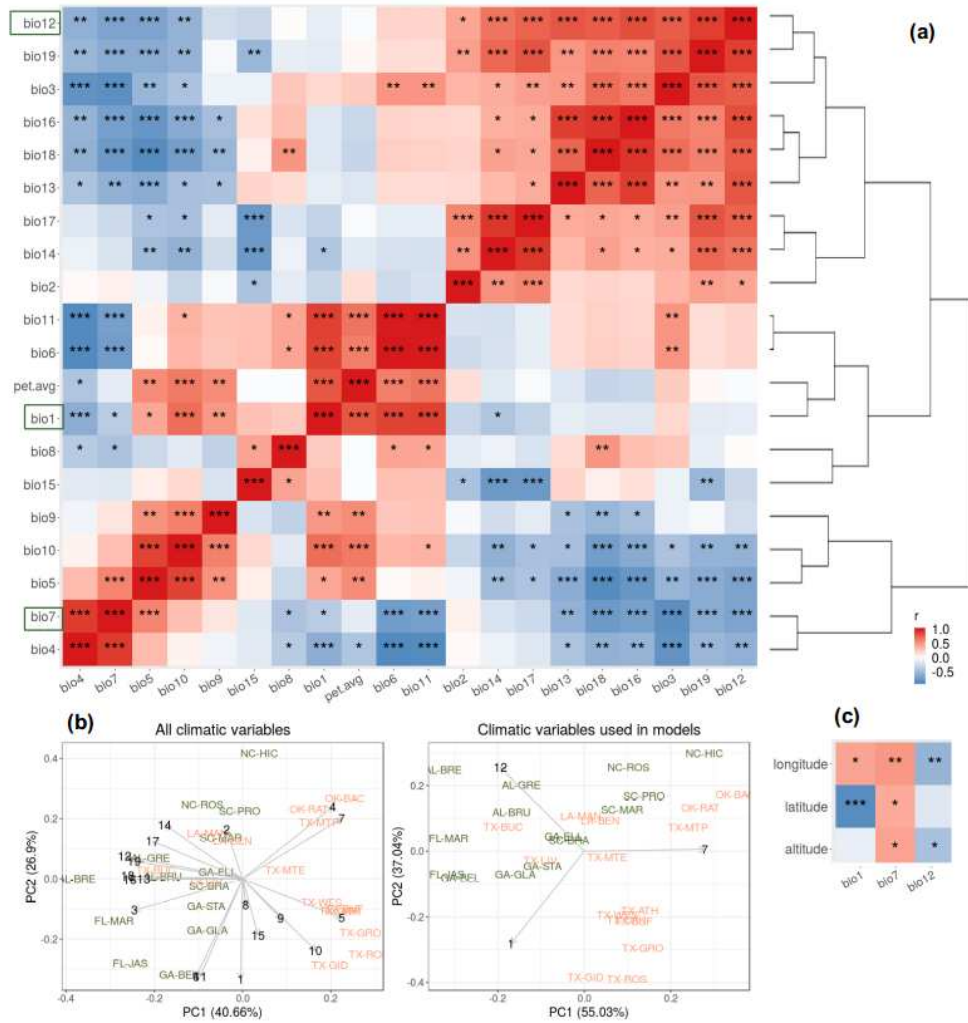


Figure S4: Bioclimatic variables across the geographical range of *Rumex hastatulus*. (A) Matrix showing the patterns of Spearman rank correlations among bioclimatic variables extracted from WorldClim (see Methods). The specifications of each one are as follows; Bio1: annual mean temperature. Bio2: mean diurnal range (mean of monthly (max temp - min temp)). Bio3: isothermality (bio2/bio7)×100. Bio4: temperature seasonality (standard deviation ×100). Bio5: max temperature of warmest month. Bio6: min temperature of coldest month. Bio7: temperature annual range (Bio5-Bio6). Bio8: mean temperature of wettest quarter. Bio9: mean temperature of driest quarter. Bio10: mean temperature of warmest quarter. Bio11: mean temperature of coldest quarter. Bio12: annual precipitation. Bio13: precipitation of wettest month. Bio14: precipitation of driest month. Bio15: precipitation seasonality (coefficient of variation). Bio16: precipitation of wettest quarter. Bio17: precipitation of driest quarter. Bio18: precipitation of warmest quarter. Bio19: precipitation of coldest quarter global potential evapotranspiration (mm). Pet.avg: global potential evapotranspiration (mm). Bio1, Bio7 and Bio12 (green squares) are the variables we used for further analyses. Populations of the North Carolina (green) and Texas (orange) chromosome races projected in the first two principal components from (B, left) all bioclimatic variables and (B, right) the three bioclimatic variables used in the models. The contribution of each principal component to the total variance is indicated in the x and y axis respectively. (C) Patterns of Spearman rank correlations between the bioclimatic variables used in the models and ecological parameters. In (A) and (C) color indicates correlation coefficient (blue for positive and red for negative). *: 0.01 < P < 0.05, **: 0.001 < P < 0.01, ***: P < 0.001

Table S1: Summary of univariate results for common glasshouse study of *Rumex hastatulus*. For each trait, “Data” included in the specific model, “Probability distribution and link function” used for the GLMM that best fitted the data (see Methods). Significance of each “Term” of the model was assessed with ANOVA type 2, which outputted the respective “Chisq” and “P”-value with the specified degrees of freedom (“DF”). The traits considered are height (cm), number of leaves, leaf size (cm), number of stems, flowering (binary: yes or no. Excluded at week 8, since all plants are flowering), proportion of flowering stems (including only flowering individuals), number of inflorescences, inflorescence size (mm, average of 3 inflorescences measured per plant), overall flowering (inflorescence number x size; as an integrative flowering measure) and biomass (reproductive, vegetative and total). See Methods for more information. In green, models used in Figure 1; in blue, models used in Figure 2; in orange, models used in Figure S3; highlighted in yellow, significant sex-by-population interactions; in bold, significant results ($P < 0.05$).

Height

Data	Probability distribution and link function	Term	DF	Chisq	P
Overall model	gaussian log link	sex	1	63.7469309	1.414738e-15
		chr.race	1	6.5934002	1.023575e-02
		timepoint	2	6521.559524	0.000000e+00
		sex:chr.race	1	1.2646441	2.607739e-01
		sex:timepoint	2	60.9566951	5.799918e-14
		chr.race:timepoint	2	26.9118293	1.432750e-06
		sex:chr.race:timepoint	2	0.6109309	7.367804e-01
Week 2 sex:chr.race	gaussian log link	sex	1	1.398911	0.236906072
		chr.race	1	8.883597	0.002877440
		sex:chr.race	1	10.681468	0.001082142
Week 2 sex in chrNC	gaussian log link	sex	1	5.758235	0.01641
Week 2 sex in chrTX	gaussian log link	sex	1	7.0128	0.008093
Week 2 sex:population	gaussian log link	sex	1	0.9044198	3.415994e-01
		population	28	120.4373685	1.962462e-13
		sex:population	28	56.8418676	1.014406e-03
Week 2 sex:population in chrNC	gaussian log link	sex	1	7.756766	0.00535116836
		population	13	42.041275	0.00006448248
		sex:population	13	31.387678	0.00295804878
Week 2 sex:population in chrTX	gaussian log link	sex	1	6.673605	0.00978510643
		population	14	51.331086	6
		sex:population	14	18.475703	0.00000364796
					8
					0.18596555656
					0
Week 4 and 8 sex:chr.race	gaussian identity link	sex	1	6.51473643	1.069842e-02
		chr.race	1	9.67085386	1.872143e-03
		timepoint	1	9534.27017079	0.000000e+00
		sex:chr.race	1	1.18668734	2.759988e-01
		sex:timepoint	1	75.28170565	4.081237e-18
		chr.race:timepoint	1	1.91703140	1.661843e-01
		sex:chr.race:timepoint	1	0.08981531	7.644121e-01
Week 4 sex:chr race	gaussian log link	sex	1	49.3117208	2.183540e-12
		chr.race	1	13.0041815	3.107962e-04
		sex:chr.race	1	0.7050846	4.010805e-01
Week 4 sex:population	gaussian identity link	sex	1	34.01873	5.458412e-09
		population	28	306.96430	1.014322e-48
		sex:population	28	25.84712	5.814477e-01
Week 8 sex:chr race	gaussian identity link	sex	1	43.5352902	4.163823e-11
		chr.race	1	3.4805425	6.209438e-02
		sex:chr.race	1	0.4136996	5.200977e-01
Week 8 sex:population	gaussian identity link	sex	1	42.84307	5.931183e-11
		population	28	124.38003	4.120350e-14
		sex:population	28	34.31265	1.907682e-01

Number of leaves

Data	Probability distribution and link function	Term	DF	Chisq	P
Overall model	poisson log link	sex	1	73.416745	1.049718e-17
		chr.race	1	7.270067	7.011317e-03
		timepoint	2	22192.361799	0.000000e+00
		sex:chr.race	1	2.974602	8.458094e-02
		sex:timepoint	2	75.198294	4.687032e-17
		chr.race:timepoint	2	731.792670	1.239484e-159
		sex:chr.race:timepoint	2	7.597839	2.239496e-02
Week 2 sex:chr.race	poisson log link	sex	1	1.7288694	1.885554e-01
		chr.race	1	119.2117480	9.412581e-28
		sex:chr.race	1	0.1774768	6.735506e-01
Week 2 sex:population	poisson log link	sex	1	1.2058196	0.2721616
		population	28	187.9635	1.268683e-25
		sex:population	28	10.5318687	0.9988671
Week 4 and 8 sex:chr.race	poisson log link	sex	1	89.02813	3.892376e-21
		chr.race	1	1.3142692	0.2516231
		timepoint	1	654.9329	1.889297e-144
		sex:chr.race	1	8.618317291	0.003327991
		sex:timepoint	1	30.176146505	0.0000000394532
		chr.race:timepoint	1	233.9688	8.125592e-53
		sex:chr.race:timepoint	1	1.240379	0.265398
Week 4 sex:chr.race	poisson log link	sex	1	12.6242005920	0.0003807847
		chr.race	1	84.43197	3.976658e-20
		sex:chr.race	1	0.7229596	0.3951748
Week 4 sex:population	poisson log link	sex	1	12.7083088276	0.0003640345
		population	28	670.6441	2.662750e-123
		sex:population	28	30.1928560	0.3540585
Week 8 sex:chr.race	poisson log link	sex	1	207.2982e	5.337548e-47
		chr.race	1	2.3678743	0.1238556
		sex:chr.race	1	6.954425910	0.008361212
Week 8 sex:chr.race in chrNC	poisson log link	sex	1	44.646	2.361e-11
Week 8 sex:chr.race in chrTX	poisson log link	sex	1	170.09	7.071646e-39
Week 8 sex:population	poisson log link	sex	1	205.6912	1.196685e-46
		population	28	313.1892	5.848013e-50
		sex:population	28	66.214854104	0.00006179246
Week 8 sex:population in chrNC	poisson log link	sex	1	44.89326	2.080726e-11
		population	13	68.1016174969	0.000000017914
		sex:population	13	38.9824332442	0.0002012385
Week 8 sex:population in chrTX	poisson log link	sex	1	168.6908	1.429244e-38
		population	14	240.0367	3.287855e-43
		sex:population	14	20.2902589	0.1212526

Leaf size

Data	Probability distribution and link function	Term	DF	Chisq	P
Overall model (weeks 4 and 8)	gaussian identity link	sex	1	21.179459869559	0.000004182227
		chr.race	1	0.3881972	0.5332486
		timepoint	1	18.89039239322	0.00001384482
		sex:chr.race	1	0.4726430	0.4917738
		sex:timepoint	1	16.53367156729	0.00004779377
		chr.race:timepoint	1	174.192938878060	8.983599e-20
		sex:chr.race:timepoint	1	0.02318004	0.87898982
Week 4 sex:chr.race	gamma log link	sex	1	1.9209890	0.1657477
		chr.race	1	14.8741446736	0.0001149275
		sex:chr.race	1	3.21651121	0.07289885
Week 4 sex:population	gamma log link	sex	1	1.8308243	0.1760302
		population	26	134.6411	6.699526e-16
		sex:population	26	31.5174769	0.2945879
Week 8 sex:chr.race	gamma log link	sex	1	30.15011275927874	0.00000003998639
		chr.race	1	4.61881143	0.03162314
		sex:chr.race	1	0.1594230	0.6896883
Week 8 sex:population	gamma log link	sex	1	30.27703310106227	0.00000003745346
		population	28	110.5428	9.281919e-12
		sex:population	28	25.8315415	0.5823039

Number of stems

Data	Probability distribution and link function	Term	DF	Chisq	P
Overall model (weeks 4 and 8)	poisson log link	sex	1	25.06500340	0.0000005542978
		chr.race	1	34.574535198	0.000000041023
		timepoint	1	1614.186 0.2770829	0.000
		sex:chr.race	1	47.44892	0.5986196
		sex:timepoint	1	138.8962 0.6449624	5.645595e-12
		chr.race:timepoint	1		4.640930e-32
		sex:chr.race:timepoint	1		0.4219195
Week 4 sex:chr.race	poisson log link	sex	1	70.47907	4.651755e-17
		chr.race	1	24.792432923	0.0000006384763
		sex:chr.race	1	658 0.2550384	0.6135495
Week 4 sex:population	poisson log link	sex	1	63.90558	1.305272e-15
		population	27	335.3494	6.108677e-55
		sex:population	27	29.3300887	0.3450777
Week 8 sex:chr.race	poisson log link	sex	1	1.169665	0.279470
		chr.race	1	34.902336126	0.0000000346660.
		sex:chr.race	1	0.2554038	6132955
Week 8 sex:population	poisson log link	sex	1	1.5619531	0.2113795
		population	28	123.0334	7.032193e-14
		sex:population	28	18.1040272	0.9234987

Flowering

Data	Probability distribution and link function	Term	DF	Chisq	P
Overall model (weeks 4 and 8)	binomial logit link	sex chr.race timepoint sex:chr.race sex:timepoint chr.race:timepoint sex:chr.race:timepoint	1 1 1 1 1 1 1	218875.1 24046.87 >1e+10 5140.366 >1e+10 >1e+10 >1e+10 >1e+10	1e<-16 1e<-16 1e<-16 1e<-16 1e<-16 1e<-16 1e<-16
Week 4 sex:chr.race	gaussian identity link	sex chr.race sex:chr.race	1 1 1	1.229424e+02 1.3760826 0.7082089	1.435582e-28 0.2407696 0.4000391
Week 4 sex:population	gaussian identity link	sex population sex:population	1 27 27	1.234959e+02 79.372986333675 33.1143852	1.086132e-28 0.000000469827 0.1933213

Proportion of flowering stems

Data	Probability distribution and link function	Term	DF	Chisq	P
Overall model (weeks 4 and 8)	binomial logit link	sex chr.race timepoint sex:chr.race sex:timepoint chr.race:timepoint sex:chr.race:timepoint	1 1 1 1 1 1 1	20.498521424223 0.02115992 8.319732e+01 5.98982707 0.05774818 3.34391227 2.1932536	0.000005967733 0.88434416 7.425829e-20 0.01438861 0.81009109 0.06745405 0.1386162
Week 4 sex:chr.race	gaussian log link	sex chr.race sex:chr.race	1 1 1	7.41244915556 2.1013490 7.455491328	0.00003008491 0.1471692 0.006324321
Week 4 sex in chrNC	gaussian log link	sex	1	0.1566383	0.6922706
Week 4 sex in chrTX	gaussian log link	sex	1	23.333985962420	0.000001361725
Week 4 sex:population	gaussian identity link	sex population sex:population	1 27 27	6.390558e+01 3.353494e+02 29.3300887	1.305272e-15 6.108677e-55 0.3450777
Week 4 sex:population chrNC	gaussian identity link	sex population sex:population	1 4 4	0.01251367 3.4241860 3.6814761	0.91093084 0.4894992 0.4508259
Week 4 sex:population chrTX	gaussian identity link	sex population sex:population	1 11 11	27.7445413269345 7.8970446 13.2382196	0.000000138438 0.7224957 0.2780411
Week 8 sex:chr.race	gaussian identity link	sex chr.race sex:chr.race	1 1 1	9.123334479 0.01248944 0.3001888	0.002523695 0.91101675 0.5837641
Week 8 sex:population	gaussian identity link	sex population sex:population	1 28 28	8.390999467 28.3408332 50.28895921	0.003770835 0.4465005 0.00600363

Number of inflorescences (of already flowering individuals)

Data	Probability distribution and link function	Term	DF	Chisq	P
Overall model (weeks 4 and 8)	poisson log link	sex	1	4.423842e+02	3.277623e-98
		chr.race	1	12.422035754	0.0004242975
		timepoint	1	1.4368.343	0.000
		sex:chr.race	1	1.1690967	0.2795869
		sex:timepoint	1	2.281527e+02	1.507389e-51
		chr.race:timepoint	1	5.814865e+01	2.430404e-14
		sex:chr.race:timepoint	1	0.5451541	0.4603045
Week 4 sex:chr.race	poisson log link	sex	1	18.072243757	0.00002126793
		chr.race	1	78.3.03020004	0.08172794 0.6077061
		sex:chr.race	1	0.2635288	
Week 4 sex:population	poisson log link	sex	1	19.176334995	0.00001191818
		population	26	43	0.002161479 0.154052
		sex:population	26	51.350271779 33.282751	
Week 8 sex:chr.race	poisson log link	sex	1	1497.218	0.000 0.0004767681
		chr.race	1	12.204404740	0.080238
		sex:chr.race	1	6.3.060074	
Week 8 sex:population	poisson log link	sex	1	1.474375e+03	1.432790e-322
		population	28	1.398100e+02	8.178347e-17
		sex:population	28	1.600115e+02	1.888116e-20

Inflorescence size

Data	Probability distribution and link function	Term	DF	Chisq	P
Overall model (weeks 4 and 8)	gaussian log link	sex	1	147.0124	7.798701e-34
		chr.race	1	13.6371083489	0.0002217587
		timepoint	1	4826.634	1e<-16
		sex:chr.race	1	8.30738953	0.00394841
		sex:timepoint	1	12.4552880108	0.0004168101
		chr.race:timepoint	1	33.30802265800	0.0000000786574
		sex:chr.race:timepoint	1	2180.0.1530384	7.0.6956485
Week 4 sex:chr.race	gaussian log link	sex	1	17.47593071722	0.00002909682
		chr.race	1	25.27507717795	0.0000004970905
		sex:chr.race	1	22.3.9829281	0.0459636
Week 4 sex in chrNC	gaussian log link	sex	1	0.2454831	0.6202737
Week 4 sex in chrTX	gaussian log link	sex	1	18.45961013566	0.00001735435
Week 4 sex:population	gamma log link	sex	1	13.702738148	0.000214142
		population	26	78.47495628019	0.0000003594530.0
		sex:population	26	94 45.61025616	1008064
Week 4 sex:population chrNC	gamma log link	sex	1	0.2017679	0.6532976
		population	1	29.244383789	0.003623662
		sex:population	1	34.0904502028	0.0006527382
Week 4 sex:population chrTX	gamma log link	sex	1	0.2017679	0.6532976
		chr.race	1	29.244383789	0.003623662
		sex:chr.race	1	34.0904502028	0.0006527382

Week 8 sex:chr.race	gamma log link			3.246676e+02 13.0536850885 32.00790194916 922	1.393839e-72 0.0003026883 0.000000015354
Week 8 sex chrNC	gamma log link	sex	1	4.203878e+01	8.948107e-11
Week 8 sex chrTX	gamma log link	sex	1	2.915468e+02	2.288311e-65
Week 8 sex:population	gamma log link	sex population sex:population	1 28 28	308.2576 216.2465 48.973760740	5.233551e-69 5.550972e-31 0.008399235
Week 8 sex:population chrNC	gamma log link	sex population sex:population	1 13 13	44.57819 43.166615154 6.0426625	2.443994e-11 0.00004214201 0.9445865
Week 8 sex:population chrTX	gamma log link	sex population sex:population	1 14 14	301.6316 121.5143 27.7636863	1.453149e-67 3.177501e-19 0.0152908

Estimated total flower number

Data	Probability distribution and link function	Term	DF	Chisq	P
Overall model (weeks 4 and 8)	gaussian log link	sex chr.race timepoint sex:chr.race sex:timepoint chr.race:timepoint sex:chr.race:timepoint	1 1 1 1 1 1 1	0.00735907 0.0002322504 133.28 0.0005282701 154.36 125.81 1.6882950	0.93163731 0.9878408974 1e<-16 0.9816629335 1e<-16 1e<-16 0.1938259
Week 4 sex:chr.race	gamma log link	sex chr.race sex:chr.race	1 1 1	23.147304667792 11.0180742999 0.1352528	0.0000015005 34 0.0009022776 0.7130468
Week 4 sex:population	gamma log link	sex population sex:population	1 26 26	84396.1 2985257 2247414	1e<-16 1e<-16 1e<-16
Week 8 sex:chr.race	gaussian log link	sex chr.race sex:chr.race	1 1 1	88.54569 1.2545504 12.2610210007	4.967414e-21 0.2626852 0.0004625184
Week 8 sex chrNC	gaussian log link	sex	1	54.109	1.896e-13
Week 8 sex chrTX	gaussian log link	sex	1	12.081	0.0005094
Week 8 sex:population	gaussian log link	sex population sex:population	1 28 28	86.32863 136.8871 96.565107947120438	1.523864e-20 2.692196e-16 0.0000000018 12
Week 8 sex:population chrNC	gaussian log link	sex population sex:population	1 13 13	47.57167 54.5243803292198 34.8779429371	5.302924e-12 0.0000004896 37 0.0008840001
Week 8 sex:population	gaussian log link	sex population	1 14	12.6518515139 103.6572	0.0003751939 9.407107e-16

chrTX		sex:population	14	25.6856266	0.0283721
-------	--	----------------	----	------------	------------------

Biomass (reprod figure + text; veg figure)

Data	Probability distribution and link function	Term	DF	Chisq	P
Reproductive biomass sex:chr.race	gaussian log link	sex	1	1.6597645	0.1976351
		chr.race	1	2.96716602	0.08497059
		sex:chr.race	1	4.59407313	0.03208269
Reproductive biomass sex:chr.race chrNC	gaussian log link	sex	1	4.8975	0.0269
Reproductive biomass sex:chr.race chrTX	gaussian log link	sex	1	0.0358	0.8499
Reproductive biomass sex:population	gaussian log link	sex	1	1.3818597	0.2397846
		population	28	59.1968599805	0.0005152761
		sex:population	28	37.8861887	0.1005714
Reproductive biomass sex:population chrNC	gaussian log link	sex	1	5.0284297	0.0249345
		population	13	9.0509717	0.7690831
		sex:population	13	12.9372494	0.4526703
Reproductive biomass sex:population chrTX	gaussian log link	sex	1	0.1694783	0.6805759
		population	14	44.424483782	0.00005055958
		sex:population	14	4 25.06949530	0.03388748
Vegetative biomass sex:chr.race	gamma log link	sex	1	174.3556	8.278210e-40
		chr.race	1	1.3031933	0.2536308
		sex:chr.race	1	0.3122547	0.5762999
Vegetative biomass sex:population	gamma log link	sex	1	190.1270	2.982722e-43
		population	28	127.3601	1.255878e-14
		sex:population	28	37.2637506	0.1131571
Total biomass sex:chr.race	gamma log link	sex	1	163.5808	1.867832e-37
		chr.race	1	0.9036169	0.3418137
		sex:chr.race	1	0.05196842	0.81967281
Total biomass sex: population	gamma log link	sex	1	178.6623	9.494910e-41
		population	28	122.2484	9.596837e-14
		sex:population	28	37.2204009	0.1140791

Trait	Altitude	Latitude	Longitude
No. leaves (week 8)		***	
No. stems (week 4)	**		
No. stems (week 8)		*	
No. inflorescences (week 8)	*		
Inflorescence size (week 4)		**	**
Inflorescence size (week 8)			**
Total No. flowers (week 4)		*	*
Total No. flowers (week 8)	**	**	**

Table S2: Variation of sexual dimorphism along ecological gradients for populations of *Rumex hastatulus*. Results of multiple regression of percent sexual dimorphism (%SD) of different reproductive and vegetative traits at weeks 4 and 8 among populations on altitude, latitude and longitude. Only significant contributions are displayed. Specific models are: No. leaves (week 8) = 160.255 - 4.496 Latitude ($R^2 = 0.35$, $P = 0.0004$); No. stems (week 4) = -12.146 - 0.245 Altitude ($R^2 = 0.22$, $P = 0.007$); No. stems (week 8) = 117.864 - 3.614 Latitude ($R^2 = 0.16$, $P = 0.0374$); No. inflorescences (week 8) = 48.208 + 0.2535 Altitude ($R^2 = 0.14$, $P = 0.027$); Inflorescence size (week 4) = -894.198 + 28.31 Latitude ($R^2 = 0.29$, $P = 0.0023$); Inflorescence size (week 4) = 441.094 - 4.806 Longitude ($R^2 = 0.23$, $P = 0.0065$); Inflorescence size (week 8) = 60.5 - 0.996 Longitude ($R^2 = 0.4261$, $P = 7.43e-05$); Total flower number (week 4) = 602.548 - 6.748 Longitude ($R^2 = 0.17$, $P = 0.018$); Total flower number (week 4) = -1121.55 + 35.03 Latitude ($R^2 = 0.16$, $P = 0.022$); Total flower number (week 8) = 580.979 + 0.338 Altitude - 10.03 Latitude - 3.044 Longitude ($R^2 = 0.33$, $P = 0.004$). Color indicates the direction of the correlation (red for positive and blue for negative). *: $0.01 < P < 0.05$, **: $0.001 < P < 0.01$, ***: $P < 0.001$

The Molecular Basis of Sexual Dimorphism

	Temperature annual mean		Temperature annual range		Precipitation annual	
	Coeff	P	Coeff	P	Coeff	P
Height (week 4)	-0.6145	0.00428				
	0.1312	0.00611				
	0.21363	0.000329				
No. stems (week 4)	-1.11871	0.049	-1.27514	0.000427	-0.12069	0.002103
	0.03362	0.00118	0.00305	0.640	-0.002054	0.00769
	0.04132	0.0039	0.009822	0.261	-0.002409	0.0234
Inflorescence size (week 4)	-3.476	0.00487				
	0.3259	0.00321				
	0.4963	0.00122				
Overall flowering (week 4)	-8.3239	0.000803	-4.0849	0.003361	-0.3566	0.015412
	1.718	0.0124	-0.282	0.496	-0.08364	0.1023
	2.738	0.0199	-0.2174	0.758	-0.10388	0.2379
No. leaves (week 8)	0.5601	0.001084				
	-0.17956	0.047942				
	-0.31876	0.000166				
No. stems (week 8)	0.5468	0.01124				
	0.033839	0.000694				
	0.01145	0.329				
Inflorescence size (week 8)	-0.45049	0.004442	-0.38975	7.19e-05		
	0.07978	0.00603	-0.01445	0.4145		
	0.12474	0.00262	0.01830	0.476		

Table S3: Sexual dimorphism and sex-specific trait mean variation along climatic gradients for populations of *Rumex hastatulus*. For each trait, grey (first) line shows the correlation coefficients and P-values of the significant results of the multiple regression analyses (Table S2): percent sexual dimorphism (%SD) across populations regressed on mean annual temperature (bio1, see Figure S4 for more details on climatic variables), annual temperature range (bio7) and total annual precipitation (bio12). See Methods for more details and Figure 5 for full models. Green (second) and orange (third) lines show coefficients and P-values of regression of respectively female and male trait means on bioclimatic variables.

CHAPTER 2

Sex-specific estimation of *cis* and *trans* regulation of gene expression in heads and gonads of

Drosophila melanogaster

Supplementary Material

Gemma Puixeu, Ariana Macon and Beatriz Vicoso

Dataset S1: Overall count data in parentals and hybrids estimated using Kallisto. Each column contains count gene expression for a particular sample. Each sample is labeled as follows: 1 2 3. 1 indicates the maternal (F) and paternal (M) lines of the hybrid cross. 2 is the tissue and sex: fh (female heads), fo (female ovaries), mh (male heads) and mt (male testes). 3 is the replicate: R1 or R2. Expression data for samples 392F x 757M mh R2, 392M x 392F mt R2 and 808M x 208F mt R2 are removed due to low quality, and not used in any analysis. The last two columns (chr and start) are the chromosome and position of the gene.

The dataset corresponds to Dataset S1 in this link: <https://doi.org/10.15479/AT:ISTA:12933>

Dataset S2: Overall TPM data in parentals and hybrids estimated using Kallisto. Each column contains TPM gene expression for a particular sample. Each sample is labeled as follows: 1 2 3. 1 indicates the maternal (F) and paternal (M) lines of the hybrid cross. 2 is the tissue and sex: fh (female heads), fo (female ovaries), mh (male heads) and mt (male testes). 3 is the replicate: R1 or R2. Expression data for samples 392F x 757M mh R2, 392M x 392F mt R2 and 808M x 208F mt R2 are removed due to low quality, and not used in any analysis. The last two columns (chr and start) are the chromosome and position of the gene. This dataset is used for the inheritance patterns classification.

The dataset corresponds to Dataset S2 in this link: <https://doi.org/10.15479/AT:ISTA:12933>

Dataset S3: Overall parental and allele-specific hybrid count expression estimated using ASETigar. Each column contains count gene expression for a particular sample.

Parental overall expression data has been estimated using the ASETigar pipeline (see Methods) so that the estimates are comparable to the allelic expression in the hybrids. Expression for each specific pairwise comparison is labeled as 1.2_34.5. 1 and 2 are the two lines being compared, 3 is the tissue and sex: fh (female heads), fo (female ovaries), mh (male heads) and mt (male testes), 4 is the replicate: R1 or R2. 5 is the line (corresponding with 1 or 2) for which expression is estimated. Hybrid allelic expression estimates are labeled as 1Fx2M_3.4.5. 1 and 2 indicate the maternal and paternal lines of the hybrid cross, respectively. 3 is the tissue and sex, 4 the replicate and 5 the line (corresponding with 1 or 2) for which allele-specific expression is estimated. Expression data for samples 392F x 392M mt R2, 208Fx808M_mt_R2 and 392Fx757M_mh_R2 are removed due to low quality and not used in the analysis. The last two columns (chr and start) are the chromosome and position of the gene. This dataset is used to estimate *cis* regulatory effects via the two described methods: only hybrid allele-specific expression was used for CR, PO and MG estimates following Takada et al. (2017)'s pipeline; parental and hybrid allelic expression was used for the *cis* vs *trans* estimates of regulatory variation following McManus et al. (2010)'s approach.

The dataset corresponds to Dataset S3 in this link: <https://doi.org/10.15479/AT:ISTA:12933>

Dataset S4: Overall parental and allele-specific hybrid FPKM expression estimated using ASETigar. Each column contains FPKM gene expression for a particular sample. Parental overall expression data has been estimated using the ASETigar pipeline (see Methods) so that the estimates are comparable to the allelic expression in the hybrids. Expression for each specific pairwise comparison is labeled as 1.2_34.5. 1 and 2 are the two lines being compared, 3 is the tissue and sex: fh (female heads), fo (female ovaries), mh (male heads) and mt (male testes), 4 is the replicate: R1 or R2. 5 is the line (corresponding with 1 or 2) for which expression is estimated. Hybrid allele-specific expression estimates are labeled as 1Fx2M_3.4.5. 1 and 2 indicate the maternal and paternal lines of the hybrid cross, respectively. 3 is the tissue and sex, 4 the replicate and 5 the line (corresponding with 1 or 2) for which allele-specific expression is estimated. Expression data for samples 392F x 392M mt R2, 208Fx808M_mt_R2 and 392Fx757M_mh_R2 are removed due to low quality and not used in the analysis. The last two columns (chr and start) are the chromosome and position of the gene.

The dataset corresponds to Dataset S4 in this link: <https://doi.org/10.15479/AT:ISTA:12933>

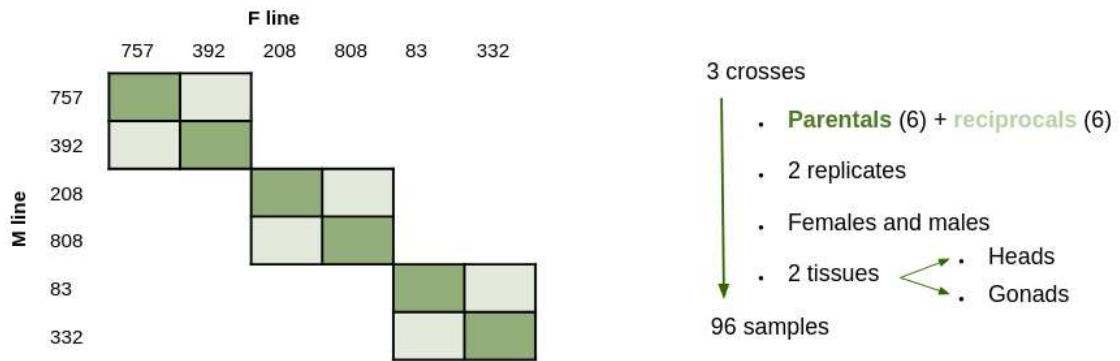


Figure S1: Outline of the experimental design. We randomly selected 6 DGRP lines without *Wolbachia* infection and main inversions and matched them into three pairs: DGRP-757 x DGRP-392, DGRP-208 x DGRP-808 and DGRP-83 x DGRP-332. For each pair, we performed within- and both reciprocal between-line crosses and obtained sex-specific head and gonad gene expression for two replicates of each sample.

The Molecular Basis of Sexual Dimorphism

Female heads							Male heads						
	757x392		208x808		83x332			757x392		208x808		83x332	
N genes	5897	1096	5854	1047	5812	1117	N genes	5767	1092	6135	1118	6291	1166
CR	610	87	460	106	447	68	CR	484	75	476	78	487	69
PO	15	4	10	4	4	0	PO	23	576	0	641	2	602
MG	16	1	7	0	3	0	MG	139	55	106	68	148	61
Female ovaries							Male testes						
	757x392		208x808		83x332			757x392		208x808		83x332	
N genes	5124	1049	4783	985	4621	992	N genes	6724	1182	6576	1138	6898	1217
CR	400	74	392	73	580	85	CR	1110	74	918	69	1076	60
PO	0	6	0	1	10	2	PO	30	667	25	612	7	713
MG	27	1	84	4	40	7	MG	26	65	295	47	81	44

Autosomes
 X chromosome

Table S1: Number of genes showing significant *cis*-regulatory (CR), parent-of-origin (PO) and maternal genotype (MG) effects in each tissue, sex and cross for both autosomal (grey) and X-linked (white) genes.

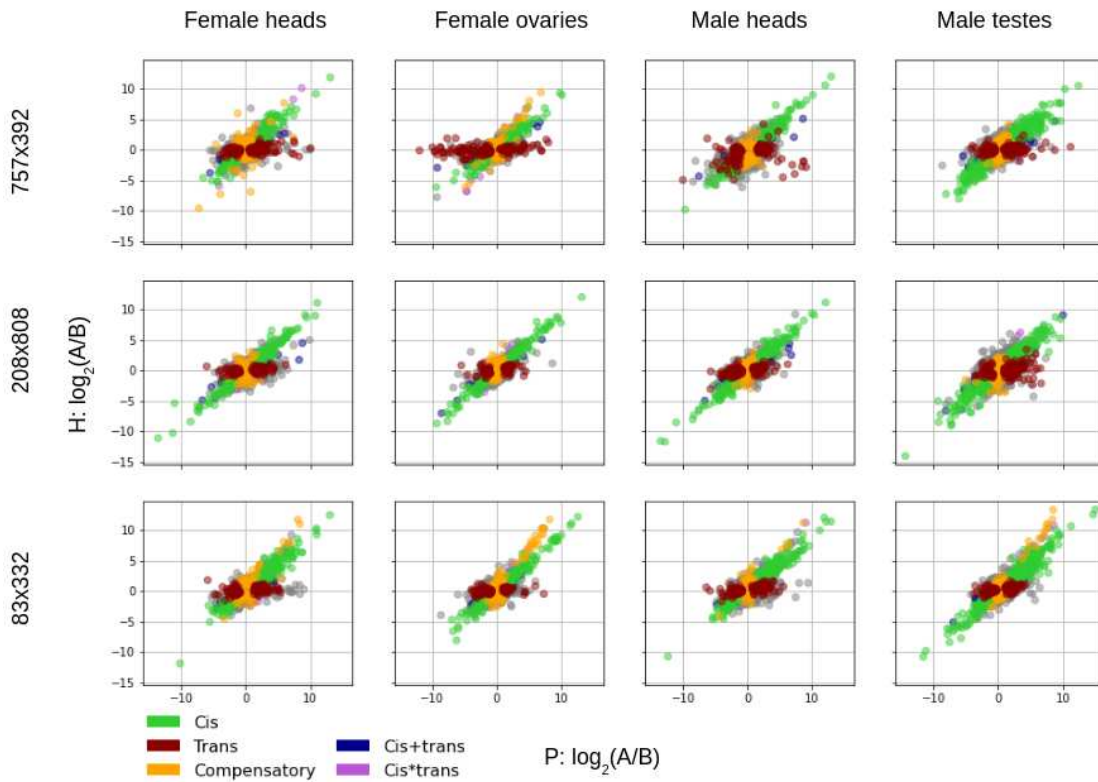
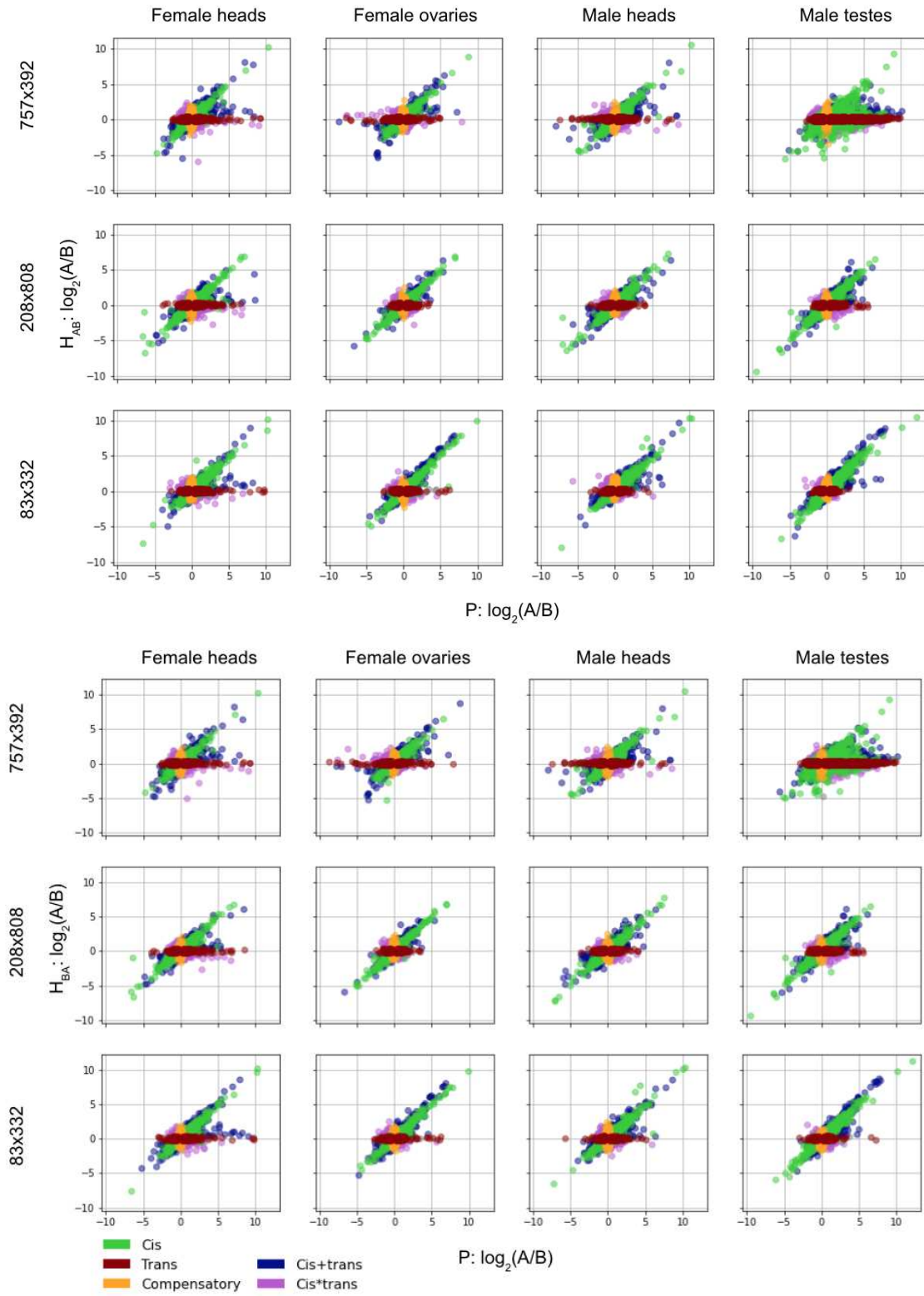


Figure S2: Inferred *cis* and *trans* regulatory mechanisms. Scatter plots of the relative averaged allele-specific expression levels in parental (P) vs hybrid (H, averaged across reciprocals) datasets in each sex, tissue and cross. Each dot is a gene and is color-coded according to the inferred mechanism of expression regulation: *cis* (green), *trans* (red), compensatory (yellow), *cis+trans* (blue) and *cis*trans* (purple).

The Molecular Basis of Sexual Dimorphism



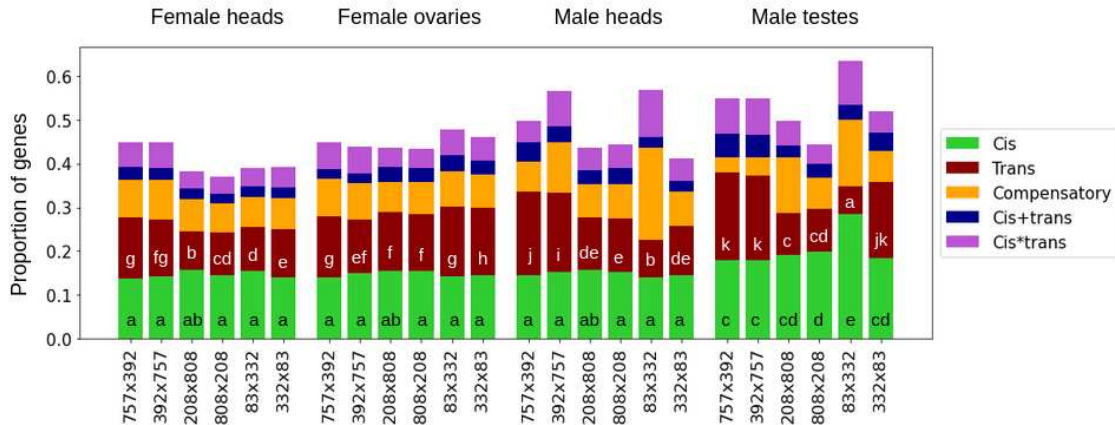


Figure S3: Inferred *cis* and *trans* regulatory mechanisms in both reciprocal crosses separately. A) Scatter plots of the relative allele-specific expression levels in parentals (P) vs hybrids (H) in each sex, tissue and reciprocal (AxB and BxA in first and second panels, respectively) for each cross. Each dot is a gene and is color-coded according to the inferred mechanism of expression regulation: *cis* (green), *trans* (red), compensatory (yellow), *cis+trans* (blue) and *cis*trans* (purple). B) Proportion of genes with each inferred regulatory mechanism in each sex, tissue and reciprocal cross. Significance groups revealing differences in the proportion of genes classified as having *cis* (black) and *trans* (white) regulation across all samples (two-proportions z-test at p-value < 0.05) are denoted by different letters (a–e and a–k).

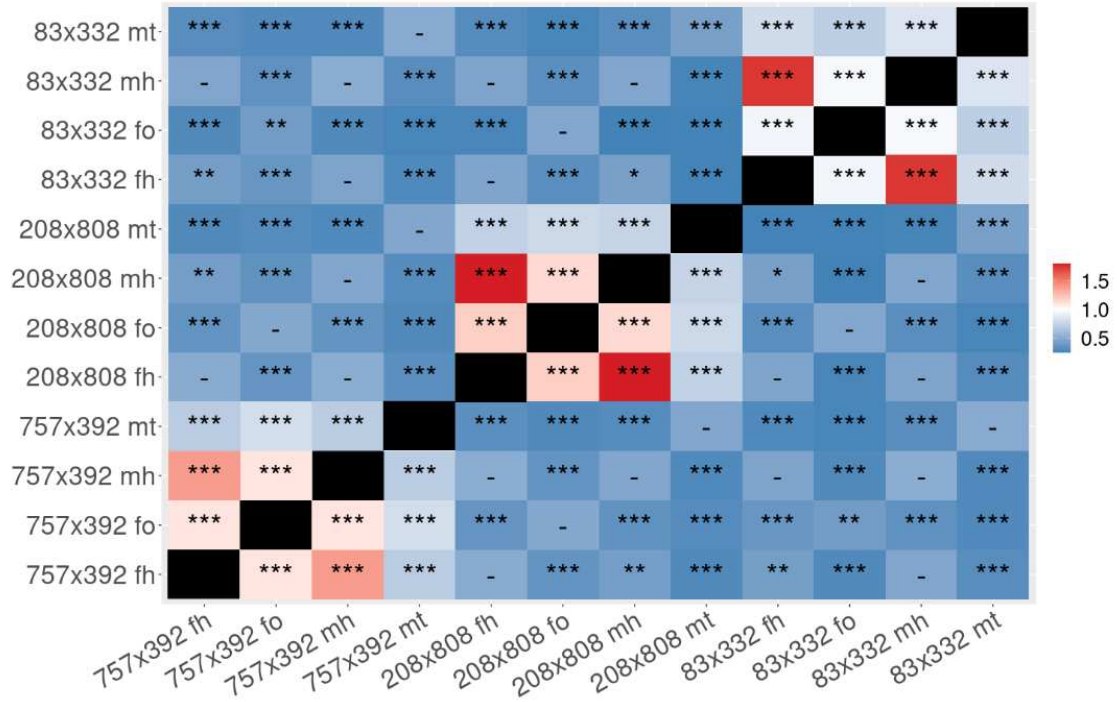


Figure S4: Overlap in *cis*-regulatory effects between samples. The color indicates the ratio between observed and expected overlap in CR effects between pairs of samples, red (blue) indicating larger (smaller) overlap than expected. fh: female heads, fo: female ovaries, mh: male heads, mt: male testes. The stars indicate significance: *** : p-value > 0.001; ** : p-value < 0.01; * : p-value < 0.05; non-significant (-): otherwise (Chi-squared tests).

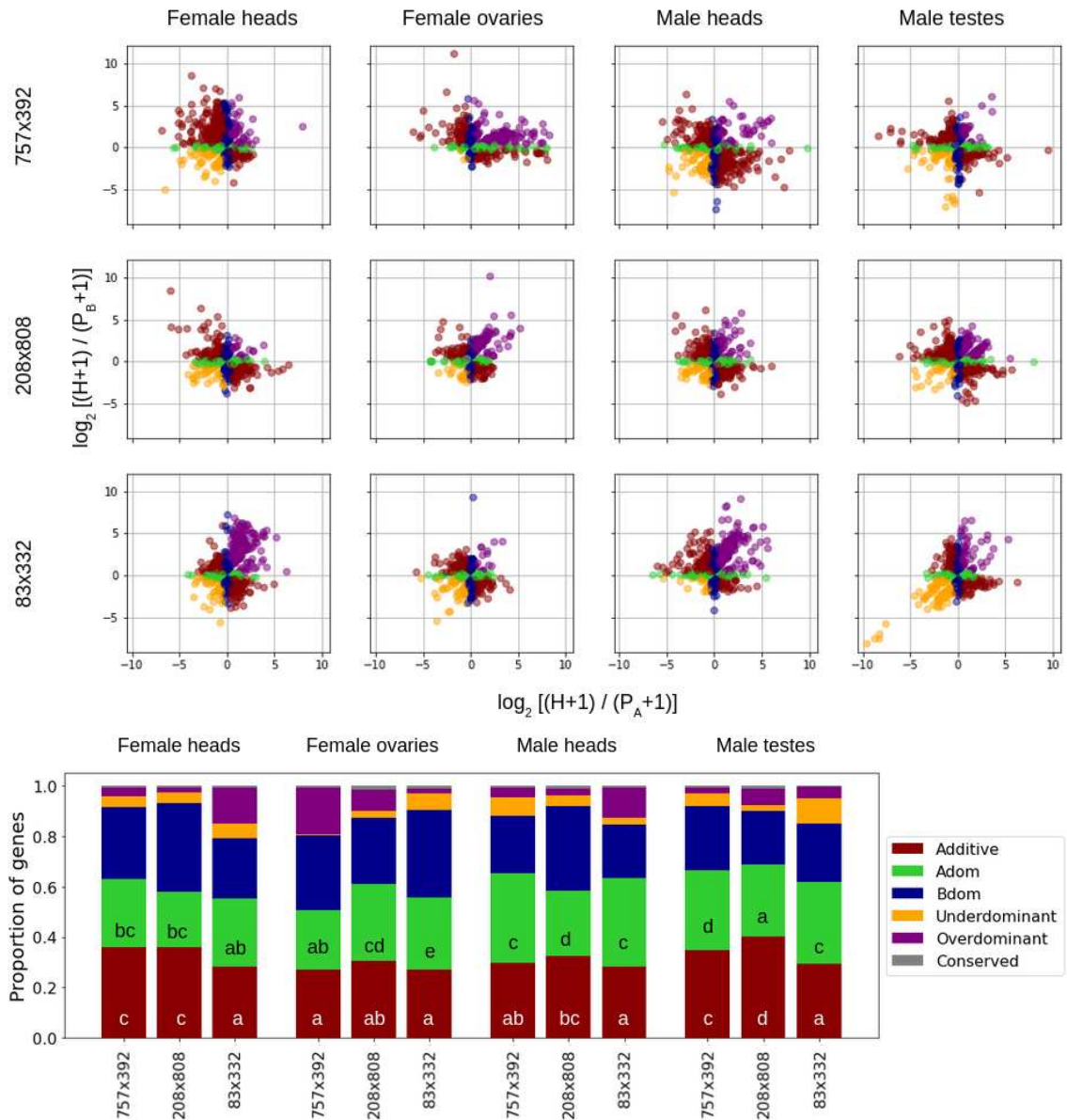
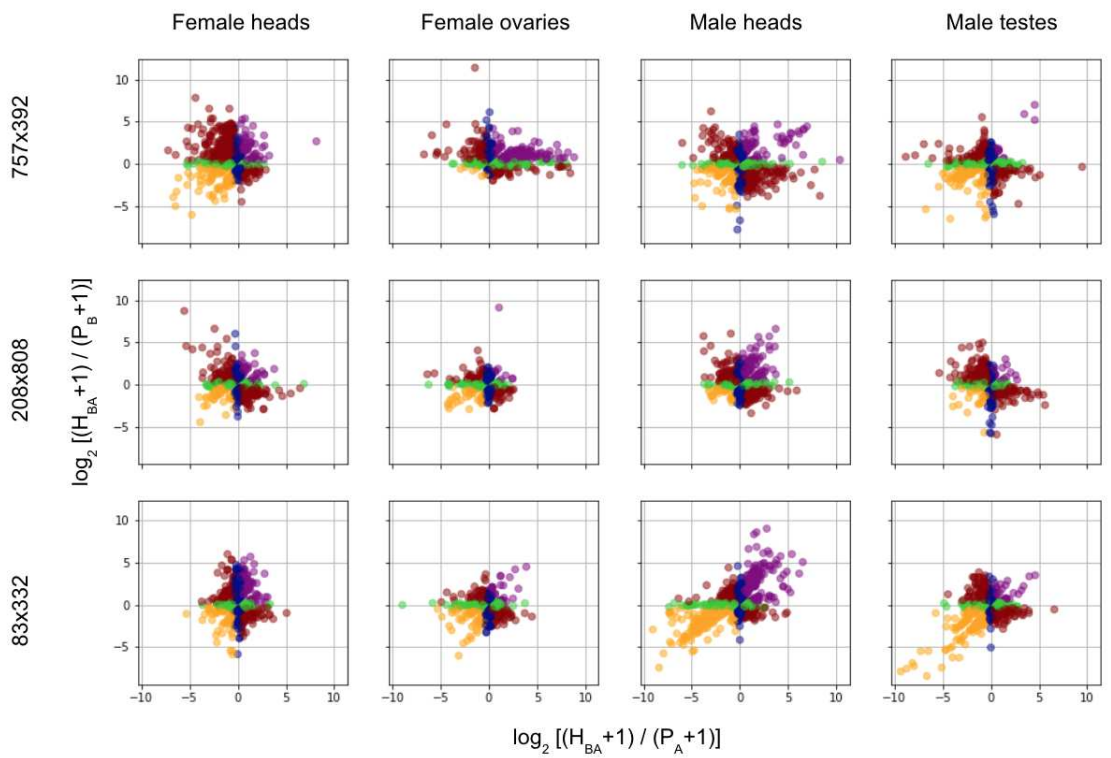
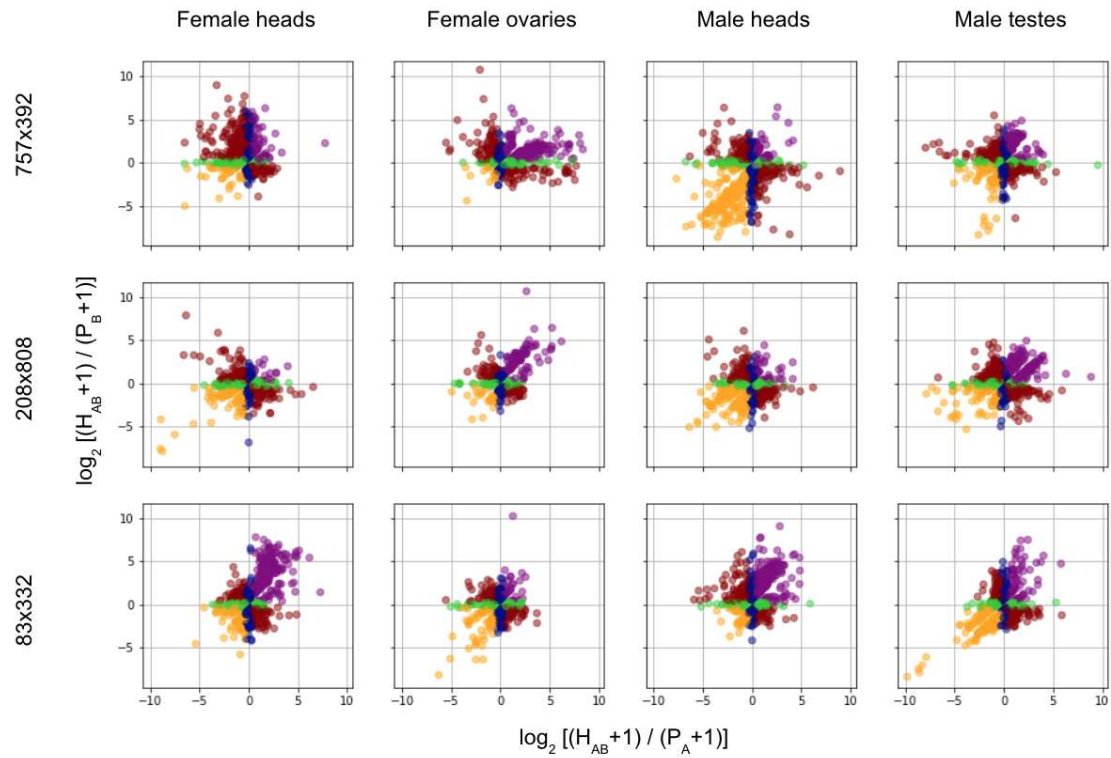


Figure S5: Inheritance patterns inferred using fold-differences. A) Scatter plots of the relative overall expression between hybrids (H) and parentals (P) in each sex, tissue and cross, averaged across reciprocals. Each dot is a gene and is color-coded according to the inheritance pattern, inferred using hierarchical classification based on fold expression differences between P and H. B) Proportion of genes with each inferred inheritance mechanism per sample. Significance groups revealing differences in the proportion of genes displaying additive and dominant –in both directions combined (in white and black respectively)– across samples (two-proportions z-test at p-value < 0.05) are denoted by different letters (a–i and a–e).

The Molecular Basis of Sexual Dimorphism



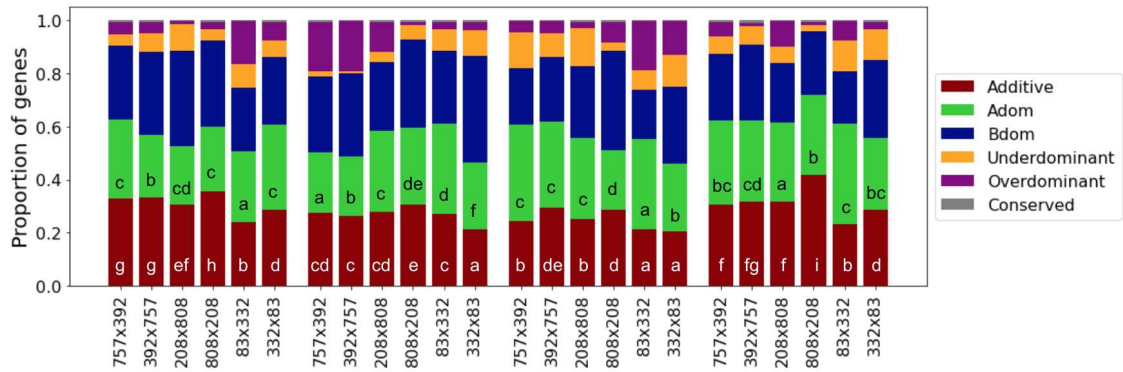


Figure S6: Inheritance patterns inferred using fold-differences in reciprocal crosses separately. A) Scatter plots of the relative overall expression between hybrids (H) and parentals (P) in each sex, tissue and both reciprocals (AxB and BxA in first and second panels, respectively) for each cross. Each dot is a gene and is color-coded according to the inheritance pattern, inferred using hierarchical classification based on fold expression differences between P and H. B) Proportion of genes with each inferred inheritance mechanism per sample. Significance groups revealing differences in the proportion of genes displaying additive and dominant –in both directions combined– (in white and black respectively) across samples (two-proportions z-test at p-value < 0.05) are denoted by different letters (a-i and a-e).

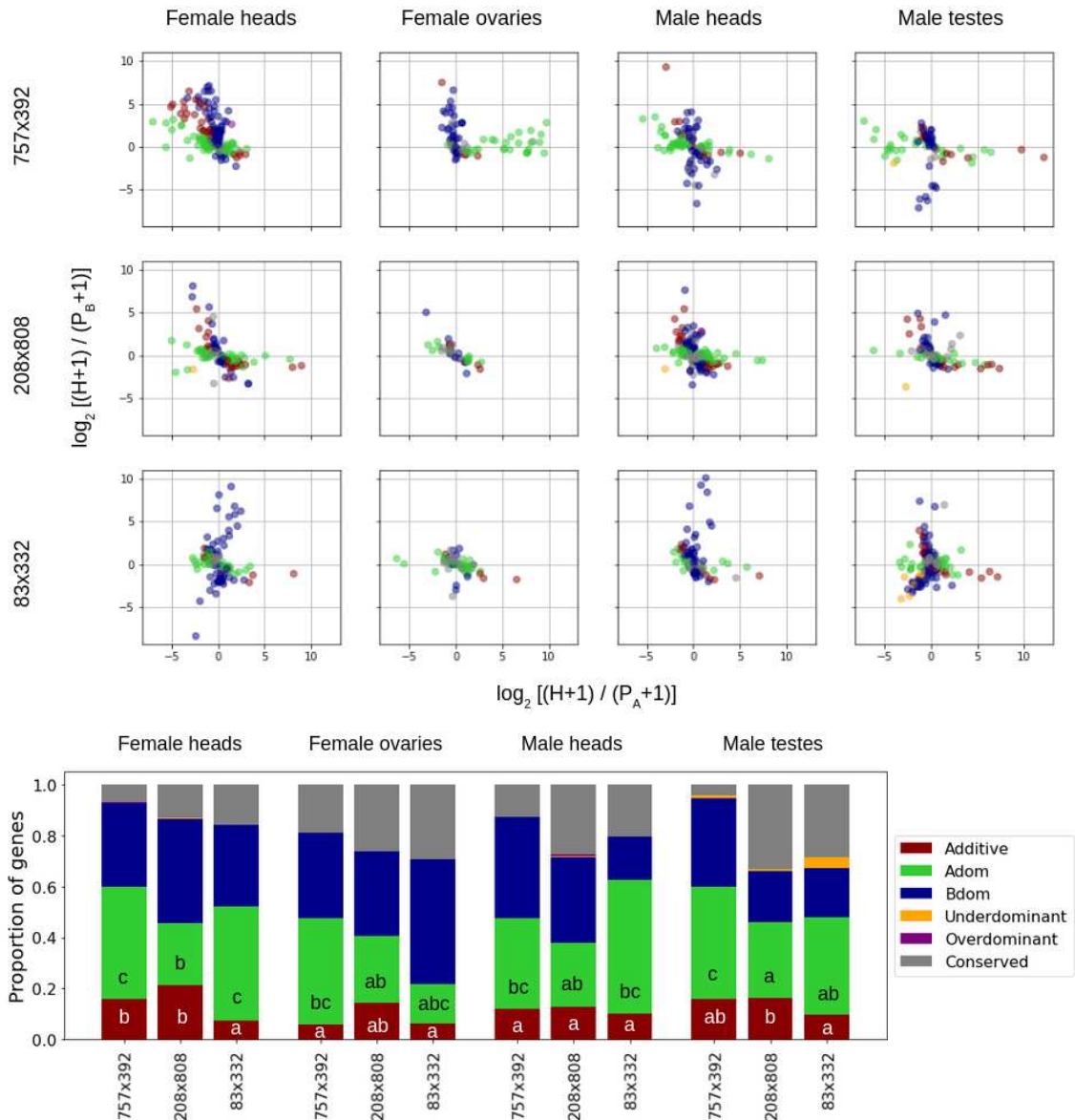


Figure S7: Inheritance patterns inferred using statistical tests. Instead of fold differences, the classification into the various inheritance patterns was done via statistical testing for differences in expression between parentals and hybrid crosses (pooling the reciprocals together) using DEseq2 at $FDR < 0.05$. A) Scatter plots of the relative overall expression between hybrids (H) and parentals (P) in each sex, tissue and cross. Each dot is a gene and is color-coded according to the inferred inheritance pattern, according to the legend in B). B) Proportion of genes with each inferred inheritance mechanism per sample. Significance groups revealing differences in the proportion of genes displaying additive and dominant –in both directions combined– (in white and black respectively) across samples (two-proportions z-test at $p\text{-value} < 0.05$) are denoted by different letters (a–b and a–c).

References

- McManus, C. J., Coolon, J. D., Duff, M. O., Eipper-Mains, J., Graveley, B. R., & Wittkopp, P. J. (2010, June). Regulatory divergence in *Drosophila* revealed by mRNA-seq. *Genome Research*, *20*(6), 816–825. doi: 10.1101/gr.102491.109
- Takada, Y., Miyagi, R., Takahashi, A., Endo, T., & Osada, N. (2017, July). A Generalized Linear Model for Decomposing Cis-regulatory, Parent-of-Origin, and Maternal Effects on Allele-Specific Gene Expression. *G3 (Bethesda, Md.)*, *7*(7), 2227–2234. doi: 10.1534/g3.117.042895

CHAPTER 3

Characterizing the regulatory architecture of sex differences in expression via sex bias eQTL analysis in heads and gonads of *Drosophila melanogaster*

Supplementary Material

Gemma Puixeu, Christine Syrowatka, Ariana Macon, Luísa Scolari,
Nick Barton and Beatriz Vicoso

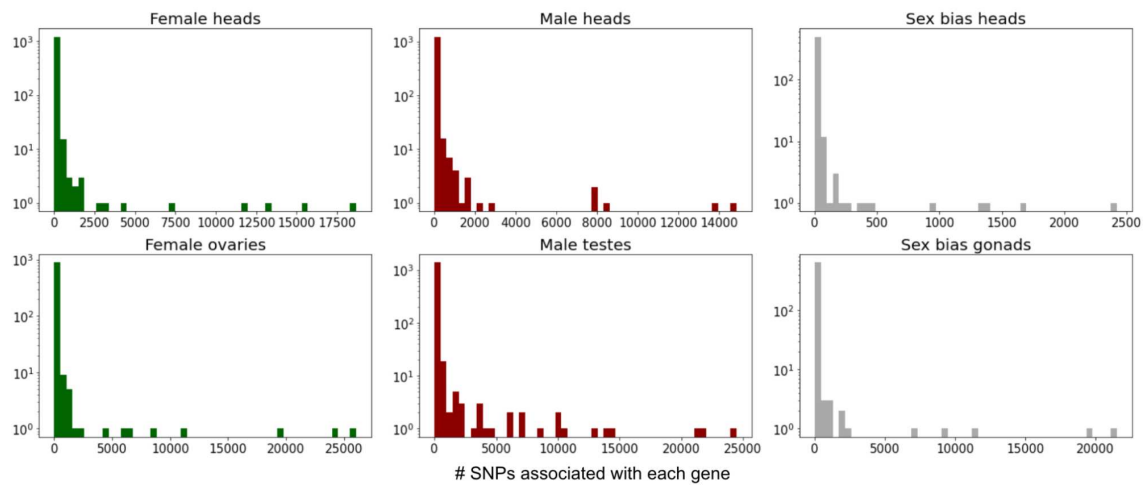


Figure S1: Distribution of the number of SNPs associated with each gene in each analysis.

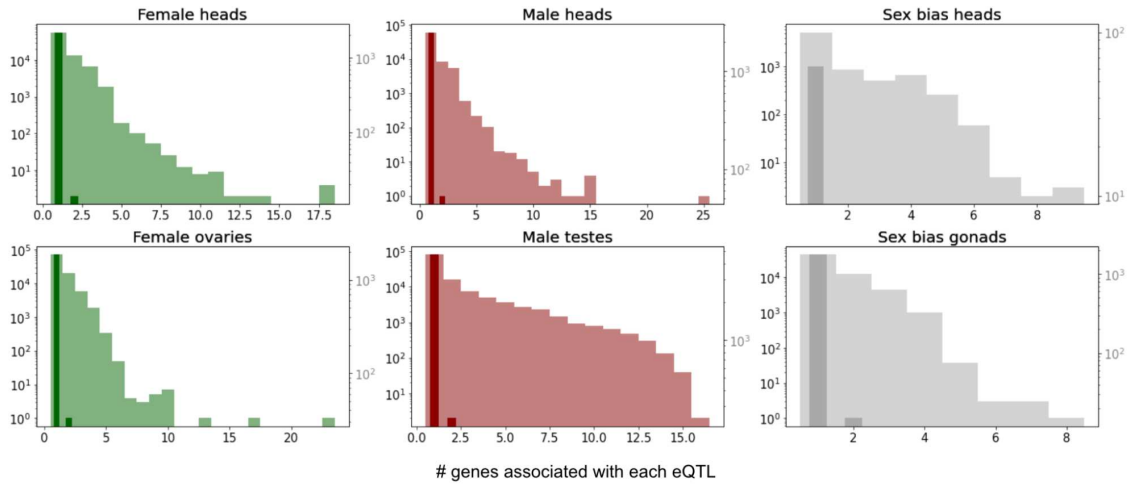


Figure S2: Distribution of the number of genes associated with each eQTL in each analysis. Light distributions (with black y axis to the left) are for *trans* interactions and dark distributions (with grey y axis to the right) are for *cis* interactions.

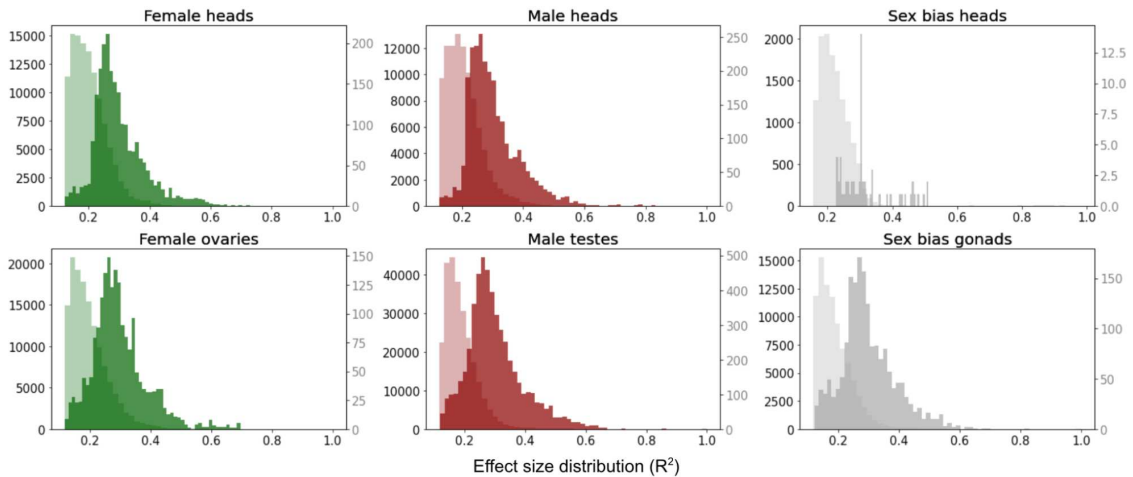


Figure S3: Distribution of effect sizes for each analysis, in *cis* (dark) and *trans* (light distributions). The effect sizes correspond to the coefficients of determination (variance explained) of each particular SNP-gene association.

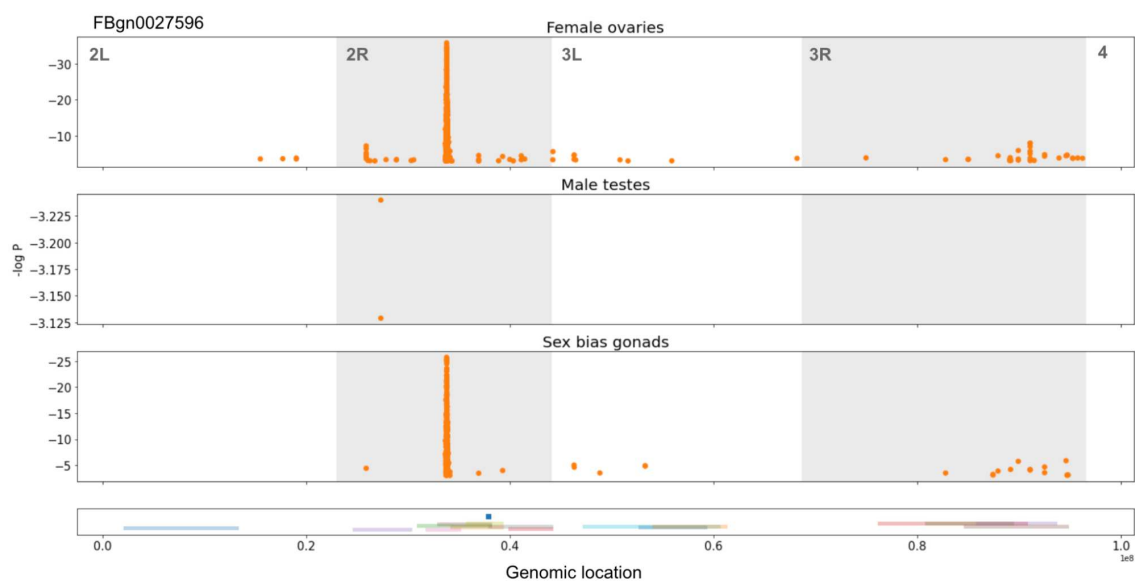


Figure S4: Manhattan plot of an example where eQTL associations generate variation in sex bias by affecting expression in females (but not males). P-values of the association of each SNP genome-wide with expression of gene FBgn0027596 in female ovaries, male testes and sex bias gonads. Only significant hits ($FDR < 0.05$) are plotted. *Cis* and *trans* interactions are plotted in orange and blue. The horizontal lines in the lowest subplot display the location of the 16 segregating inversions in the genome, and the blue square the location of the gene.

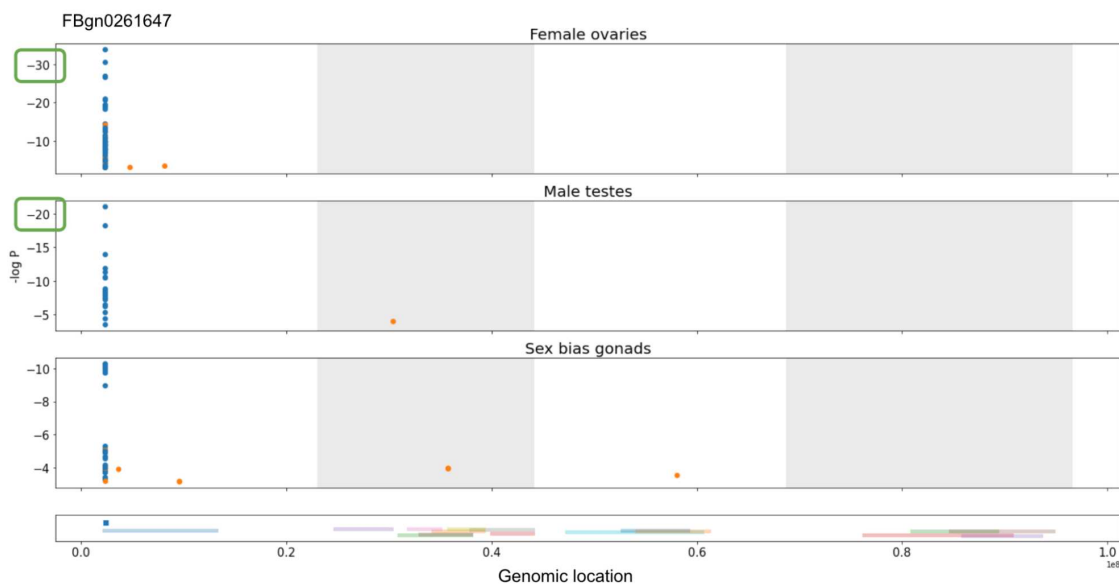


Figure S5: Manhattan plot of an example of sex-biased eQTL associations (affecting expression in the same direction but at different magnitude in the two sexes) generating variation for sex bias. P-values of the association of each SNP genome-wide with expression of gene FBgn0261647 in female ovaries, male testes and sex bias gonads. Only significant hits ($FDR < 0.05$) are plotted. *Cis* and *trans* interactions are plotted in orange and blue. The horizontal lines in the lowest subplot display the location of the 16 segregating inversions in the genome, and the blue square the location of the gene.

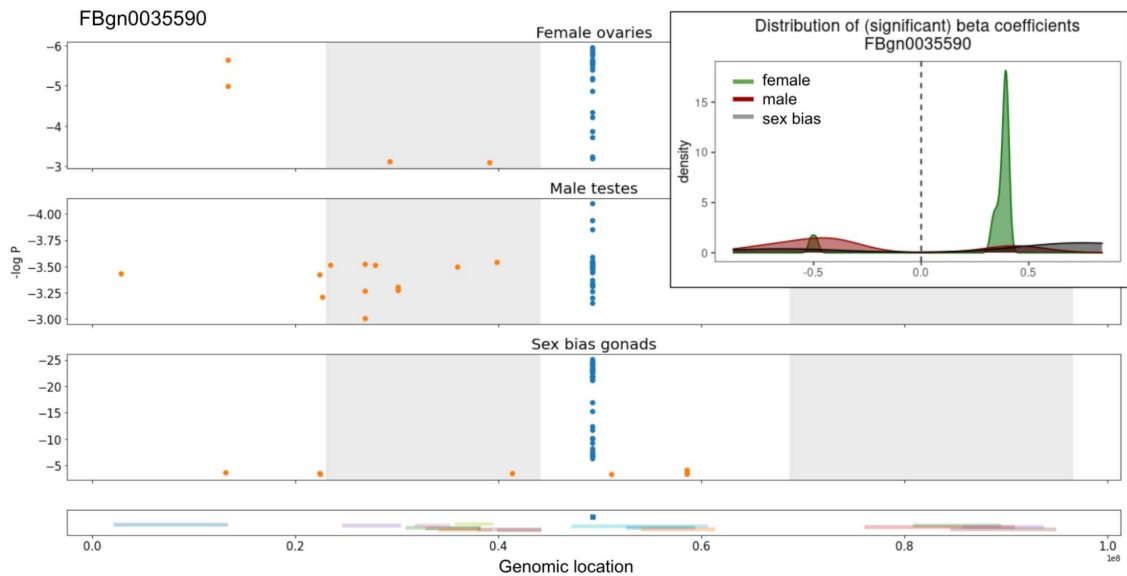


Figure S6: Manhattan plot of an example where sexually-antagonistic mutations (affecting expression in different directions in the two sexes – see subplot of the sex-specific distribution of the regression coefficients for the significant hits) generating variation for sex bias. P-values of the association of each SNP genome-wide with expression of gene FBgn0035590 in female ovaries, male testes and sex bias gonads. Only significant hits ($FDR < 0.05$) are plotted. *Cis* and *trans* interactions are plotted in orange and blue. The horizontal lines in the lowest subplot display the location of the 16 segregating inversions in the genome, and the blue square the location of the gene.

CHAPTER 4

When and why should we expect a negative correlation between intersex correlation and sexual dimorphism?

Supplementary Material

Gemma Puixeu and Laura Hayward

1 Derivation of the allelic equation

Consider an allele segregating at frequency x_f and x_m with phenotypic effect a_f and a_m in females and males, respectively, with an overall frequency $x \equiv (x_f + x_m)/2$ in the population. The expected change in the allele's overall frequency in a single generation is given by

$$E[\Delta x] = \frac{1}{2} (\Delta x_f + \Delta x_m), \quad (\text{S.1})$$

where

$$\Delta x_f \equiv \frac{x_f x_m \bar{W}_0 + \frac{1}{2} (x_f (1 - x_m) + x_m (1 - x_f)) \bar{W}_1}{x_f x_m \bar{W}_0 + (x_f (1 - x_m) + x_m (1 - x_f)) \bar{W}_1 + (1 - x_f) (1 - x_m) \bar{W}_2} - x_f, \quad (\text{S.2})$$

$$\Delta x_m \equiv \frac{x_f x_m \bar{V}_0 + \frac{1}{2} (x_f (1 - x_m) + x_m (1 - x_f)) \bar{V}_1}{x_f x_m \bar{V}_0 + (x_f (1 - x_m) + x_m (1 - x_f)) \bar{V}_1 + (1 - x_f) (1 - x_m) \bar{V}_2} - x_m \quad (\text{S.3})$$

and \bar{W}_i and \bar{V}_i denote the average fitness of females and males, respectively, with $i = 0, 1$ or 2 copies of the allele, where the averaging is over the distribution of contributions to the phenotype from other sites (Kidwell et al., 1977). Rewriting Equations S.2 and S.3 in terms of the overall allele frequency, x , and the difference in allele frequency between males and females, $\delta_{fm} = x_f - x_m$, yields

$$\Delta x_f = \frac{x(1-x)(x(\bar{W}_0 - \bar{W}_1) + (1-x)(\bar{W}_1 - \bar{W}_2))}{2\bar{W}} + \frac{\delta_{fm}^2}{8\bar{W}}(\bar{W}_1 - \bar{W}_0 - x(2\bar{W}_1 - \bar{W}_0 - \bar{W}_2)) \quad \text{and} \quad (\text{S.4})$$

$$\Delta x_m = \frac{x(1-x)(x(\bar{V}_0 - \bar{V}_1) + (1-x)(\bar{V}_1 - \bar{V}_2))}{2\bar{V}} + \frac{\delta_{fm}^2}{8\bar{V}}(\bar{V}_1 - \bar{V}_0 - x(2\bar{V}_1 - \bar{V}_0 - \bar{V}_2)), \quad (\text{S.5})$$

where

$$\bar{W} \equiv x^2\bar{W}_0 + 2x(1-x)\bar{W}_1 + (1-x)^2\bar{W}_2 + \frac{\delta_{fm}^2}{4}(2\bar{W}_1 - \bar{W}_0 - \bar{W}_2) \quad \text{and} \quad (\text{S.6})$$

$$\bar{V} \equiv x^2\bar{V}_0 + 2x(1-x)\bar{V}_1 + (1-x)^2\bar{V}_2 + \frac{\delta_{fm}^2}{4}(2\bar{V}_1 - \bar{V}_0 - \bar{V}_2). \quad (\text{S.7})$$

(Tim Connallon, personal correspondence).

We expect deviations from Hardy-Weinburg to be negligible and we neglect terms of $O(\delta_{fm}^2)$, arriving at

$$\Delta x_f \approx \frac{x(1-x)(x(\bar{W}_0 - \bar{W}_1) + (1-x)(\bar{W}_1 - \bar{W}_2))}{2\bar{W}}, \quad (\text{S.8})$$

$$\Delta x_m \approx \frac{x(1-x)(x(\bar{V}_0 - \bar{V}_1) + (1-x)(\bar{V}_1 - \bar{V}_2))}{2\bar{V}} \quad (\text{S.9})$$

with

$$\bar{W} \approx x^2\bar{W}_0 + 2x(1-x)\bar{W}_1 + (1-x)^2\bar{W}_2 \quad \text{and} \quad (\text{S.10})$$

$$\bar{V} \approx x^2\bar{V}_0 + 2x(1-x)\bar{V}_1 + (1-x)^2\bar{V}_2. \quad (\text{S.11})$$

Equations S.8 and S.9 are identical in form to the expression for $E[\Delta x]$ for a single sex with a Gaussian fitness function. An identical derivation as that in Appendix 3, Section 1.1 of [Hayward and Sella \(2022\)](#), therefore shows that provided $a \ll \sqrt{V_S}$, $V_A \ll V_S$ and $D_f, D_m \lesssim \sqrt{V_S}$ (with D_f and D_m the distances of the male and

female mean trait values from their respective optima), then

$$\Delta x_f \approx \frac{a_f D_f (2\gamma_f^2)}{V_S} x(1-x) - \frac{a_f^2 (2\gamma_f^2)}{V_S} x(1-x) (1/2-x) \quad \text{and} \quad (\text{S.12})$$

$$\Delta x_m \approx \frac{a_m D_m (2\gamma_m^2)}{V_S} x(1-x) - \frac{a_m^2 (2\gamma_m^2)}{V_S} x(1-x) (1/2-x). \quad (\text{S.13})$$

Consequently, the expected change in overall allele frequency in a single generation (Equation S.1) is well approximated by

$$E[\Delta x] \approx \left(\frac{a_f D_f \gamma_f^2}{V_S} + \frac{a_m D_m \gamma_m^2}{V_S} \right) x(1-x) - \left(\frac{a_f^2 \gamma_f^2}{V_S} + \frac{a_m^2 \gamma_m^2}{V_S} \right) x(1-x) (1/2-x). \quad (\text{S.14})$$

2 Genetic variances and covariance at equilibrium

2.1 The number of segregating sites at equilibrium

At equilibrium the first two moments of change in allele frequency are given by

$$E_{eq}[\Delta x] = -\frac{a^2}{V_S} x(1-x) (1/2-x) \quad (\text{S.15})$$

$$V[\Delta x] \approx \frac{x(1-x)}{2N}, \quad (\text{S.16})$$

where $a \equiv \sqrt{a_f^2 \gamma_f^2 + a_m^2 \gamma_m^2}$ is the total phenotypic magnitude. Consequently, the density of sites segregating with total phenotypic magnitude, a , and MAF \tilde{x} per unit mutational input is

$$2\rho(a, \tilde{x}) \equiv \begin{cases} (2Nx) \cdot 4 \cdot \text{Exp}[-a^2 \tilde{x}(1-\tilde{x})] / [\tilde{x}(1-\tilde{x})] & 0 \leq \tilde{x} \leq 1/(2N) \\ 4 \cdot \text{Exp}[-a^2 \tilde{x}(1-\tilde{x})] / [\tilde{x}(1-\tilde{x})] & 1/(2N) < \tilde{x} \leq 1/2 \end{cases}. \quad (\text{S.17})$$

(Hayward & Sella, 2022, Appendix 3, Section 3). The mutational input per generation of alleles with total phenotypic magnitude, a , and angle, ϕ is $2NU \cdot g(a) \cdot h(\phi)$, where $g(a)$ is the distribution of incoming effect magnitudes and $h(\phi_a)$ is the distribution of incoming effect angles. It follows that the density of sites segregating

with total phenotypic magnitude, a , angle, ϕ , and MAF \tilde{x} is

$$2NU \cdot 2\rho(a, \tilde{x}) \quad (\text{S.18})$$

2.2 Computing the variances and covariance

The genic variance in females ($\beta = f$), and males ($\beta = m$), and the covariance between the sexes (Equations ?? and ?? in the main text) can be rewritten as

$$V_{A,\beta} = \sum_i^L 2a_{i,\beta}^2 \tilde{x}_i (1 - \tilde{x}_i); \quad B = \sum_i^L 2a_{i,f} a_{i,m} \tilde{x}_i (1 - \tilde{x}_i); \quad (\text{S.19})$$

where, here, the \tilde{x}_i are minor allele frequencies. Changing variables from sex-specific effects $a_{i,f}$ and $a_{i,m}$ to the total phenotypic magnitude, a_i , and the angle, $\phi_{i,a}$ (Equation 16 in the main text), these expressions become

$$V_{A,f} = \frac{1}{\gamma_f^2} \sum_i^L 2a_i^2 \cos^2(\phi_{i,a}) \tilde{x}_i (1 - \tilde{x}_i), \quad (\text{S.20})$$

$$V_{A,m} = \frac{1}{\gamma_m^2} \sum_i^L 2a_i^2 \sin^2(\phi_{i,a}) \tilde{x}_i (1 - \tilde{x}_i) \quad (\text{S.21})$$

$$B = \frac{1}{\gamma_f \gamma_m} \sum_i^L 2a_i^2 \cos(\phi_{i,a}) \sin(\phi_{i,a}) \tilde{x}_i (1 - \tilde{x}_i) \quad (\text{S.22})$$

Approximating the sums in Equations S.20, S.21 and S.22 by integrals over the density of segregating sites at equilibrium (Equation S.18), it follows that

$$V_{A,f} = \frac{1}{\gamma_f^2} \int_{\phi_a=0}^{\phi_a=2\pi} \int_{a=0}^{a=\infty} \int_{\tilde{x}=0}^{\tilde{x}=1/2} 2a^2 \cos^2(\phi_a) \tilde{x} (1 - \tilde{x}) [2NU \cdot 2\rho(a, \tilde{x})] d\tilde{x} da d\phi_a, \quad (\text{S.23})$$

$$V_{A,m} = \frac{1}{\gamma_m^2} \int_{\phi_a=0}^{\phi_a=2\pi} \int_{a=0}^{a=\infty} \int_{\tilde{x}=0}^{\tilde{x}=1/2} 2a^2 \sin^2(\phi_a) \tilde{x} (1 - \tilde{x}) [2NU \cdot 2\rho(a, \tilde{x})] d\tilde{x} da d\phi_a \quad (\text{S.24})$$

$$B = \frac{1}{\gamma_f \gamma_m} \int_{\phi_a=0}^{\phi_a=2\pi} \int_{a=0}^{a=\infty} \int_{\tilde{x}=0}^{\tilde{x}=1/2} 2a^2 \cos(\phi_a) \sin(\phi_a) \tilde{x} (1 - \tilde{x}) [2NU \cdot 2\rho(a, \tilde{x})] d\tilde{x} da d\phi_a \quad (\text{S.25})$$

These expressions can be rewritten as

$$V_{A,f} = \frac{1}{\gamma_f^2} \int_0^{2\pi} \cos^2(\phi_a) d\phi_a \cdot V_{A,T}, \quad (\text{S.26})$$

$$V_{A,m} = \frac{1}{\gamma_m^2} \int_0^{2\pi} \sin^2(\phi_a) d\phi_a \cdot V_{A,T} \quad (\text{S.27})$$

$$B = \frac{1}{\gamma_f \gamma_m} \int_0^{2\pi} \cos(\phi_a) \sin(\phi_a) d\phi_a \cdot V_{A,T} \quad (\text{S.28})$$

where

$$V_{A,T} = 2NU \cdot \int_0^\infty \int_0^{1/2} 2a^2 \tilde{x}(1 - \tilde{x}) \cdot 2\rho(a, \tilde{x}) d\tilde{x} da = 2NU \cdot \int_0^\infty v(a)g(a) da \quad (\text{S.29})$$

where $v(a) = 4a \cdot D_+(a/2)$ and D_+ is the Dawson function (the second equality was shown in [Hayward & Sella, 2022](#), Appendix 3, Section 3.2).

3 Exploring the limits to shift size

We explore the range of magnitudes of shifts in sex-specific optima Λ_f, Λ_m that fulfill the assumptions of the analytical framework. Concretely, we ensure that the shifts are substantially larger than the random fluctuations so that we can see a signal ($|\Lambda_f|, |\Lambda_m| > \delta$), but smaller than, or on the order of, the width of the fitness function ($|\Lambda_f|, |\Lambda_m| \lesssim \sqrt{V_S}$). To test the limits to the shift size, we computed the average of sex-specific variances divided by the analytical variance for various sizes in shift size. As Figure S1 shows, with completely shared genetic architecture between sexes ($\phi_a = \pi/4$), the realized variance remains as expected for a shift size (scaled by the width of the fitness function) of $\Lambda_f, \Lambda_m \lesssim 0.5\sqrt{V_S}$.

This tells us two things: on the one hand, that for shift sizes up to this magnitude the analytics predict well the simulation outcomes, so it is the range we should be using. However, this is likely to be relaxed when the genetic architecture is (partially) sex-specific, since sex-specific trait means are going to be closer to their optima, and thus to the center of the fitness functions.

On the other hand, we do not observe an increase in sex-specific variances within this range, confirming the prediction derived from Equation ?? that when effect sizes are the same across sexes ($\phi_a = \pi/4$), selection acts exactly symmetrically across sexes ($V_{Sf} = V_{Sm} = V_S$) and both sexes undergo exactly opposite shifts in optima

$\Delta_f = -\Delta_m$, sex-specific directional selective forces exactly cancel out and individual alleles do not experience directional selection.

4 Phenotypic evolution with multigenic genetic architecture

With multigenic genetic architecture, selection in the rapid phase drives an increase in 2nd and 3rd central moments of the phenotypic distribution (Figure S2), which lead to deviations in the phenotypic dynamics with respect to infinitesimal genetic architecture, where the 2nd and 3rd central moments remain at the equilibrium values throughout.

When considering D_a , changes in the 2nd central moments tend to accelerate phenotypic evolution during the rapid phase, while changes in 3rd central moments delay them during equilibration, leading to the quasi-static approximation (Figure S3, top). For D_d , there is a faster (slower) phenotypic evolution in the rapid phase with changes in 2nd (3rd) central moments (Figure S3, bottom). Whether phenotypic evolution given changes in the genetic architecture in the multigenic case are faster or slower than in the infinitesimal case depend on whether the specific simulation parameters lead to a higher increase in 2nd or 3rd central moments. This is well illustrated in our three choices of intersex correlation, where phenotypic evolution is faster, similar and slower with $r_{fm} = 0.90, 0.67, 0.33$.

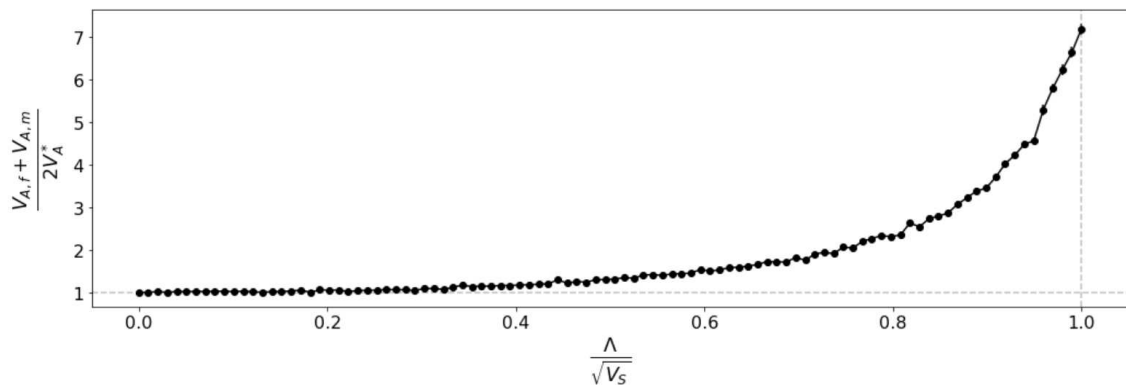


Figure S1: Exploring the limits to the shift size. Average of sex-specific variances divided by the analytical variance ($\frac{V_{A,f}+V_{A,m}}{2V_A^*}$) for various shift size scaled by the width of the fitness function ($\Lambda_f, \Lambda_m/\sqrt{V_S}$). The error bars (often smaller than the dots themselves) are the SEM around the averages across 25 replicates.

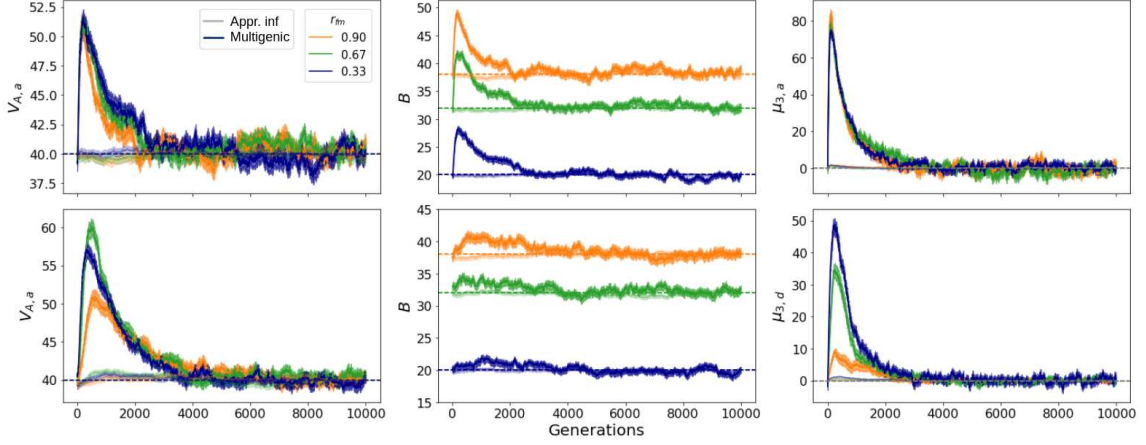


Figure S2: Second and third central moments of the phenotypic distribution along time. Top and bottom rows correspond to evolution after sexually-concordant and sexually-dimorphic shifts in optima, respectively corresponding to scenarios illustrated in main Figure 2A ($\Lambda_a = 0.25\sqrt{V_S}$ and $\Lambda_d = 0$) and Figure 2B ($\Lambda_a = 0$ and $\Lambda_d = 0.25\sqrt{V_S}$). Left, average genetic variance, $V_{A,a} = 0.5(V_{A,f} + V_{A,m})$ (average difference genetic variance, $V_{A,d} = 0.5(V_{A,f}^e - V_{A,m}^e)$, is not depicted as it is close to zero along time). Middle, between-sex covariance (B). Right, average and average difference third central moments of the phenotypic distribution. Only the relevant 3rd central moment is shown, as $\mu_{3,d}$ ($\mu_{3,a}$) remains zero for sexually-concordant, top (sexually-dimorphic, bottom) adaptation. Orange, green and blue indicate simulations with different intersex correlations ($r_{fm} = 0.90, 0.67, 0.33$). Simulations with multigenic ($E(a^2) = 16$) and approximately infinitesimal ($E(a^2) = 1$) genetic architecture are respectively plotted in bright and dim colors. Dashed horizontal lines correspond to the equilibrium values.

5 The quasi-static approximation

The quasi-static solution during equilibration relating the distances from the optimum with the second and third moments in the multigenic case can be obtained by setting $E[\Delta D_a] \approx 0$ and $E[\Delta D_d] \approx 0$ in Equation 34 which, after working through the algebra, yields:

$$\begin{aligned}
 D_a^*(t) &\approx \frac{\mu_{3,a}(t)}{V_{A,a}(t) + B(t)} \cdot (1 - \xi(t)) - \frac{\mu_{3,d}(t)}{V_{A,d}(t)} \cdot \xi(t) \\
 D_d^*(t) &\approx \frac{\mu_{3,d}(t)}{V_{A,a}(t) - B(t)} \cdot (1 - \xi(t)) - \frac{\mu_{3,a}(t)}{V_{A,d}(t)} \cdot \xi(t)
 \end{aligned} \tag{S.30}$$

where

$$\xi(t) \equiv \frac{V_{A,d}^2(t)}{V_{A,a}^2(t) - B^2(t) - V_{A,d}^2(t)}$$

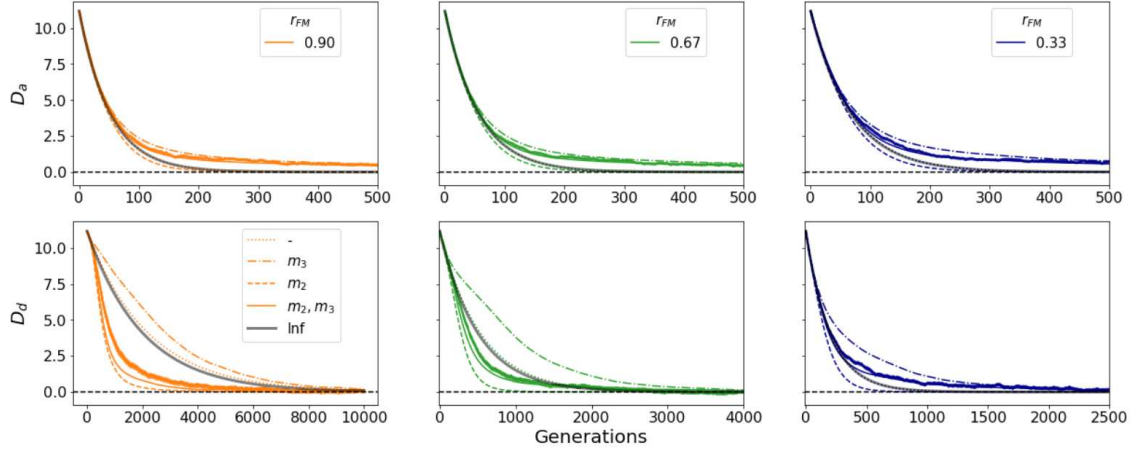


Figure S3: Phenotypic evolution in the multigenic case. Top row corresponds to D_a along time, for optima shift $\Lambda_a = 0.25\sqrt{V_S}$ and $\Lambda_d = 0$ leading to sexually-concordant adaptation (Figure 2A). Bottom row corresponds to D_d along time, for optima shift $\Lambda_a = 0$ and $\Lambda_d = 0.25\sqrt{V_S}$, leading to sexually-dimorphic adaptation (Figure 2B). Thick lines correspond to simulations with multigenic genetic architecture, grey lines to the prediction assuming infinitesimal architecture using Equation 28, and various types of thin lines to predictions using various versions of Equation 33: dotted, with constant G' matrix and with $\mu_{3,a} = \mu_{3,d} = 0$, effectively coinciding with the prediction assuming infinitesimal architecture; dash-dotted, with constant G' matrix and with $\mu_{3,a}, \mu_{3,d}$ updated generation-wise according to their values in the simulations; dashed, with elements in the G' matrix updated generation-wise according to their values in the simulations and with $\mu_{3,a} = \mu_{3,d} = 0$; solid, with both 2nd and 3rd order moments updated generation-wise according to their values in the simulations. First, second and third columns (orange, green, blue) correspond to simulations with $r_{fm} = 0.90, 0.67, 0.33$. For the simulations, we let the populations evolve for $10N$ generations so they attain a selection-mutation-drift equilibrium before applying the shift in optima. We have zoomed in the results so that the relevant dynamics can be appreciated for all cases. The error bars (often not appreciable) represent SEM across 200 replicates.

When things are perfectly symmetric between the sexes, the above simplifies further since $V_{A,d}(t)$ should remain zero after the shift. In that case we get

$$D_a^{**}(t) \approx \frac{\mu_{3,a}(t)}{V_{A,a}(t) + B(t)}; \quad D_d^{**}(t) \approx \frac{\mu_{3,d}(t)}{V_{A,a}(t) - B(t)} \quad (\text{S.31})$$

As Figure S4 shows, in the infinitesimal case at t_a and t_d (end of rapid phase, Equation 31) sex-specific means have matched their optima $D_a, D_d \approx 0$. However, with multigenic genetic architecture there is a slower equilibration phase, which is well-predicted by the quasi-static approximation (Equations S.31). This seems to be independent from r_{fm} , which determines t_a and t_d , but not the dynamics of

the quasi-static approximation. However, for $r_{fm} = 0.67$ we see that the dynamics are qualitatively different (approximation is similar for the infinitesimal as well as multigenic case). Further characterization of the quasi-static approximation with both genetic architectures and different r_{fm} is ongoing work.

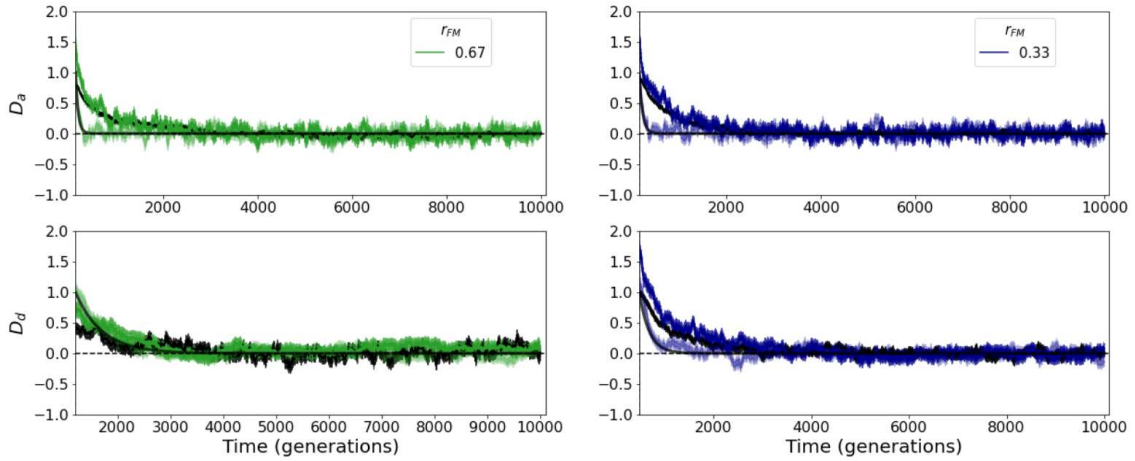


Figure S4: Quasi-static approximation during equilibration. Evolution of D_a and D_d (first and second rows), for sexually-concordant and sexually-dimorphic adaptation after shifts in optima corresponding to $\Lambda_a = 0.25\sqrt{V_S}$, $\Lambda_d = 0$ and $\Lambda_a = 0$, $\Lambda_d = 0.25\sqrt{V_S}$ (scenarios depicted in Figure 2A and 2B, respectively) for $r_{fm} = 0.67, 0.33$ (first and second columns, in green and blue) with multigenic ($E(a^2) = 16$, dark) and approximately infinitesimal ($E(a^2) = 1$, light) genetic architecture following equation 34. Black lines correspond to the quasi-static approximation (Equations S.31). Grey lines correspond to the evolution in D_a, D_d in the infinitesimal case (Equation 28). We let the populations evolve for $10N$ generations so they attain a selection-mutation-drift equilibrium before the shift in optima. The starting point of the current plots corresponds to the time where D_a and D_d to reach the typical deviation of the population mean from the optima at equilibrium, $\delta = \sqrt{V_S}/2N$, which determines the end of the rapid phase and beginning of equilibration (t_a, t_d in Equation 31). The error bars represent SEM across 200 replicates.

6 Fixed background with multigenic genetic architecture

Equations 37 and 38 predict well the evolution of the fixed background for both F_a and F_d in the multigenic case, independently of r_{fm} (Figure S4).

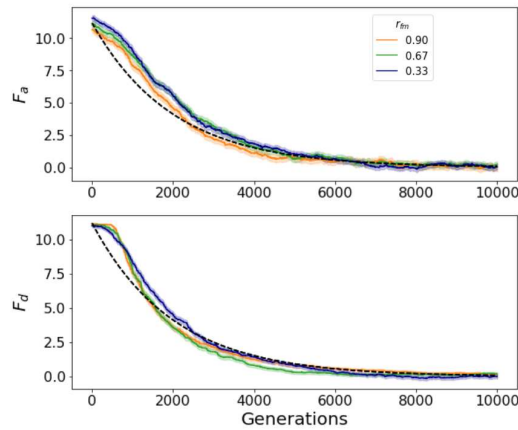


Figure S5: The fixed background with multigenic genetic architecture. F_a (top) and F_d (bottom), for sexually-concordant and sex-specific adaptation corresponding to scenarios depicted in main Figure 2A (optima shift $\Lambda_a = 0.25\sqrt{V_S}$, $\Lambda_d = 0$) and 2B (optima shift $\Lambda_a = 0$, $\Lambda_d = 0.25\sqrt{V_S}$), respectively. Coloured lines correspond to simulations with multigenic genetic architecture and the dashed black line corresponds to the prediction according to Equations 37 and 38, for $r_{fm} = 0.90, 0.67, 0.33$.

References

- Hayward, L. K., & Sella, G. (2022, September). Polygenic adaptation after a sudden change in environment. *eLife*, *11*, e66697. doi: 10.7554/eLife.66697
- Kidwell, J. F., Clegg, M. T., Stewart, F. M., & Prout, T. (1977, January). Regions of stable equilibria for models of differential selection in the two sexes under random mating. *Genetics*, *85*(1), 171–183. doi: 10.1093/genetics/85.1.171